Deregulation of DNA mismatch repair by the oncogenic tyrosine kinase NPM-ALK

by

Kathleen Marie Bone

A thesis submitted in partial fulfillment of the requirements for the degree of

Doctor of Philosophy

Department of Laboratory Medicine and Pathology
University of Alberta

Abstract

The vast majority of anaplastic lymphoma kinase positive anaplastic large cell lymphoma (ALK+ALCL) tumors carry the genetic translocation t(2;5)(p23;q35), leading to production of the constitutively active fusion tyrosine kinase NPM-ALK. NPM-ALK expression and its potent transformative properties are central to the pathogenesis of this disease. The Lai Laboratory recently identified MSH2, an integral component of the DNA mismatch repair (MMR) pathway, as a novel NPM-ALK interactor by mass spectrometry. DNA MMR proteins aid in tumor suppression through the maintenance of genomic instability, and their loss is highly oncogenic. As NPM-ALK is a tyrosine kinase that binds to and phosphorylates downstream proteins to mediate its tumorigenesis, it was hypothesized that through its interaction with MSH2, NPM-ALK interferes with its biological function, impacting MMR. The major findings of this study are that NPM-ALK indeed binds and tyrosine phosphorylates MSH2, blocking the interaction with its main MMR binding partner, MSH6, and inducing cytoplasmic retention of MSH2 in the presence of DNA damage. Correlating with these findings, ALK+ALCL patient samples displayed evidence of MMR dysfunction, including accentuated MSH2 cytoplasmic staining, and microsatellite instability. Furthermore, tyrosine 238 in the MSH2 protein was identified as the key NPM-ALK-induced tyrosine phosphorylation site in the context of MMR deregulation; overexpression

of a non-phosphorylatable mutant, $MSH2^{Y238F}$, in NPM-ALK expressing cell lines reversed MSH2 tyrosine phosphorylation, and restored the interaction of MSH2 and MSH6, resulting in a return of MMR function. Finally, using a novel antibody specifically designed against phosphorylated MSH2 at tyrosine 238, other clinically relevant oncogenic tyrosine kinases were found to interact with MSH2, inducing its phosphorylation at tyrosine 238, leading to MMR dysfunction. This is the first reported evidence of post-translational modification of MSH2 at a specific residue, tyrosine 238, by oncogenic tyrosine kinases with a direct impact on MMR function. Altogether, this study provides novel insights into the deregulation of DNA repair by oncogenic tyrosine kinases, with widespread implications for tyrosine kinase screening and targeted cancer therapy.

Preface

This thesis represents collaborative work, led by Dr. Raymond Lai at the University of Alberta.

Chapter 2 of this thesis has been published as:
Young LC, Bone KM, Wang P, Wu F, Adam BA, Hegazy S, Gelebart P, Holovati J, Li L, Andrew SE, Lai R. Fusion tyrosine kinase NPM-ALK deregulates MSH2 and suppresses DNA mismatch repair function: novel insights into a potent oncoprotein. American Journal of Pathology. 2011. Jul; 179(1):411-421. I contributed to this work as outlined on page 93 on this thesis.

Chapter 3 of this thesis has been submitted for publication as:
Bone KM, Wang P, Wu F, Wu C, Li L, Bacani, JT, Andrew SE, Lai R. NPM-ALK mediates phosphorylation of MSH2 at tyrosine 238, creating a functional deficiency in MSH2 and the loss of mismatch repair. Submitted for publication. 2014. I was first author of this submitted manuscript, and contributed to the work as outlined on page 137 of this thesis.

Chapter 4 of this thesis represents work that will be included in a manuscript in preparation:
Bone KM, Gupta N, Andrew SE, Lai R. Clinically relevant oncogenic tyrosine kinases interact with and phosphorylate MSH2: a novel mechanism underlying MMR dysfunction. In preparation. I was first author of this work, and contributed as outlined on page 184 of this thesis.

Dedicated to my J

“Some people care too much. I think it’s called love.”

- A.A. Milne (1882-1956)

Acknowledgements

This thesis would not be possible without the help of so many people in many ways. Foremost, my sincerest thanks to my supervisor, Dr. Raymond Lai, for getting me to where I am today, and for your patience, motivation, support and guidance. Your love of science is contagious.

I would also like to thank my committee member Dr. Susan Andrew for everything. Your mentorship, and support were invaluable, and your constant encouragement and smile a blessing. For these things, I am grateful.

To Dr. David Murray for serving on my committee and for your continued support throughout my graduate program.

To Dr. Monika Keelan, for not only giving guidance and support as the Graduate Studies Coordinator, but for all the other ways you have helped me throughout my program, including your willingness to listen, for which I am forever indebted.

To all the past and present members of the Lai Lab that I have been fortunate enough to work with, I appreciate you all as you have all contributed to making me a better scientist. Thank you especially to my friend and colleague Karen Jung for providing me with a little extra friendship and support.

Thank you to the University of Alberta, Killam Trusts, the Canadian Institutes of Health Research, and Alberta Innovates Health Solutions for providing me with the financial support needed during my graduate studies.

To my friends for putting up with me throughout my studies, thank you with all my heart. A special heartfelt thank you to Stephanie Grainger: although you are far and away, I think of you always and love you like a sister. Thank you for standing by me through it all.

To my family: I would by no means be where I am today if not for the support that I have received over the years from every single one of you, even if you don't really understand what I am studying – I promise, it's not *that* boring. Special thanks to my sister, Holly: you have the ability to make me laugh when no one else can, and I am not exactly sure how to express how fortunate I feel (and am, too) to have you in my life. You and your Goombas rock, for reals.

To my Mom and Dude: I never do seem to pick the easiest journey, and you both know this more than anyone. Thank you for helping me find myself.

And last but not least, to my husband, Jamie. I wouldn't have picked this journey if I weren't on it with you. And, you are pretty awesome, so that just makes it that much better.

Table of Contents

List of Abbreviations

5-FU – 5-fluorouracil
6TG – 6-thioguanine
Abl – Abelson kinase
ALCL – anaplastic large cell lymphoma
ALCLC – anaplastic large cell lymphoma, conventional
ALK – anaplastic lymphoma kinase
ALK+ALCL – anaplastic lymphoma kinase positive anaplastic large cell lymphoma
ALO17 – anaplastic lymphoma kinase (ALK) lymphoma oligomerization partner on chromosome 17
ALL – acute lymphoblastic leukemia
APC - adenomatous polyposis coli
AP-1 – activator protein-1
ATIC – 5-aminoimidazole-4-carboxamide ribonucleotide formyltransferase/IMP cyclohydrolase
ATM – ataxia telangiectasia mutated
ATR – ataxia telangiectasia and Rad3 related
ATRIP – ATR-interacting protein
BAD – Bcl2-associated death receptor
BALB – Bagg albino
BC – breast cancer
BCA – bicinchoninic acid
BCL2 – B-cell lymphoma 2
BCR – breakpoint cluster region
BCR-ABL – breakpoint cluster region fused to Abelson kinase
BER – base excision repair
BLM – Bloom syndrome, RecQ helicase-like
BP – blast phase
BRAF – v-Raf murine sarcoma viral oncogene homolog B protein

BRCA1 - breast cancer 1, early onset

C – cytoplasmic

C – cytosine

c-KIT – v-kit Hardy-Zuckerman 4 feline sarcoma viral oncogene homolog

c-MYC – V-myc avian myelocytomatosis viral oncogene homolog

C-terminal – carboxy terminal

C2orf44 – chromosome 2 open-reading-frame 44

CA – constitutively active

CARS – cysteinyl-tRNA synthetase

CASP – caspase

CDC25A – cell division cycle 25 homolog A

CHK1 – checkpoint kinase 1

CHK2 – checkpoint kinase 2

CHOP – cyclophosphamide, hydroxydaunorubicin, oncovin, prednisone

CIP – calf intestinal phosphatase

CKII – casein kinase 2

Cl – cleaved

CLTC – clathrin heavy chain

CML – chronic myelogenous leukemia

Co-IP/Co-IPP – co-immunoprecipitation

CP – chronic phase

CRC – colorectal carcinoma

CSF-1R – colony stimulating factor 1 receptor

CSR – class switch recombination

DAB – 3,3'-diaminobenzidine

DAG – diacylglycerol

DCC – deleted in colorectal carcinoma

DLBCL – diffuse large B-cell lymphoma

DMEM – Dulbecco’s modified Eagle’s media

DNMT – DNA methyltransferase

DOX/Dox – doxycycline

ECL – enhanced chemiluminescence

EGFR – epidermal growth factor receptor

ELISA – enzyme-linked immunosorbent assay

EMA – epithelial membrane antigen

EML4 – echinoderm microtubule associated protein like 4

EML4-ALK – echinoderm microtubule associated protein like 4 fused to anaplastic lymphoma kinase

ERα – estrogen receptor alpha

ERβ – estrogen receptor beta

ERK – extracellular signal-related kinase

ESCC – esophageal squamous cell carcinoma

ETS-1 – V-Ets avian erythroblastosis virus E26 oncogene homolog 1

EV – empty vector

Exo1 – exonuclease 1

F – phenylalanine

FBS – fetal bovine serum

FISH – fluorescent *in-situ* hybridization

FITC – fluorescein isothiocyanate

FN1 – fibronectin 1

FOXO3a – forkhead box O3 a

FRA2 – Fos-related antigen 2

O^6-MeG – O^6methylguanine

GI – gastrointestinal

GIST – gastrointestinal stromal tumor

GRB2 – growth factor receptor-bound protein 2

Gua – guanine

FACS – fluorescent activated cell sorter

FITC – fluorescein isothiocyanate

FGA – fibrinogen alpha chain

GLI1 – glioma-associated oncogene homolog 1

GSK – glycogen synthase kinase

H&E – Hematoxylin and eosin

HB – his-biotin

HBT – his-biotin tagged

HDAC1 – histone deacetylase 1

HDC-ASCT – high-dose chemotherapy with autologous stem cell transplantation

HEK – human embryonic kidney

Hem – hematopoietic

HER2 – human epidermal growth factor receptor 2

HL – Hodgkin lymphoma

HNPCC – hereditary non-polyposis colorectal cancer

HPC1 – hereditary prostate cancer 1

HR – homologous recombination

ICL – inter-strand crosslinks

ID2 – inhibitor of DNA binding 2

IDL – insertion-deletion loop

IGF-1R – insulin-like growth factor 1 receptor

IHC – immunohistochemistry

IL – interleukin

ILR – interleukin receptor

IMT – inflammatory myofibroblastic tumor

IP – immunoprecipitation

IP3 – inositol-1,4,5-triphosphate

IR – ionizing radiation

IRS-1 – insulin receptor substrate 1

JAK – Janus kinase

JNK – Jun-amino terminal kinase

KIF5B – kinesin family member 5B

KLC1 – kinesin light chain 1

KLH – keyhole limpet hemocyanin

LC/MS – liquid chromatography-mass spectrometry

Lck – lymphocyte protein tyrosine kinase

LTK – leukocyte tyrosine kinase

mAB – monoclonal antibody

MAPK – mitogen-activated protein kinase

MAX – MYC-associated factor X

MCL – mantle cell lymphoma

Mcl1 – myeloid cell leukemia sequence 1

MCM6 – minichromosome maintenance complex component 6

MEK – mitogen-activated protein kinase

MET/HGFR – hepatocyte growth factor receptor

MGMT – O^6MeG-DNA methyltransferase

MK - midkine

MLH – MutL homolog

MMR – mismatch repair

MNNG – N-methyl-N'-nitro-N-nitrosoguanine

MNU – *N*-methyl-*N*-nitrosourea

MSH – MutS homolog

MSI – microsatellite instability

MSI-H – microsatellite instability high

MSI-L – microsatellite instability low

MSN – moesin

MSS – microsatellite stable

mTOR – mammalian target of rapamycin

MTS – 3-(4,5-dimethylthiazol-2-yl)-5-(3-carboxymethoxyphenyl)-2-(4-sulfophenyl)-2H-tetrazolium

MUC1 – mucin 1

MutSα – mutational S alpha, MSH2:MSH6

MutSβ – mutational S beta, MSH2:MSH3

MYH9 – myosin heavy chain 9

N – nuclear

N-terminal – amino terminal

N/A – not available

NCI – National Cancer Institute

NHEJ – non-homologous end joining

NHL – non-Hodgkin lymphoma

NIPA – nuclear interaction partner of ALK

NK – natural killer

NLS – nuclear localization signal

NPM – nucleophosmin

NPM-ALK – nucleophosmin fused to anaplastic lymphoma kinase

NR – not-reported

ns – not significant

NSCLC – non-small cell lung cancer

O^6meG – O^6methylguanine

OF – out-of-frame

OMIM – Online Mendelian Inheritance in Man

P/p – phospho/phosphorylation

p-Y – phosphorylated tyrosine

PARP1 – poly (ADP ribose) polymerase 1

PBS – phosphate buffered saline

PCNA – proliferating cell nuclear antigen

PCR – polymerase chain reaction

PDGFR – platelet derived growth factor receptor

PKC – protein kinase C

PH – pleckstrin homology

PI – propidium iodide

PI3K – phosphatidylinositide 3-kinase

PINK1 – PTEN-induced putative kinase 1

PIP2 – phosphatidylinositol 4,5-bisphosphate

PLC-γ – phospholipase C gamma

PMS – postmeiotic segregation increased

PTB – phospho-tyrosine binding

PTCH – patched
PTEN – phosphatase and tensin homolog
PTN – pleiotrophin
PTPN3 – protein tyrosine phosphatase, non-receptor type 3
PPFIBP1 – protein tyrosine phosphatase receptor type F polypeptide-interacting protein-binding protein
RANBP2 – RAN-binding protein 2
RECT – rectal
RECQ1 – RecQ protein-like (DNA helicase Q1-like)
RFC – replication factor C
RMC – renal medulla carcinoma
RCC – renal cell carcinoma
ROS1 – c-ros oncogene 1
RPA – replication protein A
RPS6 – ribosomal protein s 6
RTK – receptor tyrosine kinase
SAPK – stress activated protein kinase
SDS-PAGE – sodium docedyl sulfate-polyacrylamide gel electrophoresis
SEM – standard error of the mean
SHC – Src homology region 2 domain containing
SHH – sonic hedgehog
SHP1 – Src homology region 2 domain-containing phosphatase-1
siRNA – small interfering RNA
SLC7A8 – solute carrier family 7 (amino acid transporter light chain, L system), member 8
SMO – smoothened
SOC – serous ovarian carcinoma
SRC – v-Src avian sarcoma (Schmidt-Ruppin A-2) viral oncogene homolog
STAT – signal transducer and activator of transcription
STRN – striatin

Sox2 – SRY (sex determining region Y)-box 2

SQSTM1 – sequestosome 1

T – total, or thymine

t – translocation

T-ALL – T-acute lymphoblastic leukemia

TAGC – The Applied Genomics Centre

TCR – T-cell receptor

Tet – tetracycline

TFG – TRK-fused gene

TIA-1 – T-cell-restricted intracellular antigen 1

TNR – trinucleotide repeat expansion

tTa – Tetracycline-transactivator

TMP – tropomyosin

UVB – ultraviolet B

v – variant

VCL – vinculin

Y – tyrosine

ZNF2 – zinc finger protein 2

Authorizations

AMERICAN ASSOCIATION FOR CANCER RESEARCH LICENSE TERMS AND CONDITIONS

Sep 21, 2014

This is a License Agreement between Kathleen M Bone ("You") and American Association for Cancer Research ("American Association for Cancer Research") provided by Copyright Clearance Center ("CCC"). The license consists of your order details, the terms and conditions provided by American Association for Cancer Research, and the payment terms and conditions.

All payments must be made in full to CCC. For payment instructions, please see information listed at the bottom of this form.

License Number	3413770943540
License date	Jun 21, 2014
Order Content Publisher	American Association for Cancer Research
Order Content Publication	Molecular Cancer Therapeutics
Order Content Title	Targeting Oncogenic ALK: A Promising Strategy for Cancer Treatment
Order Content Author	Enrique Grande, María-Victoria Bolós, Edurne Arriola et al.
Order Content Date	April 1, 2011
Volume number	10
Issue number	4
Type of Use	Thesis/Dissertation
Requestor type	academic/educational
Format	print and electronic
Portion	figures/tables/illustrations
Number of figures/tables/illustrations	1
Will you be translating?	no
Circulation	8
Territory of distribution	Worldwide
Title of your thesis / dissertation	Deregulation of DNA mismatch repair by the oncogenic tyrosine kinase NPM-ALK
Expected completion date	Sep 2014
Estimated size (number of pages)	230
Total	**0.00 USD**
Terms and Conditions	

American Association for Cancer Research (AACR) Terms and Conditions

NATURE PUBLISHING GROUP LICENSE TERMS AND CONDITIONS

Sep 21, 2014

This is a License Agreement between Kathleen M Bone ("You") and Nature Publishing Group ("Nature Publishing Group") provided by Copyright Clearance Center ("CCC"). The license consists of your order details, the terms and conditions provided by Nature Publishing Group, and the payment terms and conditions.

All payments must be made in full to CCC. For payment instructions, please see information listed at the bottom of this form.

License Number	3415570255974
License date	Jun 24, 2014
Order Content Publisher	Nature Publishing Group
Order Content Publication	Clinical Pharmacology & Therapeutics
Order Content Title	Current Status of Targeted Therapy for Anaplastic Lymphoma Kinase-Rearranged Non-Small Cell Lung Cancer
Order Content Author	B Solomon, K D Wilner and A T Shaw
Order Content Date	Oct 3, 2013
Volume number	95
Issue number	1
Type of Use	reuse in a dissertation / thesis
Requestor type	academic/educational
Format	print and electronic
Portion	figures/tables/illustrations
Number of figures/tables/illustrations	2
High-res required	no
Figures	Table 1 Figure 4
Author of this NPG article	no
Your reference number	None
Title of your thesis / dissertation	Deregulation of DNA mismatch repair by the oncogenic tyrosine kinase NPM-ALK
Expected completion date	Sep 2014
Estimated size (number of pages)	230
Total	**0.00 USD**

JOHN WILEY AND SONS LICENSE TERMS AND CONDITIONS

Sep 21, 2014

This is a License Agreement between Kathleen M Bone ("You") and John Wiley and Sons ("John Wiley and Sons") provided by Copyright Clearance Center ("CCC"). The license consists of your order details, the terms and conditions provided by John Wiley and Sons, and the payment terms and conditions.

All payments must be made in full to CCC. For payment instructions, please see information listed at the bottom of this form.

License Number	3404861389433
License date	Jun 09, 2014
Order Content Publisher	John Wiley and Sons
Order Content Publication	International Journal of Cancer
Order Content Title	Structure and function of the components of the human DNA mismatch repair system
Licensed copyright line	Copyright © 2006 Wiley-Liss, Inc.
Order Content Author	Thomas Jascur,C. Richard Boland
Order Content Date	Jun 27, 2006
Start page	2030
End page	2035
Type of use	Dissertation/Thesis
Requestor type	University/Academic
Format	Electronic
Portion	Figure/table
Number of figures/tables	2
Original Wiley figure/table number(s)	Figure 1, Figure 2
Will you be translating?	No
Title of your thesis / dissertation	Deregulation of DNA mismatch repair by the oncogenic tyrosine kinase NPM-ALK
Expected completion date	Sep 2014
Expected size (number of pages)	230
Total	**0.00 USD**

NATURE PUBLISHING GROUP LICENSE TERMS AND CONDITIONS

Sep 21, 2014

This is a License Agreement between Kathleen M Bone ("You") and Nature Publishing Group ("Nature Publishing Group") provided by Copyright Clearance Center ("CCC"). The license consists of your order details, the terms and conditions provided by Nature Publishing Group, and the payment terms and conditions.

All payments must be made in full to CCC. For payment instructions, please see information listed at the bottom of this form.

License Number	3416071161502
License date	Jun 25, 2014
Order Content Publisher	Nature Publishing Group
Order Content Publication	Cell Research
Order Content Title	Mechanisms and functions of DNA mismatch repair
Order Content Author	Guo-Min Li
Order Content Date	Dec 24, 2007
Volume number	18
Issue number	1
Type of Use	reuse in a dissertation / thesis
Requestor type	academic/educational
Format	print and electronic
Portion	figures/tables/illustrations
Number of figures/tables/illustrations	1
High-res required	no
Figures	Figure 2
Author of this NPG article	no
Your reference number	None
Title of your thesis / dissertation	Deregulation of DNA mismatch repair by the oncogenic tyrosine kinase NPM-ALK
Expected completion date	Sep 2014
Estimated size (number of pages)	230
Total	**0.00 USD**

SPRINGER LICENSE
TERMS AND CONDITIONS

Sep 21, 2014

This is a License Agreement between Kathleen M Bone ("You") and Springer ("Springer") provided by Copyright Clearance Center ("CCC"). The license consists of your order details, the terms and conditions provided by Springer, and the payment terms and conditions.

All payments must be made in full to CCC. For payment instructions, please see information listed at the bottom of this form.

License Number	3416560052245
License date	Jun 26, 2014
Order Content Publisher	Springer
Order Content Publication	Familial Cancer
Order Content Title	Lynch syndrome-associated neoplasms: a discussion on histopathology and immunohistochemistry
Order Content Author	Jinru Shia
Order Content Date	Jan 1, 2013
Volume number	12
Issue number	2
Type of Use	Thesis/Dissertation
Portion	Figures
Author of this Springer article	No
Order reference number	None
Original figure numbers	Table 1
Title of your thesis / dissertation	Deregulation of DNA mismatch repair by the oncogenic tyrosine kinase NPM-ALK
Expected completion date	Sep 2014
Estimated size(pages)	230
Total	**0.00 USD**

NATURE PUBLISHING GROUP LICENSE TERMS AND CONDITIONS

Sep 21, 2014

This is a License Agreement between Kathleen M Bone ("You") and Nature Publishing Group ("Nature Publishing Group") provided by Copyright Clearance Center ("CCC"). The license consists of your order details, the terms and conditions provided by Nature Publishing Group, and the payment terms and conditions.

All payments must be made in full to CCC. For payment instructions, please see information listed at the bottom of this form.

License Number	3405560196719
License date	Jun 10, 2014
Order Content Publisher	Nature Publishing Group
Order Content Publication	Cell Research
Order Content Title	Mechanisms and functions of DNA mismatch repair
Order Content Author	Guo-Min Li
Order Content Date	Dec 24, 2007
Volume number	18
Issue number	1
Type of Use	reuse in a dissertation / thesis
Requestor type	academic/educational
Format	print and electronic
Portion	figures/tables/illustrations
Number of figures/tables/illustrations	1
High-res required	no
Figures	Table 2
Author of this NPG article	no
Your reference number	None
Title of your thesis / dissertation	Deregulation of DNA mismatch repair by the oncogenic tyrosine kinase NPM-ALK
Expected completion date	Sep 2014
Estimated size (number of pages)	230
Total	**0.00 USD**

AMERICAN ASSOCIATION FOR CANCER RESEARCH LICENSE TERMS AND CONDITIONS

Sep 21, 2014

This is a License Agreement between Kathleen M Bone ("You") and American Association for Cancer Research ("American Association for Cancer Research") provided by Copyright Clearance Center ("CCC"). The license consists of your order details, the terms and conditions provided by American Association for Cancer Research, and the payment terms and conditions.

All payments must be made in full to CCC. For payment instructions, please see information listed at the bottom of this form.

License Number	3413770943540
License date	Jun 21, 2014
Order Content Publisher	American Association for Cancer Research
Order Content Publication	Molecular Cancer Therapeutics
Order Content Title	Targeting Oncogenic ALK: A Promising Strategy for Cancer Treatment
Order Content Author	Enrique Grande, María-Victoria Bolós, Edurne Arriola et al.
Order Content Date	April 1, 2011
Volume number	10
Issue number	4
Type of Use	Thesis/Dissertation
Requestor type	academic/educational
Format	print and electronic
Portion	figures/tables/illustrations
Number of figures/tables/illustrations	1
Will you be translating?	no
Circulation	8
Territory of distribution	Worldwide
Title of your thesis / dissertation	Deregulation of DNA mismatch repair by the oncogenic tyrosine kinase NPM-ALK
Expected completion date	Sep 2014
Estimated size (number of pages)	230
Total	**0.00 USD**
Terms and Conditions	

ELSEVIER LICENSE
TERMS AND CONDITIONS

Sep 21, 2014

This is a License Agreement between Kathleen M Bone ("You") and Elsevier ("Elsevier") provided by Copyright Clearance Center ("CCC"). The license consists of your order details, the terms and conditions provided by Elsevier, and the payment terms and conditions.

All payments must be made in full to CCC. For payment instructions, please see information listed at the bottom of this form.

Supplier	Elsevier Limited The Boulevard,Langford Lane Kidlington,Oxford,OX5 1GB,UK
Registered Company Number	1982084
Customer name	Kathleen M Bone
Customer address	University of Alberta Edmonton, AB T6G2E1
License number	3473721055790
License date	Sep 21, 2014
Licensed content publisher	Elsevier
Licensed content publication	The American Journal of Pathology
Licensed content title	Fusion Tyrosine Kinase NPM-ALK Deregulates MSH2 and Suppresses DNA Mismatch Repair Function Novel Insights into a Potent Oncoprotein
Licensed content author	Leah C. Young,Kathleen M. Bone,Peng Wang,Fang Wu,Benjamin A. Adam,Samar Hegazy,Pascal Gelebart,Jelena Holovati,Liang Li,Susan E. Andrew,Raymond Lai
Licensed content date	July 2011
Licensed content volume number	179
Licensed content issue number	1
Number of pages	11
Start Page	411
End Page	421
Type of Use	reuse in a thesis/dissertation
Intended publisher of new work	other
Portion	full article
Format	both print and electronic
Are you the author of this Elsevier article?	Yes
Will you be translating?	No

Title of your thesis/dissertation	Deregulation of DNA mismatch repair by the oncogenic tyrosine kinase NPM-ALK
Expected completion date	Sep 2014
Estimated size (number of pages)	
Elsevier VAT number	GB 494 6272 12
Price	0.00 USD
VAT/Local Sales Tax	0.00 USD / 0.00 GBP
Total	**0.00 USD**

List of Tables

List of Figures

CHAPTER 1

Introduction

1. Introduction

1.1 Anaplastic large cell lymphoma – an overview

Anaplastic large cell lymphoma (ALCL) is a rare type of peripheral T-cell non-Hodgkin lymphoma (NHL) that presents clinically as two distinct diseases: a widespread, systemic disease, and a localized, cutaneous disease.[1,2] Systemic ALCL comprises 2-8% of all NHL in adults, and 10-15% in children.[2,3] It was first described by Stein et al. in 1985 as a neoplastic proliferation of cells with the consistent expression of CD30 (Ki-1 antigen) on the cell surface, and the presence of large polymorphic or giant "anaplastic" cells within the cancerous population (**Figure 1.1A** and **1.1B**).[4,5] "Horseshoe"-like or "wreath" cells are hallmark markers of ALCL (arrows), as well as a CD30 membranous and Golgi region staining (**Figure 1.1C** and **1.1D**).[1,2,5] The disease was classified as lymphocytic in origin due to the presence of lymphoid markers, specifically those of T-cell origin, and the absence of markers from cells of other histological origins[1]; the diagnosis of ALCL was thus restricted to CD30 positive lymphoma with a T or null cell phenotype.[6,7] Due to the unusual cytological composition of ALCL, and because CD30 expression is common among many cancers of hematological origin, ALCL was often misdiagnosed as malignant histiocytosis or anaplastic carcinoma.[3,4]

A breakthrough in the understanding of ALCL biology and diagnosis came in the late 1980s with the discovery of a recurrent, reciprocal chromosomal translocation in CD30 positive ALCL involving chromosome 2 and chromosome 5, specifically t(2;5)(p23;q35), between 2 unknown genes.[8-13]

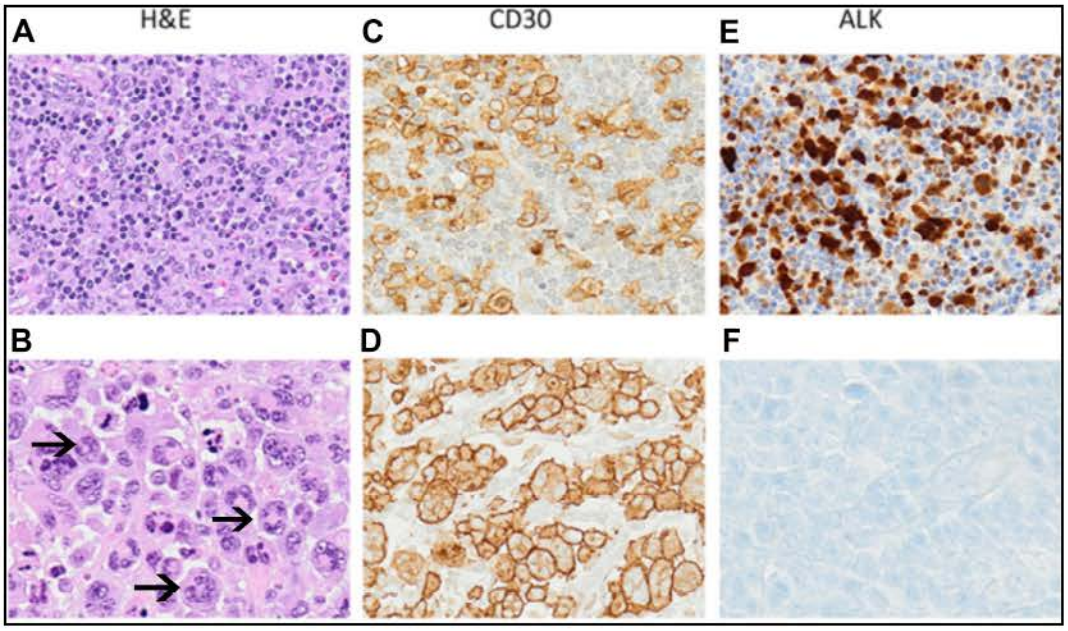

Figure 1.1. Histological features of anaplastic large cell lymphoma (ALCL). (A) Hematoxylin and eosin (H&E) staining of ALCL patient sample. (B) H&E staining of an ALCL tumor showing hallmark cells (arrows), with large "wreath" or "horseshoe" shaped nuclei and abundant cytoplasm. (C) and (D) CD30 immunoreactivity on ALCL neoplastic cells. All ALCL cells show strong membrane and perinuclear CD30 staining. (E) ALK immunoreactivity in ALK+ALCL, with strong cytoplasmic and nuclear staining associated with the NPM-ALK translocation, t(2;5)(p23;q35). (F) ALK immunoreactivity in ALK−ALCL, showing negative ALK staining due to the absence of an *ALK* translocation.

Modified from [ALK signaling and target therapy in anaplastic large cell lymphoma. Tabbo F, Barreca A, Piva R, Inghirami G and the European T Cell Lymphoma Study Group. Frontiers in Oncology. 2(41). Copyright © 2012 Tabbo F, Barreca A, Piva R, Inghirami G and the European T Cell Lymphoma Study Group.] with permission. Frontiers in Oncology is an open-access journal, which permits non-commercial use, distribution, and reproduction in other forums, provided the original authors and source are credited.

1.2 Anaplastic lymphoma kinase positive anaplastic large cell lymphoma

In 1994, the successful cloning of the genes at the chromosome breakpoint was reported by two independent research teams; the reciprocal t(2;5) translocation caused the *nucleophosmin* (*NPM*) gene, located at 5q35, to be fused with the gene *anaplastic lymphoma kinase* (*ALK*) at 2p23.[14,15] ALCL tumors with the t(2;5) translocation became a distinct clinical entity known as ALK positive (ALK+) ALCL.[16,17] In ALK+ALCL, translocations between the *ALK* gene locus and genes other than *NPM* are also possible (described below); *ALK* translocations occur in 40-60% of ALCL patients, and 80% of these carry the specific t(2;5)(p23;q35) translocation (**Figure 1.1 E)**.[2,5,18] ALCL tumors without ALK translocations are known as ALK-negative (ALK−) ALCL (**Figure 1.1F**).[5,16,19]

1.2.1 ALK

The *ALK* gene encodes a classical receptor tyrosine kinase (RTK) harboring an extracellular domain for ligand binding, a transmembrane domain, and a cytoplasmic tyrosine kinase domain.[20] It is part of a subfamily of the insulin receptor family of RTKs that also includes the leukocyte tyrosine kinase (LTK).[20,21] The activating ligand(s) of ALK in mammalian cells are controversial, and ALK was initially described as an orphan receptor with no known activating ligand for many years.[22,23] Recently, the small heparin-binding growth factors midkine (MK) and pleiotrophin (PTN) have been proposed as mammalian ALK activating ligands.[24-26]

The expression of *ALK* mRNA and ALK protein is typically limited to cells and stem cells of neural origin[20]; ALK expression is relatively high during

development, diminishing shortly after birth.[21] It is thus thought that ALK may play key roles in controlling neuronal development, although the exact physiological role of ALK in mammals is unclear. *ALK*-/- mice are fertile and viable, with only reported behavioral issues[27-29]; the behavioral phenotype does suggest a role for ALK in the mammalian brain. Aberrant ALK expression is linked to the pathogenesis of certain tumor types: full length ALK expression has been detected in tumors of neural origin, including neuroblastoma and glioblastoma, substantiating its role in neuronal cells.[20,30,31]

1.2.2 ALK translocations

The *ALK* gene locus is located in a genetic translocation hotspot, and thus far, 22 translocations involving the *ALK* gene and various fusion partners have been identified in various cancer types (**Table 1.1**).[20] In ALK+ALCL, 9 clinically significant chromosomal translocations have been identified. The known *ALK* translocations described lead to the production of ALK fusion proteins that dimerize to constitutively activate the ALK tyrosine kinase.[1,2,32] All chimera proteins occur following genomic breakpoints between exon 19 and 20 of the *ALK* gene, fusing the distal portion of ALK to the promoter region and proximal gene portion of the fusion gene[3,33]; the proximal region of the fusion protein acts as a dimerization domain, activating ALK in the absence of ligand binding (**Figure 1.2**, representative example).[5,32]

The cause of frequent and non-random chromosomal translocations in cancer is unclear, but translocations are common in hematological malignancies and are typically the primary causative factor for disease progression. Chromosomal translocations in solid tumors are often random, and occur as a consequence of tumor progression; they rarely lead to the production of oncogenic fusion protein "cancer drivers".[34] For

Table 1.1. Clinically relevant ALK fusion proteins.[20]

Chromosomal Translocation	Partner Protein	Localization	Tumor Type	Frequency % (Ref.)
t(2;5)(p23;q35)	NPM	Cytoplasm, nucleus and nucleolus	ALCL DLBCL	80 (Amin and Lai[2]) <1 (Adam et al.[35])
t(2;17)(p23;q25)	ALO17	Cytoplasm	ALCL	<1 (Cools et a.l[36])
t(2;3)(p23;q21)	TFG	Cytoplasm	ALCL NSCLC	2 (Hernandez et al.[37], Hernandez et al.[38]) <1 (Rikova et al.[39])
t(2;X)(p23;q11-12)	MSN	Cell-membrane	ALCL	<1 (Tort et al.[40])
t(1;2)(q25;p23)	TPM3	Cytoplasm	ALCL RMC/RCC IMT	12-18 (Lamant et al.[41]) <1 (Sugawara et al.[42], Sukov et al.[43]) <1 (Lawrence et al.[44])
t(2;19)(p23;p13)	TPM4	Cytoplasm	ALCL ESCC IMT	<1 (Meech at el.[45]) <1 (Du et al.[46], Jazii et al.[47]) <1 (Lawrence et al.[44])
inv(2)(p23;q35)	ATIC	Cytoplasm	ALCL IMT	2 (Colleoni et al.[48]) <1 (Debiec-Rychter et al.[49])
t(2;22)(p23;q11.2)	MYH9	Cytoplasm	ALCL	<1 (Lamant et al.[50])
t(2;17)(p23;q23)	CLTC	Granular cytoplasm	ALCL IMT DLBCL	<1(Touriol et al.[51]) <1 (Patel et al.[52], Bridge et al.[53]) <1 (Gascoyne at al.[54])
t(2;4)(p23;q21) t(2;4)(p2?4;q21)	SEC31A	Cytoplasm	IMT DLBCL	<1 (Panagopoulus et al.[55]) <1 (Van Roosbroeck et al.[56], Bedwell et al.[57])
t(2;2)(p23;q13) or inv(2)(p23;q11-13)	RANBP2	Nuclear periphery	IMT	<1 (Patel et al.[52])

t(2;12)(p23;p11)	PPFIBP1	N/A	IMT	<1(Takeuchi et al.[58])
t(2;11;2)(p23;p15;q31)	CARS	N/A	IMT	<1 (Cools et al.[36], Debelenko et al.[59])
inv(2)(p21;p23)	EML4	Cytoplasm	NSCLC Breast Colon RMC/RCC	2-7 (Lin et al.[60]) ~2 (Lin et al.[60]) ~2 (Lin et al.[60]) <1 Sugawara et al.[42])
t(2;10)(p23;p11)	KIF5B	Cytoplasm	NSCLC	<1 (Takeuchi et al.[61])
N/A	KLC1	N/A	NSCLC	<1 (Togashi et al.[62])
N/A	PTPN3	N/A	NSCLC	NR (Jung et al.[63])
N/A	STRN	Cytoplasm	NSCLC Thyroid	<1 (Majewski et al.[64]) <1
t(2;5)(p23;q35)	SQSTM1	Cytoplasm (nuclear?)	DLBCL	<1 (Takeuchi et al.[65])
t(2;10)(p23;q22)	VCL	Cytoplasm	RMC/RCC	<1(Debelenko et al.[66])
)N/A	C2orf44	N/A	CRC	<1 (Lipson et al.[67])
N/A	FN1	Cytoplasm	SOC	<1 (Ren et al.[68])

Abbreviations: ALK – anaplastic lymphoma kinase; NPM – nucleophosmin; ALCL – anaplastic large cell lymphoma; DLBCL – diffuse large B-cell lymphoma; ALO17 – ALK lymphoma oligomerization partner on chromosome 17; TFG – TRK-fused gene; NSCLC – non-small cell lung cancer; NR – not-reported; MSN – moesin; TPM – tropomyosin; RMC – renal medulla carcinoma; RCC – renal cell carcinoma; IMT – inflammatory myofibroblastic tumor; ATIC – 5-aminoimidazole-4-carboxamide ribonucleotide formyltransferase/IMP cyclohydrolase; MYH9 – myosin heavy chain 9; CLTC – clathrin heavy chain; RANBP2 – RAN-binding protein 2; PPFIBP1 – Protein tyrosine phosphatase receptor type F polypeptide-interacting protein-binding protein; N/A – not available; CARS – cysteinyl-tRNA synthetase; EML4 – echinoderm microtubule associated protein like 4; KIF5B – kinesin family member 5B; KLC1 – kinesin light chain 1; PTPN3 – protein tyrosine phosphatase, non-receptor type 3;

STRN – striatin; SQSTM1 – sequestosome 1; VCL – vinculin; C2orf44 – chromosome 2 open-reading-frame 44; CRC – colorectal carcinoma; SOC – serous ovarian carcinoma; FN1 – fibronectin 1.

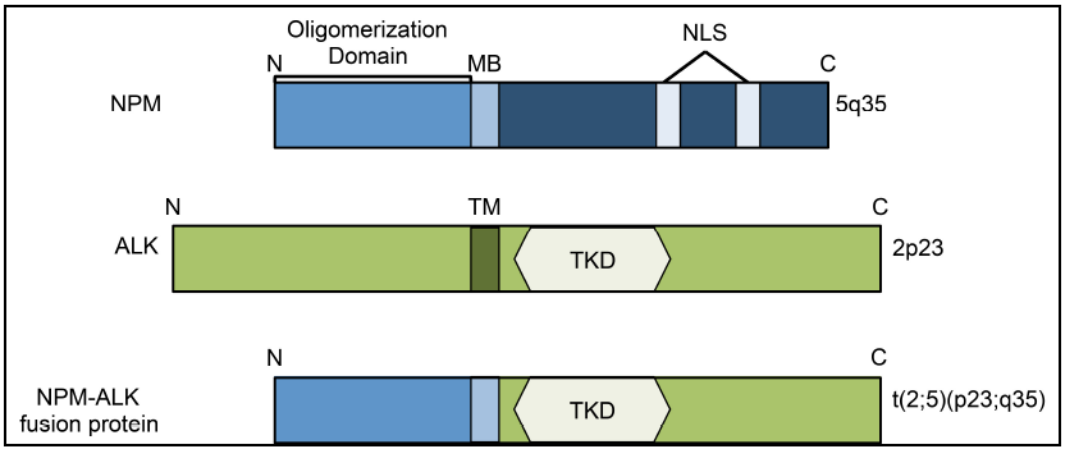

Figure 1.2. Structure of the nucleophosmin (NPM), anaplastic lymphoma kinase (ALK) and NPM-ALK fusion proteins. The NPM protein carries an oligomerization domain, a metal binding domain (MB), and 2 nuclear localization signals (NLS) flanked by acidic amino acid clusters (not shown) that act as nucleolar targeting signals. The ALK protein is a transmembrane tyrosine kinase receptor, with an N-terminal extracellular domain, a transmembrane (TM) domain, and an intercellular tyrosine kinase domain (TKD). The translocation between the *NPM* and *ALK* genes, occurring in approximately 80% of all ALK+ALCL cases, causes the N-terminal oligomerization and metal binding domains of NPM to become fused upstream of the ALK tyrosine kinase domain, producing the NPM-ALK fusion oncogenic tyrosine kinase. Abbreviations: NPM – nucleophosmin; ALK – anaplastic lymphoma kinase; N – amino terminus; C – carboxy terminus.

the translocation to happen, double stranded breaks in the DNA need to occur, and the two broken DNA ends have to be close together in the nucleus to facilitate the translocation.[69] Errors in the process of double stranded DNA break repair, including homologous recombination (HR), and non-homologous end joining (NHEJ), as well as the processes of class-switch recombination, and V(D)J recombination, contribute to chromosomal translocation.[34,70] Recombination "hot-spots" in the genome at sites, which are prone to double-stranded DNA breaks, including purine/pyrimidine repeat regions, scaffold/matrix hot-spots, and topoisomerase II cleavage sites, can also lead to chromosomal translocation.[34]

Two hypotheses have been proposed to explain how chromosomal translocations occur; in the first model, known as the "contact first" model, the chromosomes must first co-localize in the nuclear environment prior to the DNA damage.[71] The second hypothesis, called the "breakage first" model, postulates that after two independent double stranded DNA breaks occur, the "free" chromosome ends move in the nucleus to find their translocation partner.[72] Recent studies have shown that the "contact first" model is more likely to occur in cancer[34,71,73,74]; in one such study by Roix et al., the *MYC*, *BCL2* (B-cell lymphoma 2), and immunoglobulin gene loci, which are frequently involved in chromosomal translocations in B-cell lymphoma, preferentially co-localized in a non-random distribution in the center of the nucleus prior to any detectable translocation.[75] These results suggest that there may be a cell-type specific organization of the genome that favors translocation in hematological malignancies.

1.2.2.1 NPM-ALK

The predominant *ALK* translocation, t(2;5)(p23;q35) occurring in about 80% of ALK+ALCL, encodes a gene fusion tyrosine kinase protein known

as NPM-ALK.[2] NPM is a ubiquitously expressed phosphoprotein that shuttles newly synthesized proteins from the cytoplasm to the nucleolus via an amino- (N) terminal oligomerization domain, and two carboxy- (C) terminal nuclear localization signals.[76,77] The t(2;5) translocation fuses the N-terminal portion containing the oligomerization domain of NPM (amino acids 1-117) to the entire cytoplasmic portion of the ALK tyrosine kinase (**Figure 1.2**).[1,78] As a consequence of this translocation, the ubiquitous *NPM* promoter controls the expression of the *ALK* gene, changing the temporal expression of the ALK tyrosine kinase in cells of neural origin to a continual expression in cells of multiple lineages.[1,2] The NPM-ALK protein forms homodimers with other NPM-ALK proteins via the NPM oligomerization domain, and heterodimers with other wild-type NPM proteins, changing the membrane-associated expression of ALK to its expression in both the cytoplasm and the nucleus.[20] The formation of NPM-ALK homodimers leads to the constitutive activation of the ALK tyrosine kinase in the absence of ligand, making it a potent tyrosine kinase with high transformative ability.[1]

In an effort to understand the molecular mechanisms underlying the t(2;5)(p23;q35) chromosomal translocation in ALK+ALCL, Mathas et al. analyzed genes flanking the chromosomal breakpoints in four T-cell derived cell lines with the t(2;5) translocation, and four without, and, focusing on genes with known oncogenic properties, looked for a pattern of changes in protein and mRNA expression in the 8 cell lines.[69] In all cell lines, regardless of the translocation status, up-regulation of the oncogenic transcription factors Fos-related antigen 2 (FRA2) and inhibitor of DNA binding 2, dominant-negative helix-loop-helix (ID2), as well as the differentiation/metastasis promoting colony stimulating factor 1 receptor (CSF1-R) was detected. This manuscript also reported that, in cells without the t(2;5) translocation, the 2p23 and 5q35 loci were in close proximity in ALCL, and the specific t(2;5)(p23;q35) translocation could be

induced after the introduction of double stranded DNA breaks by ionizing radiation (IR). This study suggests that, in close proximity to specific chromosomal breakpoints, a non-random, patterned and predictable deregulation of oncogenic genes may favor translocation in ALK+ALCL.

1.2.3 Clinical features

Systemic ALK+ALCL (the major tumor type associated with ALK+ALCL) is an aggressive lymphoma that occurs in the first 3 decades of life with a high male predominance.[1,2,18,79-82] It typically presents at a later clinical stage (stage III to stage IV), with systemic symptoms such as high fever, and frequent extranodal involvement, including skin (26%), bone (14%), soft tissues (15%), lung (11%) and liver (8%).[1,81] Several cases with leukemic presentation have been reported; bone marrow involvement varies from 30-60%, and is typically higher in ALK+ALCL than in ALCL without the ALK translocation.[83-86]

1.2.4 Morphology

ALK+ALCL presents in a large morphological spectrum. All cases, however, do contain a varying portion of “hallmark cells” with large horseshoe, kidney shaped nuclei (**Figure 1.1A** and **Figure 1.1B**).[1,2,5] Five morphological types of ALCL are currently recognized by the WHO[16]: the common variant (70%); the lymphohistiocytic variant (10%)[87,88]; the small cell variant (10%)[89]; Hodgkin-like (1-3%)[90]; and ALCL with a composite pattern, with features of more than one variant. Other morphological types are seen, although they are not recognized by the current WHO ALCL diagnostic criteria.

1.2.5 Immunophenotype

As previously mentioned, nearly all ALCL cases show CD30 positivity on the cell membrane and in the Golgi region (Figure **1.1C** and **1.1D**).[1,5] CD30 is a member of the tumor necrosis factor receptor (TNFR) family, and its expression is typically restricted to activated lymphoid cells.[91] The majority of ALCL tumors express epithelial membrane antigen (EMA), also known as mucin 1 (MUC1), a high molecular weight glycoprotein normally expressed on the luminal surface of glandular epithelia.[92,93] ALCL tumors also typically express one or more T-cell and natural killer (NK) antigens; however, loss of the T-cell phenotype has led to some ALCL being diagnosed as "null" cell.[1,79,94] The null cell phenotype of ALCL is associated with the loss of both T-cell and B-cell marker expression. Loss of CD3, a common pan T-cell marker, is seen in approximately 75% of ALCL cases.[79] The T-cell markers CD5, and CD7 are often undetectable, while CD2, and CD4 positive staining is common and can be used for diagnosis. Expression of the T-cell marker CD8 is variable. Further, most ALCL cases express the cytotoxic cell antigens TIA-1 (T-cell-restricted intracellular antigen 1), granzyme B and perforin.[95,96] Regardless of T-cell antigen expression, approximately 90% of all ALK+ALCL cases exhibit clonal rearrangement of the T-cell receptor (TCR) genes, which is indicative of reactive and/or lymphoid tissue.[1,95] In the diagnosis of ALK+ALCL, ALK nuclear and/or cytoplasmic staining is of the highest value.

1.2.6 Conventional treatment and prognosis

ALK+ALCL has a good prognosis and responds well to chemotherapy, with a 5-year overall survival rate of 71%±6% versus 15%±11% (~40% in another study[97]) for ALK−ALCL.[81]

There is no defined treatment protocol for ALCL, and a doxorubicin-containing polychemotherapy, namely CHOP (cyclophosphamide, an alkylating agent that halts replication by crosslinking the DNA; hydroxydaunorubicin/doxorubicin, which intercalates in the DNA, inhibiting its unwinding by topoisomerase II during replication; oncovin/vincristine, a tubulin binding drug that inhibits mitosis; and prednisone, an immunosuppressant) is often the first-line of treatment.[98] The CHOP regimen is associated with an overall ~90% response rate in ALK+ALCL patients, especially in those in the pediatric population.[98,99] Patients with relapsed or refractory ALK+ALCL that did not respond well to the initial treatment protocol are typically treated with high-dose chemotherapy with autologous stem cell transplantation (HDC-ASCT).[98] Patients who are resistant to primary chemotherapy and who relapse within the first 12 months of diagnosis have a worse prognosis than those who relapse late (3-year overall survival 28% versus 68%, respectively), and pediatric patients benefit more from HDC-ASCT and allogeneic transplant than older ALK+ALCL patients.[98,100] As ALK+ALCL is relatively rare with a high chemotherapeutic response, this represents a logistical challenge for drug development. Novel therapeutic approaches based on targeted therapy are available, developed from understanding the ALK molecular signaling network important in ALK+ALCL pathogenesis.

1.2.7 Pathogenesis

ALK+ALCL depends highly on the growth promoting signals and transformative capabilities of the ALK tyrosine kinase in the chimeric proteins, and has thus been suggested to be "ALK-addicted."[82] The transformative capabilities of NPM-ALK and other ALK chimeric proteins have been demonstrated extensively both *in vitro* and *in vivo*.[30,101-103] In a recent study, the *in vitro* transformative ability of NPM-ALK was demonstrated with human CD4 positive T lymphocytes, which, following

transduction with lentiviral NPM-ALK, displayed a morphology and immunophenotype similar to patient-derived ALCL cells.[104] Implantation of these cells into mice led to tumor development indistinguishable from human ALK+ALCL tumors, underlying the oncogenic potential of NPM-ALK.

Various *in vivo* studies have demonstrated that NPM-ALK transgenic mice developed hematopoietic lymphoid tumors with short latency and high penetrance; however, in most cases, tumors were of B-cell origin, and were not the characteristic T/null cell ALCL lymphoma seen in humans, even when NPM-ALK expression was driven by a T-cell specific promoter (**Table 1.2**).[105-110] ALK translocations in transgenic mouse models may act as a molecular switch to drive transformation and oncogenic growth; however, since the various NPM-ALK transgenic mice do not develop classical ALCL, it's reasonable to postulate that ALK needs the cooperation of a number of other factors, some with oncogenic properties on their own, to drive ALK+ALCL pathogenesis. NPM-ALK and other ALK chimeric proteins interact with and activate adapter proteins that are involved in a number of downstream signaling pathways critical in the pathogenesis of ALK+ALCL, including the Janus kinase (JAK)/signal transducer and activator of transcription (STAT), Ras/extracellular signal-related kinase (ERK), phospholipase C gamma (PLC-γ), and the phosphatidylinositide 3-kinase (P13K)/AKT signaling pathways (**Figure 1.3**).[2,5,32,111-113]

1.2.7.1 The JAK/STAT pathway

One of the most well studied pathways deregulated by the NPM-ALK tyrosine kinase is the JAK/STAT pathway, and more specifically STAT3 (**Figure 1.4**). NPM-ALK binds to and promotes the activation of STAT3 via its tyrosine phosphorylation at tyrosine (Y) 705.[114,115] STAT3 is a member

Table 1.2. NPM-ALK transgenic mouse models.

Promoter	NPM-ALK expression	Tumor type	Latency (Penetrance)	Molecular	Ref. Year
CD4 – T-cell	T-cells Tumor	-Thymic lymphoblastic lymphoma -Plasma (B-cell) with bone marrow involvement	5-7 weeks (100%)	Constitutive phospho-STAT3, JAK3	Chiarle et al.[105] 2003
Vav – hem. lineage (early)	Tumor	Diffuse large B cell lymphoma (DLBCL), negative for T-cell markers	91-225 days (100%)	Hyperactive SAPK/JNK ERK/MAPK	Turner et al.[106] 2003
N/A – IL9 transgenic mice, bone marrow transplant (NPM-ALK)	Hem. and lymphoid cells	-Lympho-blastic lymphoma (T-cell) -Mature and immature plasmacytoma -Anaplastic DLBCL	13-30 weeks (100%)	N/A	Lange et al.[107] 2003
Lck – T-cell	Spleen Tumor	-Lymphoma – T-cell immature lymphoblastic lymphomas, extranodal involvement	8-15 weeks (100%)	N/A	Jager et al.[108] 2005
CD2 – T-cell	Tumor	-B cell lymphoma (some T-cell rich) -DLBCL	9-20 months (50%)	N/A	Turner et al.[109] 2006
EμSRα tTa - B and T-cells Tet-off NPM-ALK, TPM3-ALK mice	-early expression embryonic lethal -Tumors	-Leukemia and lymphoma (B-cell) with no T-cell involvement -Cutaneous disease (due to early ALK fusion protein expression)	4 weeks (100%)	Inactivation of ALK (via Dox treatment as cells are Tet-off, and ALK inhibitor) led to tumor regression	Giuriato et al.[110] 2010

Abbreviations – NPM – nucleophosmin; ALK – anaplastic lymphoma kinase; Ref – reference; STAT3 – signal transducer and activator of transcription 3; JAK3 – Janus kinase 3; SAPK – stress activated protein kinase; JNK – Jun-amino terminal kinase; ERK – extracellular signal-related kinase; MAPK – mitogen-activated protein kinase; IL9 – interleukin 9; Hem – hematopoietic; N/A – not available; Lck – lymphocyte protein tyrosine kinase; tTa – Tetracycline-transactivator; TPM3 – tropomyosin 3; Dox – doxycycline.

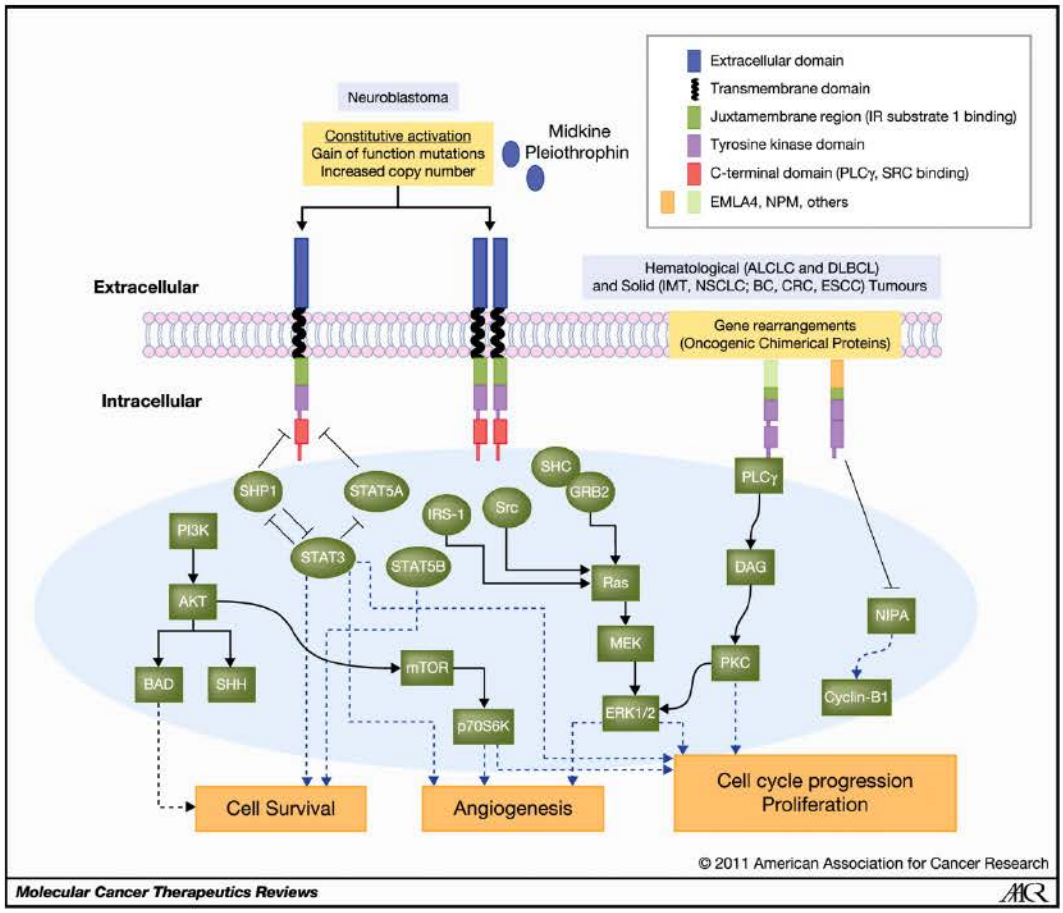

Figure 1.3. Oncogenic NPM-ALK signaling pathway. A schematic of ALK RTK. The mechanisms associated with deregulation are in solid lines. Hematologic tumors are shown in the figure's upper part. The hypothetical downstream signaling pathways and cellular responses subsequent to ALK constitutive activation in tumors are shown in the figure's lower part. Abbreviations: PLC-γ – phospholipase C gamma; ALCLC – anaplastic large cell lymphoma, conventional; DLBCL – diffuse large B cell lymphoma; IMT – inflammatory myofibroblastic tumor; NSCLC – non-small cell lung cancer; BC – breast cancer; CRC – colorectal cancer; ESCC – esophageal squamous cell carcinoma; SHP1 – Src homology region 2 domain-containing phosphatase-1; STAT – signal transducer and activator of transcription; SHC – Src homology region 2 domain-containing; GRB2 – growth factor receptor-bound protein 2; IRS-1 – insulin receptor substrate

1; PI3K – phosphatidylinositide 3-kinase; DAG – diacylglycerol; NIPA – nuclear interaction partner of ALK; MEK – mitogen-activated protein kinase kinase; BAD – Bcl2-associated death receptor; SHH – sonic hedgehog; mTOR – mammalian target of rapamycin; PKC – protein kinase C; ERK – extracellular signal-related kinase.

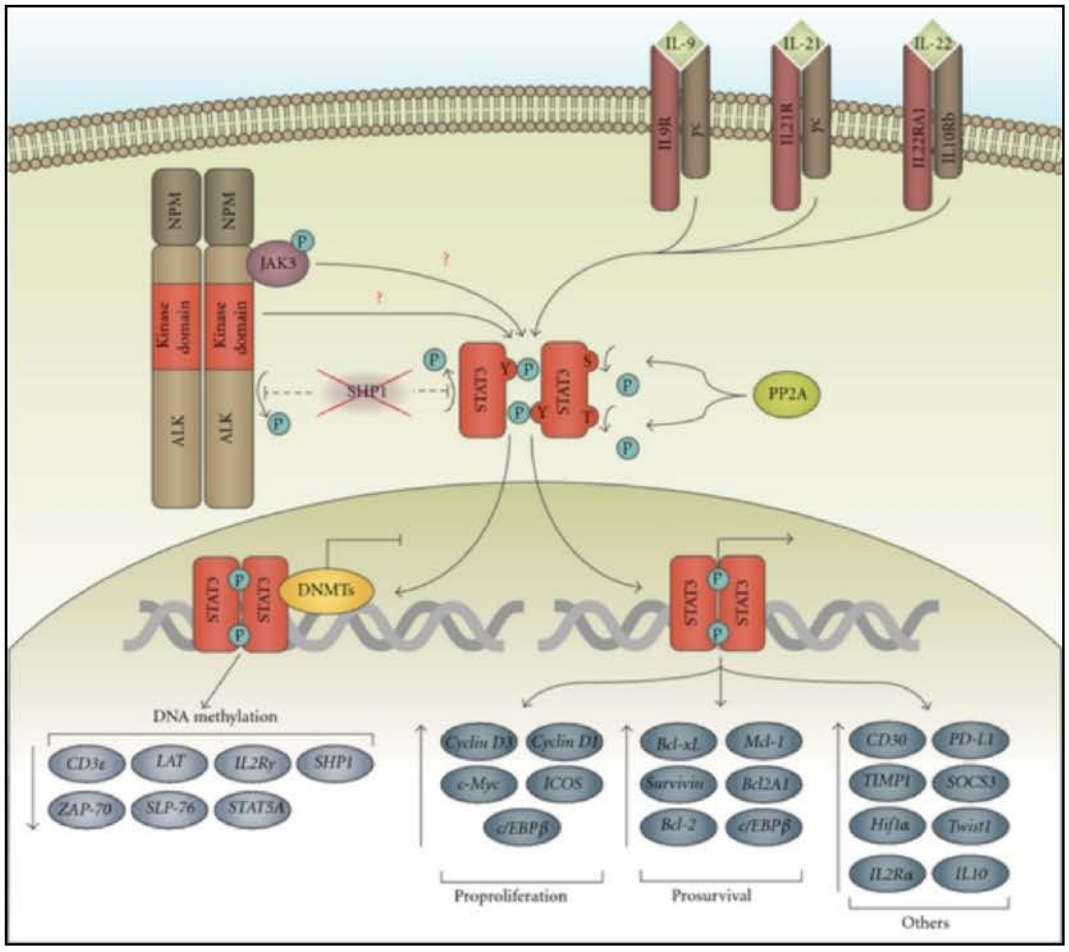

Figure 1.4. The STAT3 signaling pathway in ALK+ALCL. STAT3 is activated by NPM-ALK signaling. The phosphatase, protein phosphatase (PP)2A, and signaling through the IL-9, IL-21, and IL-22 receptors also promote STAT3 activation. STAT3 promotes the expression of genes that suppress apoptosis and enhance proliferation. STAT3 can also repress a variety of genes in this malignancy through DNA methylation. Suppression of the SHP1 phosphatase by STAT3 is particularly important in ALK+ALCL, as SHP1 inhibits NPM-ALK and STAT3 activity.

the original authors and source are credited.

of the STAT family of transcription factors that dimerize as homo and heterodimers, and translocate to the nucleus to activate the transcription of genes involved in cellular survival, proliferation, and immune responses.[116-118] The STAT signaling pathway is activated via interferon, cellular cytokines and growth factors. Strong staining for phosphorylated STAT3 and its nuclear translocation is a marker for ALK+ALCL tumor samples and cell lines.[2,112,119] Importantly, activated STAT3 is highly oncogenic on its own, underlying its importance in the pathogenesis of ALK+ALCL.[120-122] Inhibition of STAT3 activation effectively induced cell-cycle arrest and apoptosis in ALK+ALCL cell lines; thus, STAT3 is required for NPM-ALK-induced transformation.[118,123] STAT3 mediates its oncogenesis in ALK+ALCL by regulating a number of genes via direct transcriptional regulation, but also by epigenetic mechanisms. In the ALK+ALCL cell line SUP-M2, it has been shown by microarray studies following STAT3 gene knockdown with short-interfering RNA (siRNA) that STAT3 regulates at least 1500 genes, 60% of which were repressed.[124] STAT3 has been shown to interact with DNA methyltransferases (DNMTs), leading to promoter hypermethylation to epigenetically silence a number of key genes that have been shown to decrease ALK+ALCL tumor cell growth and viability and directly inhibit NPM-ALK expression, including the protein tyrosine phosphatase SHP1 (Src homology region 2 domain-containing phosphatase-1)[125-127] and STAT5A (**Figure 1.3**).[111,128]

STAT3 activation in ALK+ALCL is also achieved through the constitutive activation of JAK3, a tyrosine kinase that signals via cytokine activation to regulate STAT3.[112,113,129,130] In ALK+ALCL, JAK3, STAT3 and NPM-ALK co-immunoprecipitate, implying direct regulation by NPM-ALK[114,115,131]; JAK3 knockdown results in significant tumor cell apoptosis[132], suggesting that JAK3 is important in the molecular pathogenesis of ALK+ALCL. Cytokine signaling through interleukin 9 (IL9), IL21 and IL22 have been shown to stimulate STAT3 activation in ALK+ALCL.[129,130,133] NPM-ALK

also induces the expression of interleukin receptor 22 (IL22R), which is used by IL22 for signaling.[133] This suggests that the cytokine activation in ALK+ALCL may be autocrine in nature: NPM-ALK is capable of further activating STAT3 in this manner.

1.2.7.2 The Ras/ERK pathway

Like the STAT3 pathway, signaling through the Ras/ERK pathway (ERK1 and ERK2) promotes survival, and proliferation; this pathway also contributes to cellular differentiation and migration/metastasis.[134] ERK1 and ERK2 are serine/threonine kinases that are activated via growth factors, as well as a defined kinase cascade (**Figure 1.5**).[113,135] The ERK pathway is activated in both ALK+ALCL patient samples and cell lines, contributing to growth and proliferation[136,137]; inhibition of ERK with the inhibitor U0126 reduces ALK+ALCL cell proliferation, leading to cell death via apoptosis.[137,138] NPM-ALK-mediated activation of activator protein-1 (AP-1) transcription factors, including JunB, via the ERK pathway influences the phenotypic characteristics of ALK+ALCL tumor cells.[136,137] JunB, a protein that is highly active in ALK+ALCL[139,140], promotes the expression of the tumor marker CD30.[136,141,142] The activation of CD30 expression in turn signals through the Ras/ERK/JunB axis to further promote the expression of CD30 on ALK+ALCL tumor cells.[136]

1.2.7.3 The PLC-γ pathway

PLC-γ is activated through interaction with cell surface RTKs, leading to the hydrolysis of phosphatidylinositol 4,5-bisphosphate (PIP2) to inositol-1,4,5-triphosphate (IP3) and diacylglycerol (DAG).[143] These two molecules act as secondary messengers in signal transduction; IP3 stimulates the endoplasmic reticulum to release calcium (Ca^{2+}) into the cytoplasm, while DAG binds to and activates the serine/threonine kinase, protein kinase C

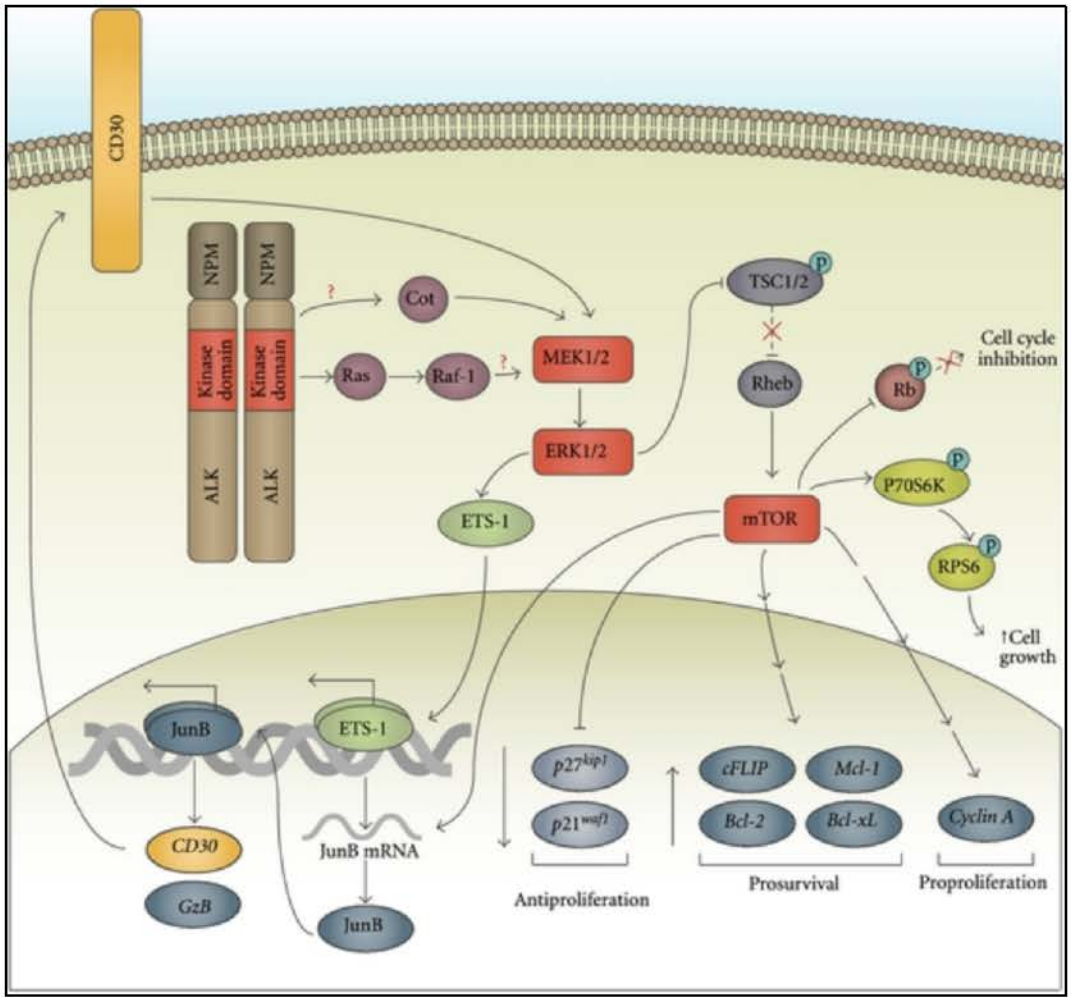

Figure 1.5. The MEK/ERK signaling pathway in ALK+ALCL. NPM-ALK activates Ras, Raf-1, MEK1/2, and ERK1/2. The ability of NPM-ALK to activate Mitogen-activated protein kinase (MAPK) 1/ERK kinase (MEK)/ERK appears not to be dependent on Raf-1. The activation of ERK1/2 promotes ALK+ALCL proliferation and survival, largely through the JunB transcription factor and serine/threonine kinase, mammalian target of rapamycin (mTOR). ERK1/2 activates the ETS-1 (V-Ets avian erythroblastosis virus E26 oncogene homolog 1) transcription factor, which promotes the transcription of JunB. JunB promotes the transcription of CD30 and Granzyme B in this lymphoma, but likely has other important targets that have not yet been identified. ERK1/2 are thought to activate mTOR signaling in ALK+ALCL by phosphorylating and inhibiting tuberous

sclerosis (TSC)1/2. mTOR phosphorylates and inhibits the cell cycle inhibitor, Rb (retinoblastoma protein). It also phosphorylates and activates p70S6K, which phosphorylates ribosomal protein s 6 (RPS6) to promote cell growth. mTOR also influences the expression of genes that contribute to the survival and proliferation of ALK+ ALCL cells. Signaling through CD30 in ALK+ALCL also activates MEK/ERK, and this leads to enhanced CD30 expression.

(PKC).[144] PKC acts to phosphorylate a number of proteins involved in cell cycle progression and cellular proliferation.[143]

Evidence linking the transforming ability of NPM-ALK to the PLC-γ pathway came from a study in 1998 by Bai and colleagues. They demonstrated a physical association between NPM-ALK and PLC-γ via Y664 of NPM-ALK.[103] Mutation of Y664 to phenylalanine, a residue structurally similar to tyrosine that can't be phosphorylated (i.e. NPM-ALK^{Y664F}), abrogated the ability of NPM-ALK to transform Ba/F3 (a murine interleukin-3 dependent pro-B-cell line) and rat fibroblast (Rat-1) cells.

1.2.7.4 The PI3K/AKT pathway

Activation of the PI3K/AKT pathway promotes cellular survival and proliferation in ALK+ALCL (**Figure 1.6**).[113] PI3K is made up of two subunits, a regulatory subunit, p85, and a catalytic subunit, p110. It phosphorylates inositol phospholipids on the 3′ position of the inositol ring, which activates proteins containing pleckstrin homology (PH) domains, such as AKT.[145] NPM-ALK interacts both directly and indirectly with PI3K, implicating the PI3K/AKT pathway in NPM-ALK-mediated oncogenic transformation.[32] The importance of PI3K/AKT in ALK+ALCL has been shown in a number of studies; the transformative ability of NPM-ALK in murine bone marrow and Ba/F3 cells was reversed with PI3K inhibitor treatment or in the presence of a dominant negative PI3K or AKT mutant.[146,147]

PI3K/AKT signaling activates many pathways, including the sonic hedgehog (SHH) pathway in ALK+ALCL (**Figure 1.6**).[113,148] The SHH pathway plays a key role in normal embryonic development; importantly, it has been implicated in the development and progression of a number of different cancer types.[149,150] SHH is a secreted protein that binds to its

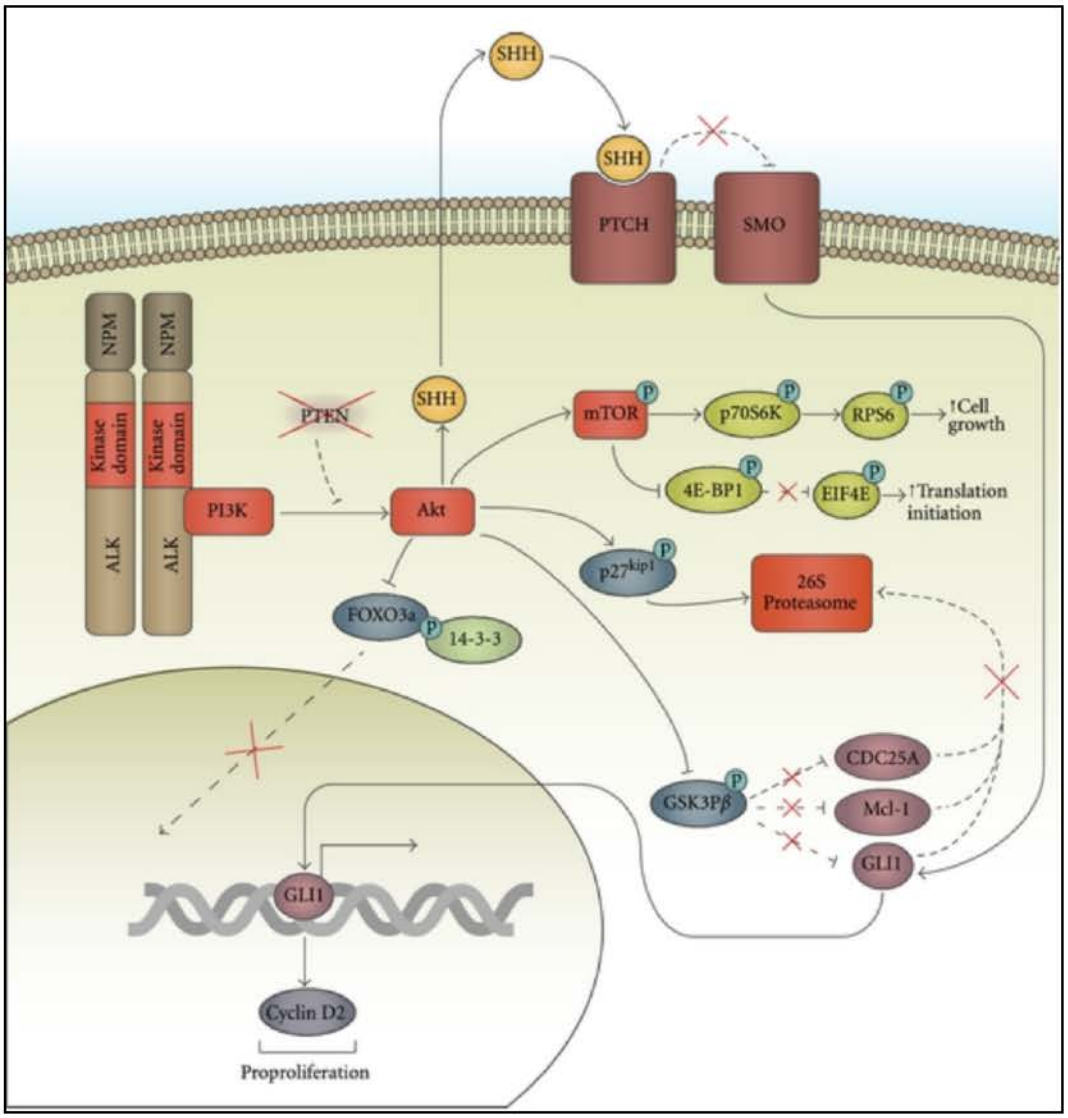

Figure 1.6. The PI3K/Akt signaling pathway in ALK+ALCL. NPM-ALK associates with and activates PI3K, which, in turn, activates the serine/threonine kinase AKT. Expression of the phosphatase and tensin homolog (PTEN) lipid phosphatase, which inhibits PI3K signaling, is lost in some ALK+ALCL tumor samples and likely contributes to AKT activation in cancers where PTEN is not expressed. AKT inhibits glycogen synthase kinase (GSK)3β activity in ALK+ALCL, which protects glioma-associated oncogene homolog 1 (GLI1), myeloid cell leukemia sequence 1 (Mcl-1), and cell division cycle 25 homolog A (CDC25A) from proteasomal

degradation. AKT also phosphorylates the cell-cycle inhibitor, p27, in ALK+ALCL and this results in the targeting of p27 for proteasomal degradation. Phosphorylation of the forkhead box O3 a (FOXO3a) transcription factor by AKT results in the binding of FOXO3a to 14-3-3 proteins. This sequesters FOXO3a in the cytoplasm, preventing it from translocating to the nucleus and transcribing pro-apoptotic and cell cycle inhibitory genes. In addition to being an important downstream target of MEK/ERK signaling in ALK+ALCL, mTOR activity may also be promoted by PI3K/Akt signaling. NPM-ALK/AKT signaling also promotes the expression of sonic hedgehog (SHH). When SHH binds its receptor, Patched (PTCH), this relieves the inhibition of the Smoothened (SMO) coreceptor by Patched. This allows Smo to activate the GLI1 transcription factor, which promotes the transcription of the pro-proliferation protein, Cyclin D2.

receptor patched (PTCH), which relieves its inhibition of smoothened (SMO).[151] SMO is then able to activate glioma-associated oncogene homolog 1 (GLI1) transcription factors; both SMO and GLI1 are activated in ALK+ALCL in a PI3K-dependent manner.[148] The SHH pathway promotes cell cycle progression in ALK+ALCL; inhibition of GLI1 by siRNA or treatment with pharmacological inhibitors reduced cell viability and promoted cell cycle arrest. The PI3K/AKT signaling pathway also contributes to ALK+ALCL neoplastic transformation via a number of other key signaling pathways outlined in **Figure 1.6**.

1.2.8 Targeting ALK in cancer therapy

As previously stated, ALK+ALCL patients respond well to conventional chemotherapy treatments, and have a good long-term prognosis; this has made it difficult to generate interest for the development of targeted therapies for ALK+ALCL. However, the landscape of targeted therapy, specifically against the ALK tyrosine kinase, changed in 2007 when the ALK translocation echinoderm microtubule-associated protein-like 4 (EML4)-ALK was first described in a set of non-small cell lung cancer (NSCLC) patients (**Table 1.1**).[39,152] This discovery, as well as the realization that full-length ALK contributes to some types of neuroblastoma, led to the development of a number of targeted ALK inhibitors in various development stages (**Table 1.3**).[5]

1.2.8.1 Crizotinib

Crizotinib (Xalkori, PF-02341066; Pfizer) is a small molecule oral, selective ATP-competitive inhibitor of ALK, c-MET/hepatocyte growth factor receptor, and ROS1 (c-ros oncogene 1) RTKs and their derivatives.[153] The efficacy of crizotinib was evaluated in a number of studies on patients with ALK+NSCLC, with some complete responses recorded, and an overall

Table 1.3. ALK inhibitors currently in development or in clinical use.

Drug	Company	Activity against L1196M ALK mutation	Other kinases inhibited	Status	Ongoing studies	Reference
Crizotinib	Pfizer	No	ROS1 c-MET	Approved	Phase III	Camidge et al.[154], Shaw et al.[155]
LDK378	Novartis	Yes	IGF-1R ROS1	Investigational (breakthrough therapy)	Phase I, Phase II, Phase III	Marsilje et al.[156], Shaw et al.[155]
CH5424802 RO5424802	Chugai/ Roche	Yes	ROS1	Investigational	Phase I/II	Sakamoto et al.[157], Kinoshita et al.[158], Seto et al.[159]
AP26113	Ariad	Yes	EGFR ROS1	Investigational	Phase I/II	Rossi et al.[160]
ASP3026	Astellas	Yes	ROS1	Investigational	Phase I	Mori et al.[161]
X-396	Xcovery	Yes	Yes	Investigational	Phase I	Solomon et al.[153]
TSR-011	Tesaro	Yes	Unknown	Investigational	Phase I	Solomon et al.[153]

Abbreviations: ALK – anaplastic lymphoma kinase; ROS1 – c-ros oncogene 1; EGFR – epidermal growth factor receptor; IGF-1R – insulin-like growth factor 1 receptor.

response rate of 50-61% depending on the patient population.[153,154,162] The average progression-free survival time was doubled in patients treated with crizotinib monotherapy versus conventional chemotherapy. In addition to ALK+NSCLC, treatment with crizotinib has achieved partial or complete responses in ALK+ inflammatory myofibroblastic tumor (IMT)[163], ALK+ diffuse large B-cell lymphoma (DLBCL)[164], ALK+ neuroblastoma[165], as well as ALK+ALCL.[164,165]

1.2.8.1.1 Resistance mechanisms

Acquired resistance to crizotinib treatment occurs in about a third of the patients with an initial positive response to therapy, leading to relapse.[154,166] The mechanisms underlying acquired resistance to ALK inhibition with crizotinib are shown in **Figure 1.7**.[153] Crizotinib binds the ALK fusion protein, inhibiting its ability to phosphorylate and activate downstream proteins (**Figure 1.7**, left panel). In the first instance, genetic alterations in the *ALK* tyrosine kinase gene disable this mechanism (**Figure 1.7**, middle panel). A variety of single amino acid substitutions in the *ALK* gene capable of conferring both *in vitro* and *in vivo* resistance have been detected in a number of relapsed patients who no longer respond to treatment, including L1156Y, G1269A, 1151Tins (threonine insertion), L1152R, G1202R, S1206Y, and L1196M.[167-172] The L1196M substitution is known as a "gate-keeper" mutation, which causes steric hindrance of drug binding, and is common among resistance seen with other RTK-targeted therapies.[153,171] Gene amplification at the *ALK* locus leading to an abundance of ALK fusion protein has also been detected in patients displaying ALK inhibitor resistance.[167,168]

In the second resistance pattern detected in relapsed patients, activation of alternative pathways for transformation occur, bypassing the ALK tyrosine kinase, and rendering ALK inhibition ineffective (**Figure 1.7**, right

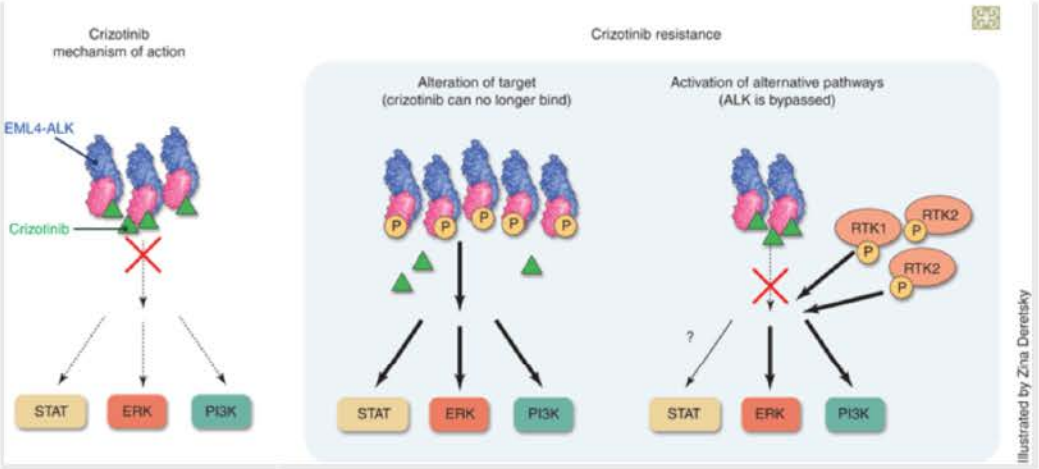

Figure 1.7 Mechanisms of crizotinib resistance. The left panel depicts crizotinib-sensitive cancer cells expressing EML4–ALK. Crizotinib binds and inactivates the ALK fusion, disrupting downstream signaling. The right panel depicts two general classes of crizotinib resistance: one mediated by genetic mutation of the target so that crizotinib can no longer bind to the active site, and the other mediated by activation of alternative pathways (or bypass tracks) that can engage downstream signaling pathways even when ALK is inhibited. Abbreviations: ALK – anaplastic lymphoma kinase; EML4 – echinoderm microtubule-associated protein-like 4; RTK – receptor tyrosine kinase; P – phosphorylation; STAT – signal transducer and activator of transcription; ERK – extracellular signal-related kinase.

panel).[153] Epidermal growth factor receptor (EGFR) upregulation has been detected in crizotinib-resistant cell lines *in vitro*; this upregulation has also been seen in relapsed patients.[167,169] Amplification of the *c-kit* (*v-kit Hardy-Zuckerman 4 feline sarcoma viral oncogene homolog)* gene also contributes to crizotinib-resistance detected in patients.[168,172] The c-KIT protein is an RTK that promotes signal transduction and proliferation of a variety of immature cell types during development.[173] Activating c-KIT mutations are associated with several human malignancies, including gastrointestinal stromal tumors, acute myeloid leukemia, mast cell leukemia, and melanoma.[174]

To bypass these resistance mechanisms, a number of second-generation ALK inhibitors are currently in varying stages of production (**Table 1.3**).[153] A number of them have shown clinical efficacy, as well as the ability to bypass known *ALK* mutations that render crizotinib ineffective. The better understanding of acquired resistance, as well as ALK downstream signaling molecules, could lead to the generation of new diagnostic and therapeutic targets in ALK-expressing cancers.

1.2.9 Identification of new NPM-ALK interacting partners

In an effort to fully understand the extent of how NPM-ALK potentiates its oncogenic potential through downstream signaling pathways, a number of laboratories have performed mass spectrometry studies to profile those proteins physically bound by NPM-ALK.[131,175,176] In one such study from the Lai Laboratory, NPM-ALK was found to be bound to 254 proteins by tandem-affinity purification mass spectrometry using the human embryonic kidney cell line, GP293, transiently transfected with a his-biotin (HB) tagged NPM-ALK plasmid.[175] A number of these proteins were previously reported NPM-ALK interactors, including PI3K, mammalian target of rapamycin (mTOR), JAK2, and AP-1; NPM-ALK was also found to bind to

previously unreported proteins involved in a number of cellular processes, such as apoptosis regulation, proteasomal degradation, biogenesis, cell cycle, and DNA repair. Among the DNA repair proteins, a novel NPM-ALK interactor was identified by mass spectrometry, and was confirmed by reciprocal co-immunoprecipitation: this protein, known as MutS homolog 2 (MSH2), is a critical component of the DNA mismatch repair process, and has been implicated in the development of a number of cancer types.

1.3 DNA mismatch repair

DNA mismatch repair (MMR) is a highly conserved DNA repair system that helps to maintain genomic stability by detecting and repairing post-replicative DNA errors.[177] Although the major DNA polymerase involved in DNA replication, DNA polymerase δ, has 3'>5' proofreading activity that detects and corrects 99% of DNA replication errors, insertions, deletions, and mispaired nucleotides are occasionally left behind.[177] The majority of these errors occur at highly repetitive genomic sequences known as microsatellites, which consist of a repeated tract of 2-5 DNA base pairs.[178] DNA replication errors are common on microsatellite sequences as the DNA polymerase often slips, or "stutters" while traversing repetitive sequences, creating mismatches and insertion-deletion-loops (IDLs).[178,179] When not corrected by the MMR system, IDLs lead to expansion and contraction of microsatellite sequences, a phenomenon known as microsatellite instability (MSI). MSI is a hallmark of MMR deficiency and is associated with a number of hereditary and sporadic human cancers.[180]

1.3.1 Mismatch repair processing

The human MMR system function can be divided into 4 stages: i) mismatch recognition; ii) repair enzyme recruitment; iii) excision; and iv) resynthesis (**Figure 1.8**).[177]

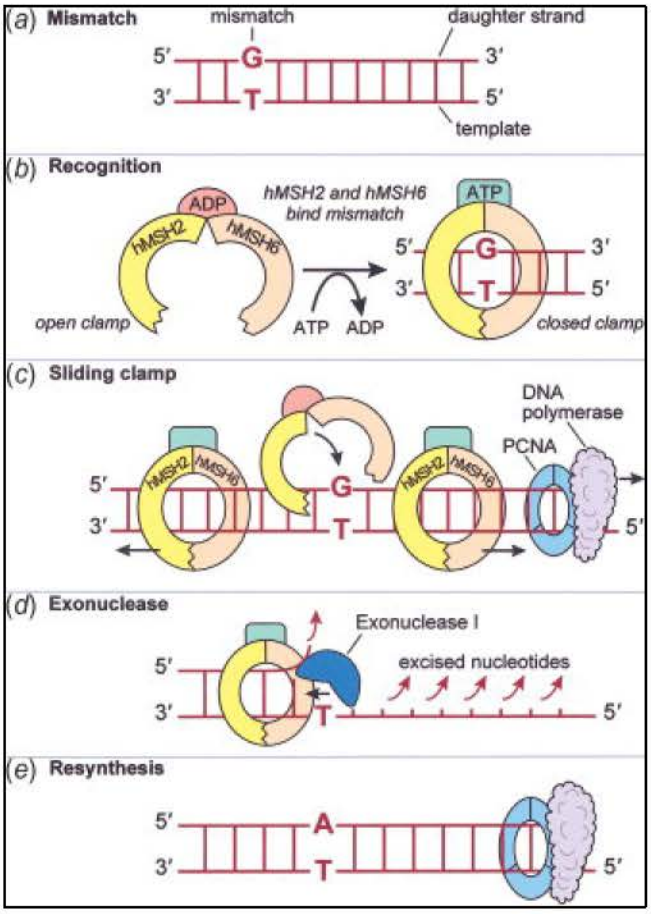

Figure 1.8. Repair of a single nucleotide mismatch in S phase by DNA MMR. (A) In this example, the polymerase has erroneously placed a G in the daughter strand across from a non-complementary T in the template, creating a mismatch during S phase. (B) The heterodimer of hMSH2 and hMSH6, bound by ADP and in an open configuration, monitors newly synthesized DNA for mispairs. Upon encountering the G-T mispair, an exchange of ATP for ADP occurs, and MutSα switches to a closed, sliding clamp along the DNA. (C) The sliding clamps can migrate in either direction from the mispair, and as this occurs, additional MutSα clamps may be recruited to the mismatch. The MutSα moving in the 5′ > 3′ direction will eventually encounter the PCNA–DNA polymerase complex, and according to one hypothesis, displace the enzymes involved in DNA synthesis. (D) Exo1 excises the newly synthesized daughter strand back

to the site of the mismatch, removing the erroneous G. (E) The error is corrected by resynthesis. Adapted from Fishel.[181]

1.3.1.1 Mismatch recognition

The DNA mismatch (**Figure 1.8A**) is first recognized by heterodimers of human MutS homolog (hMSH) proteins (**Figure 1.8B**). The predominant heterodimer consisting of MSH2 bound to MSH6, known as mutational S alpha (MutSα), recognizes single base mismatches and small IDLs (one to two nucleotides).[182,183] The secondary recognition heterodimer, MutS beta (MutSβ), composed of MSH2 bound to MSH3, is approximately 10-fold less abundant in the cell than MutSα, and corrects larger IDLs (two to fourteen nucleotides) (**Figure 1.9**).[184,185] hMSH proteins have one ATP binding site per protein, which determines the mismatch binding affinity of the heterodimer complex: in the ADP bound state, MutS heterodimers bind tightly to the mismatch, and in the ATP bound state, MutS heterodimers have been shown *in vitro* to work as "sliding clamps", moving laterally along the DNA (**Figure 1.8C**).[177,186-190] The lateral DNA movement allows for the MutS proteins to differentiate the newly synthesized strand from the parental strand; it is thought that the synthesized strand is identified by single strand nicks, such as the gaps between Okazaki fragments in the lagging DNA strand.[191,192]

1.3.1.2 Repair enzyme recruitment

Once the MutS proteins are in the activated ATP state, and bound to the DNA, the next set of repair proteins, consisting of the MutL proteins MutL homolog 1 (MLH1) and post meiotic segregation increased 2 (PMS2), are recruited to the site of the DNA mismatch.[193] MutL directly interacts with MutS at the site of the DNA damage, displacing DNA polymerase and proliferating cell nuclear antigen (PCNA) from the daughter strand, and recruiting exonuclease 1 (Exo1), which is required to excise the DNA at the damaged site.[194]

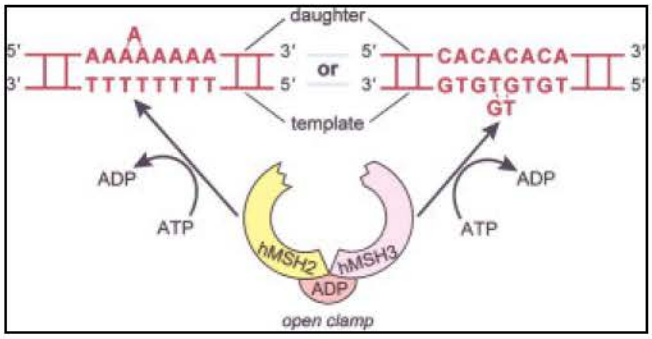

Figure 1.9. Repair of insertion/deletion errors at microsatellite sequences. These lesions are caused by "slippage" during DNA replication and are recognized by hMSH2 + hMSH3 (MutSβ) and corrected. Mononucleotide repeats such as A_n (which is T_n on the complementary strand) on the left, or dinucleotide repeats (such as $[CA:GT]_n$) on the right are recognized by hMutSβ here, triggering ATP-ADP exchange, long-patch excision and resynthesis. For purposes of illustration, the slippage has created a short "loop out" on the nascent strand for the A_n sequence, which would lead to an insertion frameshift mutation after replication, and on the template strand for the $(CA)_n$ repeat, which would lead to a deletion mutation. This particular error is best recognized by the hMSH2 + hMSH6 (MutSα) heterodimer. The heterodimer of MutSβ has greater affinity for larger insertion/deletion loops (not shown here) that commonly occur during DNA replication at microsatellite sequences.

1.3.1.3 Mismatch excision

The MutS/MutL/Exo1 complex initiates "long-patch excision repair", removing up to a kilobase from the DNA back to the mismatch site, and ending up to 150 nucleotides past the mismatch (**Figure 1.8D**).[177] DNA excision occurs in both the 5'>3' and 3'>5' directions, with MutS, Exo1 and replication protein A (RPA) needed for the 5'>3' excision, and MutL, PCNA and replication factor C (RFC) needed for the 3'>5' excision.[192,195-197] Exo1, which is a well-established 5'>3' exonuclease, has also been shown to act as a cryptic 3'>5' exonuclease in the presence of MSH2, MSH6, MLH1, PMS2, RPA, PCNA and RFC.[189] RPA binds single stranded DNA, stabilizing the remaining strand, and is needed for excision termination once the mismatch is removed. PCNA functions as a DNA sliding clamp that enhances the function of the DNA polymerase, and RFC is an ATPase responsible for loading and unloading PCNA from the DNA.[177]

1.3.1.4 DNA resynthesis

DNA resynthesis occurs following the recruitment of the replication machinery and DNA polymerase δ[198], which repairs the excised DNA on the newly synthesized DNA strand using the parental DNA strand as the template (**Figure 1.8E**).[177]

1.3.2 MMR protein regulation

Although the basics of MMR signaling and genetics have been studied extensively, there is little currently known regarding the cellular regulation of the MMR pathway.

1.3.2.1 Post-translational modification

Post-translational modification of proteins via phosphorylation is known to be involved in many cellular processes, including inactivation or activation of cellular signaling cascades, activation of transcription factors, proteasomal degradation, and protein nuclear translocation.[199-204] Of the few studies concerning MMR regulation, most have focused on the main MMR protein heterodimer, MutSα, due to its importance in the recognition of the DNA mismatch and the initiation of the MMR signaling cascade.

1.3.2.1.1 Nuclear localization

Two independent laboratories have found that the phosphorylation of MutSα greatly increases its mismatch-binding activity and nuclear translocation. In a 2002 study, both MSH2 and MSH6 were reported to be phosphorylated *in vitro* and *in vivo* by the serine/threonine kinases PKC and casein kinase 2 (CKII).[205] Similar findings were reported in a more recent paper, showing that an increase in phosphorylation of MSH6 occurred in the presence of a G:T or O^6methylguanine (O^6MeG):T mismatch, which occurs as a result of DNA adduct formation following exposure to alkylating agents such as N-methyl-N'-nitro-N-nitrosoguanine (MNNG).[206] Both studies suggest that MutSα phosphorylation regulates its nuclear translocation and DNA adduct binding activity, and that in this case, post-translational modification increases MMR signaling capability.

The regulation of MutSα appears to mostly involve the phosphorylation of MSH6, which has been shown to contain more potential phosphorylation sites than MSH2.[206] This is of particular interest since the nuclear translocation of MutSα is most likely dependent on MSH6; through computer searching of classical nuclear localization signals (NLS) in human protein sequences, MSH6 but not MSH2 was found to contain a

functional NLS.[207] However, a recent report on MutSα in yeast has shown that MSH2 can enter the nucleus in cells lacking MSH3 and MSH6.[208] Two putative MSH2 NLSs were found, mapping to the DNA binding domain of the MSH2 protein. Although MSH2 contains a NLS, less translocation occurred in the absence of MSH6, suggesting that the NLS of MSH6 is more efficient at regulating nuclear translocation than that of MSH2.

1.3.2.1.2 Proteasomal degradation and protein stability

Recently, the ubiquitin (Ub)-proteasome-mediated degradation of hMutSα was found to be regulated by phosphorylation events initiated by the atypical protein kinase C zeta (PKCζ).[209] Ubiquitination and subsequent proteasomal degradation of both MSH2 and MSH6 was previously shown to regulate the protein expression of MutSα in human cell lines.[210] Phosphorylation events have been implicated in the regulation of the ubiquitination reaction, and the degradation of targeted proteins.[211] Previous studies have also implicated the atypical PKCζ in protein inactivation and proteasome-mediated protein degradation.[200] An investigation of a panel of cell lines showed a correlation between hMutSα and PKCζ levels: cells with high PKCζ kinase activity had higher hMSH2 and hMSH6 protein levels[209]. Interestingly, an interaction between PKCζ and both hMSH2 and hMSH6 was detected, and PKCζ was found to mediate phosphorylation of MutSα, protecting the heterodimer from proteasomal degradation. Thus, in this case, phosphorylation of MutSα mediated by PKCζ not only stabilizes MutSα protein levels, but it also protects MutSα from degradation, suggesting a role for PKCζ in the regulation of MMR activity.[209]

1.3.3 Non-canonical MMR signaling

In addition to their roles in classical mismatch recognition and MMR signaling, MMR proteins also play key roles in processing DNA damage and DNA adducts from both endogenous and exogenous sources as discussed in the following sections.[177-179,189]

1.3.3.1 Cell cycle arrest and apoptosis

Mismatch repair proteins are needed for the cytotoxic effects induced by treatment with methylating and alkylating agents; MMR deficient cells are up to 100 fold more resistant to unimolecular nucleophilic substitution (S_N1)-type methylating agents.[179] Treatment with methylating agents leads to the methylation of DNA basepairs, primarily the O^6 of guanine, producing O^6-methylguanine (O^6MeG), which forms unusual basepairs in the DNA with thymine (T) and cytosine (C).[179,189] O^6MeG lesions are typically removed by MGMT (O^6MeG-DNA methyltransferase); MGMT removes the methyl group of O^6MeG, creating a G:T mismatch processes by MMR. However, MGMT inactivation is common in many cancer types.[212] O^6MeG:T mispairs are preferentially bound by MutSα, which mediates the removal of the T from the new strand; O^6MeG:C mispairs are not recognized by MMR.[213] However, the DNA repair machinery will continue to place a T opposite the O^6MeG on the newly replicated strand, leading to a "futile repair" cycle, signaling to MMR-dependent S-phase G_2 cell cycle arrest and apoptosis (**Figure 1.10**, left).[178,214] An alternative model for how cytotoxicity of these drugs is dependent on MMR, known as the "direct signaling model", postulates that MutSα/MutLα directly recruit checkpoint proteins to the site of the DNA adduct, inducing cell cycle checkpoint activation and subsequent apoptosis (**Figure 1.10**, right).[178] MMR deficient cells are unable to process O^6MeG adducts at the expense

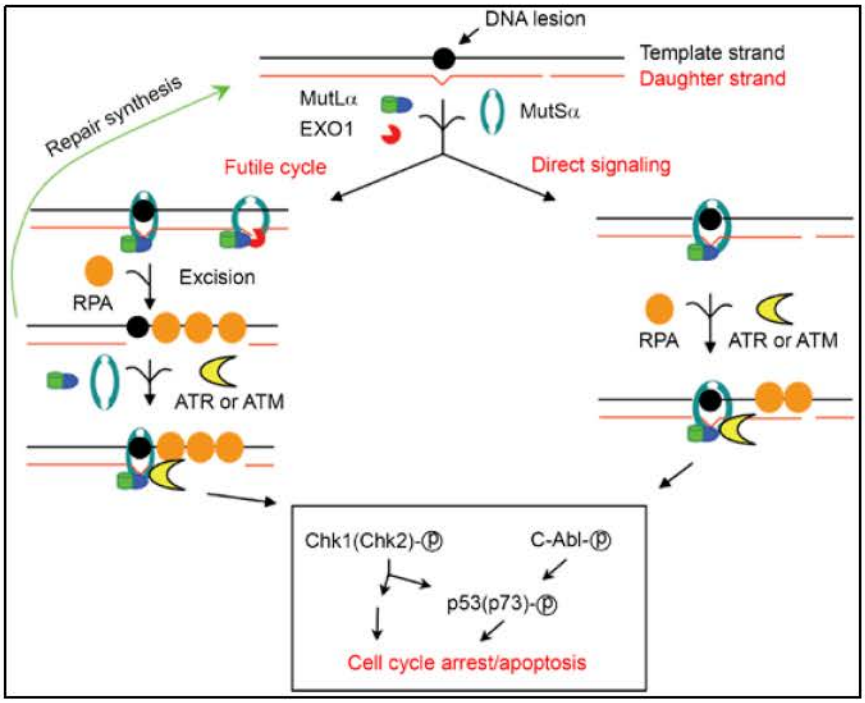

Figure 1.10. Models for MMR-dependent DNA damage signaling. The "futile DNA repair cycle" model (left) suggests that DNA adducts (solid black circle) induce misincorporation, which triggers the strand-specific MMR reaction. Since MMR only targets the newly synthesized strand for repair, the offending adduct in the template strand cannot be removed, and will provoke a new cycle of MMR upon repair resynthesis. Such a futile repair cycle persists and activates the ATR and/or ATM damage signaling network to promote cell cycle arrest and/or programmed cell death. The direct signaling model proposes that recognition of DNA adducts by MSH-MLH complexes allows the proteins to recruit ATR and/or ATM to the site, activating the downstream damage signaling.

of extensive mutation; MMR deficient cells are thus known to be DNA damage tolerant.[179,214] The MMR-dependent induction of cell cycle arrest requires the checkpoint protein ataxia telangiectasia and Rad3 related (ATR) kinase, which phosphorylates its effector checkpoint kinase 1 (CHK1), as well as the MMR proteins MLH1 and MSH2.[215-218] Apoptosis and cell cycle arrest mediated by treatment with DNA alkylating and platinating agents also requires the presence of a functional MMR, specifically MutSα[219]; hMutSα- and hMutLα-deficient cells are defective in cell cycle arrest and apoptosis in response to multiple types of DNA damaging agents, and fail to phosphorylate p53 and p73 to initiate apoptosis.[220,221] In support of this concept, an interaction between MutSα, MutLα, the checkpoint proteins ATM (ataxia telangiectasia mutated), ATR-ATRIP (ATR-interacting protein), the RTK c-Abl (Abelson kinase) that plays important roles in cell cycle, and the apoptotic protein p73 has been reported in cells treated with DNA damaging agents.[213,218,222-224] It has thus been proposed that on top of their roles in MMR, MutSα and MutLα act as DNA damage sensors in the cell[178], implicating MMR as part of a more global DNA damage response system.

1.3.3.2 Homeologous recombination

MMR proteins have been implicated in the regulation of homeologous recombination, which is the genetic recombination between two similar, but non-identical sequences. Homeologous recombination occurs at a much lower frequency in normal cells than homologous recombination (between identical sequences).[225,226] Through increasing the genetic diversity, homeologous recombination is thought to drive evolutionary adaptation. Interestingly, the frequency of homeologous recombination is higher in MMR deficient cells, suggesting that MMR may suppress this phenomenon.[227,228] Uncontrolled homeologous recombination induces DNA mispairs and heteroduplexes, leading to chromosomal inversions,

duplications, translocations, and deletions. This increases the cellular genomic instability.[229]

The mechanisms surrounding MMR regulation of homeologous recombination have been studied extensively in yeast systems, but are unclear in human cells. In yeast, it has been hypothesized that MutSα recruits the DNA helicase SGS1 to the site of DNA heteroduplex, and blocks homeologous recombination.[230-232] In humans, an interaction between MutSα and two human equivalents of SSG1, BLM (Bloom syndrome, RecQ helicase-like) and RECQ1 (RecQ protein-like (DNA helicase Q1-like)), has been demonstrated[233,234], suggesting a similar mechanism for regulation. The regulation of homeologous recombination by MMR is another way that the MMR pathway promotes genomic stability.

1.3.3.3 Relationship between MMR and other notable DNA pathways

MMR proteins have been shown to play a role in the processing of inter-strand crosslinks (ICLs) in the DNA, which are formed during natural cellular processes as well as by chemotherapeutic agents. MMR proteins coordinate in an unknown manner with double strand DNA break repair, homologous recombination, and nucleotide excision repair proteins to efficiently repair ICLs.[235-237]

MMR proteins also play roles in promoting the genetic variation needed for immunoglobulin class switching (class switch recombination, CSR) and somatic hypermutation, mechanisms for increasing the diversity of immune system antibodies during antigen-mediated B-cell differentiation.[178] When an individual MMR protein is missing, the process of CSR and somatic hypermutation is reduced 2-5 fold compared to wild-type cells; this holds true for the loss of most of the MMR proteins,

including MSH2, MSH6, MLH1, PMS2 and EXO1.[238-242] It has been postulated that MMR proteins function in CSR to increase the frequency of DNA substrates, increasing genetic diversity.[243]

1.3.4 MMR deficiency and cancer development

MMR proteins play a major role in the maintenance of genomic stability through their canonical roles in DNA mismatch repair, as well as their non-canonical functions in cell cycle arrest, apoptosis, and homeologous recombination.[178] Defects in MMR genes are thus associated with genome-wide instability, hereditary and sporadic tumor development, and resistance to some DNA damaging agents.[180] The importance of MMR genes in tumor suppression in both humans and mice has been well characterized in MMR gene knockout systems, and in genetic and biochemical studies of humans and human derived tumor cell lines from patients with hereditary non-polyposis colorectal cancer (HNPCC).[178,244]

1.3.4.1. MMR and hereditary non-polyposis colorectal cancer (HNPCC) or Lynch syndrome

Mutations leading to loss of MMR gene function in humans are directly linked to the development of hereditary non-polyposis colorectal cancer (HNPCC) or Lynch syndrome. Lynch syndrome is an early-onset cancer that affects a variety of tissues, including colon, endometrium, urothelium, ovarian, small-bowel, and renal-pelvis regions, and is inherited in an autosomal dominant manner.[244] Lynch syndrome patients have an 80% risk of developing colon cancer, and women have a 60% lifetime risk of endometrial cancer.[245] The majority of Lynch syndrome patients inherit one copy of a MMR gene mutation, and rarely, biallelic mutations are inherited, leading to constitutional MMR deficiency, which is a more severe type of Lynch syndrome.[244,246] Biallelic mutations include homozygous (2

copy) mutations with residual protein production that is non-functional, such as a truncation/missense mutation, and compound heterozygous mutations involving two unrelated recessive mutations at a given locus, leading to genetic dysfunction. Recently, constitutional MMR deficiency associated disorders has been updated to include early onset leukemia, lymphoma, brain tumors, and adenocarcinoma.[246-248]

1.3.4.1.1 MMR germline gene mutations

In Lynch syndrome patients, *MLH1* gene mutations account for approximately 50% of the inherited disease-associated mutations. *MSH2* gene mutations occur in 40% of Lynch syndrome cases. Mutations in the *MSH6* gene are more rare, accounting for only 7-10% of Lynch syndrome families, and <5% carry mutations in the *PMS2* gene.[244] Over 2000 unique mutations leading to missense, nonsense, splice site, or abnormal gene regulation mutations have been detected in the four main MMR genes: 875 in *MLH1*, 860 in *MSH2*, 290 in *MSH6* and 111 in *PMS2*.[244] Large gene deletions are common among the *MLH1* and *MSH2* genes, accounting for 5-10% and 17-50% of gene mutations detected, respectively.[244] Interestingly, germline mutations in *MSH2* and *MLH1* lead to eventual genetic loss of *MSH6* and *PMS2*, often through truncating mutations associated with MSI at microsatellites in the coding regions. The stability of MSH6 and PMS2 proteins rely heavily on their binding partners, so loss of MSH2 and MLH1 also leads to loss of MSH6 and PMS2 protein expression.

In 2009, it was reported for the first time that germline mutations associated with MMR genes confer a risk for prostate cancer, which is currently not recognized as part of the Lynch syndrome tumor spectrum.[249] In this study, 106 men from 34 different families were found to be MMR germline mutation carriers: 68 carried *MSH2* mutations, 19 with *MLHI,* 13

with *MSH6*, and 6 with *PMS2* mutations. Nine of these men from 8 different families were diagnosed with prostate cancer; by chance, only 1.52 men should have developed prostate cancer, versus the 9 observed, suggesting a correlation between germline MMR gene mutation and prostate cancer in this population, and further, that prostate cancer may be part of the Lynch syndrome-associated cancer types.[249]

1.3.4.1.2 Diagnosis by microsatellite instability testing

Patients presenting with colorectal cancer (CRC) are tested for MSI following the "Revised Bethesda Guidelines", based on the notion that hereditary, Lynch syndrome-associated and sporadic CRC have distinct features histologically.[250,251] The Bethesda Guidelines are outlined in **Table 1.4**.[251] Since nearly all Lynch-associated CRCs exhibit MSI, the first step in the diagnosis is to test for MSI by immunohistochemistry (IHC) or by PCR for microsatellite repeats.[244,252,253]

1.3.4.1.2.1. Immunohistochemistry

IHC on paraffin-embedded tissue samples from suspected Lynch syndrome tumors is performed using monoclonal antibodies against all four proteins associated with MSI: MLH1, MSH2, MSH6 and PMS2.[254] The tumor and adjacent non-neoplastic tissue is evaluated for the presence or absence of staining. Loss of MMR protein expression is highly indicative of MSI.[255-260] There are typically few cases with the MSI stable (MSS), or MSI low (MSI-L) (described below) phenotype associated with loss of MMR protein expression; in a 2002 study from the Mayo Clinic analyzing a series of 1463 tumor samples, only 0.2% of MSS/MSI-L tumors showed loss of MMR protein expression by IHC.[254] However, not all MSI positive tumors (MSI high, or MSI-H, described below) show loss of MMR protein

Table 1.4. The Revised Bethesda Guidelines for testing colorectal tumors for microsatellite instability (MSI).[250]

Tumors from individuals should be tested for MSI in the following situations:
1. Colorectal cancer diagnosis in a patient who is less than 50 years of age. 2. Presence of synchronous[a], metachronous[b] colorectal, or other HNPCC-associated tumors[c], regardless of age. 3. Colorectal cancer with the MSI-H[d] histology[e] diagnosed in a patient who is less than 60 years of age. 4. Colorectal cancer diagnosed in one or more first-degree relatives with an HNPCC-related tumor, with one of the cancers being diagnosed under age 50 years. 5. Colorectal cancer diagnosed in two or more first- or second-degree relatives with HNPCC-related tumors, regardless of age.

[a]Synchronous – occurring at the same time
[b]Metachronous – occurring consecutively
[c]Hereditary non-polyposis colorectal cancer (HNPCC)-related tumors include colorectal, endometrial, stomach, ovarian, pancreas, ureter and renal pelvis, biliary tract, and brain tumors, sebaceous gland adenomas and keratoacanthomas and carcinoma of the small bowel
[d]MSI-H – microsatellite instability high in tumors refers to changes in two or more of the five National Cancer Institute recommended panels of microsatellite markers
[e]Presence of tumor infiltrating lymphocytes, Crohn's-like lymphocytic reaction, mucinous/signet-ring differentiation, or medullary growth pattern

Adapted from [Lynch syndrome-associated neoplasms: a discussion on histopathology and immunohistochemistry. Shia J, Holck S, DePetris G, Greenson JK, Klimstra DS. Familial Cancer. 12. Copyright © 2013 Springer.] with permission (license number 3416560052245).

expression, and IHC can miss about 5-15% of Lynch-syndrome-associated tumor cases.[251,259,261] This is often due to the fact that some mutations in MMR genes, such as missense mutations, can cause loss of protein function associated with intact protein expression.[251,262,263] In some rare cases, other MMR-associated genes may be lost in the MSI-H cases that do not show loss of the aforementioned MMR proteins.[254] The specificity and sensitivity of the IHC protocol must be thoroughly tested, as IHC results for MMR protein expression are often difficult to interpret.[264] Thus, PCR-based MSI testing complements IHC detection loss of MMR-protein expression, with IHC considered as a pre-screen for MSI-positive tumors.

1.3.4.1.2.2 PCR-based microsatellite instability testing

For MSI testing by PCR, tumor DNA, as well as normal patient DNA, is isolated from paraffin-embedded tissue sections, and is subjected to PCR using fluorescently labeled primers specific to a defined set of microsatellite sequences.[254] The National Cancer Institute (NCI) panel of microsatellite repeats are typically used for PCR analysis: these include the BAT25 and BAT26 markers, which are mononucleotide repeats, and the dinucleotide repeat primers D2S123, D17S250, and D5S346.[265] A panel of quasimonomorphic mononucleotide primers has also been described for MSI testing, which include the markers BAT25, BAT26, NR21, NR22 and NR24.[266] The resultant PCR products from the tumor samples are compared to the same products from the normal samples, and are scored for MSI based on changes in the PCR product size (shifts), indicative of expansion or contraction of the microsatellite markers.[254,267] The choice of markers for MSI is important, as the microsatellite panels can give differing results from the same patient tumor DNA (**Figure 1.11**).

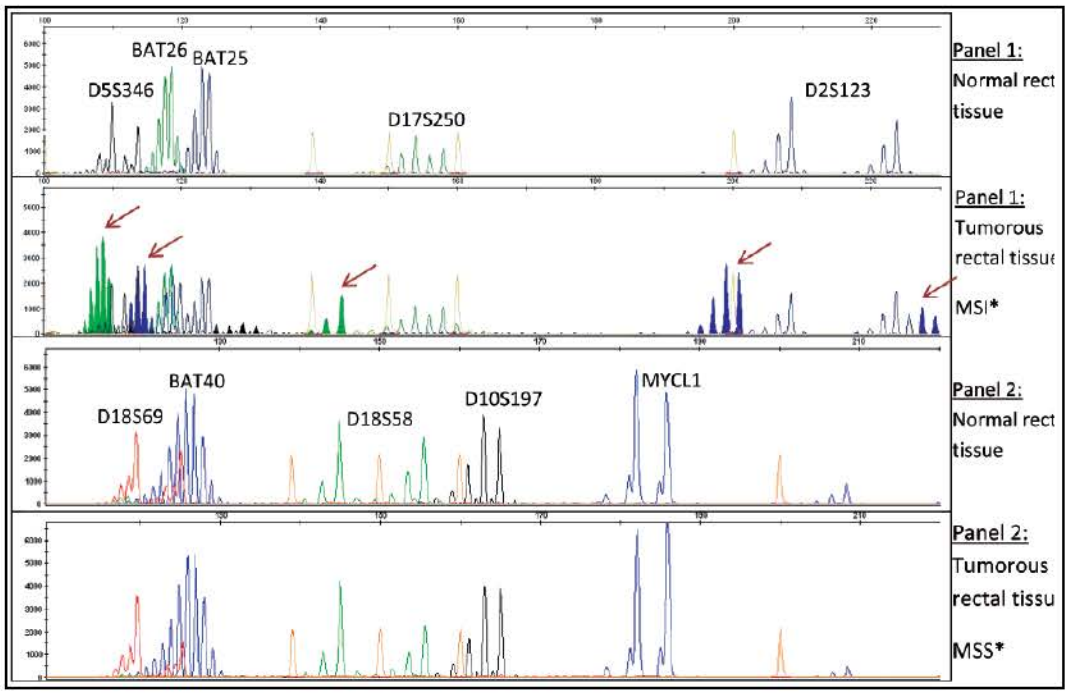

Figure 1.11. Microsatellite panel of tumor DNA and matching normal DNA. Normal rectal tissue was compared with tumorous rectal (rect) tissue using 2 panels of MSI markers. Using panel 1, the patient was classified as having microsatellite instability (MSI), due to expansion and contraction of microsatellite markers and differential PCR product size compared to the normal, matched DNA (arrows). Using panel 2, the same patient was classified as microsatellite stable (MSS); there was no perceived change in the PCR product size at the microsatellite markers in the patient tumor DNA versus the normal DNA.

Using the NCI marker panel, MSI at 2 or more of the 5 markers is classified as MSI-H, while MSI at 1 of the 5 markers is classified as MSI-L.[254] Tumors that do not show MSI are considered MSI stable, or MSS, and are not considered to be Lynch-associated. The MSI-L classification is not typically associated with Lynch syndrome, and samples with this classification are not recommended for further testing.[244] Defective MMR is associated with the MSI-H phenotype, and is seen in Lynch syndrome tumor types and a variable proportion of sporadic tumors.[254] Some patients with the MSS or MSI-L phenotype do have Lynch syndrome associated with loss of the MSH6 protein by IHC[250]; however, most patients with MSI-L status do not have abnormalities in the main MMR genes.[268] Confirmation of MSI status by IHC is required for a definitive Lynch syndrome diagnosis.

1.3.4.2 Mismatch repair knockout mice

Gene knockout mouse models have been made for a number of MMR associated genes, including *MSH2*, *MSH3*, *MSH6*, *MLH1*, *PMS1*, *PMS2*, *MLH3* and *Exo1*.[269-272] The characteristics of these mice are summarized in **Table 1.5**.[178] Interestingly, for most of the knockout mice, the primary susceptible tumor type is lymphoma, not colorectal cancer, although gastrointestinal and skin tumors, and sarcoma are reported secondary cancer sites.

MSH2-/- mice have a significantly shorter lifespan than *MSH2*+/+ mice, carry MSI, and approximately 50% succumb to lymphoma associated with MMR loss at 6 months of age.[273,274] *MSH6*-/- mice lack MSI, and develop tumors at a longer latency than *MSH2* null mice.[275-277] *MSH3* knockout mice retain the ability to repair single base mismatches, but have lost the ability to repair IDLs, and either develop tumors at a late age, or remain

Table 1.5. Phenotypes of mismatch repair deficient mice. Adapted from Li.[178]

Gene	MSI	Tumor	Fertility	Reference
MSH2	Yes	Lymphoma, GI, skin, and other tumors	Yes	de Wind et al.[273], Reitmar et al.[274]
MSH3	Yes	Tumor free or GI tumors at a very late age	Yes	de Wind et al.[276], Edelmann et al.[277]
MSH6	Low (dinucleotide repeats)	Lymphoma, GI and other tumors	Yes	Edelmann et al.[275], de Wind et al.[276],Edelmann et al.[277]
MLH1	Yes	Lymphoma, GI, skin, and other tumors	No	Baker et al.[278], Edelmann et al.[279]
PMS1	Low (mono-nucleotide repeats), or none	None	Yes	Prolla et al.[272]
PMS2	Yes	Lymphoma and sarcoma	Male infertile	Prolla et al.[272], Baker et al.[280]
MLH3	Yes	GI, extra-GI tumors	No	Chen et al.[281], Lipkin et al.[282]
Exo1	Yes	Lymphoma	No	Wei et al.[271]

Abbreviations: MSI – microsatellite instability; MSH – MutS homolog; GI – gastrointestinal; MLH – MutL homology; PMS – post meiotic segregation increased; Exo1 – exonuclease 1.

tumor free.[276,277] This highlights the importance of the MSH proteins in MMR; while MSH2 knockout results in complete MMR deficiency, loss of MSH6 or MSH3 is associated with some residual MMR due to the presence of the other MutS heterodimer. Double knockout of *MSH3* and *MSH6* in mouse models leads to tumor development that is indistinguishable from *MSH2* null mice[276,277]; like *MSH2* deficient mice, these double knockout mice can form neither MutSα nor MutSβ and are MMR deficient. Results from these mouse models have thus shown that the MSH2 protein is essential for proper MMR function. MLH deficient mice have a high susceptibility to cancer and carry genomic instability, reflective of MMR deficiency. Male and female *MLH1* and *MLH3* knockout mice and male *PMS2* knockout mice are completely sterile due to abnormal meiosis associated with MMR loss.[272,278-282] *PMS1*-/- mice have low to no MSI, do not develop tumors, and are fertile.[272] *Exo1* knockout mice carry a similar phenotype to MLH deficient mice in regards to tumor susceptibility and sterility.[271] MMR gene knockout mice highlight the important roles of MMR proteins in maintaining genomic stability as loss of most MMR genes in mice promotes cancer development.

1.3.4.3 MMR and sporadic cancer development

1.3.4.3.1 Colorectal cancer

MMR dysfunction leading to MSI is causative in approximately 10-15% of sporadic CRC, typically associated with the hypermethylation of the *MLH1* gene locus, leading to mRNA and protein loss.[283-288] More than 95% of MSI-H sporadic CRC cases are due to *MLHI* promoter methylation, which may be a heritable genetic condition.[255,289-291] Hypermethylation of *MSH2* in sporadic CRC is exceedingly rare.[178]

Mutations in the BRAF protein (v-Raf murine sarcoma viral oncogene homolog B protein) (specifically V600E) are common in about 50-70% of sporadic MSI-positive CRC tumors; *BRAF* gene mutations are not common in Lynch syndrome, allowing the distinction between sporadic tumors with MSI versus tumors associated with germline loss of MMR genes.[284,292] BRAF is a signal transduction serine/threonine kinase that regulates the mitogen activated protein kinase (MAPK)/ERK pathway, with functions in cell division, proliferation, and differentiation.[293] Mutations in BRAF occur in about 8% of all human tumors, and are frequently implicated in the development of melanoma (40-70%).[294,295]

1.3.4.3.2 Solid tumors

MMR dysfunction has been linked to the pathogenesis of a number of tumor types (2-50%, depending on the samples analyzed), including breast, prostate, lung, bladder, esophagus, squamous cell carcinoma, transitional carcinoma, ovarian, and head and neck cancer.[180] This MMR dysfunction is linked to loss of function of one or more of the major MMR genes associated with Lynch syndrome (MLHI, MSH2, MSH6, PMS2), as well as MSH3 and PMS1, whether through epigenetic silencing, or somatic mutation. Although these sporadic tumors display varying levels of MSI, the markers with instability are typically di- tri, and tetranucleotide, versus the mononucleotide repeats common in Lynch syndrome.[296]

Previous studies have demonstrated that loss of MMR is associated with genome-wide instability, especially in genetic coding regions carrying single repeat sequences, referred to as a “mutator phenotype”.[297] In MMR-deficient tumor cells, somatic frameshift mutations in key genes regulating tumor suppression, cell growth, DNA repair, cell cycle, and apoptosis, have been detected, implicating MMR loss in a multi-step tumorigenesis pathway.[178,298]

1.3.4.3.3 Lymphoid tumors

It is clear from studying MMR knockout mice that loss of MMR protein expression does lead to lymphoid tumor development (**Table 1.4**), In support of this observation, constitutional MMR deficiency associated with the congenital loss of two mutated MMR genes, including *MSH2*, has been shown to be associated with the development of childhood lymphoma[248,299], suggesting that human lymphoid tumors may also display varying degrees of MMR dysfunction.

The role of MMR dysfunction and MSI in lymphoid tumors has been controversial. The current MSI testing criteria is based on microsatellite markers known to show expansion and contraction in Lynch syndrome-associated tumors; however, there is a heterogeneity in tumor types that makes it difficult to translate results from these markers into other types of cancer and a negative result for MSI testing is not necessarily indicative of a MSS tumor. In a 2008 study, MSI was detected in 8 out of 59 (14%) of NHL tumors analyzed, and was correlated with drug resistance and poor response to chemotherapy: the probability of survival of MSI positive patients was 0.4, versus 0.771 in patients with MSS disease.[300] Interestingly, the MSI was not associated with the loss of MSH2 or MLH1 nuclear staining, suggesting that, in these tumor types, another mechanism leading to loss of MMR function may occur.

1.3.4.3.3.1 Oncogenic tyrosine kinase BCR-ABL and MMR

Like NPM-ALK, BCR-ABL is a gene-fusion tyrosine kinase resulting from the reciprocal chromosomal translocation, t(9;22)(q34;q11), between the ubiquitously expressed *Abelson kinase* (c-ABL) gene and the ubiquitously expressed (with highest expression in brain and hematopoietic cells) *breakpoint cluster region* (BCR) gene.[301] The expression of BCR-ABL

transforms normal hematopoietic stem cells to induce the development of chronic myelogenous leukemia (CML) and acute lymphoblastic leukemia (ALL). On top of its transformative ability, BCR-ABL can increase DNA damage and inhibit cellular DNA repair, promoting genomic instability.[302,303] An increase in the level of MSI is associated with the progression of chronic phase CML (CML-CP) to CML blast phase (CML-BP), which has been shown to display MSI at multiple microsatellite markers, suggestive of MMR dysfunction.[304]

In 2008, in a study by Stoklosa et al., BCR-ABL was shown to reduce the MMR ability approximately 2 fold compared to cells without BCR-ABL expression.[305] BCR-ABL positive cells were also found to be resistant to the methylating agent MNNG; cells that survived treatment displayed a mutator phenotype associated with loss of MMR. Interestingly, BCR-ABL expressing cells did not show loss of MMR protein expression, suggesting an alternative mechanism for MMR inhibition.

1.4 Thesis overview

1.4.1 Rationale

ALK+ALCL is an aggressive T/null cell lymphoma characterized by the expression of the oncogenic gene fusion tyrosine kinase NPM-ALK.[1,2,112,113] Numerous studies have demonstrated the potent transformative and oncogenic capabilities of NPM-ALK. Through signaling from its constitutive receptor tyrosine kinase, NPM-ALK activates a number of downstream signaling proteins by phosphorylation, many of which are highly tumorigenic on their own, thereby potentiating its oncogenesis.[2,98,112,113]

To further understand how NPM-ALK exerts its oncogenic pressure, our laboratory recently used liquid chromatography-mass spectrometry (LC-MS) to identify potential NPM-ALK interacting partners.[175] NPM-ALK bound to a large number of previously unidentified proteins; one of the novel interacting proteins was MutS homolog 2 (MSH2), a protein integral to DNA mismatch repair (MMR).[177,178,270] MMR proteins maintain genomic stability by correcting DNA replication errors, as well as DNA damage from both exogenous and endogenous sources. MMR dysfunction through germline mutational loss of MMR-associated genes is highly cancer promoting, and has been well characterized in Lynch syndrome, a heritable disease associated with early-onset colorectal cancer (CRC) and extra-colonic tumors.[244,306] Loss of MMR function is also associated with the development of a number of sporadic cancer types, including lymphoid malignancies.[248,299] The microsatellite instability (MSI) associated with MMR dysfunction has been directly linked to poor chemotherapeutic response in Non-Hodgkin lymphoma (NHL) patients.[300]

A direct link between MMR and oncogenic tyrosine kinases was shown in 2008, when the leukemia-associated gene fusion tyrosine kinase BCR-ABL was shown to inhibit MMR through an uncharacterized mechanism, potentiating a mutator phenotype in BCR-ABL expressing cells.[305] Oncogenic tyrosine kinases share similarities in signal transduction at the cellular level. With this in mind, ***I hypothesized that MMR deficiency in ALK+ALCL cell lines and samples from patients with ALCL is associated with an interaction of MSH2 and NPM-ALK, which interferes with cellular MMR function.***

1.4.2 Objectives

The first objective was to determine if NPM-ALK disrupts mismatch repair function, and if so, to elucidate the molecular mechanisms as to how this

may occur. This topic is covered in **Chapter 2**. Using NPM-ALK expressing cell lines and patient samples, NPM-ALK expression was evaluated for its ability to induce MMR deficiency, and it was determined if ALK+ALCL patient samples show evidence of MMR dysfunction. Finally, as NPM-ALK is a potent tyrosine kinase that binds and phosphorylates downstream proteins, the ALK tyrosine kinase was assessed for its ability to phosphorylate MSH2.

In **Chapter 3**, my second objective was to determine the specific NPM-ALK-induced tyrosine phosphorylation site in the MSH2 protein, and to evaluate the biological importance of this site in MMR using an MSH2 non-phosphorylatable mutant.

My third objective, as detailed in **Chapter 4**, was to develop and characterize a novel monoclonal antibody recognizing the MSH2 tyrosine phosphorylation site we identified. I evaluated the specificity of this antibody *in vitro* using NPM-ALK-expressing cell lines and determined its clinical relevance using immunohistochemistry on ALK expressing patient samples. We hypothesized that the ALK-mediated phosphorylation of MSH2 may be a phenomenon shared by other tyrosine kinases. Thus, I screened cells transfected with a number of known clinically relevant oncogenic tyrosine kinases for MMR deficiency, to determine if receptor tyrosine kinase-mediated tyrosine phosphorylation of MSH2 and the subsequent disruption of MMR is shared among tyrosine kinases.

1.5 References

1. Stein H, Foss HD, Durkop H, et al. CD30(+) anaplastic large cell lymphoma: a review of its histopathologic, genetic, and clinical features. *Blood* 2000;**96**(12):3681-3695.
2. Amin HM, Lai R. Pathobiology of ALK+ anaplastic large-cell lymphoma. *Blood* 2007;**110**(7):2259-2267.
3. Fornari A, Piva R, Chiarle R, Novero D, Inghirami G. Anaplastic large cell lymphoma: one or more entities among T-cell lymphoma? *Hematol Oncol* 2009;**27**(4):161-170.
4. Stein H, Mason DY, Gerdes J, et al. The expression of the Hodgkin's disease associated antigen Ki-1 in reactive and neoplastic lymphoid tissue: evidence that Reed-Sternberg cells and histiocytic malignancies are derived from activated lymphoid cells. *Blood* 1985;**66**(4):848-858.
5. Tabbo F, Barreca A, Piva R, Inghirami G, European TCLSG. ALK signaling and target therapy in anaplastic large cell lymphoma. *Front Oncol* 2012;**2**:41.
6. Kadin ME, Sako D, Berliner N, et al. Childhood Ki-1 lymphoma presenting with skin lesions and peripheral lymphadenopathy. *Blood* 1986;**68**(5):1042-1049.
7. Herbst H, Tippelmann G, Anagnostopoulos I, et al. Immunoglobulin and T-cell receptor gene rearrangements in Hodgkin's disease and Ki-1-positive anaplastic large cell lymphoma: dissociation between phenotype and genotype. *Leuk Res* 1989;**13**(2):103-116.
8. Bitter MA, Franklin WA, Larson RA, et al. Morphology in Ki-1(CD30)-positive non-Hodgkin's lymphoma is correlated with clinical features and the presence of a unique chromosomal abnormality, t(2;5)(p23;q35). *Am J Surg Pathol* 1990;**14**(4):305-316.

9. Kaneko Y, Frizzera G, Edamura S, et al. A novel translocation, t(2;5)(p23;q35), in childhood phagocytic large T-cell lymphoma mimicking malignant histiocytosis. *Blood* 1989;**73**(3):806-813.

10. Rimokh R, Magaud JP, Berger F, et al. A translocation involving a specific breakpoint (q35) on chromosome 5 is characteristic of anaplastic large cell lymphoma ('Ki-1 lymphoma'). *Br J Haematol* 1989;**71**(1):31-36.

11. Mason DY, Bastard C, Rimokh R, et al. CD30-positive large cell lymphomas ('Ki-1 lymphoma') are associated with a chromosomal translocation involving 5q35. *Br J Haematol* 1990;**74**(2):161-168.

12. Fischer P, Nacheva E, Mason DY, et al. A Ki-1 (CD30)-positive human cell line (Karpas 299) established from a high-grade non-Hodgkin's lymphoma, showing a 2;5 translocation and rearrangement of the T-cell receptor beta-chain gene. *Blood* 1988;**72**(1):234-240.

13. Benz-Lemoine E, Brizard A, Huret JL, et al. Malignant histiocytosis: a specific t(2;5)(p23;q35) translocation? Review of the literature. *Blood* 1988;**72**(3):1045-1047.

14. Morris SW, Kirstein MN, Valentine MB, et al. Fusion of a kinase gene, ALK, to a nucleolar protein gene, NPM, in non-Hodgkin's lymphoma. *Science* 1994;**263**(5151):1281-1284.

15. Shiota M, Fujimoto J, Semba T, Satoh H, Yamamoto T, Mori S. Hyperphosphorylation of a novel 80 kDa protein-tyrosine kinase similar to Ltk in a human Ki-1 lymphoma cell line, AMS3. *Oncogene* 1994;**9**(6):1567-1574.

16. Swerdlow A, Campo E, Harris NL, et al. WHO Classification of Tumours of Haematopoietic and Lymphoid Tissue. Vol. 2nd (ed 4th). Lyon: World Health Organization; 2008.

17. Campo E, Swerdlow SH, Harris NL, Pileri S, Stein H, Jaffe ES. The 2008 WHO classification of lymphoid neoplasms and beyond: evolving concepts and practical applications. *Blood* 2011;**117**(19):5019-5032.

18. Falini B, Bigerna B, Fizzotti M, et al. ALK expression defines a distinct group of T/null lymphomas ("ALK lymphomas") with a wide morphological spectrum. *Am J Pathol* 1998;**153**(3):875-886.

19. Ferreri AJ, Govi S, Pileri SA, Savage KJ. Anaplastic large cell lymphoma, ALK-negative. *Crit Rev Oncol Hematol* 2013;**85**(2):206-215.

20. Hallberg B, Palmer RH. Mechanistic insight into ALK receptor tyrosine kinase in human cancer biology. *Nat Rev Cancer* 2013;**13**(10):685-700.

21. Iwahara T, Fujimoto J, Wen D, et al. Molecular characterization of ALK, a receptor tyrosine kinase expressed specifically in the nervous system. *Oncogene* 1997;**14**(4):439-449.

22. Souttou B, Carvalho NB, Raulais D, Vigny M. Activation of anaplastic lymphoma kinase receptor tyrosine kinase induces neuronal differentiation through the mitogen-activated protein kinase pathway. *J Biol Chem* 2001;**276**(12):9526-9531.

23. Bennasroune A, Mazot P, Boutterin MC, Vigny M. Activation of the orphan receptor tyrosine kinase ALK by zinc. *Biochem Biophys Res Commun* 2010;**398**(4):702-706.

24. Stoica GE, Kuo A, Aigner A, et al. Identification of anaplastic lymphoma kinase as a receptor for the growth factor pleiotrophin. *J Biol Chem* 2001;**276**(20):16772-16779.

25. Stoica GE, Kuo A, Powers C, et al. Midkine binds to anaplastic lymphoma kinase (ALK) and acts as a growth factor for different cell types. *J Biol Chem* 2002;**277**(39):35990-35998.

26. Lu KV, Jong KA, Kim GY, et al. Differential induction of glioblastoma migration and growth by two forms of pleiotrophin. *J Biol Chem* 2005;**280**(29):26953-26964.

27. Bilsland JG, Wheeldon A, Mead A, et al. Behavioral and neurochemical alterations in mice deficient in anaplastic lymphoma kinase suggest therapeutic potential for psychiatric indications. *Neuropsychopharmacology* 2008;**33**(3):685-700.

28. Lasek AW, Lim J, Kliethermes CL, et al. An evolutionary conserved role for anaplastic lymphoma kinase in behavioral responses to ethanol. *PLoS One* 2011;**6**(7):e22636.

29. Weiss JB, Xue C, Benice T, Xue L, Morris SW, Raber J. Anaplastic lymphoma kinase and leukocyte tyrosine kinase: functions and genetic interactions in learning, memory and adult neurogenesis. *Pharmacol Biochem Behav* 2012;**100**(3):566-574.

30. Lamant L, Pulford K, Bischof D, et al. Expression of the ALK tyrosine kinase gene in neuroblastoma. *Am J Pathol* 2000;**156**(5):1711-1721.

31. Wallace GCt, Dixon-Mah YN, Vandergrift WA, 3rd, et al. Targeting oncogenic ALK and MET: a promising therapeutic strategy for glioblastoma. *Metab Brain Dis* 2013;**28**(3):355-366.

32. Kutok JL, Aster JC. Molecular biology of anaplastic lymphoma kinase-positive anaplastic large-cell lymphoma. *J Clin Oncol* 2002;**20**(17):3691-3702.

33. Chiarle R, Voena C, Ambrogio C, Piva R, Inghirami G. The anaplastic lymphoma kinase in the pathogenesis of cancer. *Nat Rev Cancer* 2008;**8**(1):11-23.

34. Aplan PD. Causes of oncogenic chromosomal translocation. *Trends Genet* 2006;**22**(1):46-55.

35. Adam P, Katzenberger T, Seeberger H, et al. A case of a diffuse large B-cell lymphoma of plasmablastic type associated with the t(2;5)(p23;q35) chromosome translocation. *Am J Surg Pathol* 2003;**27**(11):1473-1476.

36. Cools J, Wlodarska I, Somers R, et al. Identification of novel fusion partners of ALK, the anaplastic lymphoma kinase, in anaplastic large-cell lymphoma and inflammatory myofibroblastic tumor. *Genes Chromosomes Cancer* 2002;**34**(4):354-362.

37. Hernandez L, Pinyol M, Hernandez S, et al. TRK-fused gene (TFG) is a new partner of ALK in anaplastic large cell lymphoma producing two

structurally different TFG-ALK translocations. *Blood* 1999;**94**(9):3265-3268.

38. Hernandez L, Bea S, Bellosillo B, et al. Diversity of genomic breakpoints in TFG-ALK translocations in anaplastic large cell lymphomas: identification of a new TFG-ALK(XL) chimeric gene with transforming activity. *Am J Pathol* 2002;**160**(4):1487-1494.

39. Rikova K, Guo A, Zeng Q, et al. Global survey of phosphotyrosine signaling identifies oncogenic kinases in lung cancer. *Cell* 2007;**131**(6):1190-1203.

40. Tort F, Pinyol M, Pulford K, et al. Molecular characterization of a new ALK translocation involving moesin (MSN-ALK) in anaplastic large cell lymphoma. *Lab Invest* 2001;**81**(3):419-426.

41. Lamant L, Dastugue N, Pulford K, Delsol G, Mariame B. A new fusion gene TPM3-ALK in anaplastic large cell lymphoma created by a (1;2)(q25;p23) translocation. *Blood* 1999;**93**(9):3088-3095.

42. Sugawara E, Togashi Y, Kuroda N, et al. Identification of anaplastic lymphoma kinase fusions in renal cancer: large-scale immunohistochemical screening by the intercalated antibody-enhanced polymer method. *Cancer* 2012;**118**(18):4427-4436.

43. Sukov WR, Hodge JC, Lohse CM, et al. ALK alterations in adult renal cell carcinoma: frequency, clinicopathologic features and outcome in a large series of consecutively treated patients. *Mod Pathol* 2012;**25**(11):1516-1525.

44. Lawrence B, Perez-Atayde A, Hibbard MK, et al. TPM3-ALK and TPM4-ALK oncogenes in inflammatory myofibroblastic tumors. *Am J Pathol* 2000;**157**(2):377-384.

45. Meech SJ, McGavran L, Odom LF, et al. Unusual childhood extramedullary hematologic malignancy with natural killer cell properties that contains tropomyosin 4--anaplastic lymphoma kinase gene fusion. *Blood* 2001;**98**(4):1209-1216.

46. Du XL, Hu H, Lin DC, et al. Proteomic profiling of proteins dysregulted in Chinese esophageal squamous cell carcinoma. *J Mol Med (Berl)* 2007;**85**(8):863-875.

47. Jazii FR, Najafi Z, Malekzadeh R, et al. Identification of squamous cell carcinoma associated proteins by proteomics and loss of beta tropomyosin expression in esophageal cancer. *World J Gastroenterol* 2006;**12**(44):7104-7112.

48. Colleoni GW, Bridge JA, Garicochea B, Liu J, Filippa DA, Ladanyi M. ATIC-ALK: A novel variant ALK gene fusion in anaplastic large cell lymphoma resulting from the recurrent cryptic chromosomal inversion, inv(2)(p23q35). *Am J Pathol* 2000;**156**(3):781-789.

49. Debiec-Rychter M, Marynen P, Hagemeijer A, Pauwels P. ALK-ATIC fusion in urinary bladder inflammatory myofibroblastic tumor. *Genes Chromosomes Cancer* 2003;**38**(2):187-190.

50. Lamant L, Gascoyne RD, Duplantier MM, et al. Non-muscle myosin heavy chain (MYH9): a new partner fused to ALK in anaplastic large cell lymphoma. *Genes Chromosomes Cancer* 2003;**37**(4):427-432.

51. Touriol C, Greenland C, Lamant L, et al. Further demonstration of the diversity of chromosomal changes involving 2p23 in ALK-positive lymphoma: 2 cases expressing ALK kinase fused to CLTCL (clathrin chain polypeptide-like). *Blood* 2000;**95**(10):3204-3207.

52. Patel AS, Murphy KM, Hawkins AL, et al. RANBP2 and CLTC are involved in ALK rearrangements in inflammatory myofibroblastic tumors. *Cancer Genet Cytogenet* 2007;**176**(2):107-114.

53. Bridge JA, Kanamori M, Ma Z, et al. Fusion of the ALK gene to the clathrin heavy chain gene, CLTC, in inflammatory myofibroblastic tumor. *Am J Pathol* 2001;**159**(2):411-415.

54. Gascoyne RD, Lamant L, Martin-Subero JI, et al. ALK-positive diffuse large B-cell lymphoma is associated with Clathrin-ALK rearrangements: report of 6 cases. *Blood* 2003;**102**(7):2568-2573.

55. Panagopoulos I, Nilsson T, Domanski HA, et al. Fusion of the SEC31L1 and ALK genes in an inflammatory myofibroblastic tumor. *Int J Cancer* 2006;**118**(5):1181-1186.

56. Van Roosbroeck K, Cools J, Dierickx D, et al. ALK-positive large B-cell lymphomas with cryptic SEC31A-ALK and NPM1-ALK fusions. *Haematologica* 2010;**95**(3):509-513.

57. Bedwell C, Rowe D, Moulton D, Jones G, Bown N, Bacon CM. Cytogenetically complex SEC31A-ALK fusions are recurrent in ALK-positive large B-cell lymphomas. *Haematologica* 2011;**96**(2):343-346.

58. Takeuchi K, Soda M, Togashi Y, et al. Pulmonary inflammatory myofibroblastic tumor expressing a novel fusion, PPFIBP1-ALK: reappraisal of anti-ALK immunohistochemistry as a tool for novel ALK fusion identification. *Clin Cancer Res* 2011;**17**(10):3341-3348.

59. Debelenko LV, Arthur DC, Pack SD, Helman LJ, Schrump DS, Tsokos M. Identification of CARS-ALK fusion in primary and metastatic lesions of an inflammatory myofibroblastic tumor. *Lab Invest* 2003;**83**(9):1255-1265.

60. Lin E, Li L, Guan Y, et al. Exon array profiling detects EML4-ALK fusion in breast, colorectal, and non-small cell lung cancers. *Mol Cancer Res* 2009;**7**(9):1466-1476.

61. Takeuchi K, Choi YL, Togashi Y, et al. KIF5B-ALK, a novel fusion oncokinase identified by an immunohistochemistry-based diagnostic system for ALK-positive lung cancer. *Clin Cancer Res* 2009;**15**(9):3143-3149.

62. Togashi Y, Soda M, Sakata S, et al. KLC1-ALK: a novel fusion in lung cancer identified using a formalin-fixed paraffin-embedded tissue only. *PLoS One* 2012;**7**(2):e31323.

63. Jung Y, Kim P, Jung Y, et al. Discovery of ALK-PTPN3 gene fusion from human non-small cell lung carcinoma cell line using next generation RNA sequencing. *Genes Chromosomes Cancer* 2012;**51**(6):590-597.

64. Majewski IJ, Mittempergher L, Davidson NM, et al. Identification of recurrent FGFR3 fusion genes in lung cancer through kinome-centred RNA sequencing. *J Pathol* 2013;**230**(3):270-276.

65. Takeuchi K, Soda M, Togashi Y, et al. Identification of a novel fusion, SQSTM1-ALK, in ALK-positive large B-cell lymphoma. *Haematologica* 2011;**96**(3):464-467.

66. Debelenko LV, Raimondi SC, Daw N, et al. Renal cell carcinoma with novel VCL-ALK fusion: new representative of ALK-associated tumor spectrum. *Mod Pathol* 2011;**24**(3):430-442.

67. Lipson D, Capelletti M, Yelensky R, et al. Identification of new ALK and RET gene fusions from colorectal and lung cancer biopsies. *Nat Med* 2012;**18**(3):382-384.

68. Ren H, Tan ZP, Zhu X, et al. Identification of anaplastic lymphoma kinase as a potential therapeutic target in ovarian cancer. *Cancer Res* 2012;**72**(13):3312-3323.

69. Mathas S, Kreher S, Meaburn KJ, et al. Gene deregulation and spatial genome reorganization near breakpoints prior to formation of translocations in anaplastic large cell lymphoma. *Proc Natl Acad Sci U S A* 2009;**106**(14):5831-5836.

70. Lieber MR, Yu K, Raghavan SC. Roles of nonhomologous DNA end joining, V(D)J recombination, and class switch recombination in chromosomal translocations. *DNA Repair (Amst)* 2006;**5**(9-10):1234-1245.

71. Nikiforova MN, Stringer JR, Blough R, Medvedovic M, Fagin JA, Nikiforov YE. Proximity of chromosomal loci that participate in radiation-induced rearrangements in human cells. *Science* 2000;**290**(5489):138-141.

72. Aten JA, Stap J, Krawczyk PM, et al. Dynamics of DNA double-strand breaks revealed by clustering of damaged chromosome domains. *Science* 2004;**303**(5654):92-95.

73. Meaburn KJ, Misteli T, Soutoglou E. Spatial genome organization in the formation of chromosomal translocations. *Semin Cancer Biol* 2007;**17**(1):80-90.

74. Soutoglou E, Dorn JF, Sengupta K, et al. Positional stability of single double-strand breaks in mammalian cells. *Nat Cell Biol* 2007;**9**(6):675-682.

75. Roix JJ, McQueen PG, Munson PJ, Parada LA, Misteli T. Spatial proximity of translocation-prone gene loci in human lymphomas. *Nat Genet* 2003;**34**(3):287-291.

76. Lischwe MA, Smetana K, Olson MO, Busch H. Proteins C23 and B23 are the major nucleolar silver staining proteins. *Life Sci* 1979;**25**(8):701-708.

77. Michalik J, Yeoman LC, Busch H. Nucleolar localization of protein B23 (37/5.1) by immunocytochemical techniques. *Life Sci* 1981;**28**(12):1371-1379.

78. Bischof D, Pulford K, Mason DY, Morris SW. Role of the nucleophosmin (NPM) portion of the non-Hodgkin's lymphoma-associated NPM-anaplastic lymphoma kinase fusion protein in oncogenesis. *Mol Cell Biol* 1997;**17**(4):2312-2325.

79. Benharroch D, Meguerian-Bedoyan Z, Lamant L, et al. ALK-positive lymphoma: a single disease with a broad spectrum of morphology. *Blood* 1998;**91**(6):2076-2084.

80. Gascoyne RD, Aoun P, Wu D, et al. Prognostic significance of anaplastic lymphoma kinase (ALK) protein expression in adults with anaplastic large cell lymphoma. *Blood* 1999;**93**(11):3913-3921.

81. Falini B, Pileri S, Zinzani PL, et al. ALK+ lymphoma: clinico-pathological findings and outcome. *Blood* 1999;**93**(8):2697-2706.

82. Shiota M, Nakamura S, Ichinohasama R, et al. Anaplastic large cell lymphomas expressing the novel chimeric protein p80NPM/ALK: a distinct clinicopathologic entity. *Blood* 1995;**86**(5):1954-1960.

83. Takahashi D, Nagatoshi Y, Nagayama J, et al. Anaplastic large cell lymphoma in leukemic presentation: a case report and a review of the literature. *J Pediatr Hematol Oncol* 2008;**30**(9):696-700.

84. Fraga M, Brousset P, Schlaifer D, et al. Bone marrow involvement in anaplastic large cell lymphoma. Immunohistochemical detection of minimal disease and its prognostic significance. *Am J Clin Pathol* 1995;**103**(1):82-89.

85. Mussolin L, Pillon M, d'Amore ES, et al. Prevalence and clinical implications of bone marrow involvement in pediatric anaplastic large cell lymphoma. *Leukemia* 2005;**19**(9):1643-1647.

86. Damm-Welk C, Busch K, Burkhardt B, et al. Prognostic significance of circulating tumor cells in bone marrow or peripheral blood as detected by qualitative and quantitative PCR in pediatric NPM-ALK-positive anaplastic large-cell lymphoma. *Blood* 2007;**110**(2):670-677.

87. Pileri S, Falini B, Delsol G, et al. Lymphohistiocytic T-cell lymphoma (anaplastic large cell lymphoma CD30+/Ki-1 + with a high content of reactive histiocytes). *Histopathology* 1990;**16**(4):383-391.

88. Pileri SA, Pulford K, Mori S, et al. Frequent expression of the NPM-ALK chimeric fusion protein in anaplastic large-cell lymphoma, lympho-histiocytic type. *Am J Pathol* 1997;**150**(4):1207-1211.

89. Kinney MC, Collins RD, Greer JP, Whitlock JA, Sioutos N, Kadin ME. A small-cell-predominant variant of primary Ki-1 (CD30)+ T-cell lymphoma. *Am J Surg Pathol* 1993;**17**(9):859-868.

90. Vassallo J, Lamant L, Brugieres L, et al. ALK-positive anaplastic large cell lymphoma mimicking nodular sclerosis Hodgkin's lymphoma: report of 10 cases. *Am J Surg Pathol* 2006;**30**(2):223-229.

91. Chiarle R, Podda A, Prolla G, Gong J, Thorbecke GJ, Inghirami G. CD30 in normal and neoplastic cells. *Clin Immunol* 1999;**90**(2):157-164.

92. ten Berge RL, Snijdewint FG, von Mensdorff-Pouilly S, et al. MUC1 (EMA) is preferentially expressed by ALK positive anaplastic large cell

lymphoma, in the normally glycosylated or only partly hypoglycosylated form. *J Clin Pathol* 2001;**54**(12):933-939.

93. Delsol G, Al Saati T, Gatter KC, et al. Coexpression of epithelial membrane antigen (EMA), Ki-1, and interleukin-2 receptor by anaplastic large cell lymphomas. Diagnostic value in so-called malignant histiocytosis. *Am J Pathol* 1988;**130**(1):59-70.

94. Jacobsen E. Anaplastic large-cell lymphoma, T-/null-cell type. *Oncologist* 2006;**11**(7):831-840.

95. Foss HD, Anagnostopoulos I, Araujo I, et al. Anaplastic large-cell lymphomas of T-cell and null-cell phenotype express cytotoxic molecules. *Blood* 1996;**88**(10):4005-4011.

96. Krenacs L, Wellmann A, Sorbara L, et al. Cytotoxic cell antigen expression in anaplastic large cell lymphomas of T- and null-cell type and Hodgkin's disease: evidence for distinct cellular origin. *Blood* 1997;**89**(3):980-989.

97. Savage KJ, Harris NL, Vose JM, et al. ALK- anaplastic large-cell lymphoma is clinically and immunophenotypically different from both ALK+ ALCL and peripheral T-cell lymphoma, not otherwise specified: report from the International Peripheral T-Cell Lymphoma Project. *Blood* 2008;**111**(12):5496-5504.

98. Ferreri AJ, Govi S, Pileri SA, Savage KJ. Anaplastic large cell lymphoma, ALK-positive. *Crit Rev Oncol Hematol* 2012;**83**(2):293-302.

99. Brugieres L, Deley MC, Pacquement H, et al. CD30(+) anaplastic large-cell lymphoma in children: analysis of 82 patients enrolled in two consecutive studies of the French Society of Pediatric Oncology. *Blood* 1998;**92**(10):3591-3598.

100. Bordon V, De Paepe P, Dhooge C, Vandecruys E, Benoit Y, Laureys G. Successful treatment with allogeneic bone marrow transplantation of an early relapse of ALK-positive anaplastic large cell lymphoma. *Haematologica* 2005;**90**(3):ECR19.

101. Fujimoto J, Shiota M, Iwahara T, et al. Characterization of the transforming activity of p80, a hyperphosphorylated protein in a Ki-1 lymphoma cell line with chromosomal translocation t(2;5). *Proc Natl Acad Sci U S A* 1996;**93**(9):4181-4186.

102. Mason DY, Pulford KA, Bischof D, et al. Nucleolar localization of the nucleophosmin-anaplastic lymphoma kinase is not required for malignant transformation. *Cancer Res* 1998;**58**(5):1057-1062.

103. Bai RY, Dieter P, Peschel C, Morris SW, Duyster J. Nucleophosmin-anaplastic lymphoma kinase of large-cell anaplastic lymphoma is a constitutively active tyrosine kinase that utilizes phospholipase C-gamma to mediate its mitogenicity. *Mol Cell Biol* 1998;**18**(12):6951-6961.

104. Zhang Q, Wei F, Wang HY, et al. The potent oncogene NPM-ALK mediates malignant transformation of normal human CD4(+) T lymphocytes. *Am J Pathol* 2013;**183**(6):1971-1980.

105. Chiarle R, Gong JZ, Guasparri I, et al. NPM-ALK transgenic mice spontaneously develop T-cell lymphomas and plasma cell tumors. *Blood* 2003;**101**(5):1919-1927.

106. Turner SD, Tooze R, Maclennan K, Alexander DR. Vav-promoter regulated oncogenic fusion protein NPM-ALK in transgenic mice causes B-cell lymphomas with hyperactive Jun kinase. *Oncogene* 2003;**22**(49):7750-7761.

107. Lange K, Uckert W, Blankenstein T, et al. Overexpression of NPM-ALK induces different types of malignant lymphomas in IL-9 transgenic mice. *Oncogene* 2003;**22**(4):517-527.

108. Jager R, Hahne J, Jacob A, et al. Mice transgenic for NPM-ALK develop non-Hodgkin lymphomas. *Anticancer Res* 2005;**25**(5):3191-3196.

109. Turner SD, Merz H, Yeung D, Alexander DR. CD2 promoter regulated nucleophosmin-anaplastic lymphoma kinase in transgenic mice causes B lymphoid malignancy. *Anticancer Res* 2006;**26**(5A):3275-3279.

110. Giuriato S, Foisseau M, Dejean E, et al. Conditional TPM3-ALK and NPM-ALK transgenic mice develop reversible ALK-positive early B-cell lymphoma/leukemia. *Blood* 2010;**115**(20):4061-4070.

111. Grande E, Bolos MV, Arriola E. Targeting oncogenic ALK: a promising strategy for cancer treatment. *Mol Cancer Ther* 2011;**10**(4):569-579.

112. Lai R, Ingham RJ. The pathobiology of the oncogenic tyrosine kinase NPM-ALK: a brief update. *Ther Adv Hematol* 2013;**4**(2):119-131.

113. Pearson JD, Lee JK, Bacani JT, Lai R, Ingham RJ. NPM-ALK: the prototypic member of a family of oncogenic fusion tyrosine kinases. *J Signal Transduct* 2012;**2012**:123253.

114. Zamo A, Chiarle R, Piva R, et al. Anaplastic lymphoma kinase (ALK) activates Stat3 and protects hematopoietic cells from cell death. *Oncogene* 2002;**21**(7):1038-1047.

115. Zhang Q, Raghunath PN, Xue L, et al. Multilevel dysregulation of STAT3 activation in anaplastic lymphoma kinase-positive T/null-cell lymphoma. *J Immunol* 2002;**168**(1):466-474.

116. Santos CI, Costa-Pereira AP. Signal transducers and activators of transcription-from cytokine signalling to cancer biology. *Biochim Biophys Acta* 2011;**1816**(1):38-49.

117. Levy DE, Darnell JE, Jr. Stats: transcriptional control and biological impact. *Nat Rev Mol Cell Biol* 2002;**3**(9):651-662.

118. Chiarle R, Simmons WJ, Cai H, et al. Stat3 is required for ALK-mediated lymphomagenesis and provides a possible therapeutic target. *Nat Med* 2005;**11**(6):623-629.

119. Khoury JD, Medeiros LJ, Rassidakis GZ, et al. Differential expression and clinical significance of tyrosine-phosphorylated STAT3 in ALK+ and ALK- anaplastic large cell lymphoma. *Clin Cancer Res* 2003;**9**(10 Pt 1):3692-3699.

120. Bromberg JF, Wrzeszczynska MH, Devgan G, et al. Stat3 as an oncogene. *Cell* 1999;**98**(3):295-303.

121. Devarajan E, Huang S. STAT3 as a central regulator of tumor metastases. *Curr Mol Med* 2009;**9**(5):626-633.

122. Alvarez JV, Febbo PG, Ramaswamy S, Loda M, Richardson A, Frank DA. Identification of a genetic signature of activated signal transducer and activator of transcription 3 in human tumors. *Cancer Res* 2005;**65**(12):5054-5062.

123. Amin HM, McDonnell TJ, Ma Y, et al. Selective inhibition of STAT3 induces apoptosis and G(1) cell cycle arrest in ALK-positive anaplastic large cell lymphoma. *Oncogene* 2004;**23**(32):5426-5434.

124. Piva R, Agnelli L, Pellegrino E, et al. Gene expression profiling uncovers molecular classifiers for the recognition of anaplastic large-cell lymphoma within peripheral T-cell neoplasms. *J Clin Oncol* 2010;**28**(9):1583-1590.

125. Khoury JD, Rassidakis GZ, Medeiros LJ, Amin HM, Lai R. Methylation of SHP1 gene and loss of SHP1 protein expression are frequent in systemic anaplastic large cell lymphoma. *Blood* 2004;**104**(5):1580-1581.

126. Hegazy SA, Wang P, Anand M, Ingham RJ, Gelebart P, Lai R. The tyrosine 343 residue of nucleophosmin (NPM)-anaplastic lymphoma kinase (ALK) is important for its interaction with SHP1, a cytoplasmic tyrosine phosphatase with tumor suppressor functions. *J Biol Chem* 2010;**285**(26):19813-19820.

127. Han Y, Amin HM, Franko B, Frantz C, Shi X, Lai R. Loss of SHP1 enhances JAK3/STAT3 signaling and decreases proteosome degradation of JAK3 and NPM-ALK in ALK+ anaplastic large-cell lymphoma. *Blood* 2006;**108**(8):2796-2803.

128. Zhang Q, Wang HY, Liu X, Wasik MA. STAT5A is epigenetically silenced by the tyrosine kinase NPM1-ALK and acts as a tumor suppressor by reciprocally inhibiting NPM1-ALK expression. *Nat Med* 2007;**13**(11):1341-1348.

129. Qiu L, Lai R, Lin Q, et al. Autocrine release of interleukin-9 promotes Jak3-dependent survival of ALK+ anaplastic large-cell lymphoma cells. *Blood* 2006;**108**(7):2407-2415.

130. Dien Bard J, Gelebart P, Anand M, et al. IL-21 contributes to JAK3/STAT3 activation and promotes cell growth in ALK-positive anaplastic large cell lymphoma. *Am J Pathol* 2009;**175**(2):825-834.

131. Crockett DK, Lin Z, Elenitoba-Johnson KS, Lim MS. Identification of NPM-ALK interacting proteins by tandem mass spectrometry. *Oncogene* 2004;**23**(15):2617-2629.

132. Amin HM, Medeiros LJ, Ma Y, et al. Inhibition of JAK3 induces apoptosis and decreases anaplastic lymphoma kinase activity in anaplastic large cell lymphoma. *Oncogene* 2003;**22**(35):5399-5407.

133. Bard JD, Gelebart P, Anand M, Amin HM, Lai R. Aberrant expression of IL-22 receptor 1 and autocrine IL-22 stimulation contribute to tumorigenicity in ALK+ anaplastic large cell lymphoma. *Leukemia* 2008;**22**(8):1595-1603.

134. Geest CR, Coffer PJ. MAPK signaling pathways in the regulation of hematopoiesis. *J Leukoc Biol* 2009;**86**(2):237-250.

135. Steelman LS, Franklin RA, Abrams SL, et al. Roles of the Ras/Raf/MEK/ERK pathway in leukemia therapy. *Leukemia* 2011;**25**(7):1080-1094.

136. Watanabe M, Sasaki M, Itoh K, et al. JunB induced by constitutive CD30-extracellular signal-regulated kinase 1/2 mitogen-activated protein kinase signaling activates the CD30 promoter in anaplastic large cell lymphoma and reed-sternberg cells of Hodgkin lymphoma. *Cancer Res* 2005;**65**(17):7628-7634.

137. Staber PB, Vesely P, Haq N, et al. The oncoprotein NPM-ALK of anaplastic large-cell lymphoma induces JUNB transcription via ERK1/2 and JunB translation via mTOR signaling. *Blood* 2007;**110**(9):3374-3383.

138. Marzec M, Kasprzycka M, Liu X, Raghunath PN, Wlodarski P, Wasik MA. Oncogenic tyrosine kinase NPM/ALK induces activation of the

MEK/ERK signaling pathway independently of c-Raf. *Oncogene* 2007;**26**(6):813-821.

139. Rassidakis GZ, Thomaides A, Atwell C, et al. JunB expression is a common feature of CD30+ lymphomas and lymphomatoid papulosis. *Mod Pathol* 2005;**18**(10):1365-1370.

140. Mathas S, Hinz M, Anagnostopoulos I, et al. Aberrantly expressed c-Jun and JunB are a hallmark of Hodgkin lymphoma cells, stimulate proliferation and synergize with NF-kappa B. *EMBO J* 2002;**21**(15):4104-4113.

141. Hsu FY, Johnston PB, Burke KA, Zhao Y. The expression of CD30 in anaplastic large cell lymphoma is regulated by nucleophosmin-anaplastic lymphoma kinase-mediated JunB level in a cell type-specific manner. *Cancer Res* 2006;**66**(18):9002-9008.

142. Watanabe M, Itoh K, Togano T, et al. Ets-1 activates overexpression of JunB and CD30 in Hodgkin's lymphoma and anaplastic large-cell lymphoma. *Am J Pathol* 2012;**180**(2):831-838.

143. Black AR, Black JD. Protein kinase C signaling and cell cycle regulation. *Front Immunol* 2012;**3**:423.

144. Koivunen J, Aaltonen V, Peltonen J. Protein kinase C (PKC) family in cancer progression. *Cancer Lett* 2006;**235**(1):1-10.

145. Fresno Vara JA, Casado E, de Castro J, Cejas P, Belda-Iniesta C, Gonzalez-Baron M. PI3K/Akt signalling pathway and cancer. *Cancer Treat Rev* 2004;**30**(2):193-204.

146. Bai RY, Ouyang T, Miething C, Morris SW, Peschel C, Duyster J. Nucleophosmin-anaplastic lymphoma kinase associated with anaplastic large-cell lymphoma activates the phosphatidylinositol 3-kinase/Akt antiapoptotic signaling pathway. *Blood* 2000;**96**(13):4319-4327.

147. Slupianek A, Nieborowska-Skorska M, Hoser G, et al. Role of phosphatidylinositol 3-kinase-Akt pathway in nucleophosmin/anaplastic lymphoma kinase-mediated lymphomagenesis. *Cancer Res* 2001;**61**(5):2194-2199.

148. Singh RR, Cho-Vega JH, Davuluri Y, et al. Sonic hedgehog signaling pathway is activated in ALK-positive anaplastic large cell lymphoma. *Cancer Res* 2009;**69**(6):2550-2558.

149. Amakye D, Jagani Z, Dorsch M. Unraveling the therapeutic potential of the Hedgehog pathway in cancer. *Nat Med* 2013;**19**(11):1410-1422.

150. Villavicencio EH, Walterhouse DO, Iannaccone PM. The sonic hedgehog-patched-gli pathway in human development and disease. *Am J Hum Genet* 2000;**67**(5):1047-1054.

151. Riobo NA, Lu K, Ai X, Haines GM, Emerson CP, Jr. Phosphoinositide 3-kinase and Akt are essential for Sonic Hedgehog signaling. *Proc Natl Acad Sci U S A* 2006;**103**(12):4505-4510.

152. Soda M, Choi YL, Enomoto M, et al. Identification of the transforming EML4-ALK fusion gene in non-small-cell lung cancer. *Nature* 2007;**448**(7153):561-566.

153. Solomon B, Wilner KD, Shaw AT. Current status of targeted therapy for anaplastic lymphoma kinase-rearranged non-small cell lung cancer. *Clin Pharmacol Ther* 2014;**95**(1):15-23.

154. Camidge DR, Bang YJ, Kwak EL, et al. Activity and safety of crizotinib in patients with ALK-positive non-small-cell lung cancer: updated results from a phase 1 study. *Lancet Oncol* 2012;**13**(10):1011-1019.

155. Shaw AT, Yeap BY, Solomon BJ, et al. Effect of crizotinib on overall survival in patients with advanced non-small-cell lung cancer harbouring ALK gene rearrangement: a retrospective analysis. *Lancet Oncol* 2011;**12**(11):1004-1012.

156. Marsilje TH, Pei W, Chen B, et al. Synthesis, structure-activity relationships, and in vivo efficacy of the novel potent and selective anaplastic lymphoma kinase (ALK) inhibitor 5-chloro-N2-(2-isopropoxy-5-methyl-4-(piperidin-4-yl)phenyl)-N4-(2-(isopropylsulf onyl)phenyl)pyrimidine-2,4-diamine (LDK378) currently in phase 1 and phase 2 clinical trials. *J Med Chem* 2013;**56**(14):5675-5690.

157. Sakamoto H, Tsukaguchi T, Hiroshima S, et al. CH5424802, a selective ALK inhibitor capable of blocking the resistant gatekeeper mutant. *Cancer Cell* 2011;**19**(5):679-690.

158. Kinoshita K, Asoh K, Furuichi N, et al. Design and synthesis of a highly selective, orally active and potent anaplastic lymphoma kinase inhibitor (CH5424802). *Bioorg Med Chem* 2012;**20**(3):1271-1280.

159. Seto T, Kiura K, Nishio M, et al. CH5424802 (RO5424802) for patients with ALK-rearranged advanced non-small-cell lung cancer (AF-001JP study): a single-arm, open-label, phase 1-2 study. *Lancet Oncol* 2013;**14**(7):590-598.

160. Rossi A, Maione P, Sacco PC, et al. ALK inhibitors and advanced non-small cell lung cancer (Review). *Int J Oncol* 2014;**45**(2):499-508.

161. Mori M, Ueno Y, Konagai S, et al. The selective anaplastic lymphoma receptor tyrosine kinase inhibitor ASP3026 induces tumor regression and prolongs survival in non-small cell lung cancer model mice. *Mol Cancer Ther* 2014;**13**(2):329-340.

162. Kwak EL, Bang YJ, Camidge DR, et al. Anaplastic lymphoma kinase inhibition in non-small-cell lung cancer. *N Engl J Med* 2010;**363**(18):1693-1703.

163. Butrynski JE, D'Adamo DR, Hornick JL, et al. Crizotinib in ALK-rearranged inflammatory myofibroblastic tumor. *N Engl J Med* 2010;**363**(18):1727-1733.

164. Gambacorti Passerini C, Farina F, Stasia A, et al. Crizotinib in advanced, chemoresistant anaplastic lymphoma kinase-positive lymphoma patients. *J Natl Cancer Inst* 2014;**106**(2):djt378.

165. Mosse YP, Lim MS, Voss SD, et al. Safety and activity of crizotinib for paediatric patients with refractory solid tumours or anaplastic large-cell lymphoma: a Children's Oncology Group phase 1 consortium study. *Lancet Oncol* 2013;**14**(6):472-480.

166. Shaw AT, Kim DW, Nakagawa K, et al. Crizotinib versus chemotherapy in advanced ALK-positive lung cancer. *N Engl J Med* 2013;**368**(25):2385-2394.

167. Katayama R, Shaw AT, Khan TM, et al. Mechanisms of acquired crizotinib resistance in ALK-rearranged lung Cancers. *Sci Transl Med* 2012;**4**(120):120ra117.

168. Doebele RC, Pilling AB, Aisner DL, et al. Mechanisms of resistance to crizotinib in patients with ALK gene rearranged non-small cell lung cancer. *Clin Cancer Res* 2012;**18**(5):1472-1482.

169. Sasaki T, Koivunen J, Ogino A, et al. A novel ALK secondary mutation and EGFR signaling cause resistance to ALK kinase inhibitors. *Cancer Res* 2011;**71**(18):6051-6060.

170. Huang D, Kim DW, Kotsakis A, et al. Multiplexed deep sequencing analysis of ALK kinase domain identifies resistance mutations in relapsed patients following crizotinib treatment. *Genomics* 2013;**102**(3):157-162.

171. Choi YL, Soda M, Yamashita Y, et al. EML4-ALK mutations in lung cancer that confer resistance to ALK inhibitors. *N Engl J Med* 2010;**363**(18):1734-1739.

172. Kim S, Kim TM, Kim DW, et al. Heterogeneity of genetic changes associated with acquired crizotinib resistance in ALK-rearranged lung cancer. *J Thorac Oncol* 2013;**8**(4):415-422.

173. Liang J, Wu YL, Chen BJ, Zhang W, Tanaka Y, Sugiyama H. The C-kit receptor-mediated signal transduction and tumor-related diseases. *Int J Biol Sci* 2013;**9**(5):435-443.

174. Stankov K, Popovic S, Mikov M. C-KIT signaling in cancer treatment. *Curr Pharm Des* 2014;**20**(17):2849-2880.

175. Wu F, Wang P, Young LC, Lai R, Li L. Proteome-wide identification of novel binding partners to the oncogenic fusion gene protein, NPM-ALK, using tandem affinity purification and mass spectrometry. *Am J Pathol* 2009;**174**(2):361-370.

176. Galietta A, Gunby RH, Redaelli S, et al. NPM/ALK binds and phosphorylates the RNA/DNA-binding protein PSF in anaplastic large-cell lymphoma. *Blood* 2007;**110**(7):2600-2609.

177. Jascur T, Boland CR. Structure and function of the components of the human DNA mismatch repair system. *Int J Cancer* 2006;**119**(9):2030-2035.

178. Li GM. Mechanisms and functions of DNA mismatch repair. *Cell Res* 2008;**18**(1):85-98.

179. Jiricny J. The multifaceted mismatch-repair system. *Nat Rev Mol Cell Biol* 2006;**7**(5):335-346.

180. Peltomaki P. Role of DNA mismatch repair defects in the pathogenesis of human cancer. *J Clin Oncol* 2003;**21**(6):1174-1179.

181. Fishel R. The selection for mismatch repair defects in hereditary nonpolyposis colorectal cancer: revising the mutator hypothesis. *Cancer Res* 2001;**61**(20):7369-7374.

182. Jiricny J. Replication errors: cha(lle)nging the genome. *EMBO J* 1998;**17**(22):6427-6436.

183. Drummond JT, Li GM, Longley MJ, Modrich P. Isolation of an hMSH2-p160 heterodimer that restores DNA mismatch repair to tumor cells. *Science* 1995;**268**(5219):1909-1912.

184. Palombo F, Iaccarino I, Nakajima E, Ikejima M, Shimada T, Jiricny J. hMutSbeta, a heterodimer of hMSH2 and hMSH3, binds to insertion/deletion loops in DNA. *Curr Biol* 1996;**6**(9):1181-1184.

185. Marra G, Iaccarino I, Lettieri T, Roscilli G, Delmastro P, Jiricny J. Mismatch repair deficiency associated with overexpression of the MSH3 gene. *Proc Natl Acad Sci U S A* 1998;**95**(15):8568-8573.

186. Iaccarino I, Marra G, Dufner P, Jiricny J. Mutation in the magnesium binding site of hMSH6 disables the hMutSalpha sliding clamp from translocating along DNA. *J Biol Chem* 2000;**275**(3):2080-2086.

187. Gradia S, Subramanian D, Wilson T, et al. hMSH2-hMSH6 forms a hydrolysis-independent sliding clamp on mismatched DNA. *Mol Cell* 1999;**3**(2):255-261.

188. Blackwell LJ, Martik D, Bjornson KP, Bjornson ES, Modrich P. Nucleotide-promoted release of hMutSalpha from heteroduplex DNA is consistent with an ATP-dependent translocation mechanism. *J Biol Chem* 1998;**273**(48):32055-32062.

189. Stojic L, Brun R, Jiricny J. Mismatch repair and DNA damage signalling. *DNA Repair (Amst)* 2004;**3**(8-9):1091-1101.

190. Gradia S, Acharya S, Fishel R. The human mismatch recognition complex hMSH2-hMSH6 functions as a novel molecular switch. *Cell* 1997;**91**(7):995-1005.

191. Thomas DC, Roberts JD, Kunkel TA. Heteroduplex repair in extracts of human HeLa cells. *J Biol Chem* 1991;**266**(6):3744-3751.

192. Genschel J, Bazemore LR, Modrich P. Human exonuclease I is required for 5' and 3' mismatch repair. *J Biol Chem* 2002;**277**(15):13302-13311.

193. Li GM, Modrich P. Restoration of mismatch repair to nuclear extracts of H6 colorectal tumor cells by a heterodimer of human MutL homologs. *Proc Natl Acad Sci U S A* 1995;**92**(6):1950-1954.

194. Fang WH, Modrich P. Human strand-specific mismatch repair occurs by a bidirectional mechanism similar to that of the bacterial reaction. *J Biol Chem* 1993;**268**(16):11838-11844.

195. Guo S, Presnell SR, Yuan F, Zhang Y, Gu L, Li GM. Differential requirement for proliferating cell nuclear antigen in 5' and 3' nick-directed excision in human mismatch repair. *J Biol Chem* 2004;**279**(17):16912-16917.

196. Umar A, Boyer JC, Thomas DC, et al. Defective mismatch repair in extracts of colorectal and endometrial cancer cell lines exhibiting microsatellite instability. *J Biol Chem* 1994;**269**(20):14367-14370.

197. Dzantiev L, Constantin N, Genschel J, Iyer RR, Burgers PM, Modrich P. A defined human system that supports bidirectional mismatch-provoked excision. *Mol Cell* 2004;**15**(1):31-41.

198. Longley MJ, Pierce AJ, Modrich P. DNA polymerase delta is required for human mismatch repair in vitro. *J Biol Chem* 1997;**272**(16):10917-10921.

199. Desclozeaux M, Poulat F, de Santa Barbara P, et al. Phosphorylation of an N-terminal motif enhances DNA-binding activity of the human SRY protein. *J Biol Chem* 1998;**273**(14):7988-7995.

200. Scott MT, Ingram A, Ball KL. PDK1-dependent activation of atypical PKC leads to degradation of the p21 tumour modifier protein. *EMBO J* 2002;**21**(24):6771-6780.

201. Sakamoto Y, Yoshida M, Semba K, Hunter T. Inhibition of the DNA-binding and transcriptional repression activity of the Wilms' tumor gene product, WT1, by cAMP-dependent protein kinase-mediated phosphorylation of Ser-365 and Ser-393 in the zinc finger domain. *Oncogene* 1997;**15**(17):2001-2012.

202. Ghosh S, Baltimore D. Activation in vitro of NF-kappa B by phosphorylation of its inhibitor I kappa B. *Nature* 1990;**344**(6267):678-682.

203. Gould KL, Woodgett JR, Cooper JA, Buss JE, Shalloway D, Hunter T. Protein kinase C phosphorylates pp60src at a novel site. *Cell* 1985;**42**(3):849-857.

204. Ye Y, Raychaudhuri B, Gurney A, Campbell CE, Williams BR. Regulation of WT1 by phosphorylation: inhibition of DNA binding, alteration of transcriptional activity and cellular translocation. *EMBO J* 1996;**15**(20):5606-5615.

205. Christmann M, Tomicic MT, Kaina B. Phosphorylation of mismatch repair proteins MSH2 and MSH6 affecting MutSalpha mismatch-binding activity. *Nucleic Acids Res* 2002;**30**(9):1959-1966.

206. Kaliyaperumal S, Patrick SM, Williams KJ. Phosphorylated hMSH6: DNA mismatch versus DNA damage recognition. *Mutat Res* 2011;**706**(1-2):36-45.

207. Christmann M, Kaina B. Nuclear translocation of mismatch repair proteins MSH2 and MSH6 as a response of cells to alkylating agents. *J Biol Chem* 2000;**275**(46):36256-36262.

208. Hayes AP, Sevi LA, Feldt MC, Rose MD, Gammie AE. Reciprocal regulation of nuclear import of the yeast MutSalpha DNA mismatch repair proteins Msh2 and Msh6. *DNA Repair (Amst)* 2009;**8**(6):739-751.

209. Hernandez-Pigeon H, Quillet-Mary A, Louat T, et al. hMutS alpha is protected from ubiquitin-proteasome-dependent degradation by atypical protein kinase C zeta phosphorylation. *J Mol Biol* 2005;**348**(1):63-74.

210. Hernandez-Pigeon H, Laurent G, Humbert O, Salles B, Lautier D. Degradration of mismatch repair hMutSalpha heterodimer by the ubiquitin-proteasome pathway. *FEBS Lett* 2004;**562**(1-3):40-44.

211. Kubbutat MH, Jones SN, Vousden KH. Regulation of p53 stability by Mdm2. *Nature* 1997;**387**(6630):299-303.

212. Sharma S, Salehi F, Scheithauer BW, Rotondo F, Syro LV, Kovacs K. Role of MGMT in tumor development, progression, diagnosis, treatment and prognosis. *Anticancer Res* 2009;**29**(10):3759-3768.

213. Yoshioka K, Yoshioka Y, Hsieh P. ATR kinase activation mediated by MutSalpha and MutLalpha in response to cytotoxic O6-methylguanine adducts. *Mol Cell* 2006;**22**(4):501-510.

214. Karran P. Mechanisms of tolerance to DNA damaging therapeutic drugs. *Carcinogenesis* 2001;**22**(12):1931-1937.

215. Hawn MT, Umar A, Carethers JM, et al. Evidence for a connection between the mismatch repair system and the G2 cell cycle checkpoint. *Cancer Res* 1995;**55**(17):3721-3725.

216. Adamson AW, Beardsley DI, Kim WJ, Gao Y, Baskaran R, Brown KD. Methylator-induced, mismatch repair-dependent G2 arrest is activated through Chk1 and Chk2. *Mol Biol Cell* 2005;**16**(3):1513-1526.

217. Cejka P, Stojic L, Mojas N, et al. Methylation-induced G(2)/M arrest requires a full complement of the mismatch repair protein hMLH1. *EMBO J* 2003;**22**(9):2245-2254.

218. Stojic L, Mojas N, Cejka P, et al. Mismatch repair-dependent G2 checkpoint induced by low doses of SN1 type methylating agents requires the ATR kinase. *Genes Dev* 2004;**18**(11):1331-1344.

219. Hickman MJ, Samson LD. Apoptotic signaling in response to a single type of DNA lesion, O(6)-methylguanine. *Mol Cell* 2004;**14**(1):105-116.

220. Duckett DR, Drummond JT, Murchie AI, et al. Human MutSalpha recognizes damaged DNA base pairs containing O6-methylguanine, O4-methylthymine, or the cisplatin-d(GpG) adduct. *Proc Natl Acad Sci U S A* 1996;**93**(13):6443-6447.

221. Gong JG, Costanzo A, Yang HQ, et al. The tyrosine kinase c-Abl regulates p73 in apoptotic response to cisplatin-induced DNA damage. *Nature* 1999;**399**(6738):806-809.

222. Brown KD, Rathi A, Kamath R, et al. The mismatch repair system is required for S-phase checkpoint activation. *Nat Genet* 2003;**33**(1):80-84.

223. Kim WJ, Rajasekaran B, Brown KD. MLH1- and ATM-dependent MAPK signaling is activated through c-Abl in response to the alkylator N-methyl-N'-nitro-N'-nitrosoguanidine. *J Biol Chem* 2007;**282**(44):32021-32031.

224. Shimodaira H, Yoshioka-Yamashita A, Kolodner RD, Wang JY. Interaction of mismatch repair protein PMS2 and the p53-related transcription factor p73 in apoptosis response to cisplatin. *Proc Natl Acad Sci U S A* 2003;**100**(5):2420-2425.

225. Kolodner RD, Putnam CD, Myung K. Maintenance of genome stability in Saccharomyces cerevisiae. *Science* 2002;**297**(5581):552-557.

226. Vogelstein B, Kinzler KW. Cancer genes and the pathways they control. *Nat Med* 2004;**10**(8):789-799.

227. Modrich P, Lahue R. Mismatch repair in replication fidelity, genetic recombination, and cancer biology. *Annu Rev Biochem* 1996;**65**:101-133.

228. Harfe BD, Jinks-Robertson S. DNA mismatch repair and genetic instability. *Annu Rev Genet* 2000;**34**:359-399.

229. Surtees JA, Argueso JL, Alani E. Mismatch repair proteins: key regulators of genetic recombination. *Cytogenet Genome Res* 2004;**107**(3-4):146-159.

230. Goldfarb T, Alani E. Distinct roles for the Saccharomyces cerevisiae mismatch repair proteins in heteroduplex rejection, mismatch repair and nonhomologous tail removal. *Genetics* 2005;**169**(2):563-574.

231. Sugawara N, Goldfarb T, Studamire B, Alani E, Haber JE. Heteroduplex rejection during single-strand annealing requires Sgs1 helicase and mismatch repair proteins Msh2 and Msh6 but not Pms1. *Proc Natl Acad Sci U S A* 2004;**101**(25):9315-9320.

232. Myung K, Datta A, Chen C, Kolodner RD. SGS1, the Saccharomyces cerevisiae homologue of BLM and WRN, suppresses genome instability and homeologous recombination. *Nat Genet* 2001;**27**(1):113-116.

233. Doherty KM, Sharma S, Uzdilla LA, et al. RECQ1 helicase interacts with human mismatch repair factors that regulate genetic recombination. *J Biol Chem* 2005;**280**(30):28085-28094.

234. Pedrazzi G, Bachrati CZ, Selak N, et al. The Bloom's syndrome helicase interacts directly with the human DNA mismatch repair protein hMSH6. *Biol Chem* 2003;**384**(8):1155-1164.

235. Wu Q, Christensen LA, Legerski RJ, Vasquez KM. Mismatch repair participates in error-free processing of DNA interstrand crosslinks in human cells. *EMBO Rep* 2005;**6**(6):551-557.

236. Zhang N, Liu X, Li L, Legerski R. Double-strand breaks induce homologous recombinational repair of interstrand cross-links via cooperation of MSH2, ERCC1-XPF, REV3, and the Fanconi anemia pathway. *DNA Repair (Amst)* 2007;**6**(11):1670-1678.

237. Zhang N, Lu X, Zhang X, Peterson CA, Legerski RJ. hMutSbeta is required for the recognition and uncoupling of psoralen interstrand cross-links in vitro. *Mol Cell Biol* 2002;**22**(7):2388-2397.

238. Bardwell PD, Woo CJ, Wei K, et al. Altered somatic hypermutation and reduced class-switch recombination in exonuclease 1-mutant mice. *Nat Immunol* 2004;**5**(2):224-229.

239. Ehrenstein MR, Rada C, Jones AM, Milstein C, Neuberger MS. Switch junction sequences in PMS2-deficient mice reveal a microhomology-mediated mechanism of Ig class switch recombination. *Proc Natl Acad Sci U S A* 2001;**98**(25):14553-14558.

240. Ehrenstein MR, Neuberger MS. Deficiency in Msh2 affects the efficiency and local sequence specificity of immunoglobulin class-switch recombination: parallels with somatic hypermutation. *EMBO J* 1999;**18**(12):3484-3490.

241. Schrader CE, Edelmann W, Kucherlapati R, Stavnezer J. Reduced isotype switching in splenic B cells from mice deficient in mismatch repair enzymes. *J Exp Med* 1999;**190**(3):323-330.

242. Martomo SA, Yang WW, Gearhart PJ. A role for Msh6 but not Msh3 in somatic hypermutation and class switch recombination. *J Exp Med* 2004;**200**(1):61-68.

243. Eccleston J, Yan C, Yuan K, Alt FW, Selsing E. Mismatch repair proteins MSH2, MLH1, and EXO1 are important for class-switch recombination events occurring in B cells that lack nonhomologous end joining. *J Immunol* 2011;**186**(4):2336-2343.

244. Hegde M, Ferber M, Mao R, et al. ACMG technical standards and guidelines for genetic testing for inherited colorectal cancer (Lynch syndrome, familial adenomatous polyposis, and MYH-associated polyposis). *Genetics in Medicine* 2014;**16**(1):101-116.

245. Strafford JC. Genetic testing for lynch syndrome, an inherited cancer of the bowel, endometrium, and ovary. *Rev Obstet Gynecol* 2012;**5**(1):42-49.

246. Bougeard G, Olivier-Faivre L, Baert-Desurmont S, et al. Diversity of the clinical presentation of the MMR gene biallelic mutations. *Fam Cancer* 2014;**13**(1):131-135.

247. Wimmer K, Etzler J. Constitutional mismatch repair-deficiency syndrome: have we so far seen only the tip of an iceberg? *Hum Genet* 2008;**124**(2):105-122.

248. Felton KE, Gilchrist DM, Andrew SE. Constitutive deficiency in DNA mismatch repair. *Clin Genet* 2007;**71**(6):483-498.

249. Grindedal EM, Moller P, Eeles R, et al. Germ-line mutations in mismatch repair genes associated with prostate cancer. *Cancer Epidemiol Biomarkers Prev* 2009;**18**(9):2460-2467.

250. Umar A, Boland CR, Terdiman JP, et al. Revised Bethesda Guidelines for hereditary nonpolyposis colorectal cancer (Lynch syndrome) and microsatellite instability. *J Natl Cancer Inst* 2004;**96**(4):261-268.

251. Shia J, Holck S, Depetris G, Greenson JK, Klimstra DS. Lynch syndrome-associated neoplasms: a discussion on histopathology and immunohistochemistry. *Fam Cancer* 2013;**12**(2):241-260.

252. Poulogiannis G, Frayling IM, Arends MJ. DNA mismatch repair deficiency in sporadic colorectal cancer and Lynch syndrome. *Histopathology* 2010;**56**(2):167-179.

253. Bartley AN, Luthra R, Saraiya DS, Urbauer DL, Broaddus RR. Identification of cancer patients with Lynch syndrome: clinically significant discordances and problems in tissue-based mismatch repair testing. *Cancer Prev Res (Phila)* 2012;**5**(2):320-327.

254. Baudhuin LM, Burgart LJ, Leontovich O, Thibodeau SN. Use of microsatellite instability and immunohistochemistry testing for the identification of individuals at risk for Lynch syndrome. *Fam Cancer* 2005;**4**(3):255-265.

255. Thibodeau SN, French AJ, Cunningham JM, et al. Microsatellite instability in colorectal cancer: different mutator phenotypes and the principal involvement of hMLH1. *Cancer Res* 1998;**58**(8):1713-1718.

256. Dietmaier W, Wallinger S, Bocker T, Kullmann F, Fishel R, Ruschoff J. Diagnostic microsatellite instability: definition and correlation with mismatch repair protein expression. *Cancer Res* 1997;**57**(21):4749-4756.

257. Lindor NM, Burgart LJ, Leontovich O, et al. Immunohistochemistry versus microsatellite instability testing in phenotyping colorectal tumors. *J Clin Oncol* 2002;**20**(4):1043-1048.

258. Terdiman JP, Gum JR, Jr., Conrad PG, et al. Efficient detection of hereditary nonpolyposis colorectal cancer gene carriers by screening for tumor microsatellite instability before germline genetic testing. *Gastroenterology* 2001;**120**(1):21-30.

259. Ruszkiewicz A, Bennett G, Moore J, et al. Correlation of mismatch repair genes immunohistochemistry and microsatellite instability status in HNPCC-associated tumours. *Pathology* 2002;**34**(6):541-547.

260. Stone JG, Robertson D, Houlston RS. Immunohistochemistry for MSH2 and MHL1: a method for identifying mismatch repair deficient colorectal cancer. *J Clin Pathol* 2001;**54**(6):484-487.

261. Halvarsson B, Lindblom A, Rambech E, Lagerstedt K, Nilbert M. Microsatellite instability analysis and/or immunostaining for the diagnosis of hereditary nonpolyposis colorectal cancer? *Virchows Arch* 2004;**444**(2):135-141.

262. Peltomaki P, Vasen H. Mutations associated with HNPCC predisposition -- Update of ICG-HNPCC/INSiGHT mutation database. *Dis Markers* 2004;**20**(4-5):269-276.

263. Salahshor S, Koelble K, Rubio C, Lindblom A. Microsatellite Instability and hMLH1 and hMSH2 expression analysis in familial and sporadic colorectal cancer. *Lab Invest* 2001;**81**(4):535-541.

264. Muller W, Burgart LJ, Krause-Paulus R, et al. The reliability of immunohistochemistry as a prescreening method for the diagnosis of hereditary nonpolyposis colorectal cancer (HNPCC)--results of an international collaborative study. *Fam Cancer* 2001;**1**(2):87-92.

265. Sood AK, Holmes R, Hendrix MJ, Buller RE. Application of the National Cancer Institute international criteria for determination of microsatellite instability in ovarian cancer. *Cancer Res* 2001;**61**(11):4371-4374.

266. Buhard O, Suraweera N, Lectard A, Duval A, Hamelin R. Quasimonomorphic mononucleotide repeats for high-level microsatellite instability analysis. *Dis Markers* 2004;**20**(4-5):251-257.

267. Demes M, Scheil-Bertram S, Bartsch H, Fisseler-Eckhoff A. Signature of microsatellite instability, KRAS and BRAF gene mutations in German patients with locally advanced rectal adenocarcinoma before and after neoadjuvant 5-FU radiochemotherapy. *J Gastrointest Oncol* 2013;**4**(2):182-192.

268. Hatch SB, Lightfoot HM, Jr., Garwacki CP, et al. Microsatellite instability testing in colorectal carcinoma: choice of markers affects sensitivity of detection of mismatch repair-deficient tumors. *Clin Cancer Res* 2005;**11**(6):2180-2187.

269. Wei K, Kucherlapati R, Edelmann W. Mouse models for human DNA mismatch-repair gene defects. *Trends Mol Med* 2002;**8**(7):346-353.

270. Buermeyer AB, Deschenes SM, Baker SM, Liskay RM. Mammalian DNA mismatch repair. *Annu Rev Genet* 1999;**33**:533-564.

271. Wei K, Clark AB, Wong E, et al. Inactivation of Exonuclease 1 in mice results in DNA mismatch repair defects, increased cancer susceptibility, and male and female sterility. *Genes Dev* 2003;**17**(5):603-614.

272. Prolla TA, Baker SM, Harris AC, et al. Tumour susceptibility and spontaneous mutation in mice deficient in Mlh1, Pms1 and Pms2 DNA mismatch repair. *Nat Genet* 1998;**18**(3):276-279.

273. de Wind N, Dekker M, Berns A, Radman M, te Riele H. Inactivation of the mouse Msh2 gene results in mismatch repair deficiency, methylation tolerance, hyperrecombination, and predisposition to cancer. *Cell* 1995;**82**(2):321-330.

274. Reitmair AH, Schmits R, Ewel A, et al. MSH2 deficient mice are viable and susceptible to lymphoid tumours. *Nat Genet* 1995;**11**(1):64-70.

275. Edelmann W, Yang K, Umar A, et al. Mutation in the mismatch repair gene Msh6 causes cancer susceptibility. *Cell* 1997;**91**(4):467-477.

276. de Wind N, Dekker M, Claij N, et al. HNPCC-like cancer predisposition in mice through simultaneous loss of Msh3 and Msh6 mismatch-repair protein functions. *Nat Genet* 1999;**23**(3):359-362.

277. Edelmann W, Umar A, Yang K, et al. The DNA mismatch repair genes Msh3 and Msh6 cooperate in intestinal tumor suppression. *Cancer Res* 2000;**60**(4):803-807.

278. Baker SM, Plug AW, Prolla TA, et al. Involvement of mouse Mlh1 in DNA mismatch repair and meiotic crossing over. *Nat Genet* 1996;**13**(3):336-342.

279. Edelmann W, Cohen PE, Kane M, et al. Meiotic pachytene arrest in MLH1-deficient mice. *Cell* 1996;**85**(7):1125-1134.

280. Baker SM, Bronner CE, Zhang L, et al. Male mice defective in the DNA mismatch repair gene PMS2 exhibit abnormal chromosome synapsis in meiosis. *Cell* 1995;**82**(2):309-319.

281. Chen PC, Dudley S, Hagen W, et al. Contributions by MutL homologues Mlh3 and Pms2 to DNA mismatch repair and tumor suppression in the mouse. *Cancer Res* 2005;**65**(19):8662-8670.

282. Lipkin SM, Moens PB, Wang V, et al. Meiotic arrest and aneuploidy in MLH3-deficient mice. *Nat Genet* 2002;**31**(4):385-390.

283. Kim YS, Deng G. Epigenetic changes (aberrant DNA methylation) in colorectal neoplasia. *Gut Liver* 2007;**1**(1):1-11.

284. Kim YH, Kakar S, Cun L, Deng G, Kim YS. Distinct CpG island methylation profiles and BRAF mutation status in serrated and adenomatous colorectal polyps. *Int J Cancer* 2008;**123**(11):2587-2593.

285. Deng G, Bell I, Crawley S, et al. BRAF mutation is frequently present in sporadic colorectal cancer with methylated hMLH1, but not in hereditary nonpolyposis colorectal cancer. *Clin Cancer Res* 2004;**10**(1 Pt 1):191-195.

286. Deng DJ, Zhou J, Zhu BD, Ji JF, Harper JC, Powell SM. Silencing-specific methylation and single nucleotide polymorphism of hMLH1 promoter in gastric carcinomas. *World J Gastroenterol* 2003;**9**(1):26-29.

287. Deng G, Peng E, Gum J, Terdiman J, Sleisenger M, Kim YS. Methylation of hMLH1 promoter correlates with the gene silencing with a region-specific manner in colorectal cancer. *Br J Cancer* 2002;**86**(4):574-579.

288. Deng G, Chen A, Hong J, Chae HS, Kim YS. Methylation of CpG in a small region of the hMLH1 promoter invariably correlates with the absence of gene expression. *Cancer Res* 1999;**59**(9):2029-2033.

289. Chan TL, Yuen ST, Kong CK, et al. Heritable germline epimutation of MSH2 in a family with hereditary nonpolyposis colorectal cancer. *Nat Genet* 2006;**38**(10):1178-1183.

290. Hitchins MP, Wong JJ, Suthers G, et al. Inheritance of a cancer-associated MLH1 germ-line epimutation. *N Engl J Med* 2007;**356**(7):697-705.

291. Suter CM, Martin DI, Ward RL. Germline epimutation of MLH1 in individuals with multiple cancers. *Nat Genet* 2004;**36**(5):497-501.

292. Loughrey MB, Waring PM, Tan A, et al. Incorporation of somatic BRAF mutation testing into an algorithm for the investigation of hereditary non-polyposis colorectal cancer. *Fam Cancer* 2007;**6**(3):301-310.

293. Cantwell-Dorris ER, O'Leary JJ, Sheils OM. BRAFV600E: implications for carcinogenesis and molecular therapy. *Mol Cancer Ther* 2011;**10**(3):385-394.

294. Rahman MA, Salajegheh A, Smith RA, Lam AK. B-Raf mutation: a key player in molecular biology of cancer. *Exp Mol Pathol* 2013;**95**(3):336-342.

295. Garnett MJ, Marais R. Guilty as charged: B-RAF is a human oncogene. *Cancer Cell* 2004;**6**(4):313-319.

296. Boland CR, Thibodeau SN, Hamilton SR, et al. A National Cancer Institute Workshop on Microsatellite Instability for cancer detection and familial predisposition: development of international criteria for the determination of microsatellite instability in colorectal cancer. *Cancer Res* 1998;**58**(22):5248-5257.

297. Kinzler KW, Vogelstein B. Cancer-susceptibility genes. Gatekeepers and caretakers. *Nature* 1997;**386**(6627):761, 763.

298. Duval A, Hamelin R. Mutations at coding repeat sequences in mismatch repair-deficient human cancers: toward a new concept of target genes for instability. *Cancer Res* 2002;**62**(9):2447-2454.

299. Felton KE, Gilchrist DM, Andrew SE. Constitutive deficiency in DNA mismatch repair: is it time for Lynch III? *Clin Genet* 2007;**71**(6):499-500.

300. Miyashita K, Fujii K, Yamada Y, et al. Frequent microsatellite instability in non-Hodgkin lymphomas irresponsive to chemotherapy. *Leuk Res* 2008;**32**(8):1183-1195.

301. Allen PB, Morgan GJ, Wiedemann LM. Philadelphia chromosome-positive leukaemia: the translocated genes and their gene products. *Baillieres Clin Haematol* 1992;**5**(4):897-930.

302. Nowicki MO, Falinski R, Koptyra M, et al. BCR/ABL oncogenic kinase promotes unfaithful repair of the reactive oxygen species-dependent DNA double-strand breaks. *Blood* 2004;**104**(12):3746-3753.

303. Koptyra M, Falinski R, Nowicki MO, et al. BCR/ABL kinase induces self-mutagenesis via reactive oxygen species to encode imatinib resistance. *Blood* 2006;**108**(1):319-327.

304. Wada C, Shionoya S, Fujino Y, et al. Genomic instability of microsatellite repeats and its association with the evolution of chronic myelogenous leukemia. *Blood* 1994;**83**(12):3449-3456.

305. Stoklosa T, Poplawski T, Koptyra M, et al. BCR/ABL inhibits mismatch repair to protect from apoptosis and induce point mutations. *Cancer Res* 2008;**68**(8):2576-2580.

306. Plotz G, Zeuzem S, Raedle J. DNA mismatch repair and Lynch syndrome. *J Mol Histol* 2006;**37**(5-7):271-283.

CHAPTER 2

Fusion tyrosine kinase NPM-ALK deregulates MSH2 and suppresses DNA mismatch repair function: novel insights into a potent oncoprotein

---

This chapter has been modified from a previous publication:
Young LC, **Bone KM**, Wang P, Wu F, Adam BA, Hegazy S, Gelebart P, Holovati J, Li L, Andrew SE, Lai R. Fusion tyrosine kinase NPM-ALK deregulates MSH2 and suppresses DNA mismatch repair function: novel insights into a potent oncoprotein. American Journal of Pathology. 2011. Jul; 179(1):411-421.

As second author, I performed the experiments shown in Figures 2.2 (A and B), 2.3 (A and B), 2.4 (B), 2.6 (A, B and C) and 2.10 (A and B). I also contributed technically to the experiments shown in Figure 2.1 (A and B), 2.4 (A and C), 2.8 and 2.9 (C and D), as well as the writing of the manuscript.

2.1 Abstract

The fusion tyrosine kinase NPM-ALK is central to the pathogenesis of ALK-positive anaplastic large cell lymphoma (ALK+ALCL). The Lai Laboratory recently identified that MSH2, a key DNA mismatch repair (MMR) protein integral to the suppression of tumorigenesis, is an NPM-ALK-interacting protein. In this study, *in vitro* evidence that enforced expression of NPM-ALK in HEK293 cells suppressed MMR function was found. Correlating with these findings, six of nine ALK+ALCL tumors displayed evidence of microsatellite instability, as opposed to none of the eight normal DNA control samples (p=0.007, Student's t-test). Using co-immunoprecipitation, increasing levels of NPM-ALK expression in HEK293 cells resulted in decreased levels of MSH6 bound to MSH2, whereas MSH2:NPM-ALK binding was increased. The NPM-ALK:MSH2 interaction was dependent on the activation/autophosphorylation of NPM-ALK, and the Y191 residue of NPM-ALK was a crucial site for this interaction and for NPM-ALK-mediated MMR suppression. MSH2 was found to be tyrosine phosphorylated in the presence of NPM-ALK. Finally, NPM-ALK impeded the expected DNA damage-induced translocation of MSH2 out of the cytoplasm. To conclude, the data support a model in which the suppression of MMR by NPM-ALK is attributed to its ability to interfere with normal MSH2 biochemistry and function.

2.2 Introduction

NPM-ALK is an oncogenic fusion tyrosine kinase found exclusively in ALK-positive anaplastic large-cell lymphoma (ALK+ALCL), a lymphoid malignancy of mature T/null immunophenotype occurring most frequently in children.[1,2] The fusion gene encoding NPM-ALK is a consequence of the reciprocal chromosomal translocation t(2;5)(p23;q35) that fuses the promoter and 5' portion of the *nucleophosmin* (*NPM*) gene directly upstream of the DNA segment encoding the kinase domain of the *anaplastic lymphoma kinase (ALK*) gene (reviewed by Amin and Lai[3]). Normally, the tyrosine kinase activity of ALK is controlled by ligand binding, and the expression of the ALK receptor tyrosine kinase is restricted to a subset of neuronal cells. In contrast, the expression of *NPM-ALK* in ALK+ALCL cells is driven by the strong and ubiquitous *NPM* promoter; the tyrosine kinase embedded in NPM-ALK is constitutively phosphorylated and activated via its dimerization mediated through the NPM oligomerization domain.[4,5] The expression of NPM-ALK has been shown to be sufficient to promote malignant transformation, in both cell lines and murine models.[6-9] The mechanisms underlying its oncogenic potential are attributed to the fact that NPM-ALK phosphorylates and deregulates a host of cellular signaling proteins, which often leads to cell cycle progression and suppression of apoptosis (reviewed by Amin and Lai[3]).

To further explore the scope of NPM-ALK oncogenic pressure, the Lai Laboratory recently used tandem affinity purified NPM-ALK and mass spectrometry to generate a comprehensive catalogue of proteins that interact with NPM-ALK.[10] NPM-ALK was determined to bind a large number of proteins that are involved in a great diversity of biological functions. Specifically, the DNA mismatch repair (MMR) protein MSH2, but not its normal binding partners MSH6 or MSH3, interacted with NPM-

ALK.[10] In view of the importance of MSH2 in MMR, it was hypothesized that NPM-ALK may disrupt MMR function. Regarding the MMR function, it is documented that several MMR proteins are required to work in concert to fully exert this biological property (reviewed by Li[11]). MMR proteins are highly and ubiquitously expressed[12], and evidence suggests that the correct ratio between these proteins is key to their function.[13-19] The MMR protein heterodimer MSH2:MSH6 (also known as MutSα) detects both single base mismatches and small insertion-deletion loops (one or two nucleotides), whereas the MSH2:MSH3 heterodimer (also known as MutSβ) detects only insertion-deletion loops (two to 14 nucleotides).[11] Normally, MSH2:MSH6 is 10-fold more abundant than MSH2:MSH3.[14] Once a MutS heterodimer is bound to the site of DNA error, a second MMR heterodimer consisting of MutL orthologs (e.g., MLH1:PMS2) is recruited, followed by the recruitment of additional proteins that mediate the removal of the erroneous DNA bases, using the unaffected strand as a template to resynthesize the DNA.[11] The formation of heterodimers stabilizes these MMR proteins. Cells lacking MSH2 can form neither MSH2:MSH6 nor MSH2:MSH3 and are completely deficient in MMR function, whereas cells lacking one of MSH6 or MSH3 retain MSH2:MSH3 or MSH2:MSH6, respectively, and hence some residual error correction.[20-26] The MSH2:MSH6 heterodimer performs the majority of mutation repair[27], an observation that is supported by tumor latency studies using MMR-null mice.[21,22,26,28] By 6 and 11 months, 50% of *Msh2*-/- and *Msh6*-/- mice succumb to MMR-related tumors, whereas *Msh3*-/- survival is at least 18 months and tumor incidence is low.[28]

The importance of MMR function to tumor suppression in humans has been characterized most extensively in Lynch syndrome, an early-onset cancer syndrome affecting a heterogeneous group of tissues (e.g., colon, endometrium, urothelium; OMIM (Online Mendelian Inheritance in Man) #120435, *http://www.ncbi.nlm. nih.gov/omim*). In addition, acquired

inactivation of MMR contributes to a proportion of sporadic cancers.[29] The congenital loss of MMR function through the inheritance of two mutated copies of a gene encoding a MMR protein, including *MSH2*, is associated with the development of lymphoid cancer presenting in childhood.[30] In their recent review of the literature and analysis of microsatellite instability (MSI) in non-Hodgkin lymphoma, Miyashita et al. concluded that MSI was not infrequent in lymphoma and was associated with poor clinical outcomes and resistance to chemotherapy.[31] These studies suggest that MMR deficiency is pathogenetically important in human lymphoid malignancies. With this background, this study aims to determine whether the scope of NPM-ALK oncogenicity includes interference with MSH2 biology and MMR function.

2.3 Materials and Methods

2.3.1 Cells and gene transfection

Karpas 299 and SUP-M2 are ALK+ALCL cell lines and were maintained in RPMI-1640 with 10% fetal bovine serum (FBS; Sigma-Aldrich, Oakville, ON, Canada). The purchased Tet-on (tetracycline-on) HEK293 (human embryonic kidney 293) Advanced cells (Clontech, Mountain View, CA) carried the rtTA2S-M2 (Tet-On® Advanced) transactivator under stable transfection, which was maintained via 100 μg/mL G418 in the medium. *NPM-ALK* cDNA was inserted into the pTRE-TIGHT vector (Clontech), linearized, and introduced into the Tet-on HEK293 cells via stable transfection in conjunction with a linear hygromycin marker. The resulting clonal Tet-on HEK293 Advanced cells carrying *pTRE-TIGHT/NPM-ALK* were maintained in Dulbecco's modified Eagle's medium supplemented with 10% Tet-System Approved FBS (Clontech), 100 μg/mL G418 and 50 μg/mL hygromycin B (Clontech) and termed "Tet-on HEK293/NPM-ALK" cells throughout this article. All cells were grown at 37°C in 5% CO2. In

some experiments, standard HEK293 cells were transiently transfected in 10 cm dishes with 10 μg various *NPM-ALK* expression vectors using Lipofectamine 2000 (Invitrogen, Burlington, ON, Canada) in accordance with the manufacturer's suggested protocol. In the case of vectors that result in a His-biotin (HB) tag, the culture media was supplemented with 4 μmol/L biotin to improve the biotinylation efficiency of HB-tagged proteins.

2.3.2 NPM-ALK expression vectors

His-biotin tagged (HBT) *NPM-ALK* was constructed as described previously [10]; HBT consists of an RGS-hexahistidine (H) tag and a bacterially derived biotinylation (B) signal peptide. HB/NPM-ALK expresses functional NPM-ALK at levels similar to those found in ALK+ALCL cell lines.[10] Site-directed mutagenesis (tyrosine to phenylalanine, Y→F) was used to change one or more of the three tyrosine residues of NPM-ALK in the kinase activation loop (including Y338, Y342, and Y343) to phenylalanine (F).[32] Specifically, mutation of all these three tyrosine residues (termed FFF in Figures) resulted in a loss of i) NPM-ALK phosphorylation, ii) phosphorylation of many known NPM-ALK downstream targets, and iii) NPM-ALK–induced growth advantage on clonogenic assay.[32]

2.3.3 Nuclear and cytoplasmic fractionation

Nuclear and cytoplasmic proteins were isolated from 10-cm dishes of cells using the Pierce NE-PER kit following the suggested protocol (Fisher Scientific Canada, Ottawa, ON, Canada). β-tubulin and lamin A/C were used as cytoplasmic and nuclear markers, respectively, during sodium docedyl sulfate–polyacrylamide gel electrophoresis (SDS-PAGE) analysis.

2.3.4 Immunoprecipitation and his-based protein purification

Unless noted otherwise, co-immunoprecipitations (co-IPPs) were performed using 2 mg cell lysate proteins harvested in Cell Lytic M Lysis Buffer supplemented with protease and phosphatase inhibitors (Sigma-Aldrich). Briefly, cells were washed twice in ice cold PBS (phosphate buffered saline), and then 1 mL ice cold cell lytic M with inhibitors was added to each cell pellet (1 mL per 10-cm dish) and the cell pellet was disrupted by pipetting up and down 50 times on ice. The lysate was incubated for 20 minutes on ice, cleared by cold centrifugation at 15 000 x g, and the protein quantification was done by BCA (bicinchoninic acid) assay (Fisher Scientific Canada). Cell lysate was pre-cleared using 30 μL of a 33% slurry of protein G+/A agarose beads (EMD Biosciences, Gibbstown, NJ) for 2 hours. For each co-IPP, the pre-cleared lysate was first incubated with 10 μg monoclonal antibody overnight, and then 50 μL G+/A agarose beads (packed volume of washed bead) were added and the resulting mixture was incubated overnight. The bead/antibody complexes were washed twice with ice-cold PBS and then twice with ice-cold lysis buffer. All liquid was removed and the proteins eluted from the beads with 50 μL protein loading buffer under standard denaturing conditions. For IPPs, the final steps included washing in RIPA buffer. For the purification of NPM-ALK (mutant or native) tagged with HBT, NPM-ALK was purified on streptavidin-coated beads as previously published.[10] For the co-IPP of MSH2-containing MMR heterodimers, 1.0 mg lysate/IPP was used. Purified proteins resulting from IPP, co-IPP, and streptavidin purification, as well as regular cell lysates, were separated by electrophoresis using 8% or gradient Pierce Precise Protein Gels (Fisher Scientific Canada). Antibodies used include: anti-MSH2 (clones NA27, NA26, EMD Biosciences), anti-MSH6 (BD Biosciences, Mississauga, ON, Canada), anti-MSH3 (Santa Cruz Biotechnologies, Santa Cruz, CA), and anti–phospho-tyrosine (mAb P-Tyr-102, Cell Signaling, Danvers, MA).

2.3.5 Detection of microsatellite instability in ALK+ALCL tumors

Six quasi-monomorphic microsatellites (**Table 2.1**) were amplified using the Qiagen Multiplex PCR kit. Two of the markers, BAT25 and BAT26, are components of the panel of five markers recommended for Lynch testing[33]; because the remaining three markers in the recommended panel require a patient-matched non-tumor DNA sample, they were not used in this study. Instead, four additional monomorphic markers that are mononucleotide repeats proved to be informative for the detection of microsatellite instability (MSI) in Lynch syndrome associated with the loss of MSH6 were chosen.[34-36] DNA samples were isolated from eight normal donors and nine ALK+ALCL tumors. Tumor DNA was isolated from paraffin curls using the Qiagen Blood and Tissue Kit (Qiagen, Mississauga, ON, Canada) following the suggested protocol. The University of Alberta Human Research Ethics Board approved the use of the human samples. Resulting PCR products were analyzed on an ABI 3130xl Genetic Analyzer (Applied Biosystems, Foster City, CA, The Applied Genomics Centre, TAGC, University of Alberta). Normal DNA samples were used to define the normal profile for the six microsatellites, and the microsatellite profiles of the eight tumors were compared with those of the normal samples. As two of the eight normal samples demonstrated shifts at one microsatellite marker each, only the tumor samples that demonstrated shift at two or more microsatellite markers were considered to be positive for MSI.

2.3.6 Immunohistochemistry

Formalin fixed, paraffin embedded ALK+ALCL tumors (n=5) were used for this study. All cases were retrieved from the file at the Department of Laboratory Medicine and Pathology, Cross Cancer Institute. The diagnosis of these cases was based on the criteria established by the World Health

Table 2.1. Primer sequences used in microsatellite analysis.

Locus	Primer Sequence	Reference
Mononucleotide microsatellites		
BAT26		
Forward Primer	5' TGACTACTTTTGACTTCAGCC 3'	37
Reverse Primer	5'GTTTCTTAACCATTCAACATTTTTAACCC 3'	37
BAT25		
Forward Primer	5' TCGCCTCCAAGAATGTTAGT 3'	37
Reverse Primer	5' GTTTCTTTGGCTCTAAAATGCTCTGTTCT 3'	Primer3
CAT25		
Forward Primer	5' CCTAGAAACCTTTATCCCTGCTT 3'	38
Reverse Primer	5' GTTTCTTAGCTGAGATCGTGCCACTG 3'	Primer3
NR21		
Forward Primer	5' GAGTCGCTGGCACAGTTCTA 3'	39
Reverse Primer	5' GTTTCTTGCATTCACACTTTCTGGTCA 3'	Primer3
NR24		
Forward Primer	5' GCTGAATTTTACCTCCTGAC 3'	39
Reverse Primer	5' GTTTCTTCATTCCAACCTGGGTA 3'	Primer3
NR27		
Forward Primer	5' AACCATGCTTGCAAACCACT 3'	39
Reverse Primer	5' GTTTCTTTCAACAGCAGAGACCTTGTCA 3'	Primer3
Dinucleotide microsatellites		
D2S123		
Forward Primer	5' GCCAGAGAAATTAGACACAGTC 3'	37
Reverse Primer	5' GTTTCTTCTGACTTGGATACCATCTATCTA 3'	37
D5S346		
Forward Primer	5' TACTCACTCTAGTGATAAATCGG 3'	37
Reverse Primer	5' GTTTCTTTTCAGGGAATTGAGAGTTACAG 3'	37
D17S250		
Forward Primer	5' AATACACAATAAAAATATGTGTGTG 3'	37
Reverse Primer	5' GTTTCTTTTACAGGCATGAGCCACT 3'	Primer3

Underlined markers are components of the National Cancer Institute recommended panel of MSI markers for Lynch testing. Primers unique to the laboratory of the authors of the current work were designed using Primer3.[40]

Organization classification scheme, and all cases were confirmed to express ALK by immunohistochemistry. The University of Alberta Human Research Ethics Board approved the use of these tissues. Immunohistochemical detection of MSH2, MSH3, and MSH6 was performed using standard techniques. Briefly, formalin-fixed, paraffin-embedded tissue sections of 4 μm thickness were deparaffinized in xylene and hydrated in graded ethanol (100% to 50%). Antigen retrieval was performed using citrate buffer (pH 6.0) microwaved in a pressure cooker for 20 minutes and left to cool for 20 minutes. After antigen retrieval, tissue sections were incubated with 10% hydrogen peroxide (H_2O_2) and methanol for 10 minutes to block endogenous peroxidase activity, followed by washing in running tap water for 5 minutes. Subsequently, the sections were incubated for 20 minutes in antibody diluent (Dako, Mississauga, ON, Canada), followed by incubation overnight at 4°C with a mouse monoclonal anti-MSH2 antibody (1:30, Novocastra, Newcastle, UK), a rabbit polyclonal antibody reactive with anti-MSH3 (1:50 dilution, Santa Cruz Biotechnology), or a mouse monoclonal anti-MSH6 antibody (1:50 dilution, BD Transduction Laboratories). All antibodies were diluted in antibody diluent (Dako) Immunostaining was visualized with a labeled streptavidin-biotin method (20 minutes in biotinylated link and 20 minutes in streptavidin horse radish peroxidase, both from Dako) using (3, 3-diaminobenzidine/ H_2O_2) DAB as a chromogen (Dako). Hematoxylin was used as a counter stain. Following staining, sections were dehydrated in graded ethanol (50%-100%), followed by xylene incubation. Coverslips were applied using permount solution (Fisher Scientific).

2.3.7 MMR functional assay using 6TG

The sensitivity of cells to 6-thioguanine (6TG, Sigma) was tested in 96-well format, and the resulting cell viability was assayed using the WST-1 cell proliferation reagent (Clontech) with the absorbance read using a μQuant

96-well plate reader and the associated KC4 software (BioTek, Winooski, VT). Each sample was performed in quadruplicate with appropriate controls, and the assay repeated three times. In the case of transient transfection, HEK293 cells were harvested and mixed with the plasmid/Attractene Transfection Reagent solution as per the FastForward protocol (Qiagen), and immediately aliquoted into the 96-well plate. Tet-on HEK293/ NPM-ALK cells were plated at 4000 cells per well, and the appropriate wells were supplemented with doxycycline/medium or medium alone after 24 hours. After another 24 hours of incubation with doxycycline, the medium was removed and replaced with fresh medium containing doxycycline and 6TG as required.

2.3.8 MMR functional assay: reporter plasmid for insertion/deletion correction

Tet-on HEK293/NPM-ALK cells were seeded in 24-well plates and transfected with the pCAR-OF (out-of-frame) vector (Addgene plasmid 16627, Cambridge, MA) created in the laboratory of Dr. Bert Vogelstein (Johns Hopkins Kimmel Cancer Center).[41] The pCAR–OF vector contains a $(CA)_{29}$ repeat at the 5' end of the coding region that places the *β-galactosidase* cDNA out of frame; strand-slippage resulting from MMR suppression is manifested by the acquisition of β-galactosidase expression and resultant activity. Seventy–two hours after transfection, cells were harvested and counted. The activity of β-galactosidase was analyzed using the β-Galactosidase Enzyme Assay System (Promega, Madison, WI) as per the manufacturer's instructions; the β-galactosidase activity was reported relative to the total cell number.

2.3.9 Detection of NPM-ALK-induced MSI

Tet-on HEK293/NPM-ALK cells were plated at a concentration of 1

cell/well in a 96-well microplate format; limiting dilution was used such that at least half the plated wells failed to grow. After 48 hours the media was adjusted to either 0 or 1000 ng/mL doxycycline, and the cells were grown to confluence (10 days). Media was not changed during the 10-day expansion and, therefore, doxycycline levels were initiated at the higher level to accommodate the 48-hour half-life of doxycycline (in culture media) and maintain NPM-ALK expression. From each well, DNA was harvested using the QIAGEN Blood and Tissue Kit. Therefore, each DNA sample represents a single clonal expansion, either in the presence or absence of physiologically relevant NPM-ALK levels. Microsatellites were analyzed as above, with the addition of three di-nucleotide markers D2S123, D5S346 and D17S250 (**Table 2.1**); the recommended panel of markers for Lynch testing (BAT25, BAT26, D2S123, D5S346, D17S250) were encompassed by the mono- and di-nucleotide microsatellites tested. Cells not treated with doxycycline, but also subjected to clonal expansion, provided the matched DNA controls. SUP-M2 and Karpas 299 cells were included as positive controls.

2.4 Results

2.4.1 NPM-ALK interferes with MSH2:MSH6 heterodimerization

Using liquid chromatography-mass spectrometry and co-immunoprecipitation (co-IPP) experiments, the Lai Laboratory previously found evidence that MSH2 is a binding partner of NPM-ALK.[10] Interestingly, MSH6 or MSH3 were not detected in the NPM-ALK-interacting complex by mass spectrometry.[10] In the present study, using co-IPP, no evidence of binding between MSH6 and NPM-ALK in ALK+ALCL cell lines (data not shown) and HEK293 cells transfected with *NPM-ALK* (see below) was found. These findings led to the hypothesis that NPM-ALK may interfere with the normal dimerization between MSH2

and MSH6. In support of this hypothesis, using the Tet-on HEK-293/NPM-ALK cells and co-IPP with an MSH2-specific antibody, the ratio of MSH6 bound to MSH2 decreased as the NPM-ALK levels were gradually increased in a dose-dependent manner (**Figure 2.1**). Using the same experimental model, I found a dose-dependent increase in the MSH2:NPM-ALK binding as the NPM-ALK levels were gradually increased (**Figure 2.2**). These findings support the model in which NPM-ALK sequestrates MSH2 away from MSH6. This model is further supported by the finding that siRNA knock-down of NPM-ALK in ALK+ALCL cells resulted in an increase in the MSH2:MSH6 interaction in co-IPP experiments (**Figure 2.3**).

2.4.2 NPM-ALK suppresses DNA mismatch repair function

In view of the importance of the MSH2:MSH6 interaction in the context of MMR, the finding that NPM-ALK interferes with this interaction led to the hypothesis that NPM-ALK suppresses MMR function. This hypothesis was supported by the results of three different *in vitro* assays described below.

2.4.2.1 6TG assay

The 6TG assay, a widely accepted test for evaluating MMR function[42,43], was used to assess the impact of NPM-ALK on MMR function. As described in the literature, the incorporation of 6TG metabolites into DNA is not in itself cytotoxic, but the resulting aberrant base requires MMR processing to exert its cytotoxic effects.[42] Thus, in cells with normal MMR function, 6TG is cytotoxic; in the absence of MMR, 6TG is not cytotoxic.[44] As shown in **Figure 2.4A**, doxycycline-induced expression of NPM-ALK in the Tet-on HEK293/NPM-ALK cells resulted in a significantly high number of viable cells than without NPM-ALK expression. This increased viability was significant at a relatively low-level of NPM-ALK expression (100

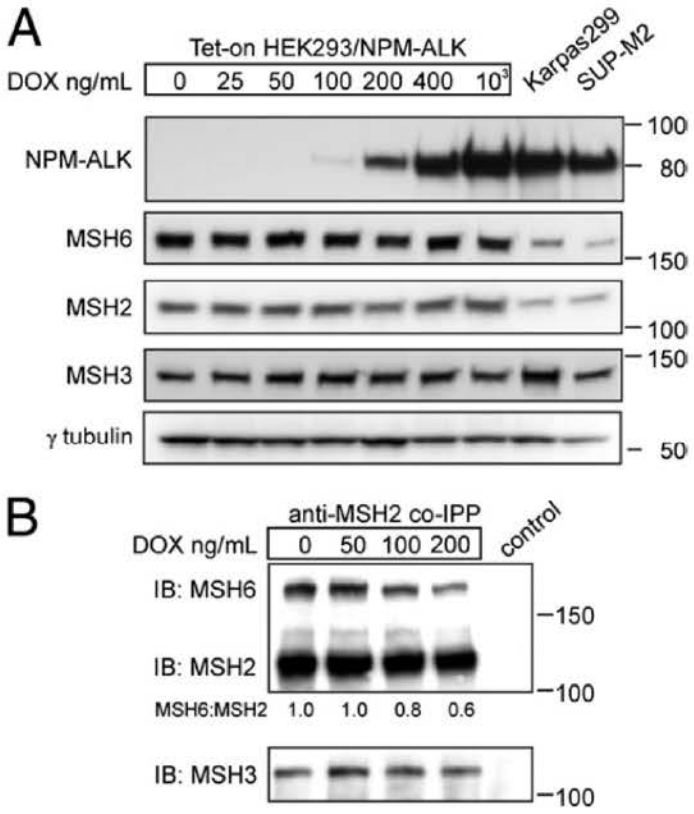

Figure 2.1. NPM-ALK interferes with MSH2:MSH6 binding. (A) Tet-on HEK293 cells were constructed such that the expression of NPM-ALK was induced by the addition of doxycycline (DOX) to the media. The cell lysate was subjected to western blotting. An anti-ALK antibody was used to show expression of NPM-ALK, and anti-MSH6, anti-MSH2, and MSH3 antibodies were used to show expression of the MMR-associated proteins. γ-Tubulin served as the protein loading control. Lysates from two ALK+ALCL cell lines, Karpas 299 and SUP-M2, were included as positive controls for NPM-ALK expression. The numbers on the right hand side represent the protein size in kiloDaltons (kDa). (n=3). (B) Tet-on HEK293/NPM-ALK cells were cultured in increasing concentrations of doxycycline. Co-IPP was performed on the lysate with a specific anti-MSH2 antibody, and the resulting immunoblot was probed to assess the levels of immunoprecipitated MSH6 and MSH3 relative to MSH2. A control co-IPP with no added antibody was included to account for nonspecific binding. Densitometry values for MSH6:MSH2 are shown (n=3).

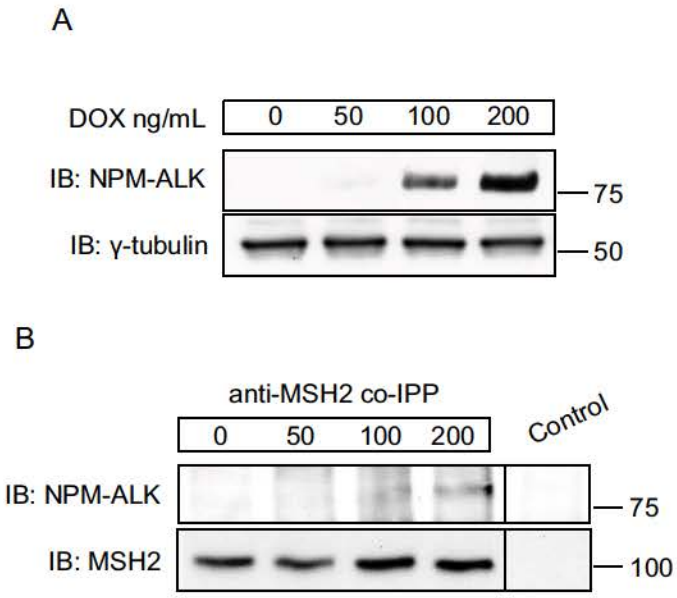

Figure 2.2. NPM-ALK binds MSH2 in a dose-dependent manner. (A) Tet-on HEK293/NPM-ALK cells were cultured in increasing concentrations of doxycycline and the resulting cell lysate was subjected to western blotting. An anti-ALK antibody was used to show expression of NPM-ALK at 75 kDa. γ-tubulin served as a protein loading control. (B) Lysate from A was subjected to co-IPP with an anti-MSH2 antibody. The resultant western blot was probed with an anti-ALK antibody to measure the NPM-ALK interaction with MSH2. The western was stripped and probed with anti-MSH2 antibody to show immunoprecipitation of MSH2 (100 kDa). A control co-IPP was included for each sample with no antibody, and a representative control is shown. A representative result from three independent experiments is shown.

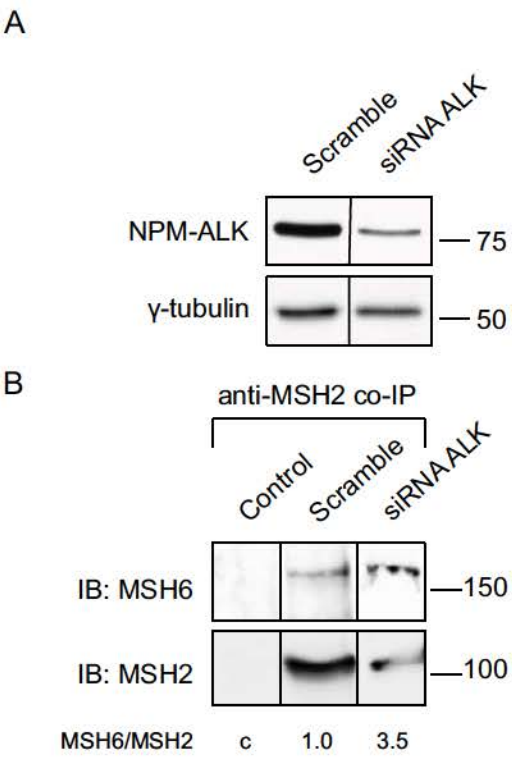

Figure 2.3 NPM-ALK knockdown restores MSH6:MSH2 binding. (A) SUP-M2 cells were transfected with ALK siRNA, and the resulting cell lysate was subjected to western blotting with an anti-ALK antibody to show NPM-ALK expression. A scramble siRNA sequence was used as a negative control. Anti-γ-tubulin antibody was used as a protein loading control. (B) Lysates from A were subjected to co-IPP with an anti-MSH2 specific antibody, and the resulting immunoblot was probed with anti-MSH6 and anti-MSH2 antibodies to compare levels of co-immunoprecipitated MSH6 relative to MSH2. A control co-IPP without added antibody was included to account for non-specific binding for each sample, and a representative control is shown. Densitometry values are for the amount of MSH6 bound to MSH2 relative to the control sample transfected with scramble siRNA. Three independent experiments were performed, and a representative result is shown.

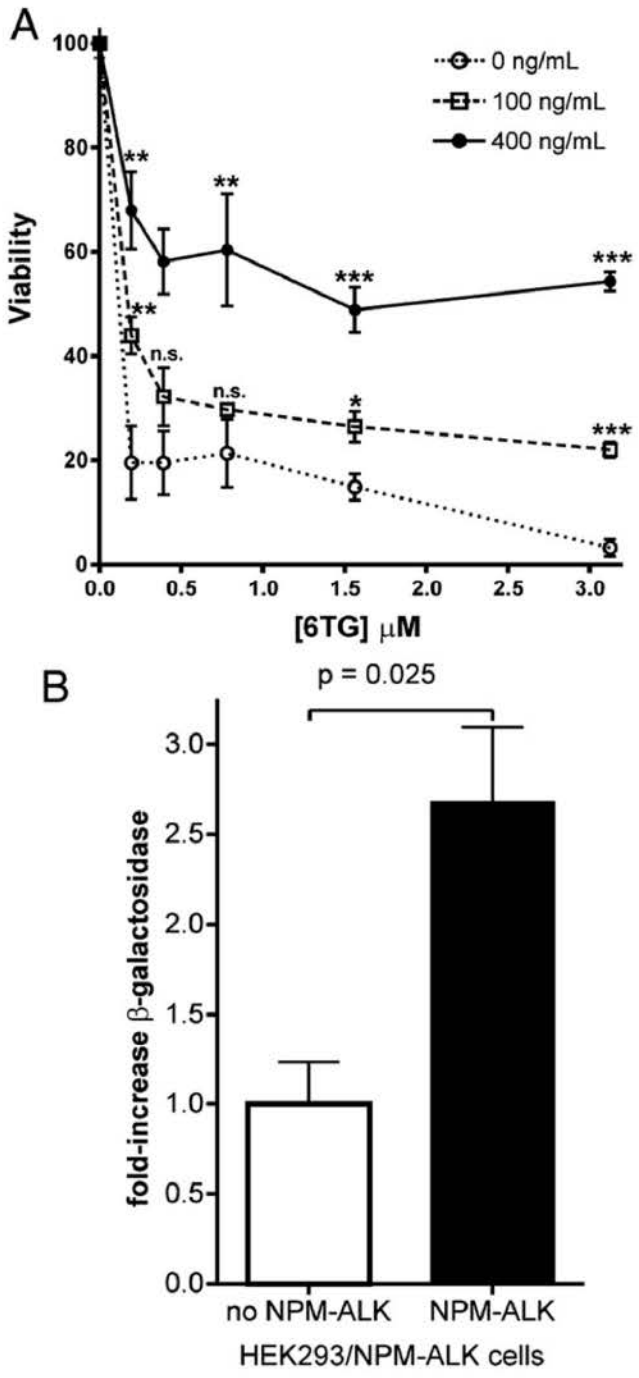
A
0 ng/mL
100 ng/mL
400 ng/mL
Viability
[6TG] μM
n.s.
B
p = 0.025
fold-increase β-galactosidase
no NPM-ALK
NPM-ALK
HEK293/NPM-ALK cells

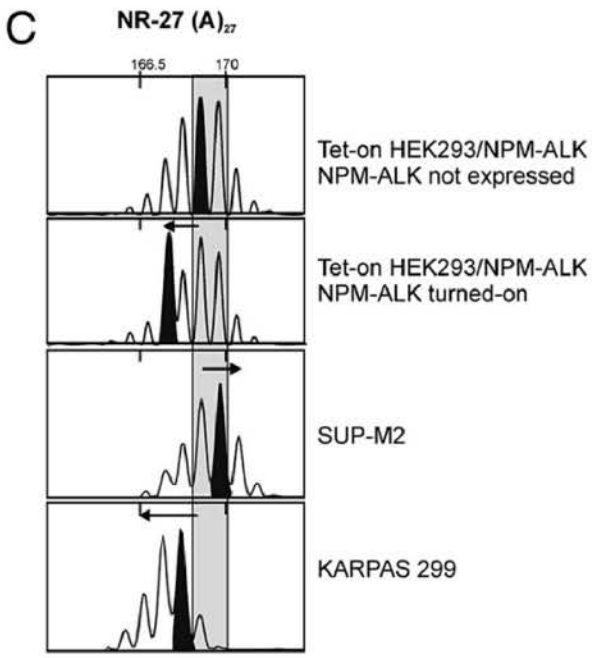

Figure 2.4. NPM-ALK suppresses MMR function *in vitro*. (A) Tet-on HEK-293/NPM-ALK cells were grown in three specified doxycycline concentrations (0, 100 ng/mL, and 400 ng/mL) for 24 hours, and then 6TG was added for an additional 48 hours. The WST-1 assay was used to compare relative cell viability/proliferation, and the resulting colorimetric response was measured with a μQuant BioTeck plate reader. Each experiment was plated in quadruplicate. Figure A shows a representative result from three independent experiments. Data are represented as mean ± SEM. Stars denote statistical difference between 0 ng/mL doxycycline and doxycycline-induced cells using one-way analysis of variance and the Newman-Keuls multiple comparison test (GraphPad Prism); *p<0.05, **p<0.01, and ***p<0.001. n.s. = not significant (p>0.05). (B) Tet-on HEK293/NPM-ALK cells were transiently transfected with the pCAR-OF vector, which carries cDNA encoding *β-galactosidase* placed out of frame by a $(CA)_{29}$ repeat. Four hours after transfection, the medium was supplemented by either 400 ng/mL doxycycline (with NPM-ALK expression) or 0 ng/mL doxycycline (no NPM-ALK). Seventy-two hours after transfection, the cell lysates were assayed for β-galactosidase activity as outlined in the Materials and Methods. Cell lysates were

measured in triplicate, and a representative result of three independent experiments is shown. β-galactosidase enzyme activity is shown relative to cell number, with cells without NPM-ALK expression set at 1. (C) Tet-on HEK293/NPM-ALK cells were subjected to clonal expansion for 10 days in the presence (1000 ng/mL doxycycline at the initial concentration) or absence (0 ng/mL doxycycline) of NPM-ALK expression. DNA was harvested and MSI tested at both mono- and di-nucleotide microsatellites. The shaded area represents the location of the predominant peaks in MMR-proficient cells, which are the cells without NPM-ALK expression, and was used as the reference normal sample. DNA from the ALK+ALCL cell lines, Karpas 299 and SUP-M2 was also subjected to MSI analysis and were included as positive controls. A representative result from three independent experiments is shown.

ng/mL doxycycline) and the difference was more pronounced at relatively high-level NPM-ALK expression (400 ng/mL doxycycline), indicating a dose-dependent relationship between NPM-ALK levels and MMR suppression.

2.4.2.2 Reporter assay for MMR function

MMR function after NPM-ALK expression also was tested using a previously described reporter plasmid containing the cDNA encoding *β-galactosidase* placed out of frame by a $(CA)_{29}$ repeat.[41] As described in the Materials and Methods, strand slippage resulting from MMR suppression is manifested by the acquisition of *β-galactosidase* expression and its resultant activity. As shown in **Figure 2.4B**, I found that induced expression of NPM-ALK in Tet-on HEK293/NPM-ALK cells resulted in a significant increase of *β*-galactosidase activity, as compared to cells with no added doxycycline (p=0.025), and this finding further supports that MMR function was suppressed by NPM-ALK.

2.4.2.3 Microsatellite instability

As described above, MMR function includes the repair of insertion-deletion-loops in areas of highly repetitive DNA sequence (i.e. microsatellites); expansion/contraction of microsatellites, commonly referred to microsatellite instability (MSI), is a hallmark of MMR deficiency. It was thus asked if NPM-ALK is capable of inducing MSI in non-cancerous cells. Single-cell clonal expansion was performed in both the presence and absence of NPM-ALK expression for 10 days, after which DNA was harvested from each expansion and subjected to MSI analysis. Of the 5 NPM-ALK expressing samples, 1 demonstrated evidence of MSI at the genomic DNA marker NR-27, an $(A)_{27}$ repeat (**Figure 2.4C**). The other microsatellites tested did not display evidence of MSI at this time-

point. In contrast, MSI was not observed for any of the 15 control expansions (no NPM-ALK expression). These results represent the first demonstration that suppression of MMR in non-neoplastic cells can directly result in MSI detectable at conventional genomic DNA microsatellites. Karpas 299 and SUP-M2 cells were included as positive controls.

2.4.3 Interference of NPM-ALK:MSH2 binding restores MMR

Thus far, the data have supported a model in which NPM-ALK suppresses MMR function via sequestrating MSH2 away from MSH6. This model predicts that abrogation of the NPM-ALK:MSH2 binding may restore the normal interaction between MSH2 and MSH6 and thus, the MMR function. Because NPM-ALK is known to interact with other proteins primarily through its phosphorylated tyrosine residues, it was hypothesized that mutation (i.e. replacement by phenylalanine) of one of the tyrosine residues involved in phosphorylation may decrease NPM-ALK:MSH2 binding. Of the eight tyrosine residues that are outside the kinase activation loop of ALK and are known to be involved in phosphorylation[32,44], only NPM-ALK^{Y191F} showed an appreciable (60% reduction by densitometry) decrease in the NPM-ALK:MSH2 interaction (**Figure 2.5A**). NPM-ALK^{Y191F} has not been identified as contributing to any previously reported NPM-ALK activated signaling pathway, thus minimizing the contribution of off-target effects, and the Y191F mutation does not result in reduced NPM-ALK conferred growth advantage.[32] Compared with native NPM-ALK, transient transfection of the NPM-ALK^{Y191F} mutant conferred a significantly lower suppressive effect on MMR function, as measured by 6TG assay (**Figure 2.5B**), demonstrating that the binding between MSH2 and NPM-ALK is essential for mediating NPM-ALK–induced MMR suppression. The observed decrease in cell viability (thus, a partial restoration in MMR function) on mutation of NPM-ALK at

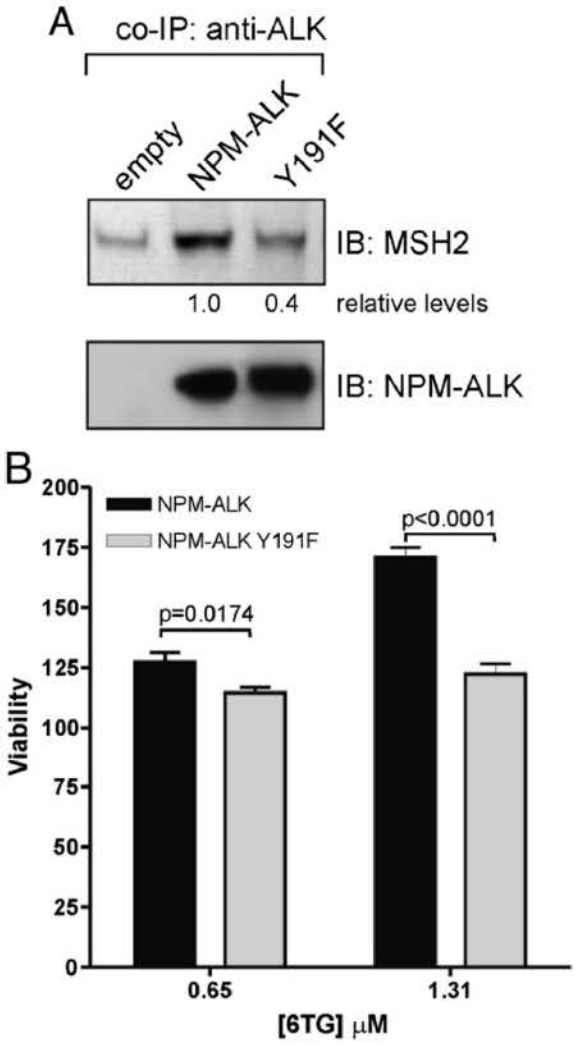

Figure 2.5 Disruption of NPM-ALK:MSH2 binding restores MMR function. (A) HEK293 cells were transiently transfected with empty vector, *NPM-ALK* or *NPM-ALK*^{Y191F}. NPM-ALK was immunoprecipitated from the resulting lysates under co-IPP conditions, and the resulting immunoblot was probed with an anti-MSH2 antibody to detect MSH2 and an anti-ALK antibody to detect NPM-ALK. Densitometry values shown are for the amount of MSH2 pulled down relative to NPM-ALK, with cells expressing NPM-ALK set at 1. Triplicate experiments were performed and results from a representative experiment are shown. (B) HEK293 cells were transiently transfected with empty vector, *NPM-ALK,* or *NPM-ALK Y191F* and treated with 6TG for 48 hours. Viability was measured using the WST-1 proliferation assay, and is expressed as a percentage relative to the

empty vector, which was set as 100%. Statistical significance was calculated using one-way analysis of variance and the Newman-Keuls multiple comparison test (GraphPad Prism), with a p value >0.05 not significant, and p<0.05 carrying statistical significance. Samples were measured in triplicate, and a representative result of three independent experiments is shown.

tyrosine 191 (**Figure 2.5B**) is in agreement with the 60% reduction in MSH2-binding observed for NPM-ALK^{Y191F} (**Figure 2.5A**). Regarding the question as to how the mutation of Y191 results in a lesser degree of MMR suppression, the possibility that NPM-ALK^{Y191F} may not interfere with the MSH2:MSH6 interaction as effectively as native NPM-ALK does was considered. To test this possibility, I performed co-IPP experiments using Tet-on HEK293/NPM-ALK cells transiently transfected with NPM-ALK or NPM-ALK^{Y191F}. In the absence of doxycycline, MSH2 pulled down substantially more MSH6 with the transient expression of NPM-ALK^{Y191F} as compared with NPM-ALK (**Figure 2.6**). Furthermore, in the presence of doxycycline, MSH2 also pulled down more MSH6 in the transient transfection of NPM-ALK^{Y191F} as compared with NPM-ALK.

2.4.4 Evidence of MMR dysfunction in ALK+ALCL tumors from patients

Given that NPM-ALK expressing cells show signs of MSI, it was then asked whether ALK+ALCL patient tumor samples display evidence of MMR dysfunction. The presence of MSI in a panel of 9 ALK+ALCL tumor samples and 8 normal DNA samples (non-patient matched) was evaluated, and the results are illustrated in **Figure 2.7A**. A significant increase in the frequency of MSI in ALK+ALCL tumors (six of nine) as compared with the normal DNA samples (none of eight) (p=0.007, relative risk=3.00; illustrated in **Figure 2.7B**) was found. Karpas 299 and SUP-M2, two ALK+ALCL cell lines, also displayed evidence of MSI (**Figure 2.4C**).

MSH2 is predominantly localized to the nucleus in normal cells[45,46], and nuclear MMR protein levels increase in rapidly proliferating non-tumor cells.[47,48] Using immunohistochemistry and paraffin-embedded ALK+ALCL tumors, it was examined whether there is any evidence of abnormal subcellular localization of MSH2 in ALK+ALCL cells. As shown in **Figure**

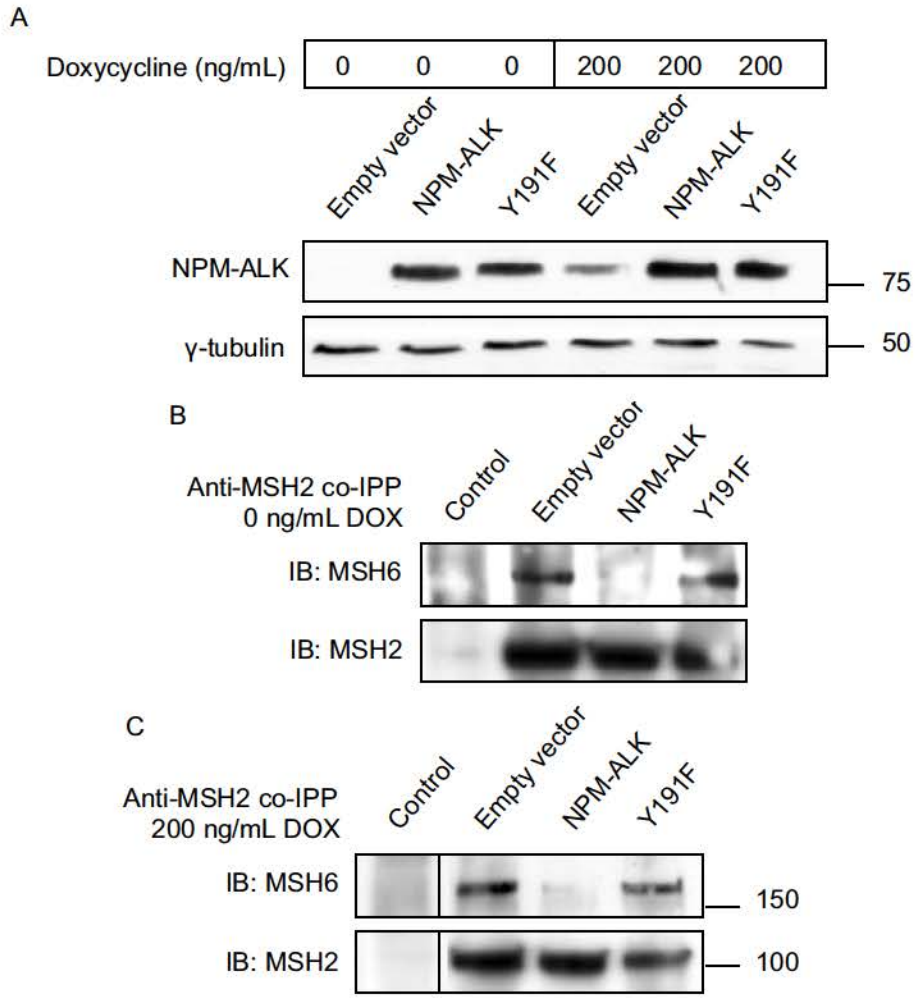

Figure 2.6 Disruption of NPM-ALK:MSH2 binding restores MutSα formation. (A) Tet-on HEK293/NPM-ALK cells were cultured in 0ng/mL and 200 ng/mL doxycycline (DOX), and were transfected with empty vector, *NPM-ALK* or *NPM-ALKY191F*. The resulting lysate was subjected to Western blotting with an anti-ALK antibody to detect NPM-ALK expression at 80 kDa. γ-tubulin (50 kDa) served as a loading control. (B) Lysate from 0 ng/mL doxycycline treated cell lysate and (C) 200 ng/mL doxycycline treated cell lysate from A were subject to co-IPP with an anti-MSH2 antibody, and the resulting immunoblots were probed with an MSH6 and MSH2 antibody to detect the amount of immunoprecipitated MSH6 relative to MSH2. A control with no antibody was included to account for non-specific binding for each sample, and a representative control is shown. Three independent experiments were performed.

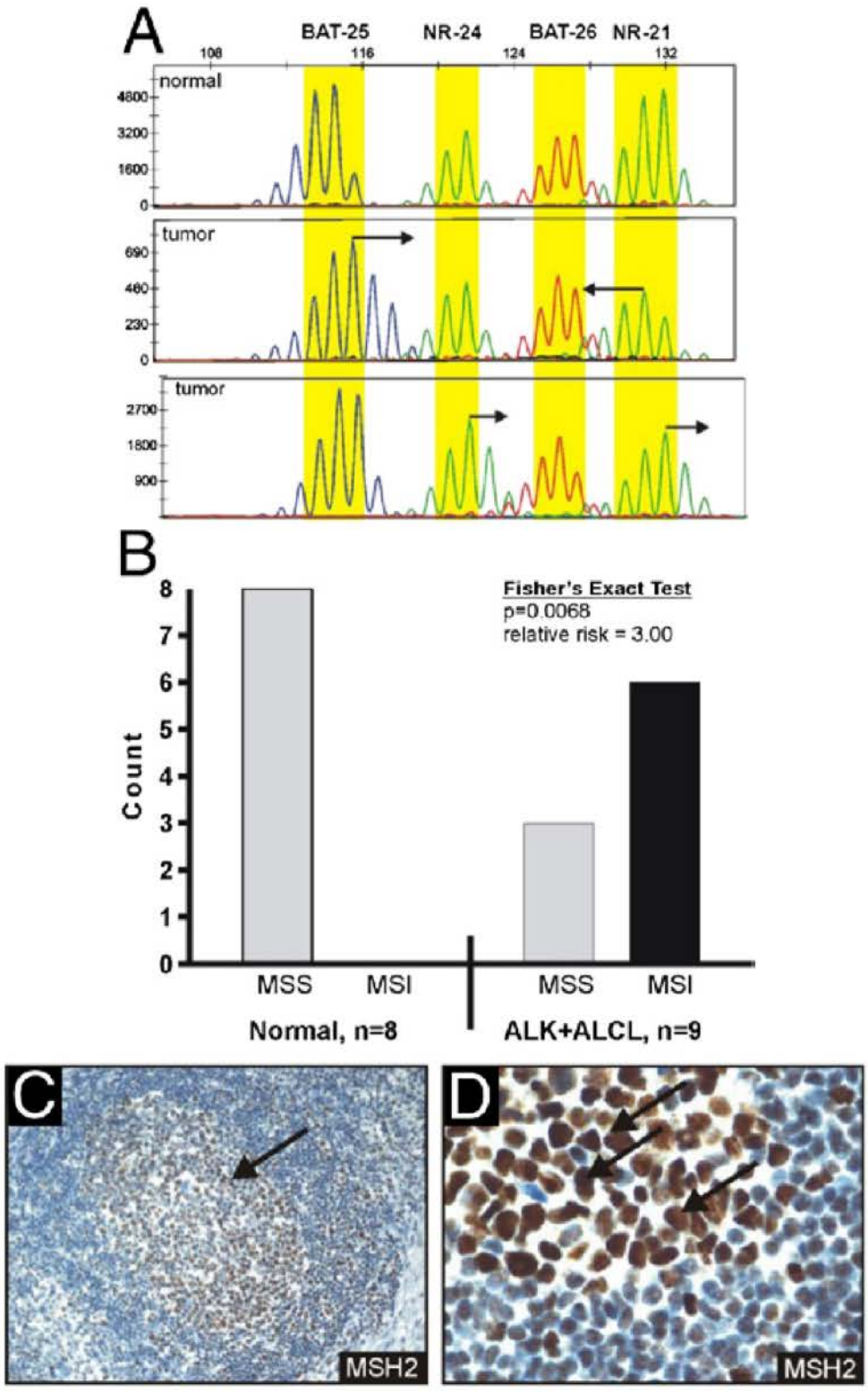
A
BAT-25
NR-24
BAT-26
NR-21
108
116
124
132
normal
4800
3200
1600
0
tumor
690
460
230
0
tumor
2700
1800
900
B
Fisher's Exact Test
p=0.0068
relative risk = 3.00
Count
8
7
6
5
4
3
2
1
0
MSS
MSI
MSS
MSI
Normal, n=8
ALK+ALCL, n=9
C
MSH2
D
MSH2

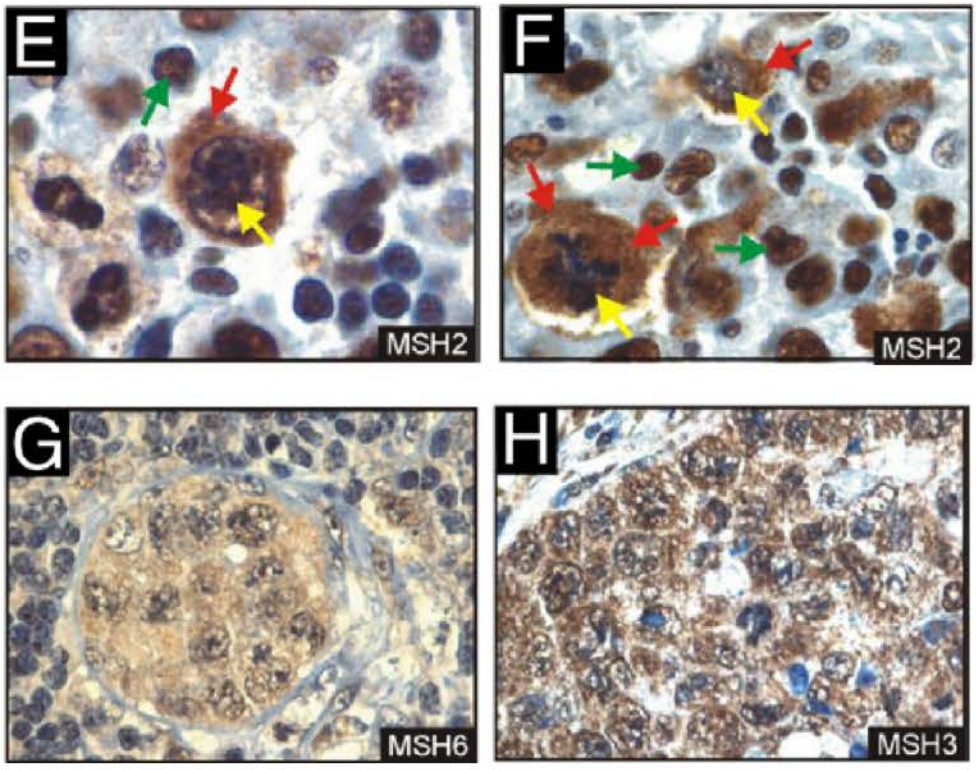

Figure 2.7. Evidence of MMR dysfunction in ALK+ALCL tumor samples. (A) Six quasi-monomorphic microsatellites were amplified using the QIAGEN Multiplex PCR kit and previously reported primers (Table 2.1) from patient DNA. Eight DNA samples were isolated from normal donors, and nine DNA samples were isolated from nine ALK+ALCL tumors. Resulting PCR samples were analyzed for MSI. Yellow depicts the range of the normal DNA traces, as determined by analysis of eight normal individuals. Arrows indicate shifts of the predominant peaks in the two representative ALK+ALCL tumors. (B) Summary of the MSI analysis of normal samples (n=8) and ALK+ALCL tumors (n=9). The significance was calculated using Fisher exact test (p=0.0068) and relative risk was calculated by GraphPad prism. MSS = microsatellite stable. (C) IHC using an anti-MSH2 antibody on reactive tonsil with benign lymphoid cells (normal sample). The arrow indicates the germinal center. (D) A high magnification of C showing nuclear MSH2 staining of benign lymphoid cells (arrows). (E) and (F) Two high-magnification views of ALK+ALCL

cells following IHC with an anti-MSH2 antibody. The red arrows show cytoplasmic staining of MSH2 in neoplastic cells. The yellow arrows highlight the nuclei of the neoplastic cells. The green arrows highlight benign lymphocyte nuclear MSH2 staining. (G) and (H) IHC of ALK+ALCL patient samples with an anti-MSH6 and anti-MSH3 antibody, respectively.

2.7C and **Figure 2.7D**, lymphocytes in benign reactive tonsils showed a predominantly nuclear staining pattern. In contrast, in large ALK+ ALCL cells, MSH2 cytoplasmic staining was readily identified cytoplasmic (**Figure 2.7E** and **2.7F**). In these tumorous samples, one can also appreciate that the small benign lymphocytes, which are often found admixed with the large lymphomatous cells, displayed the expected, predominantly MSH2 nuclear staining pattern. Similar studies for MSH3 and MSH6 were performed. As shown in **Figure 2.7G** and **Figure 2.7H**, cytoplasmic staining of MSH3 and MSH6 was readily detectable in ALK+ALCL cells. These findings provide further evidence to support that the biochemistry/function of MSH proteins is deregulated in these cells.

2.4.5 NPM-ALK impedes the DNA adduct-induced relocalization of MSH2

The exposure of cells to DNA damaging agents has been previously shown to induce a movement of MSH2·MSH6 heterodimer out of the cytoplasm.[45,46] Considering that NPM-ALK interfered with the MSH2:MSH6 binding and that heterodimerization with MSH6 is required for effective nuclear import of MSH2[49,50], it was asked whether NPM-ALK affected this normal MMR response to DNA adducts. Using the Tet-on HEK293/NPM-ALK cells, subcellular fractionation following exposure to 6TG was performed. As shown in **Figure 2.8**, in the absence of NPM-ALK (i.e. no doxycycline added), an expected reduction in cytoplasmic MSH2 and MSH6 levels on exposure to 6TG was observed. In contrast, expression of NPM-ALK abrogated the 6TG-induced reduction in MSH2 cytoplasmic levels, whereas the normal decrease in the cytoplasmic MSH6 levels was not changed. These changes correlate with the observation that the cytoplasmic MSH2:MSH6 ratios were skewed in the presence of NPM-ALK after 6TG exposure, whereas the ratios remained relatively consistent in the absence of NPM-ALK expression (**Figure 2.8**).

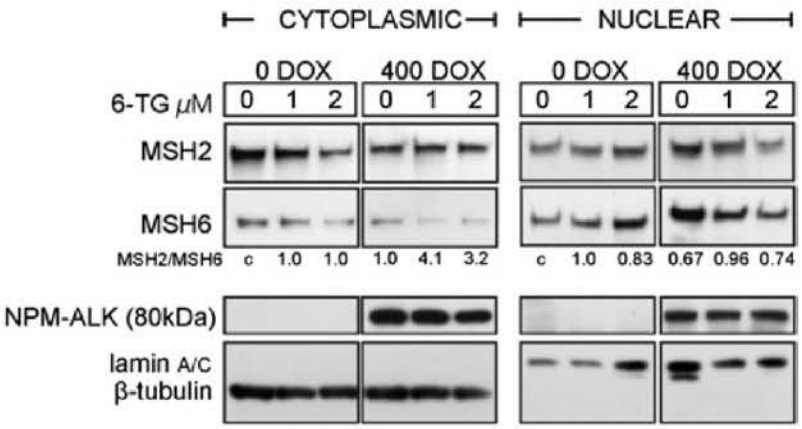

Figure 2.8. NPM-ALK impedes the DNA adduct-induced re-localization of MSH2. Tet-on HEK293/NPM-ALK cells were cultured in 0 ng/mL doxycycline (DOX) (no NPM-ALK) or 400 ng/mL doxycycline (which induced NPM-ALK expression at a level similar to that in ALK+ALCL cell lines) for 24 hours, and then exposed to 6TG for an additional 24 hours. Cells were harvested and the nuclear/cytoplasmic fractionation was performed. The resulting lysate was subjected to western blotting using anti-MSH2, anti-MSH6, and anti-ALK (NPM-ALK) antibodies. The ratio of MSH6 to MSH2, as determined by densitometry, is indicated; protein levels were normalized to 0 ng/mL doxycycline and 0 μmol/L 6TG for each fraction (indicated by c, control). The purity of the cytoplasmic and nuclear fractions was confirmed by γ-tubulin and lamin A/C, respectively. A representative result of three independent experiments is shown.

The isolation of β-tubulin to the cytoplasm and lamin A/C to the nucleus confirmed the purity of the resulting subcellular fractions. These data support a model in which NPM-ALK suppresses MMR function at the level of MSH2-related biochemistry.

2.4.6 The NPM-ALK:MSH2 interaction is dependent on the activation status of NPM-ALK

The accumulated evidence that NPM-ALK suppressed MMR function through interference with normal MMR biochemistry culminated in the question of whether the NPM-ALK:MSH2 interaction was dependent on NPM-ALK tyrosine kinase activity. To address this question, a panel of NPM-ALK mutants in which one of more of the three tyrosine residues in the kinase activation loop had been replaced by phenylalanine (Y→F mutations) was used.[32] Mutation within the kinase activation loop alters the autophosphorylation of NPM-ALK, and mutation of all three residues (FFF mutant) abrogates NPM-ALK autophosphorylation and NPM-ALK–induced growth advantage.[32] As shown in **Figure 2.9A**, affinity purification and subsequent immunoblot analysis of various NPM-ALK mutants was performed. In contrast with native NPM-ALK (denoted by YYY), inactive NPM-ALK (denoted by FFF) failed to demonstrate an interaction with MSH2. With the exception of the YFF mutant, the activation loop mutants displayed reduced levels of MSH2 interaction. The observed variations in NPM-ALK:MSH2 interaction levels were not attributable to the relative levels of NPM-ALK that were purified (**Figure 2.9A**) or the overall levels of MSH2 (**Figure 2.9B**). It should also be noted that immunoblot analysis of native NPM-ALK (denoted by YYY) revealed a readily detectable interaction with MSH2, but not MSH6 (**Figure 2.9A**), which is in keeping with previous observations from the Lai Laboratory.[10] Therefore, the NPM-ALK:MSH2 interaction was dependent on the activation state of NPM-ALK.

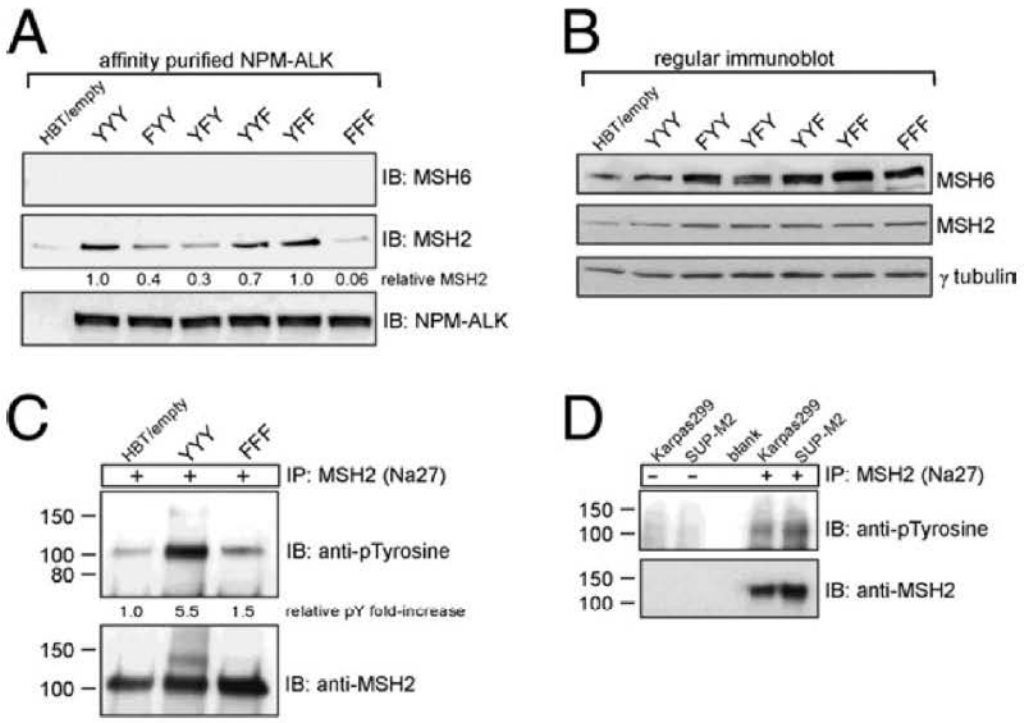

Figure 2.9. NPM-ALK mediates tyrosine phosphorylation of MSH2. (A) NPM-ALK contains the YxxxYY insulin receptor subfamily motif in its activation loop, and modulation of this loop has been shown to change the autophosphorylation characteristics of NPM-ALK and the oncogenic pressure exerted on the cells.[32] HEK293 cells were transiently transfected with empty vector, unmodified NPM-ALK (YYY), inactive NPM-ALK (FFF), as well as intermediate Y→F mutations of the activation loop. Resulting lysates were subjected to purification using on the basis of streptavidin/biotin binding; these NPM-ALK constructs were HB tagged. The resulting immunoblot was probed for MSH2, MSH6, and NPM-ALK, and the densitometry quantification of relative levels of co-precipitated MSH2 is noted. (B) HEK293 cells were transfected with various NPM-ALK expression vectors or HBT-empty vector, and the resulting lysate was subjected to western blotting with anti-MSH2, anti-MSH6 to show MSH2 and MSH6 protein expression. γ-tubulin served as a protein loading control. (C) HEK293 cells were transfected with empty vector, *NPM-ALK*, *NPM-ALK*^{FFF}. MSH2 was purified from the resulting lysates under IPP conditions, and the resulting immunoblot was probed with a phospho-

tyrosine antibody. To compare the levels of phospho-MSH2 with total MSH2, the blot was stripped and then probed with anti-MSH2. Densitometry values show the amount of tyrosine phosphorylated MSH2 relative to cells expressing empty vector, which was set at 1. (D) MSH2 was immunoprecipitated from the ALK+ALCL cell lines Karpas 299 and SUP-M2 under IP conditions, and the protein was subjected to western blotting with an anti-p-tyrosine antibody to assess MSH2 tyrosine phosphorylation. The western was stripped and probed with an anti-MSH2 antibody to confirm immunoprecipitation of MSH2. No-antibody controls (-) were included to account for non-specific binding, and a blank sample with no protein was run to ensure that the samples were sufficiently spaced on the gel. A representative result of three independent experiments is shown.

2.4.7 NPM-ALK induces MSH2 tyrosine phosphorylation

The specific interaction of MSH2 with NPM-ALK raised the question of whether MSH2 may be a direct or indirect target of NPM-ALK tyrosine kinase activity. Comparing MSH2 immunoprecipitated from cells expressing active NPM-ALK to cells expressing the inactive NPM-ALK, the Lai Laboratory found that tyrosine phosphorylation on MSH2 greatly increased in the presence of native NPM-ALK (**Figure 2.9C**). The kinase dead NPM-ALK^{K210R} (Amrogio et al.[51]), also demonstrated a failure to tyrosine phosphorylate MSH2 (not shown). Moreover, tyrosine phosphorylation of MSH2 in two ALK+ALCL cell lines was observed (**Figure 2.9D**). Finally, to determine whether NPM-ALK is directly responsible for MSH2 tyrosine phosphorylation in ALK+ALCL cells, I knocked down NPM-ALK in these cells using siRNA. The tyrosine phosphorylation of MSH2 was dramatically decreased after NPM-ALK knock-down (**Figure 2.10**).

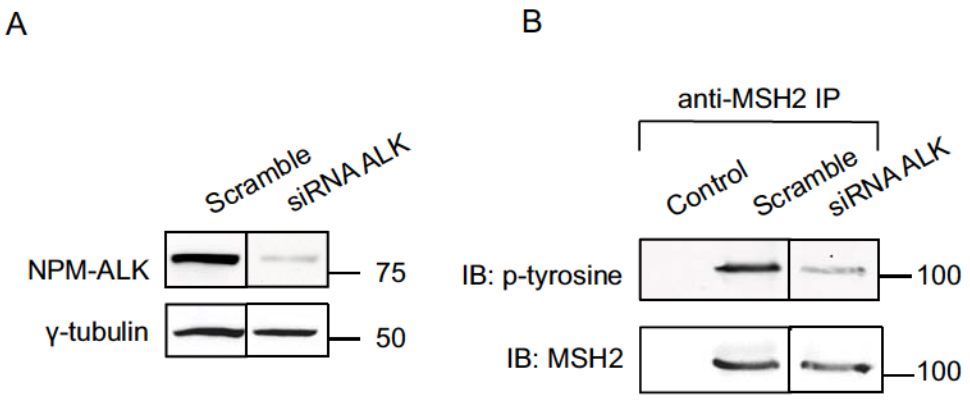

Figure 2.10. Knockdown of NPM-ALK expression significantly reduced tyrosine phosphorylation of MSH2. (A) ALK specific siRNA was used to downregulate NPM-ALK in the ALK+ALCL cell line SUP-M2. A scramble siRNA was used as a negative control. The resulting cell lysate was subjected to western blotting using an anti-ALK antibody for NPM-ALK expression (80 kDa), and a γ-tubulin antibody, which served as a protein loading control (50 kDa) .(B) MSH2 was purified from the lysates depicted in A under IPP conditions, and the resulting immunoblot was probed with anti-phospho-tyrosine (p-Y) antibody. The blot was stripped and probed with an anti-MSH2 antibody to compare the amount of phospho-MSH2 (100 kDa) with total MSH2 (100 kDa). No-antibody controls were included for all samples and a representative control is shown. A representative result from three independent experiments is shown.

2.5 Discussion

Recent studies have revealed that the mechanisms by which oncogenic tyrosine kinases mediate tumorigenesis are rather diverse. Directly relevant to the current study, there is accumulating evidence that oncogenic tyrosine kinases can redirect cellular processes to favor error-prone DNA repair pathways and to suppress cellular responses to DNA damage/errors.[52-56] It has been recently shown that expression of the fusion tyrosine kinase BCR/ABL reduced the MMR response to single base mismatches and DNA damage-induced signaling.[57] Nevertheless, how these oncogenic tyrosine kinases impair MMR function is largely unknown.

One of the key findings of this study is that NPM-ALK indeed suppresses MMR. This conclusion is primarily based on the results of three well-established *in vitro* assays for MMR functions. First, the impact of NPM-ALK on MMR function was measured by assessing the cell viability after 6TG treatment. The second assay involves the use of a previously described pCAR-OF vector. The third assay involves the novel assessment of MSI in NPM-ALK expressing non-neoplastic cultured cells. Because the conclusion that NPM-ALK suppresses MMR is based on experiments performed on HEK293 cells, an easy-to-transfect, human embryonic kidney cell line, ALK+ALCL tumors were examined for evidence of MMR dysfunction. A relatively high incidence of MSI, a hallmark of MMR dysfunction, was detected in ALK+ALCL patient samples. As NPM-ALK is considered the central pathogenetic factor in this tumor type, the frequent finding of MSI in ALK+ALCL is in support of the hypothesis. Of note, the choice of microsatellite markers used in this study was somewhat dictated by the intrinsic limitation that all of the study cases were retrospective samples, and normal DNA samples from these same individuals were not available for comparison. With this in mind,

microsatellites that are considered to be of relatively consistent length (quasi-monomorphic) in normal tissues within the Northern European ancestry were used.[39,58,59] Two of these markers are part of the five markers recommended by the National Cancer Institute. Moreover, the loci examined in this study have demonstrated increased efficacy for accurately identifying MSI-positive samples in tumor samples in which only the MSH2·MSH6 heterodimer is affected (e.g. MSH6-deficient endometrial carcinoma).[34] It is noteworthy that in tumors associated with the loss of a key MMR protein (e.g. Lynch and sporadic), MSI is not always detectable, likely because of the loci selected for analysis and tumor heterogeneity. The finding of a relatively high frequency of MSI in ALK+ALCL differs from that of a previously study in which four ALK+ALCL cases were examined and found to have no evidence of MSI at seven dinucleotide repeats.[60] In this regard, it is known that MSI results are dependent on the markers chosen for analysis, the threshold chosen for instability, and the sensitivity of the assay used.[35]

Although other oncogenic tyrosine kinases, such as BCR-ABL, have been reported to suppress MMR[57], the mechanisms have not been previously studied. This study has shed light on the possible mechanisms by which oncogenic tyrosine kinases deregulate MMR. Specifically, based on the findings that NPM-ALK binds to MSH2 but not MSH3 or MSH6, it was hypothesized that NPM-ALK may suppress MMR by interfering with the MSH2:MSH6 interaction. As mentioned above, MSH2:MSH6 is the predominant MMR protein complex responsible for the detection of postreplicative DNA errors, as well as exogenous and endogenous DNA damage. The experimental data showed that increasing expression levels of NPM-ALK decreases MSH2:MSH6 binding and promote MSH2:NPM-ALK in a dose-dependent fashion.

To further delineate the mechanism underlying NPM-ALK-mediated MMR

suppression, an NPM-ALK mutant, in which the tyrosine 191 was mutated into phenylalanine was constructed. As this mutant does not bind to MSH2 as well as native NPM-ALK does, this mutant was used to address the question of whether the MSH2:NPM-ALK interaction is important for the MMR suppression mediated by NPM-ALK. The NPM-ALK^{Y191F} mutant is less efficient in suppressing MMR functions. Furthermore, more MSH6 protein was pulled down with MSH2 in the presence of NPM-ALK^{Y191F}, as compared with native NPM-ALK. Taken together, the findings support a model in which NPM-ALK suppresses MMR via sequestrating MSH2 away from MSH6.

The finding that the MSH2:NPM-ALK binding is dependent on the activation/phosphorylation status of NPM-ALK is not surprising, as it is well documented that the interactions between NPM-ALK and its binding partners are largely abrogated when the autophosphorylation of NPM-ALK is reduced or abolished.[3] Nevertheless, as opposed to the vast majority of the proteins known to interact with NPM-ALK, MSH2 does not contain a SH2 domain. Although the Y191 residue and the overall activation status of NPM-ALK are important in mediating the MSH2:NPM-ALK interaction, the mechanism is not completely understood. The possibility that the phospho-tyrosine binding (PTB) domain present in MSH2 may play a role in mediating a direct physical interaction between NPM-ALK and MSH2 has been considered. It is also possible that the MSH2:NPM-ALK interaction is indirect and that yet-to-be identified intermediate(s) are involved.

In view of the fact that NPM-ALK is a constitutively active tyrosine kinase, whether MSH2 can be phosphorylated in the presence of NPM-ALK was investigated. In HEK293 cells, enforced expression of *NPM-ALK* indeed resulted in tyrosine phosphorylation of MSH2, and in ALK+ALCL cells, MSH2 is also tyrosine phosphorylated. Importantly, NPM-ALK is directly

responsible for the tyrosine phosphorylation of MSH2, as siRNA knock-down of NPM-ALK in these cells resulted in a dramatic decrease in the MSH2 tyrosine phosphorylation. The biological significance of MSH2 tyrosine phosphorylation is currently under investigation in the Lai laboratories. Nevertheless, a small number of reports suggest that phosphorylation of MSH2 carries biological importance. For instance, phosphorylation of MSH2:MSH6 has been shown to alter its DNA binding properties, although tyrosine phosphorylation of MSH2 was not clearly demonstrated to be involved [46]. In two other studies, threonine phosphorylation of MSH2 was found to modulate its stability.[61,62] Tyrosine tyrosine phosphorylation of MSH2 is a highly interesting phenomenon, and studies of its importance are underway in the Lai laboratories.

Normally, MSH2 is predominantly localized to the nucleus, with lower levels in the cytoplasm, and it is in the cytoplasm that newly translated MSH2 binds MSH6 to form MSH2:MSH6.[45,46] MSH2 does not contain a clear nuclear localization signal and is largely dependent on MSH6 for co-import into the nucleus.[49,50] It has previously been shown that there is a movement of the cytoplasmic MSH2 into the nucleus on the induction of DNA damage.[45,46] In keeping with the concept that NPM-ALK disrupts the MSH2:MSH6 interaction, evidence that NPM-ALK also interferes with the MSH2 nuclear translocation on DNA damage was found. The observation that MSH6 re-localization was not affected by NPM-ALK is in keeping with the concept that its nuclear translocation is independent of MSH2.[50] Correlating with these *in vitro* data, the immunohistochemical studies revealed that MSH2 was readily detectable in the cytoplasm in ALK+ALCL tumor cells, but not the infiltrating small lymphocytes. Although the biological importance of these abnormalities needs to be further defined, reduced (but not abrogated) levels of MMR proteins have been shown to be sufficient to confer MMR dysfunction.[14,19,63,64] In other words, it is highly likely that this “cytoplasmic retention” of MSH2 is sufficient to confer MMR

dysfunction.

In summary, the evidence presented in this study suggest that NPM-ALK suppresses MMR function, and this conclusion echoes the observed high frequency of MSI in ALK+ALCL tumor samples. This study also has provided evidence that the biology/biochemistry of MSH2 is affected by NPM-ALK, and these alterations may represent some of the underlying mechanisms by which NPM-ALK suppresses MMR function. Further studies are clearly needed to clarify this complicated biological process. The biological importance of tyrosine phosphorylation of MSH2 in the context of oncogenesis also needs to be further delineated.

2.6 Acknowledgments

Supported by research grants from the Alberta Cancer Foundation and the Canadian Institutes of Health Research (R.L.). S.E.A is an Alberta Heritage Foundation for Medical Research Senior Scholar. K.M.B. is a recipient of the Izaak Walton Killam Memorial Scholarship (University of Alberta). B.A.A. was supported by a summer studentship provided by the Alberta Heritage Foundation for Medical Research. L.L. is a Canada Research Chair in Chemistry.

2.7 References

1. Kutok JL, Aster JC. Molecular biology of anaplastic lymphoma kinase-positive anaplastic large-cell lymphoma. *J Clin Oncol* 2002;**20**(17):3691-3702.
2. Falini B. Anaplastic large cell lymphoma: pathological, molecular and clinical features. *Br J Haematol* 2001;**114**(4):741-760.
3. Amin HM, Lai R. Pathobiology of ALK+ anaplastic large-cell lymphoma. *Blood* 2007;**110**(7):2259-2267.

4. Bischof D, Pulford K, Mason DY, Morris SW. Role of the nucleophosmin (NPM) portion of the non-Hodgkin's lymphoma-associated NPM-anaplastic lymphoma kinase fusion protein in oncogenesis. *Mol Cell Biol* 1997;**17**(4):2312-2325.

5. Duyster J, Bai RY, Morris SW. Translocations involving anaplastic lymphoma kinase (ALK). *Oncogene* 2001;**20**(40):5623-5637.

6. Jager R, Hahne J, Jacob A, et al. Mice transgenic for NPM-ALK develop non-Hodgkin lymphomas. *Anticancer Res* 2005;**25**(5):3191-3196.

7. Wellmann A, Doseeva V, Butscher W, et al. The activated anaplastic lymphoma kinase increases cellular proliferation and oncogene up-regulation in rat 1a fibroblasts. *FASEB J* 1997;**11**(12):965-972.

8. Kuefer MU, Look AT, Pulford K, et al. Retrovirus-mediated gene transfer of NPM-ALK causes lymphoid malignancy in mice. *Blood* 1997;**90**(8):2901-2910.

9. Chiarle R, Gong JZ, Guasparri I, et al. NPM-ALK transgenic mice spontaneously develop T-cell lymphomas and plasma cell tumors. *Blood* 2003;**101**(5):1919-1927.

10. Wu F, Wang P, Young LC, Lai R, Li L. Proteome-wide identification of novel binding partners to the oncogenic fusion gene protein, NPM-ALK, using tandem affinity purification and mass spectrometry. *Am J Pathol* 2009;**174**(2):361-370.

11. Li GM. Mechanisms and functions of DNA mismatch repair. *Cell Res* 2008;**18**(1):85-98.

12. Rasmussen LJ, Rasmussen M, Lee B, et al. Identification of factors interacting with hMSH2 in the fetal liver utilizing the yeast two-hybrid system. In vivo interaction through the C-terminal domains of hEXO1 and hMSH2 and comparative expression analysis. *Mutat Res* 2000;**460**(1):41-52.

13. Gibson SL, Narayanan L, Hegan DC, Buermeyer AB, Liskay RM, Glazer PM. Overexpression of the DNA mismatch repair factor, PMS2,

confers hypermutability and DNA damage tolerance. *Cancer Lett* 2006;**244**(2):195-202.

14. Marra G, Iaccarino I, Lettieri T, Roscilli G, Delmastro P, Jiricny J. Mismatch repair deficiency associated with overexpression of the MSH3 gene. *Proc Natl Acad Sci U S A* 1998;**95**(15):8568-8573.

15. Zhang H, Richards B, Wilson T, et al. Apoptosis induced by overexpression of hMSH2 or hMLH1. *Cancer Res* 1999;**59**(13):3021-3027.

16. Young LC, Listgarten J, Trotter MJ, Andrew SE, Tron VA. Evidence that dysregulated DNA mismatch repair characterizes human nonmelanoma skin cancer. *Br J Dermatol* 2008;**158**(1):59-69.

17. Norris AM, Woodruff RD, D'Agostino RB, Jr., Clodfelter JE, Scarpinato KD. Elevated levels of the mismatch repair protein PMS2 are associated with prostate cancer. *Prostate* 2007;**67**(2):214-225.

18. Shcherbakova PV, Kunkel TA. Mutator phenotypes conferred by MLH1 overexpression and by heterozygosity for mlh1 mutations. *Mol Cell Biol* 1999;**19**(4):3177-3183.

19. Claij N, Te Riele H. Methylation tolerance in mismatch repair proficient cells with low MSH2 protein level. *Oncogene* 2002;**21**(18):2873-2879.

20. Edelmann L, Edelmann W. Loss of DNA mismatch repair function and cancer predisposition in the mouse: animal models for human hereditary nonpolyposis colorectal cancer. *Am J Med Genet C Semin Med Genet* 2004;**129C**(1):91-99.

21. Edelmann W, Umar A, Yang K, et al. The DNA mismatch repair genes Msh3 and Msh6 cooperate in intestinal tumor suppression. *Cancer Res* 2000;**60**(4):803-807.

22. Edelmann W, Yang K, Umar A, et al. Mutation in the mismatch repair gene Msh6 causes cancer susceptibility. *Cell* 1997;**91**(4):467-477.

23. Andrew SE, McKinnon M, Cheng BS, et al. Tissues of MSH2-deficient mice demonstrate hypermutability on exposure to a DNA methylating agent. *Proc Natl Acad Sci U S A* 1998;**95**(3):1126-1130.

24. Reitmair AH, Risley R, Bristow RG, et al. Mutator phenotype in Msh2-deficient murine embryonic fibroblasts. *Cancer Res* 1997;**57**(17):3765-3771.

25. Lowsky R, DeCoteau JF, Reitmair AH, et al. Defects of the mismatch repair gene MSH2 are implicated in the development of murine and human lymphoblastic lymphomas and are associated with the aberrant expression of rhombotin-2 (Lmo-2) and Tal-1 (SCL). *Blood* 1997;**89**(7):2276-2282.

26. Reitmair AH, Schmits R, Ewel A, et al. MSH2 deficient mice are viable and susceptible to lymphoid tumours. *Nat Genet* 1995;**11**(1):64-70.

27. Genschel J, Littman SJ, Drummond JT, Modrich P. Isolation of MutSbeta from human cells and comparison of the mismatch repair specificities of MutSbeta and MutSalpha. *J Biol Chem* 1998;**273**(31):19895-19901.

28. Wei K, Kucherlapati R, Edelmann W. Mouse models for human DNA mismatch-repair gene defects. *Trends Mol Med* 2002;**8**(7):346-353.

29. Coleman WB, Tsongalis GJ. The role of genomic instability in human carcinogenesis. *Anticancer Res* 1999;**19**(6A):4645-4664.

30. Felton KE, Gilchrist DM, Andrew SE. Constitutive deficiency in DNA mismatch repair. *Clin Genet* 2007;**71**(6):483-498.

31. Miyashita K, Fujii K, Yamada Y, et al. Frequent microsatellite instability in non-Hodgkin lymphomas irresponsive to chemotherapy. *Leuk Res* 2008;**32**(8):1183-1195.

32. Wang P, Wu F, Ma Y, Li L, Lai R, Young LC. Functional characterization of the kinase activation loop in nucleophosmin (NPM)-anaplastic lymphoma kinase (ALK) using tandem affinity purification and liquid chromatography-mass spectrometry. *J Biol Chem* 2010;**285**(1):95-103.

33. Umar A, Boland CR, Terdiman JP, et al. Revised Bethesda Guidelines for hereditary nonpolyposis colorectal cancer (Lynch

syndrome) and microsatellite instability. *J Natl Cancer Inst* 2004;**96**(4):261-268.

34. Wong YF, Cheung TH, Lo KW, et al. Detection of microsatellite instability in endometrial cancer: advantages of a panel of five mononucleotide repeats over the National Cancer Institute panel of markers. *Carcinogenesis* 2006;**27**(5):951-955.

35. Oda S, Maehara Y, Ikeda Y, et al. Two modes of microsatellite instability in human cancer: differential connection of defective DNA mismatch repair to dinucleotide repeat instability. *Nucleic Acids Res* 2005;**33**(5):1628-1636.

36. Plaschke J, Engel C, Kruger S, et al. Lower incidence of colorectal cancer and later age of disease onset in 27 families with pathogenic MSH6 germline mutations compared with families with MLH1 or MSH2 mutations: the German Hereditary Nonpolyposis Colorectal Cancer Consortium. *J Clin Oncol* 2004;**22**(22):4486-4494.

37. Umetani N, Sasaki S, Watanabe T, Ishigami H, Ueda E, Nagawa H. Diagnostic primer sets for microsatellite instability optimized for a minimal amount of damaged DNA from colorectal tissue samples. *Ann Surg Oncol* 2000;**7**(4):276-280.

38. Findeisen P, Kloor M, Merx S, et al. T25 repeat in the 3' untranslated region of the CASP2 gene: a sensitive and specific marker for microsatellite instability in colorectal cancer. *Cancer Res* 2005;**65**(18):8072-8078.

39. Buhard O, Suraweera N, Lectard A, Duval A, Hamelin R. Quasimonomorphic mononucleotide repeats for high-level microsatellite instability analysis. *Dis Markers* 2004;**20**(4-5):251-257.

40. Rozen S, Skaletsky H. Primer3 on the WWW for general users and for biologist programmers. *Methods Mol Biol* 2000;**132**:365-386.

41. Nicolaides NC, Littman SJ, Modrich P, Kinzler KW, Vogelstein B. A naturally occurring hPMS2 mutation can confer a dominant negative mutator phenotype. *Mol Cell Biol* 1998;**18**(3):1635-1641.

42. Karran P. Thiopurines, DNA damage, DNA repair and therapy-related cancer. *Br Med Bull* 2006;**79-80**:153-170.

43. Yan T, Berry SE, Desai AB, Kinsella TJ. DNA mismatch repair (MMR) mediates 6-thioguanine genotoxicity by introducing single-strand breaks to signal a G2-M arrest in MMR-proficient RKO cells. *Clin Cancer Res* 2003;**9**(6):2327-2334.

44. Boccalatte FE, Voena C, Riganti C, et al. The enzymatic activity of 5-aminoimidazole-4-carboxamide ribonucleotide formyltransferase/IMP cyclohydrolase is enhanced by NPM-ALK: new insights in ALK-mediated pathogenesis and the treatment of ALCL. *Blood* 2009;**113**(12):2776-2790.

45. Christmann M, Kaina B. Nuclear translocation of mismatch repair proteins MSH2 and MSH6 as a response of cells to alkylating agents. *J Biol Chem* 2000;**275**(46):36256-36262.

46. Christmann M, Tomicic MT, Kaina B. Phosphorylation of mismatch repair proteins MSH2 and MSH6 affecting MutSalpha mismatch-binding activity. *Nucleic Acids Res* 2002;**30**(9):1959-1966.

47. Iwanaga R, Komori H, Ohtani K. Differential regulation of expression of the mammalian DNA repair genes by growth stimulation. *Oncogene* 2004;**23**(53):8581-8590.

48. Wilson TM, Ewel A, Duguid JR, et al. Differential cellular expression of the human MSH2 repair enzyme in small and large intestine. *Cancer Res* 1995;**55**(22):5146-5150.

49. Knudsen NO, Andersen SD, Lutzen A, Nielsen FC, Rasmussen LJ. Nuclear translocation contributes to regulation of DNA excision repair activities. *DNA Repair (Amst)* 2009;**8**(6):682-689.

50. Hong Z, Jiang J, Hashiguchi K, Hoshi M, Lan L, Yasui A. Recruitment of mismatch repair proteins to the site of DNA damage in human cells. *J Cell Sci* 2008;**121**(Pt 19):3146-3154.

51. Ambrogio C, Voena C, Manazza AD, et al. p130Cas mediates the transforming properties of the anaplastic lymphoma kinase. *Blood* 2005;**106**(12):3907-3916.

52. Dierov J, Sanchez PV, Burke BA, et al. BCR/ABL induces chromosomal instability after genotoxic stress and alters the cell death threshold. *Leukemia* 2009;**23**(2):279-286.

53. Fernandes MS, Reddy MM, Gonneville JR, et al. BCR-ABL promotes the frequency of mutagenic single-strand annealing DNA repair. *Blood* 2009;**114**(9):1813-1819.

54. Poplawski T, Blasiak J. BCR/ABL downregulates DNA-PK(CS)-dependent and upregulates backup non-homologous end joining in leukemic cells. *Mol Biol Rep* 2010;**37**(5):2309-2315.

55. Lal MA, Bae D, Camilli TC, Patierno SR, Ceryak S. AKT1 mediates bypass of the G1/S checkpoint after genotoxic stress in normal human cells. *Cell Cycle* 2009;**8**(10):1589-1602.

56. Penserga ET, Skorski T. Fusion tyrosine kinases: a result and cause of genomic instability. *Oncogene* 2007;**26**(1):11-20.

57. Stoklosa T, Poplawski T, Koptyra M, et al. BCR/ABL inhibits mismatch repair to protect from apoptosis and induce point mutations. *Cancer Res* 2008;**68**(8):2576-2580.

58. Brennetot C, Buhard O, Jourdan F, Flejou JF, Duval A, Hamelin R. Mononucleotide repeats BAT-26 and BAT-25 accurately detect MSI-H tumors and predict tumor content: implications for population screening. *Int J Cancer* 2005;**113**(3):446-450.

59. Buhard O, Cattaneo F, Wong YF, et al. Multipopulation analysis of polymorphisms in five mononucleotide repeats used to determine the microsatellite instability status of human tumors. *J Clin Oncol* 2006;**24**(2):241-251.

60. Hodges KB, Vnencak-Jones CL, Larson RS, Kinney MC. Rarity of genomic instability in pathogenesis of systemic anaplastic large cell lymphoma (ALCL) in immunocompetent patients. *Hum Pathol* 1999;**30**(2):173-177.

61. Hernandez-Pigeon H, Quillet-Mary A, Louat T, et al. hMutS alpha is protected from ubiquitin-proteasome-dependent degradation by atypical protein kinase C zeta phosphorylation. *J Mol Biol* 2005;**348**(1):63-74.

62. Hernandez-Pigeon H, Laurent G, Humbert O, Salles B, Lautier D. Degradration of mismatch repair hMutSalpha heterodimer by the ubiquitin-proteasome pathway. *FEBS Lett* 2004;**562**(1-3):40-44.

63. Ollila S, Sarantaus L, Kariola R, et al. Pathogenicity of MSH2 missense mutations is typically associated with impaired repair capability of the mutated protein. *Gastroenterology* 2006;**131**(5):1408-1417.

64. Pepponi R, Graziani G, Falcinelli S, et al. hMSH3 overexpression and cellular response to cytotoxic anticancer agents. *Carcinogenesis* 2001;**22**(8):1131-1137.

CHAPTER 3

NPM-ALK mediates phosphorylation of MSH2 at tyrosine 238, creating a functional deficiency in MSH2 and the loss of mismatch repair

---

This chapter has been modified from a manuscript that has been submitted for publication:

Bone KM, Wang P, Wu F, Wu C, Li L, Bacani, JT, Andrew SE, Lai R. NPM-ALK mediates phosphorylation of MSH2 at tyrosine 238, creating a functional deficiency in MSH2 and the loss of mismatch repair. Submitted for publication. 2014.

As first author, I designed and performed all the experiments described herein, except for the following: Wang P, and Wu F performed the mass spectrometry experiments, and subsequent analysis shown in Figure 3.2; Wu C took the Tet-on ALK+ALCL cells lines (that I made) and performed the viral infection and selection to make the Tet-on $MSH2^{Y238F}$ ALK+ALCL cell lines used in Figures 3.7-3.9. I also wrote the manuscript.

3.1 Abstract

The vast majority of ALK+ALCL cases express the characteristic oncogenic fusion protein NPM-ALK, which mediates tumorigenesis by exerting its constitutive tyrosine kinase activity on various substrates. MSH2, a central protein to DNA mismatch repair (MMR), was recently identified as a novel binding partner and phosphorylation substrate of NPM-ALK. Here, using liquid chromatography-mass spectrometry, it is reported for the first time that MSH2 is phosphorylated by NPM-ALK at a specific residue, tyrosine 238. Using GP293 cells transfected with NPM-ALK, I confirmed that the $MSH2^{Y238F}$ mutant is not tyrosine phosphorylated. Furthermore, transfection of $MSH2^{Y238F}$ into these cells substantially decreased the tyrosine phosphorylation of endogenous MSH2. Importantly, gene transfection of $MSH2^{Y238F}$ abrogated the binding of NPM-ALK with endogenous MSH2, re-established the dimerization of MSH2:MSH6, and restored the sensitivity to DNA mismatch-inducing drugs, indicative of MMR return. Parallel findings were observed in two ALK+ALCL cell lines, Karpas 299 and SUP-M2. Additionally, I found that enforced expression of $MSH2^{Y238F}$ into ALK+ALCL cells alone was sufficient to induce spontaneous apoptosis. To conclude, my findings have identified NPM-ALK-induced phosphorylation of MSH2 at Y238 as a crucial event in suppressing MMR. These studies have provided novel insights into the mechanism by which oncogenic tyrosine kinases disrupt MMR.

3.2 Introduction

Anaplastic lymphoma kinase-positive anaplastic large cell lymphoma (ALK+ALCL) is a specific type of T/null-cell non-Hodgkin's lymphoma recognized by the World Health Organization Classification Scheme for hematologic malignancies.[1] Most of these tumors are characterized by the expression of the oncogenic fusion protein NPM-ALK, which results from the reciprocal translocation t(2;5)(p23;q35) involving the *anaplastic lymphoma kinase* (ALK) and *nucleophosmin* (NPM) genes.[2-5] Previous studies have demonstrated that NPM-ALK mediates tumorigenesis by constitutively activating various signaling pathways leading to cell cycle deregulation and enhanced survival.[6-8]

The Lai Laboratory previously reported that MutS homolog 2 (MSH2), a protein central to DNA mismatch repair (MMR), is tyrosine phosphorylated by NPM-ALK, leading to the disruption of MMR.[9] MSH2 and other MMR proteins are highly expressed in normal cells and their key function is to maintain genomic stability by correcting DNA damage and replication errors from endogenous and exogenous sources.[10-12] They do so by binding and correcting single base mismatches and insertion-deletion loops, which occur when the replication machinery "stutters" on highly repetitive microsatellite sequences.[13,14] The predominant MMR protein heterodimer is composed of MSH2:MSH6 (MutSα), and it repairs single base mismatches, small insertion-deletion loops and DNA damage adducts.[10,15,16] The importance of MMR in tumor biology has been highlighted in Lynch syndrome, which is caused by hereditary germline mutations in MMR genes.[13,16-19] Loss of MMR function and the resultant microsatellite instability (MSI) have been associated with the development and progression of a number of hematological malignancies, including acute and chronic myeloid leukemia, myelodysplastic syndrome and non-Hodgkin's lymphoma.[20-23] In a previous study from the Lai Laboratory,

evidence of MSI in 6 out of 9 ALK+ALCL tumors was shown.[9] MMR dysfunction as a result of progressive loss of MMR genes is also a frequent event in a variety of sporadic cancers, where MMR-deficient cells display a significantly higher mutation rate and resistance to some chemotherapeutic agents.[24-33]

Post-translational modification of MMR proteins has not been extensively characterized[34-36], and the Lai research group described tyrosine phosphorylation of MSH2 for the first time in 2011.[9] Specifically, evidence that NPM-ALK mediates tyrosine phosphorylation of MSH2 and deregulates MMR was found. In this study, I sought to further delineate this process and explore the biological significance of MSH2 tyrosine phosphorylation. First, the specific tyrosine residue(s) on MSH2 that is/are phosphorylated by NPM-ALK were determined by mass spectrometry. Using a specific MSH2 mutant in which NPM-ALK-mediated tyrosine phosphorylation of MSH2 is largely abrogated, I assessed if this newly described phosphorylation event underlies the NPM-ALK-induced MMR deficiency.

3.3 Materials and Methods

3.3.1 Cell lines, cell culture and gene transfection

GP293 cells were maintained in Dulbecco's Modified Eagles Medium (Invitrogen, Life Technologies, Grand Island, NY) supplemented with 10% FBS (Invitrogen) and 100 units/mL penicillin,100 µg/mL streptomycin (Invitrogen). GP293 cells are a derivative of HEK293 cells with higher transfection efficiency. Tet-on HEK293/NPM-ALK cells, in which the expression of NPM-ALK is controlled by doxycycline, were maintained in Dulbecco's Modified Eagle's Medium supplemented with 10% Tet-System Approved FBS (Clontech, Mountain View, CA), 100 µg/mL G418

(Invitrogen) and 50 μg/mL hygromycin B (Invitrogen) as previously described.[9] ALK+ALCL cell lines Karpas 299 and SUP-M2 were grown in RPMI-1640 (Invitrogen) supplemented with 10% FBS and 100 units/mL penicillin,100 μg/mL streptomycin. GP293 cells were transiently transfected with 10 μg plasmid DNA in 10-cm plates using Lipofectamine 2000 (Invitrogen) according to the manufacturer's protocol.

3.3.2 Gene expression vectors and site-directed mutagenesis

His-biotin (HB) tagged MSH2 was constructed by ligating MSH2 cDNA from pcDNA3-MSH2[37] (a gift from Dr. Meuth) into the his-biotin (HB)-tagged vector described previously.[38] Site-directed mutagenesis of tyrosine (Y) 238 of MSH2 to phenylalanine (F; $MSH2^{Y238F}$) was done using the QuikChange Site Directed Mutagenesis Kit (Agilent Technologies, Mississauga, ON, Canada) following the manufacturer's suggested protocol for 2 or more mutagenic primers. The mutation was confirmed by sequencing at The Applied Genomics Centre (TAGC), University of Alberta. The NPM-ALK expression vector was a gift from Dr. Morris[39]; pcDNA3 (Invitrogen) was used as a negative control for NPM-ALK expression.

3.3.3 Tandem affinity purification under denaturing conditions, on bead protein digestion and liquid chromatography-mass spectrometry

Tandem affinity purification and liquid chromatography-mass spectrometry (LC-MS) under denaturing conditions using GP293 cells transfected with HB-MSH2 and NPM-ALK was performed as previously described.[38,40] Assigned sequence and spectra were imported into a manual database including the peptide sequences of MSH2. An increased molecular weight of ~110 kDa on a tyrosine residue was indicative of phosphorylation.

Peptide fragments containing a phosphorylated tyrosine residue were manually examined. The phosphorylation profile for the native MSH2 peptide was an assembly of three independent experiments and was considered true if it was identified in at least two independent experiments.

3.3.4 Generation of Tet-on ALK+ALCL MSH2/MSH2^{Y238F} cell lines

Tet-on ALK+ALCL MSH2^{Y238F} cell lines were generated using the RetroX Tet-on Advanced Inducible Expression System (Clontech). To generate the viral supernatant, Phoenix packaging cells were transfected with the pRetro-X Tet-on Advanced plasmid using Lipofectamine 2000. The cell supernatant was collected 48 hours post-transfection, filtered and was used to resuspend 5 X 10^6 Karpas 299 and SUP-M2 cells, along with 6 µg/mL polybrene (Santa Cruz Biotechnology, Santa Cruz, CA). The cells were placed in a 25 cm^2 flask and were centrifuged 1.5 hours at 2000 X g, 32° Celsius, after which fresh media was added to the cells. The following day, the cells were reinfected. The cells were washed three times 24 hours later and plated in media with 200 µg/mL G418,100 units/mL penicillin and 100 µg/mL streptomycin to select for stable cells. The presence of the Tet-repressor protein, a component necessary for functioning Tet-on cell lines, was confirmed by western blotting with a TetR antibody (Clontech; data not shown).

The company Genscript (Piscataway, NJ) cloned the MSH2^{Y238F} cDNA into the pRetroX Tight-Pur vector (Clontech), which is a low-copy plasmid difficult to grow and screen by conventional methods in the laboratory. To generate the double stable RetroX Tet-on Karpas 299 and SUP-M2 MSH2^{Y238F} Advanced cell lines, GP2-293 (a retroviral packaging cell line) cells were transfected with the pRetroX Tight-Pur MSH2 or MSH2^{Y238F} vector along with the pAmpho vector (Clontech) using Lipofectamine 2000. Forty-eight hours post-transfection, 5 X 10^6 Tet-on SUP-M2 and Karpas

299 cells were resuspended in viral supernatant. Following retroviral infection, the cells were grown in RPM1-1640 media with 10% Tet-System Approved FBS, 200 µg/mL G418, 100 units/mL penicillin,100 µg/mL streptomycin and 2.2 µg/mL puromycin (Invitrogen). The inducible expression of $MSH2^{Y238F}$ after doxycycline treatment was confirmed by western blotting.

3.3.5 Immunoprecipitation, his-based protein purification and western blotting

All co-immunoprecipitation (co-IP) and immunoprecipitation (IP) experiments were done as using 1000 µg lysate collected in Cell Lytic M (Sigma Aldrich, Oakville, Ontario, Canada). Briefly, cells were resuspended in 1 mL of ice-cold Cell Lytic M (supplemented with protease and phosphatase inhibitors) by pipetting up and down 50 times on ice, incubated on ice for 20 minutes, and the lysate was cleared by centrifugation. Protein was measured by BCA assay (Fisher Scientific Canada, Ottawa, ON, Canada). 1000 µg protein lysate was incubated with 5 µg monoclonal antibody overnight, and 50 µL protein G+/A agarose bead slurry (EMD Biosciences, Gibbstown, NJ) was added and incubated overnight. No-antibody controls were included although not always shown. The bead antibody complexes were washed twice with cold-PBS, and twice with ice-cold RIPA buffer (IP) or ice-cold Cell Lytic M (co-IP). Protein was eluted of the beads using 4X protein loading buffer incubated at 100°C for 5 minutes, and loaded on SDS-PAGE gels.

Biotin based protein purification was done using 500 µg lysate collected in RIPA buffer [38]. The lysate was incubated overnight in streptavidin agarose resin (Fisher Scientific Canada) that was pre-washed in ice-cold PBS. The following day, the resin was washed three times in ice-cold PBS, and protein was eluted as previously described for SDS-PAGE analysis.

Antibodies used were: anti-MSH2 (EMD, Billerica MA, IP/co-IP), anti-MSH6 (BD Biosciences, San Jose, CA), anti-MSH2, anti-phospho-tyrosine, anti-ALK, anti-total caspase 3 (Cell Signaling Technologies, Danvers, MA) and anti-β-actin (Santa Cruz Biotechnology, Santa Cruz, CA).

3.3.6 Functional assay for MMR: β-galactosidase reporter plasmid

Tet-on HEK293/NPM-ALK cells were transfected with the pCAR-OF *β-galactosidase* reporter plasmid[41], treated with doxycycline to induce NPM-ALK expression and analyzed for β-galactosidase production as previously described.[9]

3.3.7 Functional assay for MMR: sensitivity to DNA damage-inducing drugs

GP293 cells were transfected with HB-EV, or HB-MSH2^{Y238F} and NPM-ALK for 24 hours, and then were plated evenly into 48-well plates. Twenty-four hours later, the cells were treated with 0, 0.5, 1, 2, 3 or 4 mM *N*-methyl-*N*-nitrosourea (MNU) for 48 hours in fresh media, and cell viability was assessed by CellTiter 96® AQueous One Solution Cell Proliferation Assay (also known as MTS assay ((3-(4,5-dimethylthiazol-2-yl)-5-(3-carboxymethoxyphenyl)-2-(4-sulfophenyl)-2H-tetrazolium), Promega, Madison, WI) following the manufacturer's protocol. Tet-on SUP-M2 MSH2^{Y238F} cells were treated with 0 or 500 ng/mL doxycycline for 48 hours, followed by the addition of 0 or 100 μM MNU or 5 μg/mL 5-fluorouracil (5-FU) in fresh media. After 24 hours, cell viability was assessed by MTS assay, and then re-measured every 2 days.

3.3.8 Apoptosis analysis

Apoptosis analysis was done on Tet-on SUP-M2 and Karpas 299 MSH2^{Y238F} cells treated with 0, 100, and 500 ng/mL doxycycline, and stained after 48 hours with Annexin-V-FITC (fluorescein isothiocyanate) /PI (propidium iodide) (BD Biosciences) following the suggested protocol. Analysis was done on a BD FACS Calibur (Flow Cytometry Laboratory, Department of Experimental Oncology, Cross Cancer Institute). Cell cycle analysis was done using propidium iodide (PI) staining followed by flow cytometry as previously described[42] on Tet-on SUP-M2 MSH2^{Y238F} cells treated with 0 and 500 ng/mL doxycycline for 48 and 120 hours. For the 120 hour time-point, doxycycline was added to the media at 0 hours, and was not replenished. The half-life of doxycycline in media is only 24 hours; this time-point was included to determine if the apoptosis induced by early expression of MSH2^{Y238F} was lasting over time. Analysis was done on a BD FACS (fluorescent activated cell sorter) Calibur.

3.3.9 Statistical analysis

Data is expressed as mean ± the standard error of the mean (SEM), and significance was determined from three independent experiments by Student's T-test (GraphPad Prism, La Jolla, CA), with significance denoted by * (p<0.05), **(p<0.01), and ***(p<0.001).

3.4 Results

3.4.1 Identification of tyrosine 238 of MSH2 as the crucial site for NPM-ALK-induced tyrosine phosphorylation

Using NetPhos 2.0[43], I analyzed the MSH2 protein sequence for potential tyrosine phosphorylation sites that may be targeted by NPM-ALK. I identified 13 putative sites in the MSH2 protein (**Figure 3.1** and **Table 3.1**). The tyrosine (Y) residue with the highest score was Y238 (0.981,

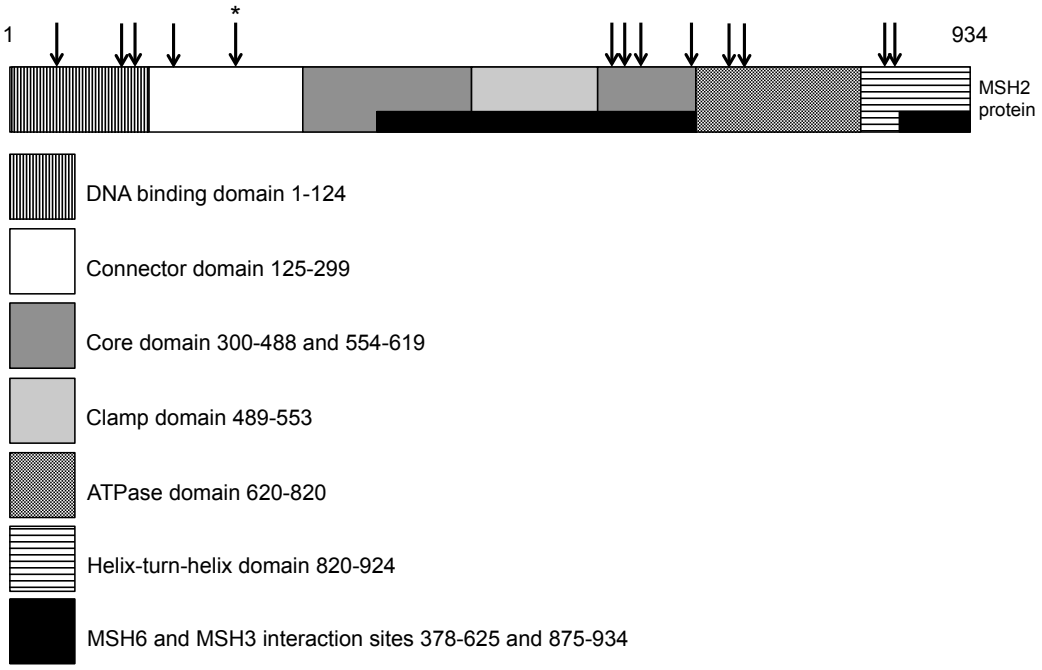

Figure 3.1. Predicted tyrosine phosphorylation sites in the MSH2 protein. MSH2 has 13 predicted tyrosine phosphorylation residues**.** Schematic diagram showing predicted MSH2 tyrosine phosphorylation residues in the MSH2 protein by domain, as proposed by NetPhos 2.0.[43] The highest predicted tyrosine phosphorylation site was at Y238 (phosphorylation score 0.980; denoted by * in the Figure), located in the MSH2 connecter domain. Figure adapted from Ollila *et al*., 2006.[44]

Table 3.1. NetPhos 2.0[a] server predicted tyrosine phosphorylation sites in the MSH2 protein sequence.

Amino Acid Sequence	Position	Phosphorylation Score
RGDF*YTAHG	43	0.863
RVEV*YKNRA	103	0.815
ENDW*YLAYK	118	0.867
VGVG*YVDSI	165	0.657
TKDI*YQDLN	238	0.981
LNEE*YTKNK	563	0.896
NKTE*YEEAQ	570	0.974
ISSG*YVEPM	588	0.768
APVP*YVRPA	619	0.837
PNDV*YFEKD	656	0.908
GKST*YIRQT	678	0.556
EEFQ*YIGES	856	0.830
ESQG*YDIME	863	0.910

[a]Online prediction software[43]

*Predicted phosphorylation site

denoted by a * in Figure), located in the connector domain of MSH2 required for the formation of the MMR ternary complex.[45] To identify the specific residue(s) phosphorylated in the presence of NPM-ALK, tandem-affinity purification was performed. To achieve this, GP293 cells transiently transfected with both HB-tagged MSH2 and NPM-ALK were used. Western blot studies showed the protein expression of HB-MSH2 and NPM-ALK in the transfected cells (**Figure 3.2**, lane 6; a representative western); HB-MSH2 migrated slightly slower than the endogenous protein due to the HB-tag. Using these cell lysates, Dr. Peng Wang and Dr. Fang Wu performed liquid chromatography coupled with tandem-affinity purification mass spectrometry. With the total peptide sequence coverage of MSH2 being 78%, the only detectable phosphorylated residue in the presence of NPM-ALK was Y238 (**Figure 3.3**). As a control, the same experiment was done on GP293 lysate expressing HB-MSH2 and the empty vector pcDNA3 and no evidence of phosphorylation was detected.

3.4.2 NPM-ALK mediates tyrosine phosphorylation of MSH2 at tyrosine 238

To examine the functional significance of phosphorylation of $MSH2^{Y238}$, site-directed mutagenesis was performed on the HB-MSH2 plasmid to change the residue to phenylalanine (F), a residue biochemically similar to Y that cannot be phosphorylated. HB-empty vector (HB-EV), HB-MSH2 or HB-$MSH2^{Y238F}$ was transfected into GP293 cells with or without NPM-ALK expression (**Figure 3.2A**). I then performed immunoprecipitation using an anti-MSH2 monoclonal antibody on lysate depicted in **Figure 3.2A**. In the absence of NPM-ALK (**Figure 3.2B**, lanes 1-3), there was no convincing evidence of tyrosine phosphorylation of endogenous MSH2, HB-MSH2 or HB-$MSH2^{Y238F}$, compared to the empty vector control. In the presence of NPM-ALK (**Figure 3.2B**, lanes 4-7), phosphorylation of endogenous

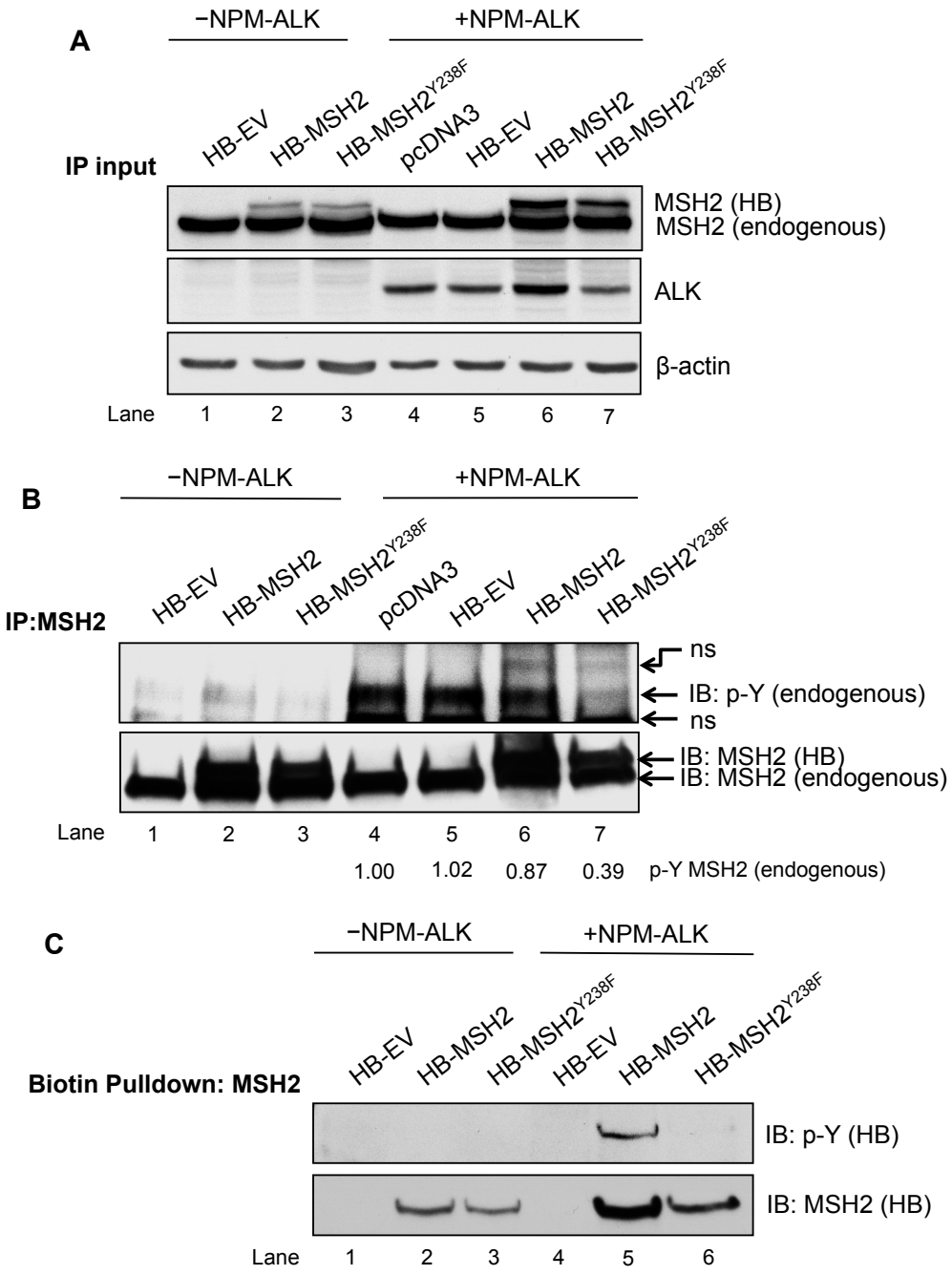

Figure 3.2. NPM-ALK mediates tyrosine phosphorylation of MSH2 at tyrosine 238. (A) Western blot analysis of cell lysate from GP293 cells transfected with HB-EV (empty vector, lane 1 and 5; negative control for HB-MSH2/MSH2^{Y238F}), HB-MSH2 (lane 2 and 6), HB-MSH2^{Y238F} (lane 3 and 7), and pcDNA3 (lane 4), with NPM-ALK (lanes 4-7) or pcDNA3 (lanes 1-3; negative control for NPM-ALK. (B) IP analysis of lysate from A showing tyrosine phosphorylation (p-Y) of endogenous and HB-tagged

MSH2 with pcDNA3 (lanes 1-3) or NPM-ALK (lanes 4-7) expression. The blot was probed with an MSH2 antibody to confirm immunoprecipitation. ns = non-specific band. Densitometry was calculated based on the intensity of endogenous p-Y (upper panel) normalized to total MSH2 (lower panel) in samples with NPM-ALK expression only (lanes 4-7). (C) Lysate from A subjected to biotin purification using streptavidin agarose resin to detect p-Y of precipitated HB-tagged MSH2 proteins in the presence of pcDNA3 (lanes 1-3) or NPM-ALK (lanes 3-6). An MSH2 antibody was used to confirm biotin pulldown of exogenous MSH2 proteins. Results shown are representative of three independent experiments.

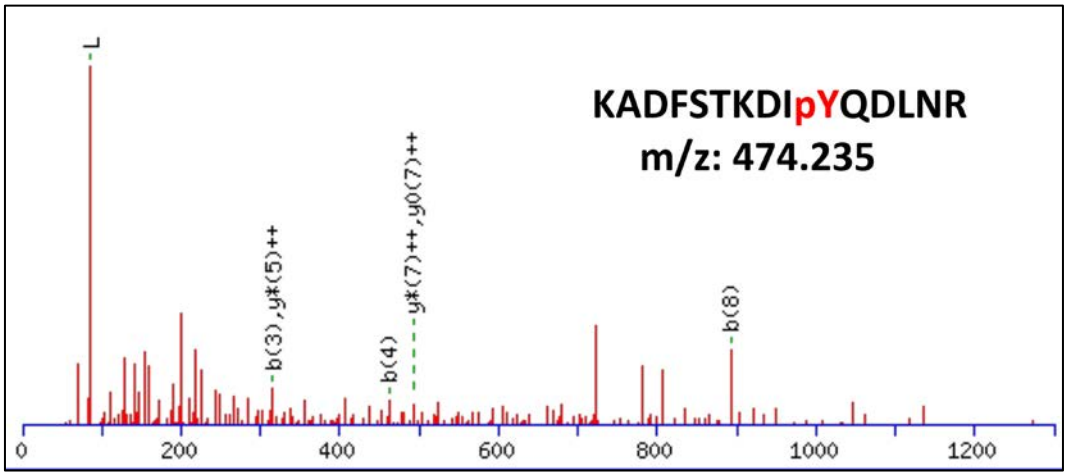

Figure 3.3. MSH2 is tyrosine phosphorylated by NPM-ALK at residue 238 by mass spectrometry. The tandem affinity mass spectrometry (MS/MS) spectrum of a representative MSH2 peptide showing Y238 phosphorylation. m/z: peptide mass to charge ratio. Results are representative of 2 independent experiments.

MSH2 was readily detectable. Importantly, the phosphorylation of endogenous MSH2 in the presence of HB-MSH2^{Y238F} was substantially (>60%) reduced (lane 7), suggesting that the MSH2^{Y238F} mutant exerts a dominant negative effect on endogenous MSH2 tyrosine phosphorylation.

Rather surprisingly, phosphorylation of the HB-tagged MSH2 proteins was not detectable in this experiment. However, as shown in **Figure 3.2C**, when streptavidin agarose resin was used to pull down the exogenous HB-MSH2 or HB-MSH2^{Y238F}, I found that NPM-ALK mediated tyrosine phosphorylation of HB-MSH2 (lane 5), whereas there was only a barely detectable signal for HB-MSH2^{Y238F} (lane 6). The discrepancy between **Figure 3.2B** and **Figure 3.2C** regarding the phosphorylation of HB-MSH2 is likely due to the fact that the anti-phospho-tyrosine antibody does not recognize its epitope on HB-MSH2 when it was pulled down by an anti-MSH2 antibody.

Taken together, these results suggest that NPM-ALK is phosphorylated at MSH2^{Y238}. Furthermore, since site-directed mutagenesis of Y238 almost completely abrogated the tyrosine phosphorylation signal induced by NPM-ALK, Y238 is the predominant tyrosine phosphorylation site on MSH2 in this context. Lastly, MSH2^{Y238F} appears to have a dominant negative effect on NPM-ALK-mediated phosphorylation of endogenous MSH2.

3.4.3 Enforced expression of HB-MSH2^{Y238F} restores MMR *in vitro*

To determine if Y238 is biologically important in the context of MMR, I expressed HB-EV, HB-MSH2, and HB-MSH2^{Y238F} in HEK293 cells in which the expression of NPM-ALK is doxycycline-inducible.[9] To assess MMR, cells were transiently transfected with the MMR β-galactosidase reporter plasmid (pCAR-OF).[9,41] This plasmid contains a 58 base-pair

poly(C-A) tract at the 5' end of its coding region, placing the start codon out of frame. Thus, in cells with dysfunctional MMR, microsatellite instability (MSI) resulting from strand slippage at the C-A repeat can place the *β-galactosidase* gene in frame, resulting in measurable enzymatic activity.

In HEK293 cells without NPM-ALK expression (i.e. no doxycycline), enforced expression of HB-MSH2 or HB-MSH2^{Y238F} led to a statistically significant increase (p<0.001 and p<0.01) in β-galactosidase activity over cells transfected with HB-EV (**Figure 3.4A** and **3.4B**). This suggests that overexpression of these MSH2 proteins alone can impair MMR, which substantiates previously published findings that overexpression of MMR proteins can lead to deregulation of MMR, mimicking what is seen in cells lacking certain MMR genes.[41,46-48]

With the induction of NPM-ALK (i.e. 400 µg of doxycycline), I identified a significant increase in β-galactosidase, which is in concordance with the previous findings from the Lai laboratory.[9] Enforced expression of HB-MSH2 resulted in a further increase in β-galactosidase activity over cells expressing HB-EV (p<0.01) (**Figure 3.4A**, 400 DOX). In contrast, enforced expression of HB-MSH2^{Y238F} did not significantly alter the β-galactosidase activity compared to cells expressing HB-EV (**Figure 3.4B,** 400 DOX). These findings suggest that the MSH2^{Y238F} has a substantial biological difference from the wild-type MSH2 in the presence of NPM-ALK.

To further assess if enforced expression of HB-MSH2^{Y238F} has the ability to neutralize the MMR-deregulating effect of NPM-ALK, I transfected HB-EV or HB-MSH2^{Y238F} into GP293 cells with or without the co-transfection of NPM-ALK. These cells were subsequently treated with MNU to assess cell viability. Of note, MNU, a mono-functional methylating agent that

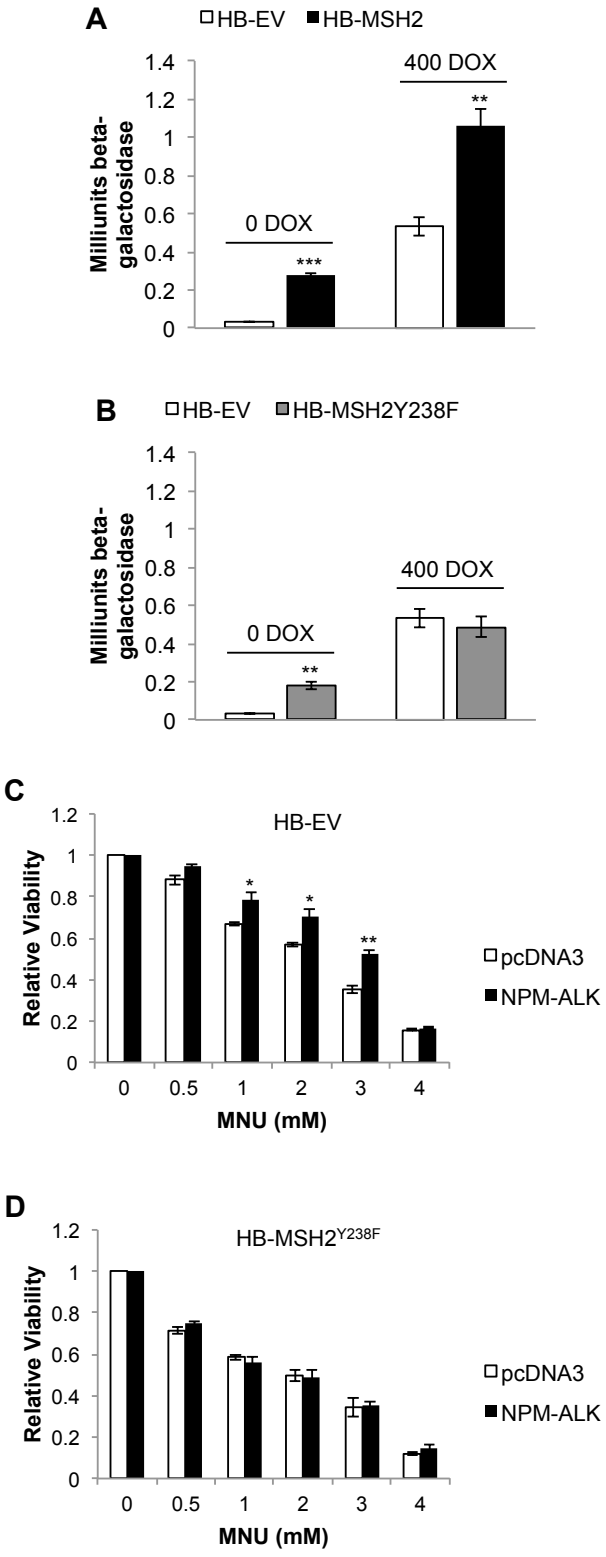

Figure 3.4. Enforced expression of HB-MSH2^{Y238F} restores MMR function *in vitro*. β-galactosidase MMR assay of Tet-on HEK293/NPM-

ALK cells transfected with the pCAR-OF plasmid plus (A) HB-EV, HB-MSH2, and (B) HB-EV or HB-MSH2^{Y238F} for 24 hours. The following day, the media was supplemented with 0 ng/mL doxycycline (0 DOX, left) and 400 ng/mL doxycycline (400 DOX, right) to induce NPM-ALK expression. β-galactosidase activity, indicative of MMR dysfunction, was measured as outlined in the Materials and Methods in triplicate 48 hours post-transfection, and at least 3 independent experiments were performed. Data is presented as mean milliunits of β-galactosidase ± SEM. Statistical significance was measured by Student's T-test, where $^{**}p<0.01$, $^{***}p<0.001$. (C) GP293 cells transfected with HB-EV, or (D) HB-MSH2^{Y238F} and pcDNA3 or NPM-ALK were treated with DMSO (0mM), 0.5, 1, 2, 3, or 4 mM MNU for 48 hours in 48 well plates. Viability was measured using the MTS cell viability assay; higher cell viability correlated with loss of DNA MMR. Data is represented as mean relative cell viability (normalized to 0 mM and pcDNA3, which was set at 1) ± SEM, and statistical significance was determined by Student's T-test, where $^{*}p<0.05$, and $^{**}p<0.01$. A representative result of 3 independent experiments is shown.

induces aberrant bases, is widely used to assess MMR *in vitro*.[49] MNU generates DNA damage-induced apoptosis that is MMR-dependent. Thus, in the absence of MMR, cells are resistant to MNU treatment.[50-53] As shown in **Figure 3.4C**, in GP293 cells transfected with HB-EV, cells co-transfected with NPM-ALK showed a significantly higher cell viability than those co-transfected with empty vector in the presence of 1 to 3 mM of MNU ($p<0.05$, 1-2 mM; $p<0.01$, 3 mM). In contrast, in cells transfected with HB-MSH2^{Y238F}, the co-transfection of NPM-ALK did not result in any significant difference in cell viability, as compared to those co-transfected with the empty vector (**Figure 3.4D**). Thus, the HB-MSH2^{Y238F} mutant appeared to have neutralized the MMR-deregulating effect of NPM-ALK.

3.4.4 Enforced expression of HB-MSH2^{Y238F} alters MSH2:MSH6 (MutSα) binding

Previously published data from the Lai research group demonstrated that NPM-ALK expression blocked the interaction of MSH6 and MSH2[9], which is critical for MMR. I hypothesized that tyrosine phosphorylation of MSH2^{Y238} is involved in this process. To test this hypothesis, I performed co-immunoprecipitation experiments using GP293 cells transiently transfected with HB-EV or HB-MSH2^{Y238F}. Cell lysate used for this experiment was initially subjected to western blots, and the expression of endogenous and HB-tagged exogenous MSH2 proteins was confirmed (**Figure 3.5A**, lane 1-2). Another set of cell lysates was similarly generated, except with the co-transfection of NPM-ALK (**Figure 3.5A**, lane 3-4).

Using these two sets of cell lysates, the physical binding between MSH2 and MSH6 was assessed using co-immunoprecipitation with an anti-MSH6 antibody. In the context of MMR, MSH2 has multiple known binding partners[54-62], whereas MSH6 only interacts with MSH2.[54,55] Thus, using an

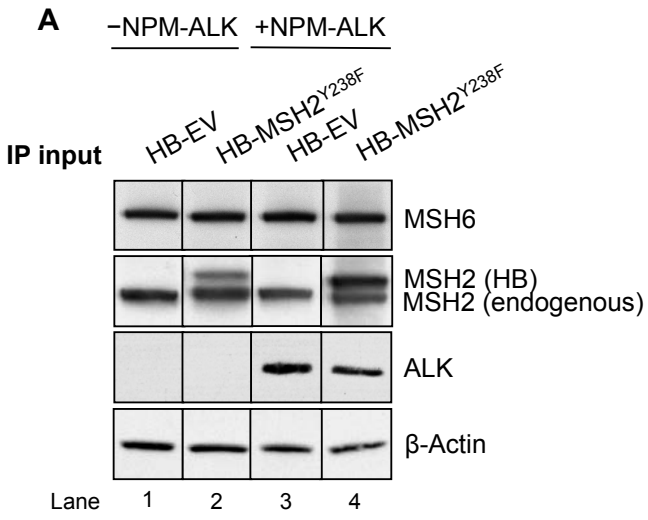
A
−NPM-ALK
+NPM-ALK
IP input
HB-EV
HB-MSH2Y238F
HB-EV
HB-MSH2Y238F
MSH6
MSH2 (HB)
MSH2 (endogenous)
ALK
β-Actin
Lane 1 2 3 4

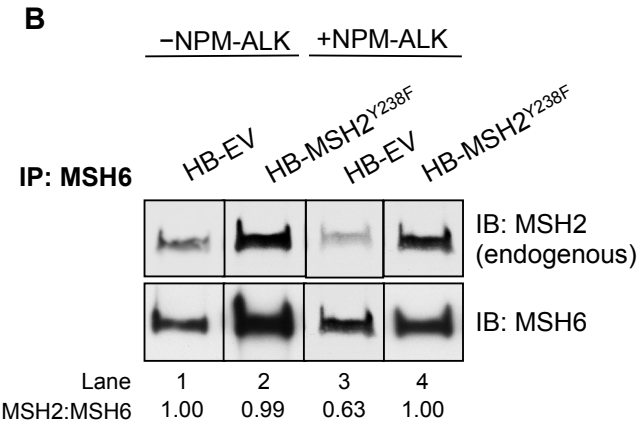
B
−NPM-ALK
+NPM-ALK
IP: MSH6
HB-EV
HB-MSH2Y238F
HB-EV
HB-MSH2Y238F
IB: MSH2 (endogenous)
IB: MSH6
Lane 1 2 3 4
MSH2:MSH6 1.00 0.99 0.63 1.00

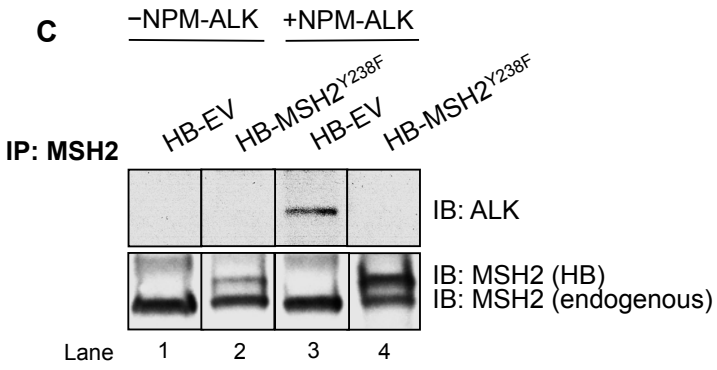
C
−NPM-ALK
+NPM-ALK
IP: MSH2
HB-EV
HB-MSH2Y238F
HB-EV
HB-MSH2Y238F
IB: ALK
IB: MSH2 (HB)
IB: MSH2 (endogenous)
Lane 1 2 3 4

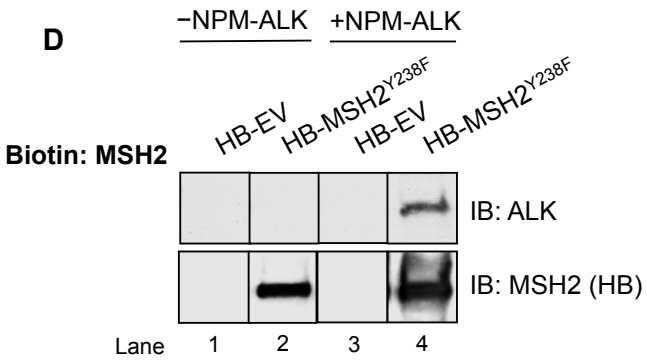

Figure 3.5. Enforced expression of HB-MSH2^{Y238F} alters MutSα (MSH2:MSH6) formation and the MSH2:NPM-ALK interaction. (A) Western blot analysis of GP293 cell lysate transfected with HB-EV, or HB-MSH2^{Y238F} and pcDNA3 (lane 1-2) or NPM-ALK (lane 3-4). The western blot was probed with anti-MSH6 and anti-ALK antibodies. Anti-MSH2 antibody was used to detect endogenous MSH2 (lower band) and HB-MSH2/HB-MSH2^{Y238F} expression levels (upper band, HB). Anti-β-actin was used as a loading control. (B) MSH6 was precipitated from cell lysate shown in A under co-IP conditions using an anti-MSH6 antibody. The resulting immunoblot was probed with MSH2 and MSH6 antibodies to measure the MSH2:MSH6 (MutSα) interaction. Densitometry shows the intensity of endogenous MSH2 normalized to MSH6, relative to lane 1. No exogenous MSH2 protein was detected by co-IP. (C) MSH2 was precipitated from cell lysate shown in A under co-IP conditions using an anti-MSH2 antibody, and the resulting immunoblot was probed with anti-ALK and anti-MSH2 to detect the interaction of MSH2 (endogenous and HB-tagged):NPM-ALK. (D) Biotin purification of HB-MSH2^{Y238F} from A, probed with anti-ALK and anti-MSH2 to measure the HB-MSH2^{Y238F}:NPM-ALK interaction. Results shown are representative of 3 independent experiments.

anti-MSH6 antibody (rather than anti-MSH2) for the pull-down is more informative. As shown in **Figure 3.5B**, I was only able to detect endogenous MSH2 bound to immunoprecipitated MSH6, suggesting that HB-MSH2^{Y238F} did not bind well to MSH6. Of note, in the absence of NPM-ALK (lane 1 and 2), when the variation in the amount of MSH6 protein pulled down was corrected, I found no difference between the interaction of MSH6 with MSH2, regardless of whether these cells were transfected with the empty vector or HB-MSH2^{Y238F}. When NPM-ALK was co-transfected, there was a 40% reduction in the interaction between MSH6 and endogenous MSH2 (lane 3), and this finding is in agreement with the previous finding from the Lai laboratory.[9] Importantly, with enforced expression of HB-MSH2^{Y238F}, the binding of MSH2 to MSH6 was almost completely restored (lane 4).

3.4.5 Enforced expression of HB-MSH2^{Y238F} alters MSH2:NPM-ALK binding

Using the cell lysate depicted in **Figure 3.5A**, I then assessed how MSH2^{Y238F} may affect the interaction of endogenous MSH2 with NPM-ALK. As shown in **Figure 3.5C**, when MSH2 was pulled down with an anti-MSH2 antibody, the interaction between NPM-ALK and endogenous MSH2 was readily detectable, as previously described.[9,38] In contrast, the MSH2:NPM-ALK interaction was not detectable by immunoprecipitation when HB-MSH2^{Y238F} was expressed (lane 4). When pull-down of HB-MSH2^{Y238F} was done by biotin pulldown assay, I readily identified an interaction between NPM-ALK and HB-MSH2^{Y238F} (**Figure 3.5D**, lane 4). Taken together, these findings suggest that HB-MSH2^{Y238F} blocks the interaction between NPM-ALK and endogenous MSH2, possibly by binding to NPM-ALK and sequestering it away from endogenous MSH2.

3.4.6 Enforced expression of MSH2^{Y238F} decreases MSH2 tyrosine phosphorylation and restores MSH2:MSH6 (MutSα) formation in ALK+ALCL cells

The biological importance of MSH2^{Y238} phosphorylation in the context of NPM-ALK pathobiology was next validated in ALK+ALCL cell lines, which express NPM-ALK at the steady state. Using retroviral vectors, Karpas 299 and SUP-M2 cells stably transduced with an inducible MSH2^{Y238F} vector were generated, and were termed Tet-on MSH2^{Y238F} cells. The Tet-on SUP-M2 and Karpas 299 MSH2^{Y238F} cells showed a dose-dependent increase in the expression of total MSH2 protein upon doxycycline treatment (**Figure 3.6A** and **3.6B**). Of note, both Karpas 299 and SUP-M2 have endogenous MSH2 expression, as evidenced at 0ng/mL doxycycline.

Using these Tet-on MSH2^{Y238F} cells, MSH2^{Y238F} expression was turned on at a low level (resulting in approximately 40% increase in the total MSH2 protein level) and MSH2 phosphorylation was assessed by immunoprecipitation. The expression of MSH2^{Y238F} in SUP-M2 cells resulted in an approximately 70% reduction in detectable tyrosine phosphorylation (**Figure 3.6C**). Similar results were achieved in Karpas 299 cells, where MSH2^{Y238F} decreased MSH2 phosphorylation by 50% (**Figure 3.6D**). Since the expression of MSH2^{Y238F} resulted in a decrease in detectable MSH2 tyrosine phosphorylation, I then asked if MSH2^{Y238F} was capable of restoring the interaction of MSH2:MSH6, which would indicate a partial restoration of MMR in these cells. As measured by co-IP using an anti-MSH2 antibody, expression of MSH2^{Y238F} in the Tet-on SUP-M2 cells (**Figure 3.6E**) and Karpas 299 cells (**Figure 3.6F**) resulted in a dose-dependent increase in the amount of MSH6 bound to MSH2.

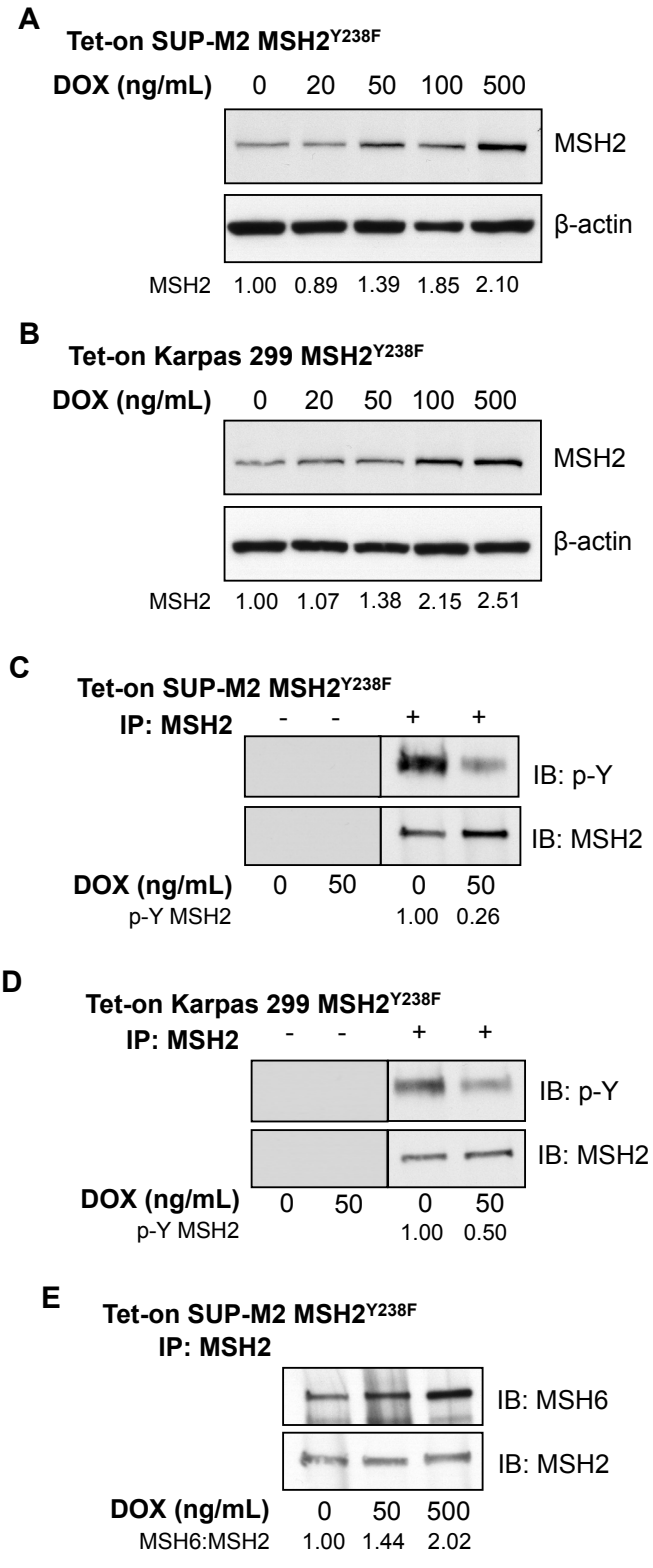
A
Tet-on SUP-M2 MSH2Y238F
DOX (ng/mL) 0 20 50 100 500
MSH2
β-actin
MSH2 1.00 0.89 1.39 1.85 2.10
B
Tet-on Karpas 299 MSH2Y238F
DOX (ng/mL) 0 20 50 100 500
MSH2
β-actin
MSH2 1.00 1.07 1.38 2.15 2.51
C
Tet-on SUP-M2 MSH2Y238F
IP: MSH2 - - + +
IB: p-Y
IB: MSH2
DOX (ng/mL) 0 50 0 50
p-Y MSH2 1.00 0.26
D
Tet-on Karpas 299 MSH2Y238F
IP: MSH2 - - + +
IB: p-Y
IB: MSH2
DOX (ng/mL) 0 50 0 50
p-Y MSH2 1.00 0.50
E
Tet-on SUP-M2 MSH2Y238F
IP: MSH2
IB: MSH6
IB: MSH2
DOX (ng/mL) 0 50 500
MSH6:MSH2 1.00 1.44 2.02

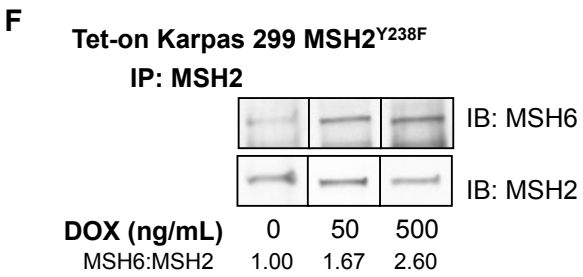

Figure 3.6. Enforced expression of MSH2^{Y238F} in ALK+ALCL cell lines alters MSH2 phosphorylation and MutSα formation. (A) Tet-on SUP-M2 MSH2^{Y238F} cell lysate, in which the expression of MSH2^{Y238F} correlated with the dose-dependent increase of doxycycline. (B) Tet-on Karpas 299 MSH2^{Y238F} cell lysate depicting the dose-dependent increase in MSH2^{Y238F} expression with doxycycline treatment. In A and B, a β-actin antibody was used as a loading control, and densitometry of MSH2 expression relative to β-actin is shown. (C) Tet-on SUP-M2 MSH2^{Y238F} and (D) Tet-on Karpas 299 MSH2^{Y238F} cells were treated with 0 and 50 ng/mL doxycycline and the resulting cell lysate was subjected to IP using an anti-MSH2 antibody (+). Tyrosine phosphorylation (p-Y) of MSH2 was measured using an anti-p-Y antibody. No-antibody controls (-) were included to account for non-specific binding to the beads. Densitometry for phosphorylated MSH2 relative to total MSH2 is shown. (E) MSH2 was precipitated from Tet-on SUP-M2 MSH2^{Y238F} lysate and (F) Tet-on Karpas 299 MSH2^{Y238F} lysate treated with 0, 50 and 500 ng/mL doxycycline under co-IP conditions. The resulting immunoblots were probed with an anti-MSH6 and an anti-MSH2 antibody to assess the amount of MSH6 precipitated relative to MSH2. Densitometry for MSH6:MSH2 is shown. Results are representative of at least three independent experiments.

3.4.7 ALK+ALCL cells are more sensitive to DNA damage-inducing drugs upon enforced expression of $MSH2^{Y238F}$

As my previous results have shown that $MSH2^{Y238F}$ is capable of restoring MSH2:MSH6 formation in ALK+ALCL, I then asked if cells expressing $MSH2^{Y238F}$ also have restored MMR function. Due to technical reasons, I was unable to use the pCAR-OF plasmid described above, since it would have involved multiple gene transfection into ALK+ALCL cells, which significantly decreased cell viability (not shown). Instead, I assessed MMR indirectly by treating these cells with MNU. In addition, I also assessed MMR by treating these cells with the thymidylate synthase inhibitor 5-FU, since resistance to 5-FU has been associated with loss of MMR.[30] As shown in **Figure 3.7A** and **3.7B**, experiments using both MNU and 5-FU showed similar results. The expression of $MSH2^{Y238F}$ (induced by the addition of 500 ng/mL of doxycycline) in the presence of the DNA-damaging drugs resulted in a significant increase in loss of viability from day 3 onward. These findings support the concept that $MSH2^{Y238F}$ restores MMR in ALK+ALCL cells. Interestingly, expression of $MSH2^{Y238F}$ alone, without the addition of MNU or 5-FU, resulted in a significant loss of viability (**Figure 3.7C**, $p<0.001$ until day 7). The decrease in statistical significance on day 9 can be attributed to the fact that only one dose of doxycycline was given at the beginning of the experiment, and the expression of $MSH2^{Y238F}$ slowly faded away.

3.4.8 Enforced expression of $MSH2^{Y238F}$ induces spontaneous apoptosis in ALK+ALCL cells

As the results depicted in **Figure 3.7** suggest that expression of $MSH2^{Y238F}$ alone can decrease cell viability of ALK+ALCL cells, I performed studies to analyze changes in the cell cycle and apoptosis induced by $MSH2^{Y238F}$. By propidium iodide staining, at 48 and 120 hours

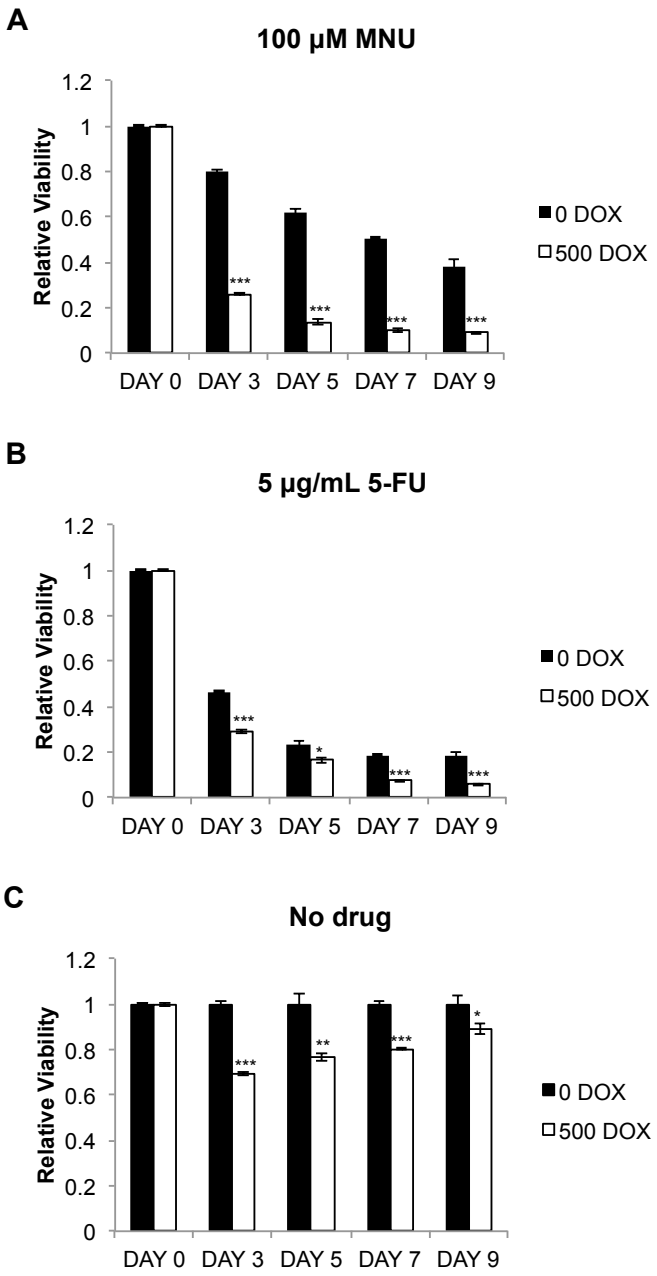

Figure 3.7. Enforced expression of MSH2^{Y238F} increases sensitivity to DNA damage-inducing drugs in ALK+ALCL cells. Tet-on SUP-M2 MSH2^{Y238F} cells were plated in 6 well plates and treated with 0 ng/mL doxycycline (0 DOX) or 500 ng/mL doxycycline (500 DOX), followed by the addition of (A) 100 µM MNU, (B) 5 µg/mL 5-FU or (C) DMSO for 24 hours. Cells were then plated in 48 well plates (day 0) and viability was assessed by MTS assay every 2 days until day 9. Viability is displayed relative to

DMSO/0 DOX, which was set at 1. Statistical significance was calculated by Student's T-test where *p<0.05, **p<0.01, and ***p<0.001. All samples were measured in sextuplicate, and results shown are representative of 3 independent experiments.

after MSH2^{Y238F} expression, there was a significant increase in the fraction of apoptotic cells in the Tet-on SUP-M2 MSH2^{Y238F} cell line (**Figure 3.8**). The average percentage of cells in each stage of cell cycle is shown in **Table 3.2** (n=3). At 48 and 120 hours post MSH2^{Y238F} expression, the increase in the percentage of cells in the apoptotic phase was statistically significant (p<0.01).

Tet-on SUP-M2 and Karpas 299 MSH2^{Y238F} cells were subjected to Annexin V/propidium iodide staining to determine if the expression of MSH2^{Y238F} resulted in a change in cells undergoing early, or late stage apoptosis. As shown in **Figure 3.9A**, increasing expression of MSH2^{Y238F} resulted in a dose-dependent increase in the fraction of cells undergoing both early (lower right quadrant) and late (upper right quadrant) apoptosis.

A graphical representation of the total apoptotic Tet-on SUP-M2 MSH2^{Y238F} cells is shown in **Figure 3.9B** (n=3); when the percentages of early, late, and dead cells were added together (i.e. total apoptotic cells), a significant increase in apoptosis was measured in cells treated with 100ng/mL doxycycline (p<0.05). In the Tet-on Karpas 299 MSH2^{Y238F} cells, a significant dose dependent increase in the percent of total apoptotic cells was detectable in cells treated with both 100 and 500 ng/mL doxycycline (p<0.05) (**Figure 3.9C**). Apoptosis in the Tet-on SUP-M2 MSH2^{Y238F} cells was confirmed by western blotting for cleaved caspase 3 expression (**Figure 3.9D**).

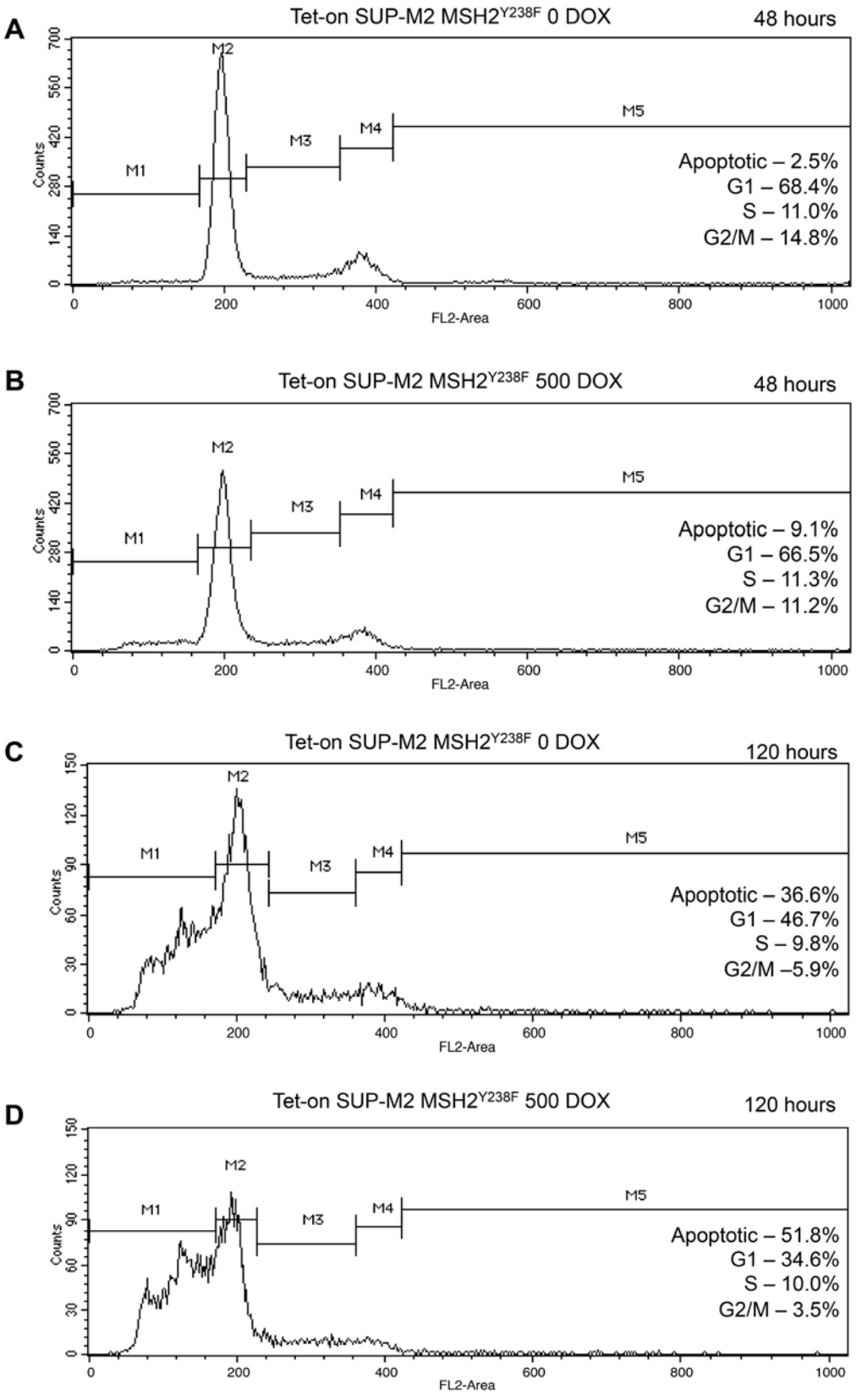
A
Tet-on SUP-M2 MSH2Y238F 0 DOX
48 hours
M1
M2
M3
M4
M5
Apoptotic – 2.5%
G1 – 68.4%
S – 11.0%
G2/M – 14.8%
Counts
FL2-Area
B
Tet-on SUP-M2 MSH2Y238F 500 DOX
48 hours
Apoptotic – 9.1%
G1 – 66.5%
S – 11.3%
G2/M – 11.2%
C
Tet-on SUP-M2 MSH2Y238F 0 DOX
120 hours
Apoptotic – 36.6%
G1 – 46.7%
S – 9.8%
G2/M –5.9%
D
Tet-on SUP-M2 MSH2Y238F 500 DOX
120 hours
Apoptotic – 51.8%
G1 – 34.6%
S – 10.0%
G2/M – 3.5%

Figure 3.8. Enforced expression of MSH2^{Y238F} shifts cells into apoptosis. (A) Tet-on SUP-M2 cells treated with 0 ng/mL and (B) 500 ng/mL doxycycline for 48 and (C) 0 ng/mL and (D) 500 ng/mL doxycycline for 120 hours were stained with propidium iodide and analyzed by flow cytometry for cell cycle distribution. A representative result of 3 independent experiments is shown.

Table 3.2. Cell cycle analysis of Tet-on SUP-M2 $MSH2^{Y238F}$ cells after enforced expression of $MSH2^{Y238F}$.

Cell Cycle (48 hours)	**0 DOX (± SEM)**	**500 DOX (± SEM)**	***P* value**
Apoptosis	4.0 ± 1.1	9.5 ± 0.3	**
G1	67.2 ± 2.0	62.7 ± 4.2	ns
S	8.8 ± 1.8	9.6 ± 1.5	ns
G2/M	12.8 ± 1.4	9.7 ± 0.9	ns
Cell Cycle (120 hours)	**0 DOX (± SEM)**	**500 DOX (± SEM)**	***P* value**
Apoptosis	31.4 ± 2.9	51.2 ± 0.7	**
G1	49.0 ± 1.7	32.6 ± 1.3	**
S	9.9 ± 0.7	9.9 ± 0.1	ns
G2/M	6.2 ± 0.2	3.8 ± 0.1	***

SEM – standard error of the mean

DOX – doxycycline

ns – non-significant ($p>0.05$), **$p<0.01$, ***$p<0.001$ (Student's T-test)

A

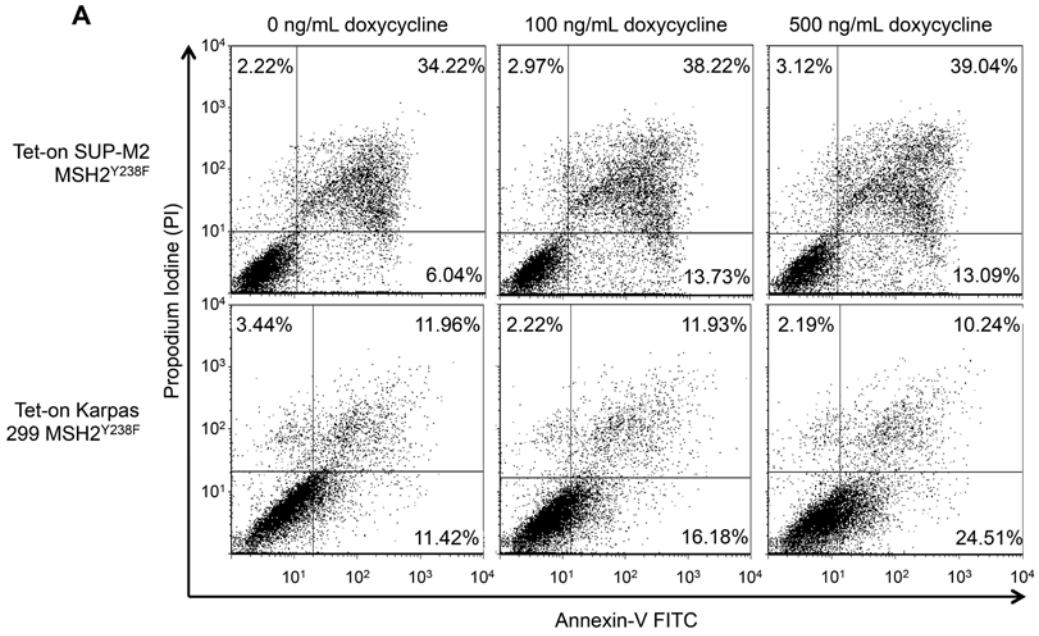

Quadrant	Viability
Lower left	Alive
Lower right	Early apoptosis
Upper right	Late apoptosis
Upper left	Dead

SUP-M2	Total Apoptosis	Karpas 299	Total Apoptosis
0 DOX	42.48%	0 DOX	26.82%
100 DOX	54.92%	100 DOX	30.33%
500 DOX	55.25%	500 DOX	36.94%

B

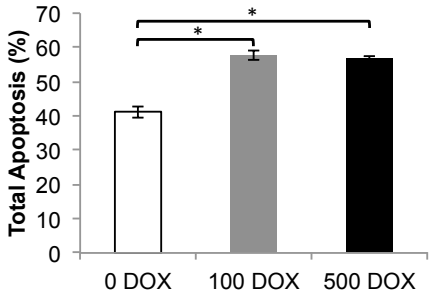

C

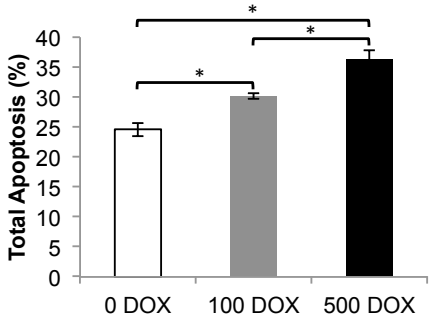

D

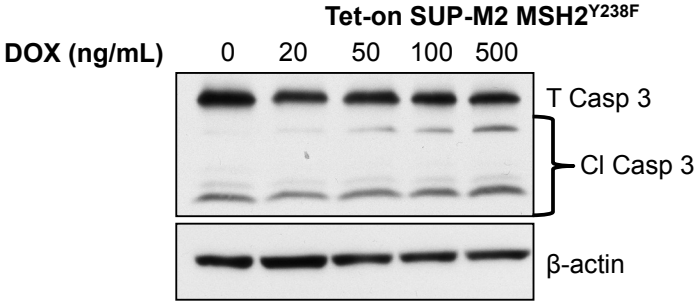

Figure 3.9. Enforced expression of MSH2^{Y238F} induces spontaneous apoptosis in ALK+ALCL cells. (A) Tet-on SUP-M2 MSH2^{Y238F} (upper 3 panels) and Tet-on Karpas 299 MSH2^{Y238F} (lower 3 panels) were treated with 0, 100, and 500 ng/mL doxycycline to enforce MSH2^{Y238F} expression, were stained with Annexin-V/FITC/propidium iodide, and were subjected to flow cytometry analysis for apoptosis. The lower left table shows the distribution of the cells in the different stages of apoptosis. The lower right table summarizes the total percent apoptosis (early, late, and dead) for each treatment group. The experiment was repeated 3 times, and a representative result is shown. (B) The percentage of Tet-on SUP-M2 MSH2^{Y238F} and (C) Tet-on Karpas 299 MSH2^{Y238F} cells in all apoptotic stages (early, late and dead) was calculated from 3 independent experiments, and the mean percent total apoptosis ± SEM is shown. Statistical significance was determined by Student's T-test, where *p<0.05 and **p<0.01. (D) Western blot analysis of the apoptotic marker cleaved caspase 3 in the Tet-on SUP-M2 MSH2^{Y238F}. The immunoblot was probed with anti-caspase 3 to detect total (T) and cleaved (Cl) caspase (casp) 3 expression. Anti-β actin was used as a loading control. Results shown are representative of 3 independent experiments.

3.5 Discussion

The finding that oncogenic tyrosine kinases can impair MMR is relatively recent, and has not been extensively studied. In 2008, it was described that BCR-ABL, an oncogenic fusion tyrosine kinase, can induce MSI, but the underlying mechanism was not investigated.[63] In a previous publication from the Lai laboratory, it was found that the oncogenic tyrosine kinase NPM-ALK induced the phosphorylation of MSH2 at unknown tyrosine residues, leading to MMR dysfunction. It was also reported that ALK+ALCL cell lines and patient samples exhibited MSI, and abnormal MSH2 cytoplasmic localization, which are both evidence of MMR deficiency.[9] In this study, I tested the hypothesis that tyrosine phosphorylation of MSH2 is a critical step in the deregulation of MMR by NPM-ALK. First, using liquid chromatography-mass spectrometry, it is shown for the first time that Y238 is a site that can be tyrosine phosphorylated by NPM-ALK. Second, I created the $MSH2^{Y238F}$ mutant and collected evidence that Y238 is the predominant site of NPM-ALK-mediated phosphorylation. Third, by performing various functional assays using $MSH2^{Y238F}$ in GP293 and ALK+ALCL cells, I found that $MSH2^{Y238F}$ can restore MMR. These findings support the concept that tyrosine phosphorylation of $MSH2^{Y238}$ is a critical step by which NPM-ALK deregulates MMR.

One of the key findings of this study is that enforced expression of $MSH2^{Y238F}$ in the presence of NPM-ALK restores MMR using both GP293 and ALK+ALCL cell lines. The *β-galactosidase* reporter assay and the MNU sensitivity assay have been used previously to assess the MMR function in other experimental systems.[9,41,64-66] While the mechanism by which $MSH2^{Y238F}$ restores MMR needs further delineation, I believe that results from this study have provided important clues. First, I found that the MSH2:MSH6 binding was disrupted in the presence of NPM-ALK[9], and

this defect was restored by MSH2^{Y238F}. Second, in the presence of NPM-ALK, the tyrosine phosphorylation of MSH2 decreased dramatically after MSH2^{Y238F} expression. Third, the expression of MSH2^{Y238F} substantially reduced the binding between NPM-ALK and endogenous MSH2, although the mutant itself can bind to NPM-ALK. Taken together, the most likely scenario I have considered is that MSH2^{Y238F} restores MMR by sequestering NPM-ALK away from the endogenous MSH2 protein, leading to a substantial increase in the availability of endogenous MSH2:MSH6 heterodimers. This is illustrated in a model shown in **Figure 3.10**, consistent with the observation that MSH2^{Y238F} exerts a dominant negative effect on NPM-ALK-mediated tyrosine phosphorylation of endogenous MSH2. In cells with NPM-ALK expression, NPM-ALK phosphorylates MSH2 at Y238, blocking the MutSα heterodimer formation between MSH2 and MSH6 (left panel). As a consequence, MMR functionality in these cells is suppressed. In cells with MSH2^{Y238F} enforced expression, NPM-ALK preferentially binds MSH2^{Y238F} (right panel). This binding event frees *endogenous* MSH2 from its interaction with NPM-ALK, allowing formation of the MutSα heterodimer, composed of endogenous MSH2 and MSH6. Thus, in these cells expressing MSH2^{Y238F}, MMR is restored.

To further understand the significance of tyrosine phosphorylation of MSH2, I assessed the effect of the MSH2^{Y238F} mutant on the sensitivity to DNA-damaging agents in ALK+ALCL cells, specifically MNU and 5-FU, which induce DNA damage processed directly and indirectly by MMR. Cells with MMR deficiencies have been reported to be more resistant to these DNA damaging drugs.[24-33] Thus, a restoration of sensitivity is associated with the return of MMR. In the context of MMR, MNU treatment creates O^6-methylguanine (O^6-meG) lesions in the DNA that are mispaired with thymine (T), and the resulting O^6-meG:T mismatch is detected by

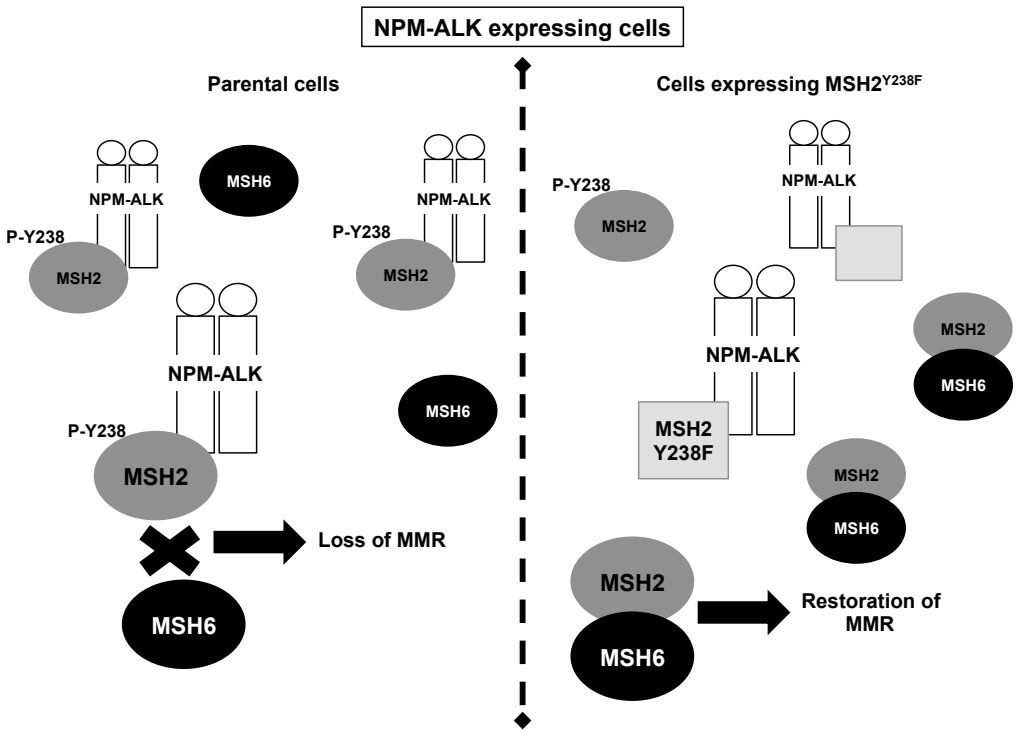

Figure 3.10. Schematic model of how MSH2^{Y238F} is postulated to restore MMR. My working model based on data published in this manuscript, as well as previously reported findings from the Lai laboratory[9], is that NPM-ALK, through an interaction with MSH2 that leads to MSH2 tyrosine phosphorylation at residue 238, sequesters MSH2 from MSH6, blocking MutSα formation and its translocation to the nucleus in the presence of DNA damage. This is shown on the left. The data from this manuscript, using both GP293 and ALK+ALCL cells, suggest that when its expression is enforced, MSH2^{Y238F} blocks the phosphorylation of *endogenous* MSH2, by preferentially binding to NPM-ALK, as shown on the right. Endogenous MSH2 is then capable of binding to MSH6, forming the MutSα heterodimer, and restoring MMR, even in the presence of NPM-ALK.

MMR proteins. Through the consequent repair process, a T is reinserted opposite the O^6-meG, reinitiating a futile MMR cycle that results in double-stranded DNA breaks, G2 arrest, and cell death.[53,67,68] MMR processing after 5-FU treatment is similar to that seen with MNU; 5-FU can cause dNTP pool imbalances, leading to frequent 5-FU:Guanine lesions detected by MutSα, leading to MMR-dependent activation of the G2-checkpoint and apoptosis.[30] I provide evidence that the expression of the $MSH2^{Y238F}$ mutant significantly increased the sensitivity to MNU and 5-FU, suggesting a restoration of MMR in ALK+ALCL cells.

My data also suggests that enforced expression of $MSH2^{Y238F}$ alone can induce apoptosis in two ALK+ALCL cell lines. Exactly how this mutant mediates this biological effect is unknown. Nevertheless, apart from its role in MMR, MSH2 is known to carry important roles in the regulation of cell-cycle checkpoint and apoptosis in both MMR proficient and deficient cells.[69] It has been reported that overexpression of MSH2 induced cell death in MMR-functional GP293 and MMR-deficient SK-UT-1 cells.[37] Although I used GP293 cells in this study, it's important to note that in most experiments, cell death was not detectable as MSH2 overexpression was only induced for 24-48 hours. Loss of MMR has been associated with a decrease in apoptosis and an increase in UVB (ultraviolet B)-associated DNA damage adducts in the epidermis of *MSH2*-null mice, accompanied by an increase in UVB-associated tumors and loss of phosphorylated p53.[70-72] The resistance of MMR deficient cells to certain DNA-damaging agents is partially through a loss of DNA-damage induced cell cycle arrest; MSH2 associates with the checkpoint proteins ATR, CHK1 and CHK2, both *in vitro* and *in vivo*, mediating the initiation of G2/M cell cycle arrest.[27,73-75] Although the exact mechanisms underlying the induction of apoptosis following overexpression of $MSH2^{Y238F}$ are not yet determined, it can be postulated that ALK+ALCL cell lines carry a large number of DNA-

damage adducts that, upon restoration of MMR, lead to an MMR-driven apoptotic signaling cascade.

There is accumulating evidence that cancers with oncogenic tyrosine kinases have dysfunctional DNA damage responses directly related to kinase-driven aberrant downstream signaling processes.[76-79] As another oncogenic tyrosine kinase, BCR-ABL has been shown to inhibit MMR[63], and receptor tyrosine kinases have similar features in regard to activity and signal transduction, MMR dysfunction through MSH2 phosphorylation may be shared across multiple oncogenic tyrosine kinases. This highly novel finding could significantly change the field of oncogenic tyrosine kinase research. Furthermore, with the emergence of ALK as a molecular driver of a number of other cancer types, including non-small-cell lung cancer, diffuse large B cell lymphoma, breast cancer, retinoblastoma, colon carcinoma, and esophageal squamous cell carcinoma[80], I believe that detection of MSH2 phosphorylation at Y238 may be of great clinical and diagnostic significance. I believe that tyrosine phosphorylation of MSH2 at Y238 and the subsequent inhibition of DNA MMR may be a universal mechanism by which oncogenic tyrosine kinases potentiate tumorigenesis. Related studies are currently underway in the Lai laboratory.

In summary, I have presented evidence that NPM-ALK phosphorylates MSH2 at a specific site, Y238, creating a functional loss of MMR by sequestration and inactivation of the function of MSH2. The data suggests that enforced expression of the $MSH2^{Y238F}$ phosphorylation-less mutant is able to restore MMR through a dominant-negative effect, whereby its expression blocks NPM-ALK interaction with endogenous MSH2, allowing for the formation of the endogenous MutSα heterodimer. The importance of detecting MSH2 tyrosine phosphorylation in oncogenic tyrosine kinase expressing cancers clinically needs to be further defined. The novel finding

of NPM-ALK-induced tyrosine phosphorylation of MSH2 leading to MMR dysfunction, an event that may be shared by other clinically significant tyrosine kinases, is an integral part of how oncogenesis is potentiated in ALK+ALCL.

3.6 Acknowledgments

This work was supported by an operating research grant from the Canadian Institute of Health Research (R.L. and S.E.A.), and by contributions by J.T.B. from the University Health Foundation – Medical Research competition (2010). K.M.B. is a graduate student supported by doctoral studentships from the Canadian Institute of Health Research, Alberta Innovates Health Solutions, and the University of Alberta (President's Doctoral Award of Distinction), and is a Killam Scholar (Izaak Walton Killam Memorial Scholarship). F.W. was supported by a post-doctoral fellowship from the Alberta Cancer Foundation. The authors would like to thank Dr. P. Kaiser for the gift of the HB-expression vector, Dr. M. Meuth for the grift of the MSH2 expression vector, and Dr. S. Morris for the gift of the MSH2 and NPM-ALK expression vectors. The authors would also like to thank Karen Jung and Dr. David Murray for proofreading the manuscript.

3.7 References

1. Campo E, Swerdlow SH, Harris NL, Pileri S, Stein H, Jaffe ES. The 2008 WHO classification of lymphoid neoplasms and beyond: evolving concepts and practical applications. *Blood* 2011;**117**(19):5019-5032.

2. Morgan R, Hecht BK, Sandberg AA, Hecht F, Smith SD. Chromosome 5q35 breakpoint in malignant histiocytosis. *N Engl J Med* 1986;**314**(20):1322.

3. Rimokh R, Magaud JP, Berger F, et al. A translocation involving a specific breakpoint (q35) on chromosome 5 is characteristic of anaplastic large cell lymphoma ('Ki-1 lymphoma'). *Br J Haematol* 1989;**71**(1):31-36.

4. Le Beau MM, Bitter MA, Larson RA, et al. The t(2;5)(p23;q35): a recurring chromosomal abnormality in Ki-1-positive anaplastic large cell lymphoma. *Leukemia* 1989;**3**(12):866-870.

5. Mathew P, Sanger WG, Weisenburger DD, et al. Detection of the t(2;5)(p23;q35) and NPM-ALK fusion in non-Hodgkin's lymphoma by two-color fluorescence in situ hybridization. *Blood* 1997;**89**(5):1678-1685.

6. Amin HM, Lai R. Pathobiology of ALK+ anaplastic large-cell lymphoma. *Blood* 2007;**110**(7):2259-2267.

7. Lai R, Ingham RJ. The pathobiology of the oncogenic tyrosine kinase NPM-ALK: a brief update. *Ther Adv Hematol* 2013;**4**(2):119-131.

8. Pearson JD, Lee JK, Bacani JT, Lai R, Ingham RJ. NPM-ALK: the prototypic member of a family of oncogenic fusion tyrosine kinases. *J Signal Transduct* 2012;**2012**:123253.

9. Young LC, Bone KM, Wang P, et al. Fusion tyrosine kinase NPM-ALK deregulates MSH2 and suppresses DNA mismatch repair function: novel insights into a potent oncoprotein. *Am J Pathol* 2011;**179**(1):411-421.

10. Li GM. Mechanisms and functions of DNA mismatch repair. *Cell Res* 2008;**18**(1):85-98.

11. Marti TM, Kunz C, Fleck O. DNA mismatch repair and mutation avoidance pathways. *J Cell Physiol* 2002;**191**(1):28-41.

12. Jascur T, Boland CR. Structure and function of the components of the human DNA mismatch repair system. *Int J Cancer* 2006;**119**(9):2030-2035.

13. Peltomaki P. Deficient DNA mismatch repair: a common etiologic factor for colon cancer. *Hum Mol Genet* 2001;**10**(7):735-740.

14. Kunkel TA, Erie DA. DNA mismatch repair. *Annu Rev Biochem* 2005;**74**:681-710.

15. Martin L, Coffey M, Lawler M, Hollywood D, Marignol L. DNA mismatch repair and the transition to hormone independence in breast and prostate cancer. *Cancer Lett* 2010;**291**(2):142-149.

16. Peltomaki P. Role of DNA mismatch repair defects in the pathogenesis of human cancer. *J Clin Oncol* 2003;**21**(6):1174-1179.

17. Rasmussen LJ, Heinen CD, Royer-Pokora B, et al. Pathological assessment of mismatch repair gene variants in Lynch syndrome: past, present, and future. *Hum Mutat* 2012;**33**(12):1617-1625.

18. Plotz G, Zeuzem S, Raedle J. DNA mismatch repair and Lynch syndrome. *J Mol Histol* 2006;**37**(5-7):271-283.

19. Lynch HT, de la Chapelle A. Hereditary colorectal cancer. *N Engl J Med* 2003;**348**(10):919-932.

20. Krskova-Honzatkova L, Cermak J, Sajdova J, Stary J, Sedlacek P, Sieglova Z. Microsatellite instability in hematological malignancies. *Leuk Lymphoma* 2002;**43**(10):1979-1986.

21. Nomdedeu JF, Perea G, Estivill C, et al. Microsatellite instability is not an uncommon finding in adult de novo acute myeloid leukemia. *Annals of Hematology* 2005;**84**(6):368-375.

22. Degroote A, Knippenberg L, Vander Borght S, et al. Analysis of microsatellite instability in gastric mucosa-associated lymphoid tissue lymphoma. *Leuk Lymphoma* 2013;**54**(4):812-818.

23. Miyashita K, Fujii K, Yamada Y, et al. Frequent microsatellite instability in non-Hodgkin lymphomas irresponsive to chemotherapy. *Leuk Res* 2008;**32**(8):1183-1195.

24. Adamsen BL, Kravik KL, De Angelis PM. DNA damage signaling in response to 5-fluorouracil in three colorectal cancer cell lines with different mismatch repair and TP53 status. *International Journal of Oncology* 2011;**39**(3):673-682.

25. Aebi S, Fink D, Gordon R, et al. Resistance to cytotoxic drugs in DNA mismatch repair-deficient cells. *Clinical Cancer Research* 1997;**3**(10):1763-1767.

26. Kinsella TJ. Coordination of DNA mismatch repair and base excision repair processing of chemotherapy and radiation damage for targeting resistant cancers. *Clinical Cancer Research* 2009;**15**(6):1853-1859.

27. O'Brien V, Brown R. Signalling cell cycle arrest and cell death through the MMR System. *Carcinogenesis* 2006;**27**(4):682-692.

28. Zeng X, Kinsella TJ. A novel role for DNA mismatch repair and the autophagic processing of chemotherapy drugs in human tumor cells. *Autophagy* 2007;**3**(4):368-370.

29. Aebi S, Kurdi-Haidar B, Gordon R, et al. Loss of DNA mismatch repair in acquired resistance to cisplatin. *Cancer Res* 1996;**56**(13):3087-3090.

30. Li LS, Morales JC, Veigl M, et al. DNA mismatch repair (MMR)-dependent 5-fluorouracil cytotoxicity and the potential for new therapeutic targets. *Br J Pharmacol* 2009;**158**(3):679-692.

31. Stojic L, Cejka P, Jiricny J. High doses of SN1 type methylating agents activate DNA damage signaling cascades that are largely independent of mismatch repair. *Cell Cycle* 2005;**4**(3):473-477.

32. Drummond JT, Anthoney A, Brown R, Modrich P. Cisplatin and adriamycin resistance are associated with MutLalpha and mismatch repair deficiency in an ovarian tumor cell line. *J Biol Chem* 1996;**271**(33):19645-19648.

33. de las Alas MM, Aebi S, Fink D, Howell SB, Los G. Loss of DNA mismatch repair: effects on the rate of mutation to drug resistance. *J Natl Cancer Inst* 1997;**89**(20):1537-1541.

34. Christmann M, Tomicic MT, Kaina B. Phosphorylation of mismatch repair proteins MSH2 and MSH6 affecting MutSalpha mismatch-binding activity. *Nucleic Acids Res* 2002;**30**(9):1959-1966.

35. Hernandez-Pigeon H, Quillet-Mary A, Louat T, et al. hMutS alpha is protected from ubiquitin-proteasome-dependent degradation by atypical protein kinase C zeta phosphorylation. *J Mol Biol* 2005;**348**(1):63-74.

36. Hernandez-Pigeon H, Laurent G, Humbert O, Salles B, Lautier D. Degradration of mismatch repair hMutSalpha heterodimer by the ubiquitin-proteasome pathway. *FEBS Lett* 2004;**562**(1-3):40-44.

37. Zhang H, Richards B, Wilson T, et al. Apoptosis induced by overexpression of hMSH2 or hMLH1. *Cancer Res* 1999;**59**(13):3021-3027.

38. Wu F, Wang P, Young LC, Lai R, Li L. Proteome-wide identification of novel binding partners to the oncogenic fusion gene protein, NPM-ALK, using tandem affinity purification and mass spectrometry. *Am J Pathol* 2009;**174**(2):361-370.

39. Hegazy SA, Wang P, Anand M, Ingham RJ, Gelebart P, Lai R. The tyrosine 343 residue of nucleophosmin (NPM)-anaplastic lymphoma kinase (ALK) is important for its interaction with SHP1, a cytoplasmic tyrosine phosphatase with tumor suppressor functions. *J Biol Chem* 2010;**285**(26):19813-19820.

40. Wang P, Wu F, Zhang J, et al. Serine phosphorylation of NPM-ALK, which is dependent on the auto-activation of the kinase activation loop, contributes to its oncogenic potential. *Carcinogenesis* 2011;**32**(2):146-153.

41. Nicolaides NC, Littman SJ, Modrich P, Kinzler KW, Vogelstein B. A naturally occurring hPMS2 mutation can confer a dominant negative mutator phenotype. *Mol Cell Biol* 1998;**18**(3):1635-1641.

42. Armanious H, Gelebart P, Anand M, Belch A, Lai R. Constitutive activation of metalloproteinase ADAM10 in mantle cell lymphoma promotes cell growth and activates the TNFalpha/NFkappaB pathway. *Blood* 2011;**117**(23):6237-6246.

43. Blom N, Gammeltoft S, Brunak S. Sequence and structure-based prediction of eukaryotic protein phosphorylation sites. *J Mol Biol* 1999;**294**(5):1351-1362.

44. Ollila S, Sarantaus L, Kariola R, et al. Pathogenicity of MSH2 missense mutations is typically associated with impaired repair capability of the mutated protein. *Gastroenterology* 2006;**131**(5):1408-1417.

45. Mendillo ML, Hargreaves VV, Jamison JW, et al. A conserved MutS homolog connector domain interface interacts with MutL homologs. *Proc Natl Acad Sci U S A* 2009;**106**(52):22223-22228.

46. Marra G, Iaccarino I, Lettieri T, Roscilli G, Delmastro P, Jiricny J. Mismatch repair deficiency associated with overexpression of the MSH3 gene. *Proc Natl Acad Sci U S A* 1998;**95**(15):8568-8573.

47. Shcherbakova PV, Kunkel TA. Mutator phenotypes conferred by MLH1 overexpression and by heterozygosity for mlh1 mutations. *Mol Cell Biol* 1999;**19**(4):3177-3183.

48. Gibson SL, Narayanan L, Hegan DC, Buermeyer AB, Liskay RM, Glazer PM. Overexpression of the DNA mismatch repair factor, PMS2, confers hypermutability and DNA damage tolerance. *Cancer Lett* 2006;**244**(2):195-202.

49. Jiricny J. The multifaceted mismatch-repair system. *Nat Rev Mol Cell Biol* 2006;**7**(5):335-346.

50. Branch P, Aquilina G, Bignami M, Karran P. Defective mismatch binding and a mutator phenotype in cells tolerant to DNA damage. *Nature* 1993;**362**(6421):652-654.

51. Kat A, Thilly WG, Fang WH, Longley MJ, Li GM, Modrich P. An alkylation-tolerant, mutator human cell line is deficient in strand-specific mismatch repair. *Proc Natl Acad Sci U S A* 1993;**90**(14):6424-6428.

52. Aquilina G, Crescenzi M, Bignami M. Mismatch repair, G(2)/M cell cycle arrest and lethality after DNA damage. *Carcinogenesis* 1999;**20**(12):2317-2326.

53. Hickman MJ, Samson LD. Apoptotic signaling in response to a single type of DNA lesion, O(6)-methylguanine. *Mol Cell* 2004;**14**(1):105-116.

54. Acharya S, Wilson T, Gradia S, et al. hMSH2 forms specific mispair-binding complexes with hMSH3 and hMSH6. *Proc Natl Acad Sci U S A* 1996;**93**(24):13629-13634.

55. Guerrette S, Wilson T, Gradia S, Fishel R. Interactions of human hMSH2 with hMSH3 and hMSH2 with hMSH6: examination of mutations found in hereditary nonpolyposis colorectal cancer. *Mol Cell Biol* 1998;**18**(11):6616-6623.

56. Plotz G, Raedle J, Brieger A, Trojan J, Zeuzem S. N-terminus of hMLH1 confers interaction of hMutLalpha and hMutLbeta with hMutSalpha. *Nucleic Acids Res* 2003;**31**(12):3217-3226.

57. Plotz G, Raedle J, Brieger A, Trojan J, Zeuzem S. hMutSalpha forms an ATP-dependent complex with hMutLalpha and hMutLbeta on DNA. *Nucleic Acids Res* 2002;**30**(3):711-718.

58. Blackwell LJ, Wang S, Modrich P. DNA chain length dependence of formation and dynamics of hMutSalpha.hMutLalpha.heteroduplex complexes. *J Biol Chem* 2001;**276**(35):33233-33240.

59. Raschle M, Dufner P, Marra G, Jiricny J. Mutations within the hMLH1 and hPMS2 subunits of the human MutLalpha mismatch repair factor affect its ATPase activity, but not its ability to interact with hMutSalpha. *J Biol Chem* 2002;**277**(24):21810-21820.

60. Schmutte C, Marinescu RC, Sadoff MM, Guerrette S, Overhauser J, Fishel R. Human exonuclease I interacts with the mismatch repair protein hMSH2. *Cancer Res* 1998;**58**(20):4537-4542.

61. Schmutte C, Sadoff MM, Shim KS, Acharya S, Fishel R. The interaction of DNA mismatch repair proteins with human exonuclease I. *J Biol Chem* 2001;**276**(35):33011-33018.

62. Rasmussen LJ, Rasmussen M, Lee B, et al. Identification of factors interacting with hMSH2 in the fetal liver utilizing the yeast two-hybrid system. In vivo interaction through the C-terminal domains of hEXO1 and hMSH2 and comparative expression analysis. *Mutat Res* 2000;**460**(1):41-52.

63. Stoklosa T, Poplawski T, Koptyra M, et al. BCR/ABL inhibits mismatch repair to protect from apoptosis and induce point mutations. *Cancer Res* 2008;**68**(8):2576-2580.

64. Chen Y, Wang J, Fraig MM, et al. Defects of DNA mismatch repair in human prostate cancer. *Cancer Res* 2001;**61**(10):4112-4121.

65. Bellacosa A, Cicchillitti L, Schepis F, et al. MED1, a novel human methyl-CpG-binding endonuclease, interacts with DNA mismatch repair protein MLH1. *Proc Natl Acad Sci U S A* 1999;**96**(7):3969-3974.

66. Mihaylova VT, Bindra RS, Yuan J, et al. Decreased expression of the DNA mismatch repair gene Mlh1 under hypoxic stress in mammalian cells. *Mol Cell Biol* 2003;**23**(9):3265-3273.

67. Quiros S, Roos WP, Kaina B. Processing of O6-methylguanine into DNA double-strand breaks requires two rounds of replication whereas apoptosis is also induced in subsequent cell cycles. *Cell Cycle* 2010;**9**(1):168-178.

68. Koryllou A, Patrinou-Georgoula M, Dimozi A, Kyrtopoulos SA, Pletsa V. Investigation of cell death induced by N-methyl-N-nitrosourea in cell lines of human origin and implication of RNA binding protein alterations. *Anticancer Res* 2011;**31**(12):4291-4299.

69. Seifert M, Reichrath J. The role of the human DNA mismatch repair gene hMSH2 in DNA repair, cell cycle control and apoptosis: implications for pathogenesis, progression and therapy of cancer. *J Mol Histol* 2006;**37**(5-7):301-307.

70. Peters AC, Young LC, Maeda T, Tron VA, Andrew SE. Mammalian DNA mismatch repair protects cells from UVB-induced DNA damage by facilitating apoptosis and p53 activation. *DNA Repair (Amst)* 2003;**2**(4):427-435.

71. Young LC, Peters AC, Maeda T, et al. DNA mismatch repair protein Msh6 is required for optimal levels of ultraviolet-B-induced apoptosis in primary mouse fibroblasts. *J Invest Dermatol* 2003;**121**(4):876-880.

72. Young LC, Thulien KJ, Campbell MR, Tron VA, Andrew SE. DNA mismatch repair proteins promote apoptosis and suppress tumorigenesis in response to UVB irradiation: an in vivo study. *Carcinogenesis* 2004;**25**(10):1821-1827.

73. Adamson AW, Beardsley DI, Kim WJ, Gao Y, Baskaran R, Brown KD. Methylator-induced, mismatch repair-dependent G2 arrest is activated through Chk1 and Chk2. *Mol Biol Cell* 2005;**16**(3):1513-1526.

74. Cejka P, Stojic L, Mojas N, et al. Methylation-induced G(2)/M arrest requires a full complement of the mismatch repair protein hMLH1. *EMBO J* 2003;**22**(9):2245-2254.

75. Wang Y, Qin J. MSH2 and ATR form a signaling module and regulate two branches of the damage response to DNA methylation. *Proc Natl Acad Sci U S A* 2003;**100**(26):15387-15392.

76. Dierov J, Sanchez PV, Burke BA, et al. BCR/ABL induces chromosomal instability after genotoxic stress and alters the cell death threshold. *Leukemia* 2009;**23**(2):279-286.

77. Lal MA, Bae D, Camilli TC, Patierno SR, Ceryak S. AKT1 mediates bypass of the G1/S checkpoint after genotoxic stress in normal human cells. *Cell Cycle* 2009;**8**(10):1589-1602.

78. Zhao R, Yang FT, Alexander DR. An oncogenic tyrosine kinase inhibits DNA repair and DNA-damage-induced Bcl-xL deamidation in T cell transformation. *Cancer Cell* 2004;**5**(1):37-49.

79. Skorski T. Oncogenic tyrosine kinases and the DNA-damage response. *Nat Rev Cancer* 2002;**2**(5):351-360.

80. Hallberg B, Palmer RH. Mechanistic insight into ALK receptor tyrosine kinase in human cancer biology. *Nat Rev Cancer* 2013;**13**(10):685-700.

CHAPTER 4

Clinically relevant oncogenic tyrosine kinases interact with and phosphorylate MSH2: a novel mechanism underlying MMR dysfunction

---

This chapter has been modified from a manuscript in preparation:
Bone KM, Gupta N, Andrew SE, Lai R. Clinically relevant oncogenic tyrosine kinases interact with and phosphorylate MSH2: a novel mechanism underlying MMR dysfunction. In preparation.

As first author, I wrote the manuscript, and designed, and performed all the experiments described herein except for the following: I equally contributed to the immunohistochemistry with Gupta N, and Gupta N provided additional experimental assistance as needed. Please note that the IHC for the Figures shown was completed in the Clinical Laboratory at the Cross Cancer Institute.

4.1 Abstract

Using the oncogenic tyrosine kinase NPM-ALK as the study model, the Lai laboratory has previously identified that the DNA mismatch repair protein MSH2 can be phosphorylated and functionally impaired in a type of T-cell lymphoma, ALK-positive anaplastic large cell lymphoma (ALK+ALCL). My subsequent biochemical studies revealed that the tyrosine 238 is the critical site of MSH2 phosphorylation in this context. In this study, I hypothesized that MSH2 phosphorylation and the resultant mismatch repair dysfunction can be mediated by tyrosine kinases other than NPM-ALK. To address this question, I report on the generation and characterization of a novel mouse monoclonal anti-phospho-MSH2 antibody, 2E4, which was designed to be specifically reactive to phospho-MSH2^{Y238}. In keeping with the understanding of the biological significance of MSH2 tyrosine phosphorylation, I found that antibody 2E4 recognizes MSH2 that is abnormally accentuated in the cytoplasm. Furthermore, MSH2 bound by MSH6 was primarily un-phosphorylated. Correlating with these findings, 2E4 immunoreactivity on ALK+ALCL tumors was predominantly cytoplasmic. Importantly, gene transfection of various clinically relevant oncogenic tyrosine kinases, including BCR-ABL, EML4-ALK, c-SRC, HER2, PDGFRα and PDGFRβ, into GP293 cells led to the phosphorylation of MSH2 and expression of the 2E4 epitope. Further, using co-immunoprecipitation, I found a physical interaction between MSH2 and these tyrosine kinases. Finally, using a plasmid-based DNA mismatch repair assay, I demonstrate that expression of these oncogenic tyrosine kinases induced mismatch repair dysfunction in GP293 cells. To conclude, using the validated phospho-MSH2^{Y238} antibody, 2E4, my novel findings demonstrate that phosphorylation of MSH2^{Y238} and subsequent deregulation of DNA mismatch repair function is a shared tyrosine kinase phenomenon.

4.2 Introduction

Tyrosine kinases are widely expressed proteins that regulate a variety of cellular processes including proliferation, differentiation, survival, and motility.[1-3] Over 100 protein tyrosine kinases have been identified, and they all function similarly by transferring phosphate from ATP to tyrosine residues on specific downstream proteins.[4] The activation and downstream signaling of tyrosine kinases is normally tightly controlled. However, tyrosine kinase deregulation and constitutive activation, through chromosomal translocation, gene amplification/overexpression, or activating mutation, has been implicated causally in the pathogenesis of a number of diseases. Once deregulated, oncogenic tyrosine kinases have been linked to the development of numerous hematological malignancies, including leukemia and lymphoma[5], as well as solid tumors, such as those in the breast, ovary, lung, brain, colon, thyroid, gastrointestinal tract, and prostate.[1,4]

Using the oncogenic tyrosine kinase NPM-ALK as a study model, the Lai laboratory has previously identified MutS homolog 2 (MSH2), a protein integral to DNA mismatch repair (MMR), as a novel binding partner and phosphorylation substrate of NPM-ALK.[6-8] Through binding with and tyrosine phosphorylating MSH2, it has been shown that NPM-ALK is capable of functionally inhibiting MMR. NPM-ALK is a gene fusion tyrosine kinase that is the central oncogenic driver of anaplastic lymphoma kinase (ALK) positive anaplastic large cell lymphoma (ALK+ALCL).[9,10] It is the result of the reciprocal chromosomal translocation t(2;5)(p23;q35), fusing the ubiquitously expressed *nucleophosmin* gene to the receptor tyrosine kinase ALK[11,12], and, through its constitutive activation, mediates tumorigenesis by phosphorylating and activating a number of downstream signaling pathways leading to cellular proliferation, cell cycle deregulation, and enhanced survival.[13-15]

Regarding DNA MMR, MSH2 and other MMR proteins are highly expressed proteins that cooperate to maintain genomic stability by correcting errors that occur during DNA replication, as well as some DNA damage that occurs from both exogenous and endogenous sources.[16,17] MMR proteins function as heterodimers, which bind to and correct single base mismatches and insertion-deletion loops, which occur when the replication machinery "stutters" on highly repetitive microsatellite sequences.[18] The predominant MMR heterodimer, MSH2 bound to MSH6, known as MutSα, repairs single base mismatches, small insertion-deletion loops, and DNA damage adducts.[16,19,20] Deregulation of MMR, through epigenetic and genetic changes resulting in loss of MMR protein expression and the resultant microsatellite instability (MSI), has been associated with the development of a number of malignancies, including hereditary non-polyposis colorectal cancer (HNPCC)/Lynch syndrome[16,21], as well as hematological cancers such as acute and chronic leukemia, and non-Hodgkin's lymphoma.[22-25] MMR dysfunction has also been linked to a number of sporadic tumor types, and is associated with a higher than average mutation rate and chemotherapeutic resistance.[18,20,26]

The Lai laboratory first identified tyrosine phosphorylation of MSH2 in 2011[7], and I have since reported on the specific tyrosine residue phosphorylated by NPM-ALK, tyrosine 238.[8] Given the understanding of the importance of phosphorylation of MSH2 at tyrosine 238 to the subsequent MMR dysfunction, and the fact that oncogenic tyrosine kinases share similarities in activation and downstream signal transduction, I hypothesized that this tyrosine phosphorylation event is shared among oncogenic tyrosine kinases. To test this hypothesis, I report on the development and characterization of a mouse monoclonal antibody, 2E4, which was designed to be specifically reactive to MSH2 phosphorylated at tyrosine 238. I then assessed if the NPM-ALK-induced tyrosine phosphorylation of MSH2 and the downstream effect on MMR

function is similarly mediated by a number of known clinically relevant oncogenic tyrosine kinases.

4.3 Methods

4.3.1 Antibody production and purification

All mouse monoclonal antibody (mAB) production steps were performed by Genscript USA, Inc. (Piscataway NJ). The phosphorylated MSH2^{Y238} peptide TKDI(pY238)QDLNRLLKGC was manufactured and purified, and subsequently conjugated with keyhole limpet hemocyanin (KLH) as an immunogen. This conjugated peptide was used to immunize 10 BALB/c (Bagg albino) mice. The mice with satisfactory immune response were chosen for hybridoma production.

The reactivity of the mAB to phospho-MSH2^{Y238} and antibody titer in the hybridoma supernatant was determined by enzyme-linked immunosorbent assay (ELISA) with MSH2 and phopsho-MSH2^{Y238} peptides used as coating antigens. This experiment was performed by Genscript. Once reactivity was confirmed, 5 mL of each hybridoma cell culture supernatant (with 0.02% sodium azide preservative) was lyophilized and shipped to the laboratory. The lyophilized powder was reconstituted in distilled deionized water prior to use, aliquoted to avoid repeated freeze-thaw cycles, and stored at -20°C.

Once the hybridoma supernatant was validated experimentally in the laboratory, the information was sent back to Genscript for mAB production (specifically for clone 2E4) in ascites using 5 BALB/c mice followed by protein G purification. The mAB 2E4 reactivity to phospho-MSH2^{Y238} and titer was determined by indirect ELISA with MSH2 and phospho-MSH2^{Y238} peptides used as coating antigens, and a goat anti-mouse IgG peroxidase

conjugated secondary antibody. The ELISA was performed by Genscript.

4.3.2 Cell lines

GP293 cells, a derivative of the human embryonic kidney cell line, HEK293, were maintained in Dulbecco's modified Eagle's medium (Invitrogen, Life Technologies, Grand Island, NY), supplemented with 10% FBS (Invitrogen), 100 units/mL penicillin and 100 µg/mL streptomycin (Invitrogen). ALK+ALCL cell lines Karpas 299 and SUP-M2, and the mantle cell lymphoma (MCL) cell line, Mino, were maintained in RPMI-1640 (Invitrogen) supplemented with 10% FBS, 100 units/mL penicillin and 100 µg/mL streptomycin. All cell lines were cultured under an atmosphere of 95% O_2 and 5% CO_2 in 98% humidity at 37°C.

4.3.3 Gene expression vectors and gene transfection

The *NPM-ALK* expression vector was a gift from Dr. S. Morris, and was cloned as previously described.[27] The *NPM-ALK*^{FFF} mutant was generated by mutating all three tyrosine residues in the kinase activation loop of ALK (Tyr^{338}, Tyr^{342}, and Tyr^{343}) to phenylalanine in pcDNA3.1(+) (Invitrogen), as previously described.[27] pcDNA3.1(+) was used as a negative expression control. His-biotin tagged *MSH2 (*HB-MSH2) was made by ligating MSH2 cDNA into the HB-tagged vector described previously.[6,8] The untagged pcDNA3-MSH2 vector was a gift from Dr. Mark Meuth.[28] Site-directed mutagenesis of tyrosine (Tyr, Y) 238 of MSH2 was done as previously described (manuscript submitted for publication).[8]

The *BCR-ABL* (*breakpoint cluster region* fused to *Abelson kinase*) expression vector (p210 pcDNA3) contains the full length *BCR-ABL* fusion gene and was purchased from Addgene (Cambridge, MA; plasmid number 27481).[29] The constitutively active *HER2* (*human epidermal growth factor*

receptor 2) (V659E) pcDNA3 plasmid (*CA-HER2*) was purchased from Addgene (plasmid number 16259).[30] The *PDGFR* (*platelet derived growth factor receptor*)*α* and *PDGFRβ* expression vectors were gifts from Dr. T. McMullen, University of Alberta. The PDGFRα and PDGFRβ proteins were activated by adding 50 ng/mL recombinant human protein PDGFaa (Invitrogen) and PDGFbb (Invitrogen) to the culture media, respectively. The constitutively active *SRC* (E381G, *CA-SRC*; *v-Src avian sarcoma (Schmidt-Ruppin A-2) viral oncogene homolog*) plasmid was a gift from Dr. D. Fujita.[31] The *c-KIT* (*v-kit Hardy-Zuckerman 4 feline sarcoma viral oncogene homolog*) vector with a constitutively active tyrosine kinase (D816V, the mutation responsible for systemic mastocytosis, *CA-KIT*) was a gift from Dr. L. Rönnstrand.[32] The *EML4* (*echinoderm microtubule associated protein like 4*)-*ALK* variant 1 (v1) plasmid contains the *EML4-ALK* inversion, which fuses exon 1-13 of *EML4* to exon 20-29 of *ALK* was a gift from Dr. J. Dalton.[33] Gene transfection of the various expression plasmids into 10-cm dishes of GP293 cells was achieved using 10 µg plasmid DNA and Lipofectamine 2000 (Invitrogen) following the manufacturer's recommended protocol.

4.3.4 Immunoprecipitation, co-immunoprecipitation, membrane phosphatase treatment, peptide dot blotting and western blotting

All immunoprecipitation (IP) experiments were done using a commercially available anti-MSH2 monoclonal antibody (2 µg, Clone NA27, EMD Biosciences, Gibbstown, NJ) and mouse monoclonal antibody 2E4 (2 µg) with 500 µg cell lysate collected in ice-cold RIPA buffer (Cell Signaling Technologies, Danvers, MA) supplemented with protease and phosphatase inhibitors (EMD) as previously described.[7,8] In all IP experiments, no-antibody controls were included, though not shown. Co-immunoprecipitation was performed using 500 µg protein lysate collected in ice-cold Cell Lytic M (Sigma Aldrich, Oakville, Ontario, Canada) and 2

µg anti-MSH2 (Clone NA27) as previously described.[7,8] Biotin pulldown experiments were done as previously described.[7]

The phosphatase treatment experiment was done on duplicate samples run by sodium docedyl sulfate–polyacrylamide gel electrophoresis (SDS-PAGE) western blot analysis, transferred to nitrocellulose membrane, cut in half, blocked for 1 hour at room temperature using 5% BSA (Santa Cruz Biotechnology, Santa Cruz, CA) in TBS 0.1% Triton X-100 (Sigma Aldrich), and incubated with calf-intestinal alkaline phosphatase (CIP) buffer (100 mM NaCl, 50 mM Tris-HCl, 10 mM $MgCl_2$, 1 mM dithiothreitol, pH 7.9) for 1 hour on a shaker at 37°C. One unit CIP (NEB, Ipswich, MA) per µg protein was added to one set of samples. Following this, the membranes were washed briefly with TBS and western blotting was done using standard techniques. Briefly, the membrane was incubated overnight with primary antibody diluted in 5% BSA (Santa Cruz) TBS 0.05% Tween 20 (Sigma Aldrich) followed by incubation with horseradish-peroxidase conjugated secondary antibody (Cell Signaling Technology). The membranes were washed in TBS 0.05% Tween 20 for 30 minutes between steps. Proteins were detected using Pierce ECL (enhanced chemiluminescence) Western Blotting Substrate (Fisher Scientific Canada, Ottawa, ON, Canada).

Peptide dot blotting was done using the phospho-MSH2^{Y238} specific immunizing peptide (used to produce the mouse mAB, TKDI(pY238)QDLNRLLKGC) and the unphosphorylated MSH2 peptide (TKDIYQDLNRLLKGC) as follows: 0, 0.125, 0.25, 0.5, 1, 2, and 4 µg peptide diluted in PBS was directly pipetted onto nitrocellulose membrane (Bio-Rad, Mississauga, ON Canada) and allowed to dry. The membrane was then blocked in 5% BSA TBS 0.05% Tween 20 for 1 hour, and incubated overnight with mAB 2E4 (1:5000). Detection was done as described above.

Antibodies for western blotting include: anti-ALK, anti-phospho-ALK, anti-MSH2, anti-STAT3, anti-pSTAT3, anti-HER2, anti-c-ABL, anti-c-KIT, anti-PDGFRα (Cell Signaling Technologies), anti-PDGFRβ, anti-c-SRC, and anti-β-actin (Santa Cruz Biotechnologies). The mAB 2E4 was used at 1:5000.

4.3.5 Nuclear cytoplasmic fractionation

Nuclear and cytoplasmic proteins were isolated from 10-cm plates using the Pierce NE-PER kit (Fisher Scientific Canada) following the manufacturer's suggested protocol. α-Tubulin and histone deacetylase 1 (HDAC-1) were used as cytoplasmic and nuclear markers, respectively, during SDS-PAGE analysis.

4.3.6 β-galactosidase reporter plasmid assay for MMR function

GP293 cells were plated into 12-well plates, transfected with various expression plasmids as well as the pCAR-OF *β-galactosidase* mismatch repair reporter plasmid, and analyzed for β-galactosidase production as previously described.[7,8]

4.3.7 Patient samples and immunohistochemistry

All cases of ALK− ALK+ALCL were diagnosed at the Cross Cancer Institute (Edmonton, Alberta, Canada), and the diagnostic criteria were based on those described by the World Health Organization Classification Scheme.[9] All cases were confirmed to express ALK by immunohistochemistry. Reactive tonsil was included as a control. All cases and ALK− and ALK+ NSCLC were diagnosed at the Cross Cancer Institute. The use of these tissues was approved by the University of Alberta Human Research Ethics Board.

To detect MSH2 phosphorylation at tyrosine 238 using antibody 2E4, antigen retrieval was done using EDTA buffer (1mM EDTA, 0.05% Tween 20, pH 8.0) for 10 minutes in a pressure cooker. The subsequent immunohistochemistry was performed using standard techniques as previously described using mouse mAB 2E4 at 1:500 overnight.[34]

4.3.8 Statistical analysis

Data is expressed as mean ± the standard error of the mean (SEM), and significance was determined from three independent experiments by Student's T-test (GraphPad Prism, La Jolla, CA), with significance denoted by * (p<0.05), **(p<0.01), and ***(p<0.001).

4.4. Results

4.4.1 Generation of the hybridoma cell lines producing anti-phopsho-MSH2^{Y238} mouse monoclonal antibodies

To generate the mouse mABs specific to MSH2 tyrosine phosphorylated at tyrosine 238 (phospho-MSH2^{Y238}), 10 BALB/c mice were immunized with a phospho-MSH2^{Y238} peptide conjugated with KLH. The mice all displayed a satisfactory immune response, and the mice with the best response were chosen for cell fusion and hybridoma production. In total, eight hybridoma cell lines derived from four parental clones were produced. The specific reactivity of the mAB produced by the hybridoma cell clones was evaluated by ELISA, and the results are shown in **Table 4.1**. All antibody production steps and the associated ELISA assays were performed by Genscript USA, Inc. Antibodies produced by all 8 hybridoma cell lines displayed preferred reactivity to the phospho-MSH2^{Y238} peptide over the unphosphorylated MSH2 peptide, with clone 1B11 showing the highest overall reactivity, and clone 5E4 showing the lowest.

Table 4.1. Reactivity of monoclonal antibodies produced from hybridoma supernatant to the peptide phospho-MSH2^{Y238} (ELISA).

Cell Lines	Supernatant Dilution (ELISA OD)						Medium	Titer*	Coating	Isotype
	1:10	1:30	1:90	1:270	1:810	1:2340				
2E4	4.203	3.955	3.790	3.720	3.582	3.239	0.077	>1:2430	A	
	0.143	0.104	0.089	0.075	0.071	0.070	0.084	<1:10	B	IgG1,k
2F12	4.027	3.813	3.753	3.627	3.435	3.087	0.077	>1:2430	A	
	0.176	0.132	0.087	0.075	0.074	0.070	0.084	<1:10	B	IgG1,k
1C7	6.000	6.000	4.643	4.467	4.084	2.896	0.077	>1:2430	A	
	0.116	0.093	0.073	0.072	0.070	0.069	0.084	<1:10	B	IgG1,k
1B11	6.000	5.546	5.245	4.944	4.847	3.055	0.077	>1:2430	A	
	0.120	0.084	0.080	0.069	0.069	0.069	0.084	<1:10	B	IgG1,k
2B10	3.554	2.566	1.143	0.527	0.229	0.142	0.077	1:810	A	
	0.127	0.085	0.073	0.071	0.070	0.063	0.084	<1:10	B	IgG1,k
2H2	3.995	2.302	1.227	0.477	0.209	0.121	0.077	1:810	A	
	0.099	0.078	0.072	0.069	0.068	0.065	0.084	<1:10	B	IgG1,k
5E4	2.897	1.856	1.209	0.382	0.196	0.083	0.077	1:810	A	
	0.125	0.097	0.094	0.082	0.081	0.081	0.084	<1:10	B	IgG1,k
5H6	3.303	2.461	1.235	0.469	0.173	0.101	0.077	1:810	A	
	0.121	0.095	0.093	0.092	0.089	0.084	0.084	<1:10	B	IgG1,k

A: phospho-MSH2^{Y238} peptide, TKDI(pY238)QDLNRLLKGC

B: MSH2 peptide, TKDIYQDLNRLLKGC

*The titer is the highest dilution with sample/blank ≥2.1

4.4.2 NPM-ALK expressing cells produce a phosphorylated MSH2 peptide that is recognized by mABs produced in hybridoma clones 2E4 and 5H6

The Lai previously reported that NPM-ALK binds and tyrosine phosphorylates MSH2 at tyrosine residue 238, and this phosphorylation event is responsible for the functional impairment of MMR induced by NPM-ALK.[6-8] As the mABs designed are meant to be specific to phospho-MSH2^{Y238}, which is induced by NPM-ALK, I asked if the hybridoma mAB clones displayed preferential reactivity to cells with NPM-ALK over cells without NPM-ALK expression. To do this, I used cell lysate from the ALK-negative cell line GP293, the ALK-negative lymphoma cell line, Mino, and the ALK+ALCL cell lines Karpas 299 and SUP-M2 (**Figure 4.1A**). MSH2 protein was immunoprecipitated from this cell lysate, and subjected to western blotting with the mABs produced in the supernatant of the 8 hybridoma cell clones (prepared as outlined in the Materials and Methods). A quick reactivity screen was performed using cell lysate from Mino and Karpas 299 and the mABs in pairs to ensure that differential reactivity to MSH2 was detectable (**Figure 4.1B**). Based on this data, each mAB was screened individually. As shown in **Figure 4.1C**, the mABs from hybridoma clones 5H6, 2E4, 2F12 and 1B11 displayed preferential reactivity with MSH2 precipitated from ALK-expressing cell lysate, while the mABs from hybridoma clones 2B10, 2H2, 1C7 and 5E4 had undesirable reactivity.

The supernatant from the 8 hybridoma clones was then used to screen for reactivity from MSH2 immunoprecipitated from GP293 cells transfected with empty vector (pcDNA3), *NPM-ALK*, or *NPM-ALK*^{FFF} (**Figure 4.1D**); NPM-ALK^{FFF} harbors tyrosine (Y) to phenylalanine (F) mutations in the three key tyrosine kinase residues of the NPM-ALK kinase activation loop. These mutations abrogate the autophosphorylation of NPM-ALK, such that

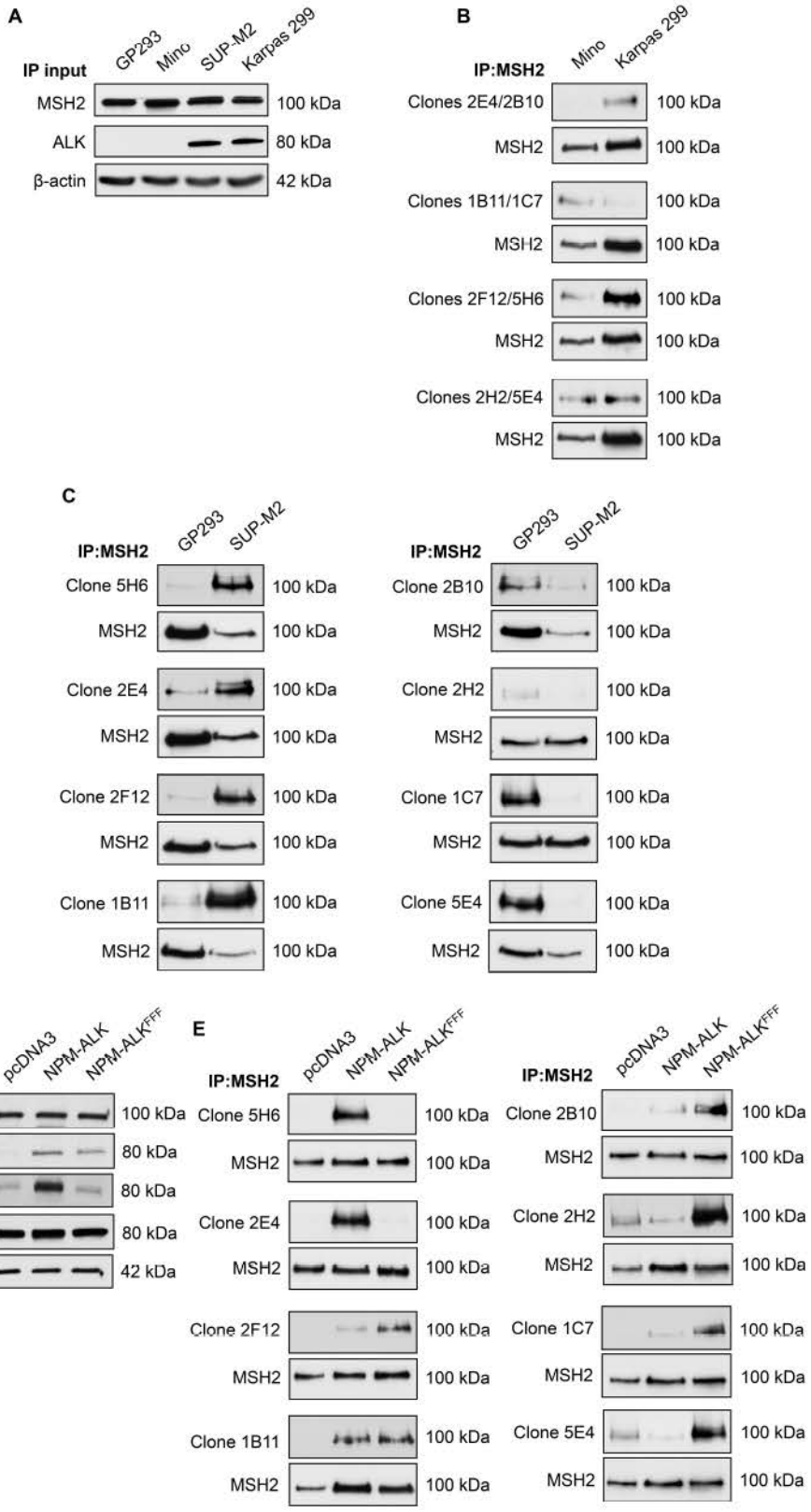
A
IP input
GP293
Mino
SUP-M2
Karpas 299
MSH2
ALK
β-actin
100 kDa
80 kDa
42 kDa
B
IP:MSH2
Mino
Karpas 299
Clones 2E4/2B10
Clones 1B11/1C7
Clones 2F12/5H6
Clones 2H2/5E4
MSH2
100 kDa
C
IP:MSH2
GP293
SUP-M2
Clone 5H6
Clone 2E4
Clone 2F12
Clone 1B11
Clone 2B10
Clone 2H2
Clone 1C7
Clone 5E4
MSH2
100 kDa
D
IP input
pcDNA3
NPM-ALK
NPM-ALKFFF
MSH2
ALK
pSTAT3
STAT3
β-actin
100 kDa
80 kDa
42 kDa
E
IP:MSH2
pcDNA3
NPM-ALK
NPM-ALKFFF
Clone 5H6
Clone 2E4
Clone 2F12
Clone 1B11
Clone 2B10
Clone 2H2
Clone 1C7
Clone 5E4
MSH2
100 kDa

Figure 4.1. NPM-ALK-expressing cells generate an epitope on the MSH2 protein recognized by monoclonal antibodies produced in the hybridoma supernatant of cell clones 2E4 and 5H6. (A) Western blot analysis of the ALK-negative GP293 and Mino cell lysate, and the ALK+ALCL Karpas 299 and SUP-M2 cell lysate. (B) IP of MSH2 was performed on Mino and Karpas 299 cell lysate from A using a monoclonal MSH2 antibody, and the resulting immunoblots were probed with paired mouse mAB raised against phopsho-MSH2^{Y238}, produced in the hybridoma supernatant of clones 2E4/2B10, 1B11/1C7, 2F12/5H6, and 2H2/5E4. The blots were probed with an anti-MSH2 antibody to confirm immunoprecipitation. (C) IP of MSH2 was performed on GP293 and SUP-M2 cell lysate shown in A using a monoclonal MSH2 antibody, and the resulting immunoblots were probed with mABs against phospho-MSH2^{Y238} produced in the supernatant of hybridoma cell clones. Mouse mAB from cell clones 5H6, 2E4, 2F12, and 1B11 showed expected immunoreactivity to cells expressing NPM-ALK (left panel), and clones 2B10, 2H2, 1C7 and 5E4 showed negative reactivity (right panel). The blots were probed with an anti-MSH2 antibody to confirm immunoprecipitation. (D) Western blot analysis of cell lysate from GP293 cells transfected with pcDNA3 (negative control for NPM-ALK expression), *NPM-ALK*, and *NPM-ALK*^{FFF}. (E) MSH2 was immunoprecipitated from lysate shown in E, and the resulting immunoblots were probed with anti-phospho-MSH2^{Y238} mABs produced in the supernatant of hybridoma cell clones. The blots were probed with an anti-MSH2 antibody to confirm immunoprecipitation.

this mutant is unable to phosphorylate downstream proteins, including STAT3. Thus, any phospho-MSH2^{Y238} mAB reactivity seen in NPM-ALK expressing cells should be lost in cells expressing NPM-ALK^{FFF}. As shown in **Figure 4.1E**, mAB produced in the supernatant of clones 2E4 and 5H6 displayed reactivity to MSH2 immunoprecipitated from lysate of cells expressing NPM-ALK, but not NPM-ALK^{FFF}. All other hybridoma produced mABs displayed undesirable immunoreactivity.

To demonstrate that the mABs produced by hybridoma clones 2E4 and 5H6 are specifically reactive to the MSH2 protein in its phosphorylated state, a phosphatase treatment strategy was employed; dephosphorylated samples should show little to no staining when compared to untreated samples. First, MSH2 was immunoprecipitated from protein of GP293 cells expressing pcDNA3, NPM-ALK or NPM-ALK^{FFF}, and the resulting IP protein was subjected to western blotting. After the protein was transferred to nitrocellulose, the membrane was incubated with calf intestinal phosphatase (CIP) prior to antibody detection as outlined in the Materials and Methods. The immunoprecipitation input western blot was also treated in the same manner; phosphatase treatment abrogated the detectable phospho-ALK (pALK) antibody signal from cell lysate expressing NPM-ALK, as expected (**Figure 4.2A**, left panel, without CIP, versus right panel with CIP, respectively). After immunoprecipitation using an anti-total-MSH2 monoclonal antibody, the mAB produced in the supernatant of hybridoma clones 2E4 and 5H6 showed specificity to MSH2 purified in the presence of wild type NPM-ALK, and this signal was lost upon CIP treatment (**Figure 4.2B**, left panels versus right panels). Taken together, these results suggest that hybridoma antibodies 2E4 and 5H6 are immunoreactive to a phospho-specific epitope of MSH2 that is induced upon NPM-ALK expression.

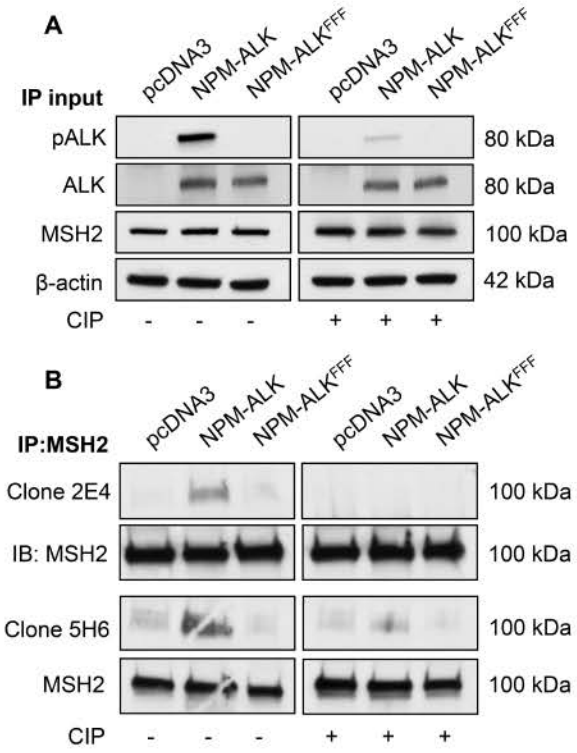

Figure 4.2. Reactivity of antibodies from hybridoma cell clones 2E4 and 5H6 to MSH2 is abrogated with phosphatase treatment. (A) Western blot analysis of GP293 cell lysate from cells transiently transfected with pcDNA3, *NPM-ALK*, and *NPM-ALK*^{FFF}, treated with (+, right panel) and without (-, left panel) calf intestinal phosphatase (CIP). (B) MSH2 was immunoprecipitated from cell lysate shown in A and the resulting immunoblot was treated with (+, right panel) and without (-, left panel) CIP, followed by incubation with mouse mABs produced in the supernatant of hybridoma cell clones 2E4 and 5H6. The blots were probed with an anti-MSH2 antibody to confirm successful immunoprecipitation.

4.4.3 Purified mouse mAB 2E4 recognizes the phopsho-Y238 epitope of MSH2 that is induced by NPM-ALK

The antibodies produced by hybridoma supernatant from clones 2E4 and 5H6 were subjected to ascites production followed by protein G purification as outlined in the Materials and Methods. These experimental procedures were completed in the laboratories of Genscript. The reactivity of the purified mAB 2E4 and 5H6, as well as the antibody titer, was determined using a phospho-MSH2Y238 and a native MSH2 peptide by ELISA (**Tables 4.2** and **Table 4.3**, respectively).

I then tested the specificity of the purified mAB to NPM-ALK-induced tyrosine phosphorylation of MSH2 by immunoprecipitation of MSH2 from GP293 cell lysate transfected with empty vector, *NPM-ALK* or *NPM-ALK*^{FFF} (**Figure 4.3A**). This was done to ensure that the purified mouse mAB 2E4 had similar reactivity to the antibody present in the hybridoma supernatant of clone 2E4. Purified mAB 2E4 reacted specifically to MSH2 purified in the presence of NPM-ALK, but not NPM-ALK^{FFF} (**Figure 4.3B**, upper panel), which is in keeping with my previous findings using antibody from the supernatant of hybridoma clone 2E4. These results were confirmed by reciprocal immunoprecipitation using the purified mAB 2E4 (**Figure 4.3B**, middle panel). Purified mAB 5H6 did not have the expected reactivity; it was immunoreactive with MSH2 immunoprecipitated from cells expressing NPM-ALK^{FFF} (**Figure 4.3B**, lower panel). Thus, purified mAB 2E4 was chosen for the subsequent experiments.

I previously reported that NPM-ALK induced tyrosine phosphorylation of MSH2 at tyrosine 238; the expression of a his-biotin (HB)-tagged MSH2^{Y238F} mutant in GP293 cells in the presence of NPM-ALK blocked NPM-ALK-induced tyrosine phosphorylation of endogenous MSH2 in a dominant negative manner, and by biotin pulldown, mutation of

Table 4.2. Reactivity of protein G purified monoclonal antibody 2E4 against the peptide phospho-MSH2^{Y238} (ELISA).

Dilution	phopsho-MSH2^{Y238} antibody (2E4)	
	A (ELISA OD)	B (ELISA OD)
1:1000	3.055	0.397
1:3000	3.035	0.159
1:9000	2.839	0.101
1:27000	2.387	0.077
1:81000	1.637	0.073
Blank	0.067	0.065
Titer*	>1:81000	1:3000

A: phospho-MSH2^{Y238} peptide, TKDI(pY238)QDLNRLLKGC

B: MSH2 peptide, TKDIYQDLNRLLKGC

Starting dilution 1:1000 = 1.0 µg/mL

*The titer is the highest dilution with sample/blank ≥2.1

Table 4.3. Reactivity of protein G purified monoclonal antibody 5H6 against the peptide phospho-MSH2^{Y238} (ELISA).

Dilution	phopsho-MSH2^{Y238} antibody (5H6)	
	A (ELISA OD)	B (ELISA OD)
1:1000	2.391	0.124
1:3000	1.449	0.085
1:9000	0.515	0.075
1:27000	0.188	0.071
1:81000	0.095	0.061
Blank	0.067	0.065
Titer*	1:27000	<1:1000

A: phospho-MSH2^{Y238} peptide, TKDI(pY238)QDLNRLLKGC

B: MSH2 peptide, TKDIYQDLNRLLKGC

Starting dilution 1:1000 = 1.0 µg/mL

*The titer is the highest dilution with sample/blank ≥2.1

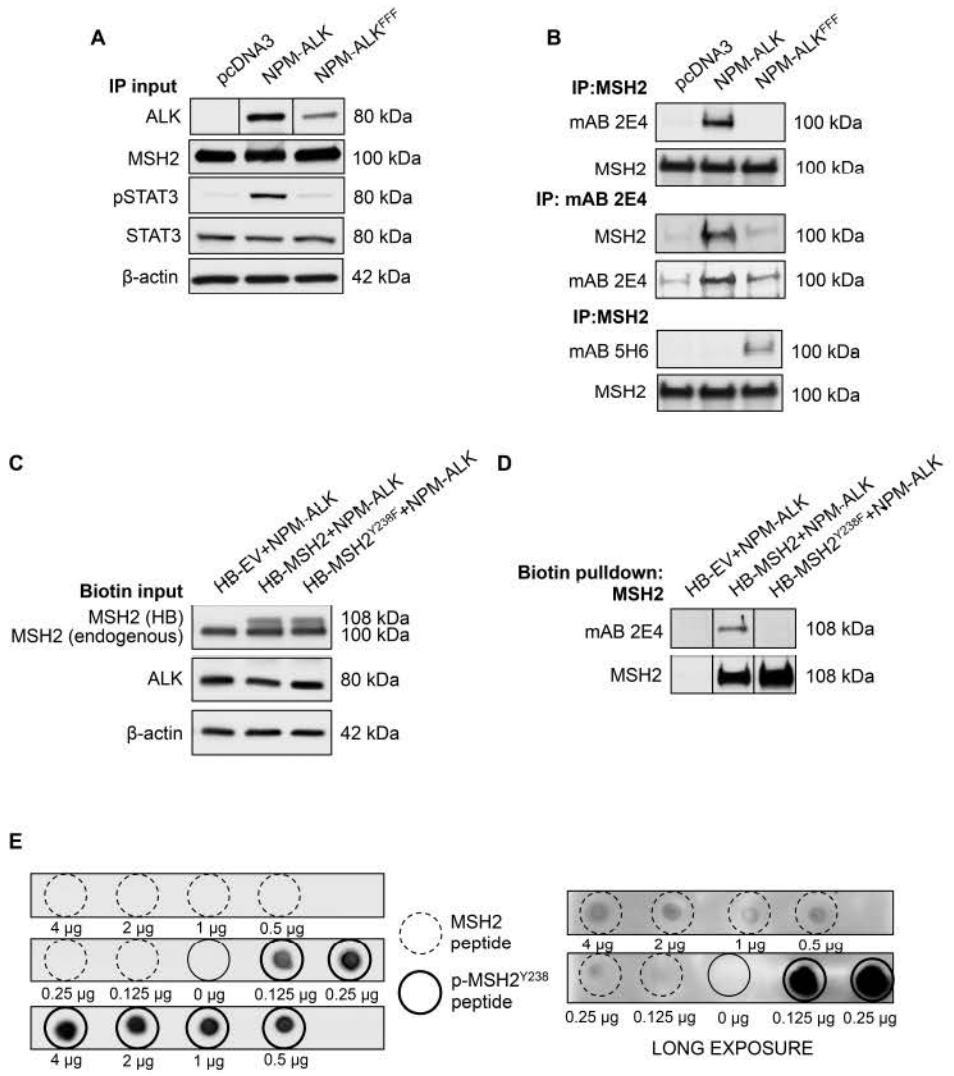

Figure 4.3. Protein G purified monoclonal antibody 2E4 recognizes an epitope of MSH2, phospho-MSH2^{Y238}, that is induced by NPM-ALK expression. (A) Western blot analysis of GP293 cell lysate expressing pcDNA3, NPM-ALK, and NPM-ALK^{FFF}. (B) MSH2 was immunoprecipitated from the lysate shown in A and the resulting immunoblot was probed with protein G purified, ascites produced, mouse mABs 2E4 (upper panel), and 5H6 (lower panel). A reciprocal immunoprecipitation was done using mAB 2E4, and probing the resulting western with MSH2 to confirm the results shown with the anti-total MSH2 antibody (middle panel). (C) Western blot analysis of GP293 cells transfected with HB-EV, HB-MSH2 and HB-MSH2^{Y238F}. (D) Streptavidin pulldown of HB-tagged MSH2/MSH2^{Y238F}

protein from lysate depicted in C. The resulting immunoblot was probed with mAB 2E4. HB-MSH2^{Y238F} abolished 2E4 immunoreactivity. The immunoblot was probed with anti-MSH2 to confirm successful immunoprecipitation. (E) Peptide dot blot analysis depicting mAB 2E4 reactivity to the phospho-MSH2^{Y238} immunizing peptide used to make the mAB, TKDI(pY238)QDLNRLLKGC (solid black circles), and the corresponding wild type MSH2 peptide, TKDIYQDLNRLLKGC (dashed circles). A long exposure of the left panel is shown in the right panel. Data shown is representative of 2 independent experiments.

HB-MSH2 to HB-MSH2^{Y238F} abrogated NPM-ALK-induced tyrosine phosphorylation.[8] Because of the inability immunoprecipitation experiments to evaluate the phosphorylation of the exogenous, HB-tagged MSH2 proteins[7], I used streptavidin agarose resin, which binds the biotinylated portion of the HB-tag, to purify the exogenous, HB-tagged MSH2 and HB-MSH2^{Y238F} proteins from GP293 cell lysates co-transfected with *NPM-ALK* (**Figure 4.3C**). Mutation of tyrosine 238 to phenylalanine (HB-MSH2^{Y238F}) abrogated any detectable phosphorylation band following incubation with purified mouse mAB 2E4 (**Figure 4.3D**). The specificity of antibody 2E4 to tyrosine 238 of MSH2 was confirmed by peptide dot blotting using the specific phospho-MSH2^{Y238} immunizing peptide and a non-phosphorylated peptide control, as detailed in the Materials and Methods. As shown in **Figure 4.3E**, mAB 2E4 was only reactive to the phospho-MSH2^{Y238} peptide (left panel; solid black circles); reactivity to the non-phosphorylated MSH2 peptide was only detected after a long film exposure time following (right panel; dashed circles). Taken together, these results suggest that mouse mAB 2E4 recognized an NPM-ALK-induced epitope of MSH2, phospho-MSH2^{Y238}.

4.4.4 Mouse mAB 2E4 recognizes MSH2 that has a weak interaction with MSH6

The Lai laboratory previously reported that, in the presence of NPM-ALK, the interaction of MSH2 with its main mismatch repair interacting partner, MSH6, is markedly reduced.[7,8] I hypothesized that the majority of MSH2 that is bound by MSH6 is not tyrosine phosphorylated; thus, the epitope of MSH2 recognized by mAB 2E4 should have weak interaction with MSH6. To test this hypothesis, I immunoprecipitated MSH6 from GP293 cell lysate transiently transfected with pcDNA3 or *NPM-ALK* (**Figure 4.4A**), and detected phopsho-MSH2^{Y238} binding with MSH6 using mAB 2E4. I found that, in the presence of NPM-ALK, mAB 2E4 had very weak

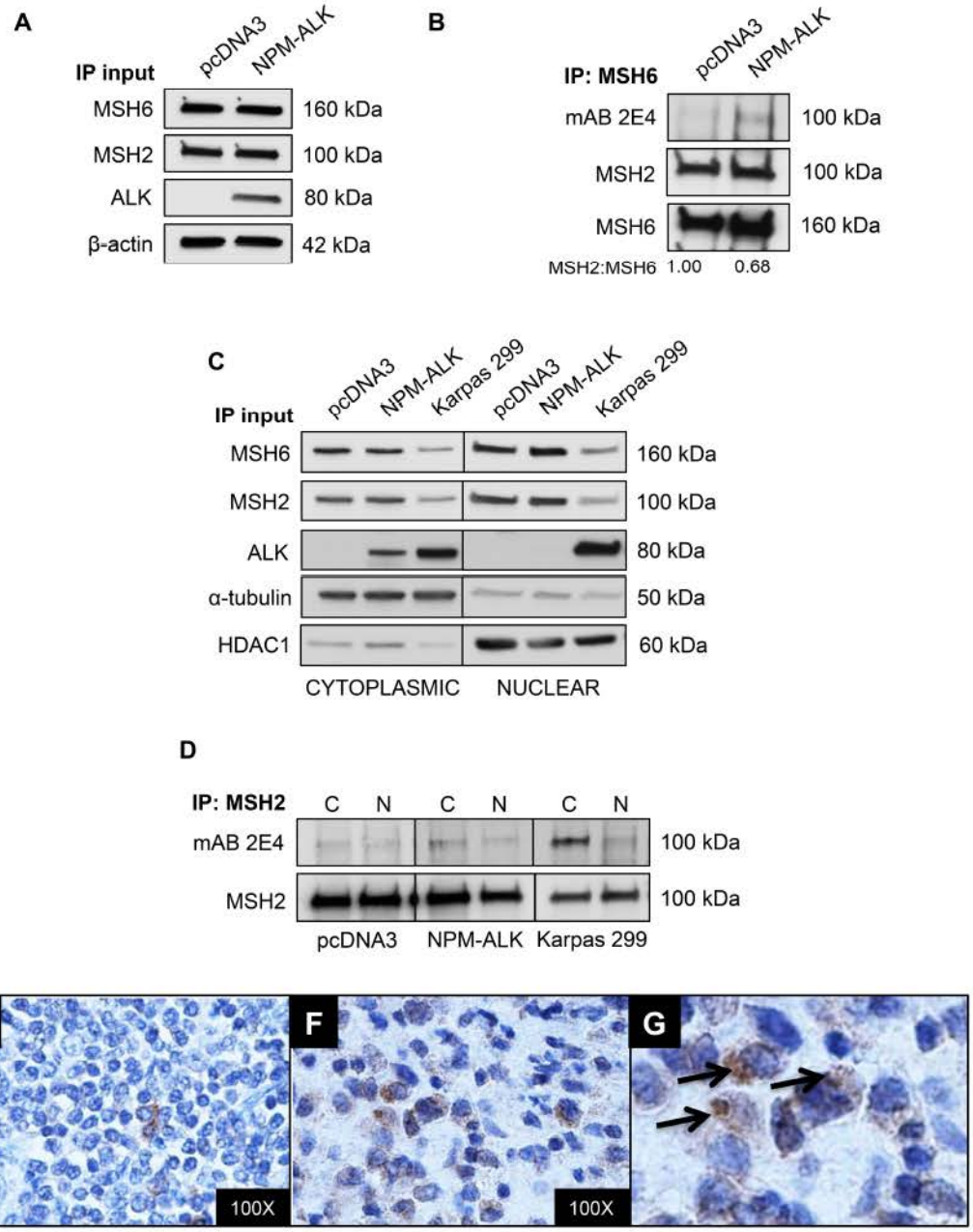

Figure 4.4. Mouse monoclonal antibody 2E4 recognizes MSH2 that is abnormally accentuated in the cytoplasm with weak MSH6 binding. (A) Western blot analysis of GP293 cell lysate from cells transfected with pcDNA3 or *NPM-ALK*. (B) MSH6 was immunoprecipitated from lysate shown in A using an anti-MSH6 mouse monoclonal antibody, and the resulting immunoblot was probed with mAB 2E4 to detect the interaction of MSH6 with phopho-MSH2^{Y238}. The western blot was probed with anti-total-

MSH2 to assess the interaction of MSH6 with total MSH2, and an anti-total-MSH6 antibody to assess MSH6 immunoprecipitation. Densitometry was calculated based on the amount of total MSH2 immunoprecipitated relative to total MSH6, with GP293 cells transfected with pcDNA3 set as 1.00. (C) Western blot analysis of nuclear/cytoplasmic fractionation from GP293 cells expressing pcDNA3 or NPM-ALK, and the ALK+ALCL cell line, Karpas 299. (D) MSH2 immunoprecipitated from cell lysate shown in C and the resulting immunoblot was probed with mAB 2E4 to detect cellular localization of the MSH2 epitope recognized by the mAB 2E4. Anti-MSH2 was included to confirm MSH2 immunoprecipitation. N – nuclear, C – cytoplasmic. (E) Immunohistochemical analysis of mAB 2E4 staining on lymphocytes of reactive tonsil, 100X magnification. (F) Mouse mAB 2E4 immunoreactivity on an ALK+ALCL tumor sample, showing 2E4 cytoplasmic staining of ALK+ALCL lymphoid cells. 100X magnification, a representative stain is shown. (G) A high magnification (400X) view of the immunohistochemical analysis of F, showing predominantly cytoplasmic staining using mAB 2E4 (black arrows). Data shown in A-D is representative of 2 independent experiments. IHC data shown in E-G is representative of at least 10 patient samples.

immunoreactivity with MSH6 (**Figure 4.4B**), suggesting that the majority of MSH2 bound to MSH6 is not tyrosine phosphorylated. Of note, the expression of NPM-ALK reduced the total MSH2:MSH6 interaction by approximately 30%, as previously reported.[7,8]

4.4.5 mAB 2E4 recognizes an epitope of MSH2 that is abnormally localized to the cytoplasm in NPM-ALK-expressing cells

The Lai laboratory has previously reported that NPM-ALK expressing cells display aberrant MSH2 cytoplasmic localization following DNA damage; in keeping with this observation, ALK+ALCL patient tumors display uncharacteristic MSH2 cytoplasmic localization.[7] MSH2 expression is normally predominantly nuclear, and its cytoplasmic retention seen in NPM-ALK expressing cells are indicative of MMR dysfunction.[35,36] Based on the understanding of tyrosine phosphorylation of MSH2 and its impact on MSH2 cellular localization, I hypothesized that mAB 2E4 should recognize an epitope of MSH2 that is abnormally localized to the cytoplasm. To test this hypothesis, I performed nuclear/cytoplasmic fractionation of cell lysate from GP293 cells expressing pcDNA3 or NPM-ALK, and the NPM-ALK-expressing cell line Karpas 299 (**Figure 4.4C**). I immunoprecipitated MSH2 from the cell lysate shown in **Figure 4.4C**, and assessed mAB 2E4 reactivity on the resultant immunoblot. As shown in **Figure 4.4D**, mAB 2E4 had weak, background reactivity to both cytoplasmic and nuclear MSH2 in GP293 cells without NPM-ALK expression. Upon NPM-ALK expression in GP293 cells, and in the ALK+ALCL cell line, Karpas 299, 2E4 was preferentially immunoreactive to a cytoplasmic epitope of MSH2. These results were confirmed by immunohistochemistry on ALK+ALCL tumors; mAB 2E4 staining was accentuated in the cytoplasm (**Figure 4.4F**, and **Figure 4.4G**, black arrows). Reactive tonsil was included as a negative control (**Figure 4.4E**).

4.4.6 Phosphorylation of MSH2^{Y238} and the subsequent MMR dysfunction is shared by other clinically relevant oncogenic tyrosine kinases

Given the understanding of the significance of MSH2 tyrosine phosphorylation in the context of NPM-ALK-expressing cell lines and patient samples, and that other receptor tyrosine kinases share similar features in regards to activation and downstream signal transduction[3,4], I hypothesized that phosphorylation of MSH2 at tyrosine 238 is a shared oncogenic tyrosine kinase phenomenon. To evaluate this hypothesis, I expressed known clinically relevant tyrosine kinases, including the constitutively active gene-fusion tyrosine kinase BCR-ABL, constitutively active (CA) SRC (E381G), CA-HER2 (V659E), CA-c-KIT (D816V), PDGFRα and PDGFRβ in GP293 cells by transient transfection. The activation of PDGFRα and PDGRFβ was mediated by the addition of their activating ligands, PDGFaa and PDGFbb, respectively, into the cell culture media. NPM-ALK expression was included as a positive control.

The expression of the oncogenic tyrosine kinases was confirmed by western blotting (**Figure 4.5A**). MSH2 protein was then immunoprecipitated from the cell lysate shown in **Figure 4.5A**, and the physical interaction of MSH2 with the oncogenic tyrosine kinases was evaluated using specific antibodies, including anti-ALK (NPM-ALK), anti-c-ABL (BCR-ABL), anti-c-SRC (SRC), anti-HER2, anti c-KIT, anti-PDGFRα and PDGFRβ. As shown in **Figure 4.5B**, an interaction between MSH2 and all 7 oncogenic tyrosine kinases was confirmed. I also evaluated MSH2:MSH6 interaction in the cell lysate expressing the oncogenic tyrosine kinases using an anti-MSH6 antibody; it has previously been shown that NPM-ALK expression blocks the heterodimerization of MSH2:MSH6 (also known as MutSα), an event that is critical for DNA

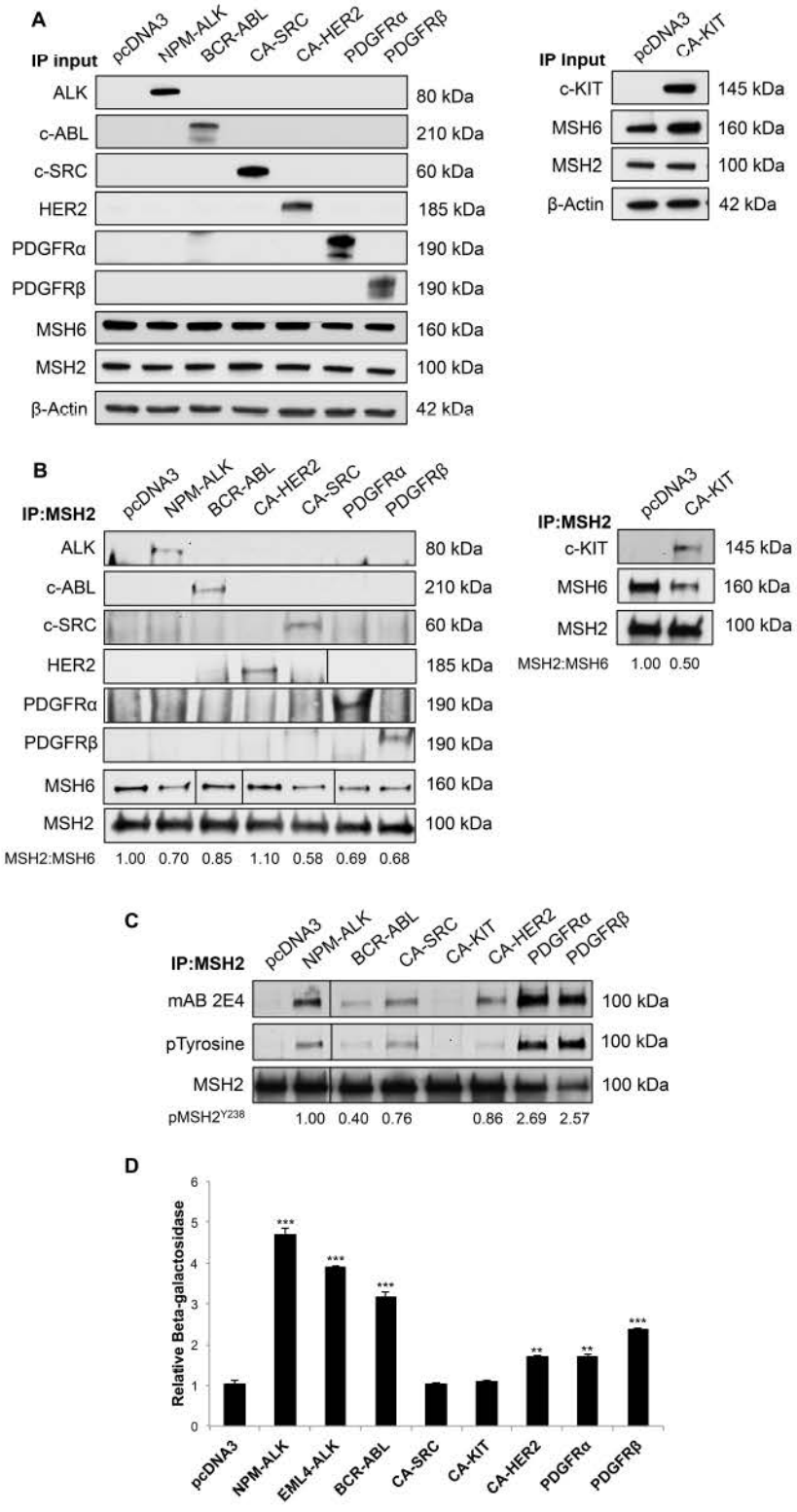
A
IP input
pcDNA3
NPM-ALK
BCR-ABL
CA-SRC
CA-HER2
PDGFRα
PDGFRβ
ALK
c-ABL
c-SRC
HER2
PDGFRα
PDGFRβ
MSH6
MSH2
β-Actin
80 kDa
210 kDa
60 kDa
185 kDa
190 kDa
190 kDa
160 kDa
100 kDa
42 kDa
IP Input
pcDNA3
CA-KIT
c-KIT
MSH6
MSH2
β-Actin
145 kDa
160 kDa
100 kDa
42 kDa
B
IP:MSH2
pcDNA3
NPM-ALK
BCR-ABL
CA-HER2
CA-SRC
PDGFRα
PDGFRβ
ALK
c-ABL
c-SRC
HER2
PDGFRα
PDGFRβ
MSH6
MSH2
MSH2:MSH6
1.00 0.70 0.85 1.10 0.58 0.69 0.68
80 kDa
210 kDa
60 kDa
185 kDa
190 kDa
190 kDa
160 kDa
100 kDa
IP:MSH2
pcDNA3
CA-KIT
c-KIT
MSH6
MSH2
MSH2:MSH6
1.00 0.50
145 kDa
160 kDa
100 kDa
C
IP:MSH2
pcDNA3
NPM-ALK
BCR-ABL
CA-SRC
CA-KIT
CA-HER2
PDGFRα
PDGFRβ
mAB 2E4
pTyrosine
MSH2
pMSH2Y238
1.00 0.40 0.76 0.86 2.69 2.57
100 kDa
100 kDa
100 kDa
D
Relative Beta-galactosidase
0
1
2
3
4
5
6
***
***
***
***
**
**
***
pcDNA3
NPM-ALK
EML4-ALK
BCR-ABL
CA-SRC
CA-KIT
CA-HER2
PDGFRα
PDGFRβ

Figure 4.5. Clinically relevant oncogenic tyrosine kinases bind and phosphorylate MSH2 at tyrosine 238, deregulating DNA MMR. (A) Western blot analysis of GP293 cells transfected with pcDNA3, *NPM-ALK*, *BCR-ABL*, constitutively active (*CA*)-*SRC* (E381G), *CA-HER2* (V659E), *PDFGRα*, *PDGFRβ*, and *CA-KIT* (D816V). Activation of PDGFRα and PDGFRβ was achieved by ligand stimulation, which involved adding recombinant human PDGFaa and PDGFbb, respectively, to the media as outlined in the Materials and Methods. Anti-MSH2 and anti-MSH6 antibodies were used to show their protein expression. β-actin served as a protein loading control. (B) MSH2 was immunoprecipitated from lysate shown in A under co-immunoprecipitation conditions, and the resulting immunoblots were probed with antibodies against ALK, ABL, SRC, HER2, PDGFRα, PDGFRβ, and c-KIT to assess the interaction of MSH2 with these clinically relevant oncogenic tyrosine kinases. The blots were probed with MSH6 to assess MSH2:MSH6 interaction, and MSH2 to confirm successful immunoprecipitation. Densitometry was calculated based on the amount of MSH6 immunoprecipitated relative to MSH2, with the value from cells transfected with pcDNA3 set as 1.00. (C) MSH2 was immunoprecipitated from lysate shown in A under immunoprecipitation conditions, and the resulting immunoblots were probed with an mAB 2E4 to measure phospho-MSH2^{Y238} expression, and a total pan-tyrosine antibody to assess general MSH2 tyrosine phosphorylation. Anti-MSH2 was included to confirm immunoprecipitation. Densitometry was calculated based on the amount of phospho-MSH2^{Y238}, as measured with mAB 2E4, relative to immunoprecipitated MSH2, with cells expressing NPM-ALK set as 1.00. (D) β-galactosidase MMR assay of GP293 cells transfected with pcDNA3, *NPM-ALK*, *EML4-ALK*, *BCR-ABL*, *CA-SRC*, *CA-KIT*, *PDFGRα*, or *PDGFRβ*, and co-transfected with the MMR plasmid pCAR-OF. Forty-eight hours post-transfection, β-galactosidase enzyme production, indicative of MMR dysfunction, was measured in triplicate as outlined in the Materials and Methods. Data is presented as β-galactosidase (A_{420}

nm) ± SEM relative to cells expressing pcDNA3, set at 1.00. Statistical significance was determined by Student's T test, where $^{**}p<0.01$, and $^{***}p<0.001$. A representative result of three independent experiments is shown for the β-galactosidase assay. A representative result of two independent experiments is shown for A-C.

MMR.[7,8] The expression of BCR-ABL, CA-SRC, PDGFRα, PDGFRβ, and CA-KIT, but not CA-HER2, decreased the amount of MSH6 bound to MSH2 to varying degrees, suggesting that these oncogenic tyrosine kinases may function to inhibit DNA MMR in a manner similar to NPM-ALK.

Using the cell lysate shown in **Figure 4.5A**, the tyrosine phosphorylation of MSH2 was evaluated by immunoprecipitating MSH2, and incubating the immunoblot with a pan-p-tyrosine antibody, to measure global MSH2 tyrosine phosphorylation, as well as mAB 2E4, to measure MSH2 phosphorylation specifically at Y238. As shown in **Figure 4.5C**, the expression of NPM-ALK (positive control), BCR-ABL, CA-SRC, CA-HER2, PDGFRα and PDGFRβ, but not CA-c-KIT induced MSH2 tyrosine phosphorylation, as well as specific phosphorylation at Y238. These results, along with those assessing MSH2:MSH6 binding, suggest that BCR-ABL, CA-SRC, PDGFRα and PDGFRβ may induce MMR dysfunction in a similar manner to NPM-ALK, by tyrosine phosphorylating $MSH2^{Y238}$, and blocking the formation of the MutSα heterodimer.

Finally, the ability of the aforementioned oncogenic tyrosine kinases, as well as the gene fusion oncogenic tyrosine kinase EML4-ALK, to deregulate DNA MMR was measured using the β-galactosidase MMR assay plasmid, pCAR-OF.[7,8,37] The pCAR-OF plasmid contains a 58 base-pair poly(C-A) tract at the 5' end of its coding region, placing the start codon out of frame. Thus, in cells with dysfunctional MMR, microsatellite instability (MSI) resulting from strand slippage at the C-A repeat can place the *β-galactosidase* gene in frame, resulting in measurable enzymatic activity.[37] The cells were transiently co-transfected with the oncogenic tyrosine kinase plasmids and pCAR-OF, and β-galactosidase enzyme production was measured 48-hours post-transfection. Expression of NPM-ALK (positive control), EML4-ALK, BCR-ABL and ligand-stimulated

PDGFRβ (p<0.001), and CA-HER2 (despite the fact that MSH2:MSH6 dimerization appeared normal), and ligand-stimulated PDGFRα (p<0.01) led to a statistically significant increase in the amount of β-galactosidase produced over cells expressing pcDNA3 (negative control) (**Figure 4.5D**). Taken together, these results suggest that the expression of BCR-ABL, PDGFRα and PDGFRβ induced DNA MMR dysfunction through the tyrosine phosphorylation of $MSH2^{Y238}$ and subsequent inhibition of MSH2:MSH6 binding. Although the β-galactosidase MMR reporter plasmid suggests that EML4-ALK can also inhibit MMR function, the importance of this gene fusion tyrosine kinase for $MSH2^{Y238}$ tyrosine phosphorylation and MSH2:MSH6 binding needs to be further evaluated.

4.5 Discussion

While it is well known that oncogenic tyrosine kinase expression induces a diversity of downstream signaling in neoplastic cells, increasing tumorigenic potential through the promotion of cellular proliferation, survival, and apoptotic resistance, the effect on the DNA damage response, specifically MMR, is not well understood. Previous studies from the Lai laboratory have revealed that the gene fusion tyrosine kinase NPM-ALK binds and tyrosine phosphorylates MSH2, inducing its cytoplasmic retention, thereby blocking the formation of the MutSα and inhibiting DNA MMR.[6,7] By mass spectrometry, the Lai laboratory has identified that NPM-ALK specifically phosphorylates MSH2 at tyrosine 238.[8] Using a phosphorylation-less mutant, $MSH2^{Y238F}$, I have shown that enforced expression of $MSH2^{Y238F}$ reverses the observed NPM-ALK-induced MMR phenotype[8], supporting the concept that phosphorylation at tyrosine 238 is a key step in the NPM-ALK-induced deregulation of MMR. Directly relevant to these studies, another oncogenic fusion protein, BCR-ABL was reported to abrogate MMR through an unknown mechanism, leading to enhanced cellular survival and the accumulation of DNA point

mutations.[38] As other tyrosine kinases have also been shown to inhibit cellular DNA repair pathways, promoting cellular transformation through the accumulation of DNA damage[39-45], I hypothesized that the NPM-ALK-induced phosphorylation of MSH2 at tyrosine 238 is a more global phenomenon shared by other oncogenic tyrosine kinases.

In this study, I report on the development and characterization of a novel mouse monoclonal antibody that was specifically raised against phospho-MSH2^{Y238}, mAB 2E4. In keeping with the understanding of the MSH2^{Y238} phosphorylation site in the context of NPM-ALK[7,8], this mAB is specifically reactive to an epitope of MSH2 that is present in NPM-ALK expressing GP293 cells, as well as ALK+ALCL cells. This reactivity is abrogated upon phosphatase treatment, and with the expression of the NPM-ALK kinase activation mutant, in which all three tyrosine residues (Y338, Y342, Y343) are mutated (i.e. NPM-ALK^{FFF}), such that NPM-ALK^{FFF} is unable to phosphorylate itself and downstream proteins, significantly affecting its tumorigenicity.[27] Importantly, in the presence of NPM-ALK, the mAB 2E4 recognizes MSH2 that is abnormally localized in the cytoplasm and that does not bind well to MSH6. These results correlate with previous findings from the Lai laboratory that NPM-ALK expression induces an MSH2 “cytoplasmic retention” phenotype, leading to the disruption of MutSα (i.e. MSH2 bound to MSH6) heterodimerization[7], and were confirmed by mAB 2E4 immunohistochemistry on ALK+ALCL tumor samples. MutSα, the primary MMR heterodimer, is 10-fold more abundant in the cell than the MutSβ heterodimer[16] (MSH2 bound to MSH3), and performs the majority of the post-replicative MMR-associated DNA damage repair[46], as well as the repair of DNA damage adducts from both endogenous and exogenous sources.[16] The importance of MutSα in tumor suppression in this context is highlighted by the fact that Lynch Syndrome patients rarely present with the genetic loss of *MSH3*.[21] The inability of MSH2 to enter the nucleus of NPM-ALK expressing cells is likely sufficient for MMR dysfunction[47,48];

thus, I believe that positive cytoplasmic staining using mAB 2E4 on tumor samples is highly indicative of potential MMR dysfunction.

One of the key findings from my study is that a number of known clinically relevant oncogenic tyrosine kinases interact with MSH2, as measured by my co-immunoprecipitation experiments. Using GP293 cells transiently transfected with activated oncogenic tyrosine kinases, I describe novel interactions between MSH2 and BCR-ABL, HER2, SRC, c-KIT, PDGFRα, and PDGFRβ. Interestingly, the expression of most of these tyrosine kinases also modulated the interaction of MSH2 to MSH6, much like the findings with cells expressing NPM-ALK. As is has been reported that the formation of MutSα (MSH2 bound to MSH6) is essential for the majority of the cellular MMR, these observations lead me to hypothesize that these other clinically relevant oncogenic tyrosine kinases may affect MMR ability.

In view of the fact that these activated tyrosine kinases function similarly to NPM-ALK, by binding and tyrosine phosphorylating downstream proteins to modulate their activity, and the fact that an interaction between the oncogenic tyrosine kinases and MSH2 was detectable, I then asked if MSH2 is tyrosine phosphorylated in cells expressing these proteins. Using GP293 cells, I found that enforced expression of activated BCR-ABL, SRC, HER2, PDGFα and PDGFRβ indeed resulted in tyrosine phosphorylation of MSH2, as measured using a pan-tyrosine phosphorylation antibody, as well as the specific phopsho-MSH2^{Y238} antibody, mAB 2E4. I did not detect tyrosine phosphorylation of cells expressing c-KIT using either the pan-p-tyrosine antibody, or mAB 2E4. I initially chose to include c-KIT in the study as gain-of-function mutations in c-KIT, typically found in exon 11 of the *c-KIT* gene, including deletions and point mutations, are common in virtually all cases of gastrointestinal stromal tumor (GIST).[49] However, the constitutively active c-KIT plasmid

available to us for this study carries the specific D816V activating mutation detected in the majority of patients with systemic mastocytosis[32,50]; this mutation is not seen in GIST patients. As I have some preliminary data showing differential mAB 2E4 staining in GIST patient tumors (data not shown), further study is needed in this context.

I have previously shown that NPM-ALK-induced phosphorylation of MSH2 at tyrosine 238 is responsible for the MMR dysfunction phenotype seen in NPM-ALK expressing cells[7,8]; when overexpressed, a tyrosine phosphorylation-less mutant, $MSH2^{Y238F}$, restored MMR function.[7] One of the key findings from this study is that a number of the clinically relevant oncogenic tyrosine kinases I surveyed, including BCR-ABL, HER-2, PDGFα and PDGFRβ, induced MMR dysfunction, as measured using the β-galactosidase reporter plasmid, pCAR-OF. The finding that BCR-ABL deregulates MMR is not a new one; using a similar EGFP MMR reporter plasmid containing a T:G heteroduplex, it has been reported that BCR-ABL-expressing leukemia cells display reduced MMR activity over control cells.[38] Nevertheless, an underlying mechanism for this dysfunction was not established, and my results suggest that tyrosine phosphorylation of MSH2 at tyrosine 238 may induce this observed phenotype.

In the MMR function assay, I included the constitutively active/gain of function EML4-ALK, v1 plasmid, which contains the inv(2)(p21;p23) chromosomal inversion, fusing exons 1-13 of EML4 to exons 20-29 of ALK; this gene fusion tyrosine kinase is important in the etiology of non-small-cell lung cancer (NSCLC).[51,52] Enforced expression of EML4-ALK in GP293 cells led to measurable β-galactosidase enzyme activity, indicative of MMR dysfunction. Although I have not yet characterized the phosphorylation of MSH2 at tyrosine 238 in the context of EML4-ALK, I do have some preliminary data that suggests that mAB 2E4 recognizes a cytoplasmically-accentuated epitope of MSH2 in EML4-ALK-expressing

NSCLC that is not present in EML4-ALK-negative tumor samples (**Figure 4.6**, panel B versus panel A, respectively). The Lai laboratory is currently in the process of confirming this staining, and assessing MSH2 phosphorylation in cells expressing EML4-ALK. As the current IHC data suggests that mAB 2E4 is reactive to ALK positive tumors, including ALK+ALCL, and EML4-ALK NSCLC, I am in the process of expanding the survey to other ALK-expressing cancers, such as neuroblastoma. In the recent years, aberrant ALK expression, whether full length, or through translocation and subsequent constitutive activation, has been reported in a diverse set of cancers, included diffuse large B cell lymphoma (DLBCL), breast cancer, retinoblastoma, renal cell carcinoma, neuroblastoma, colon cancer, serous ovarian carcinoma, and esophageal squamous cell carcinoma (ESCC) (reviewed by Hallberg and Palmer[53]). The Lai laboratory currently have a neuroblastoma tissue microarray, containing 25 neuroblastoma cases, as well as the neuroblastoma cell lines expressing full length as well as activated ALK.[54-57] Using these tools, the MSH2 tyrosine phosphorylation status using mAB 2E4 as well as the MMR function will be assessed; these experiments are currently underway.

The paradoxical findings in GP293 cells expressing CA-HER2 and CA-SRC suggest that phosphorylation of $MSH2^{Y238}$ may not always lead to MMR dysfunction. The understanding of the events leading up to MMR dysfunction in NPM-ALK expressing cells is a four step process, which includes: 1 – induction of phosphorylation of MSH2 at tyrosine 238; 2 – inhibition of MutSα (MSH2:MSH6) formation; 3 – failure of MSH2 to translocate to the nucleus, i.e. its cytoplasmic retention; and 4 – MMR dysfunction. The summary of the results from these four assays is shown in **Table 4.4**. I know that all four steps are involved in the case of NPM-ALK-induced MMR dysfunction observation, and at least steps 1, 2, and 4, are true for cells expressing BCR-ABL, PDGFα and PDGFRβ. Based on the understanding of how NPM-ALK leads to MMR deregulation via the

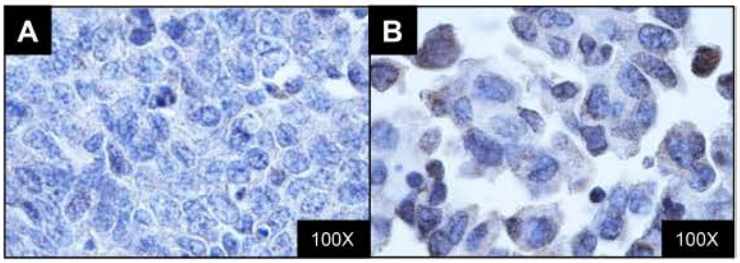

Figure 4.6. mAB 2E4 recognizes an MSH2 epitope in the cytoplasm of EML4-ALK expressing lung tumor samples. (A) Immunohistochemical analysis of mAB 2E4 staining on EML4-ALK negative non-small-cell lung cancer, 100X magnification. (B) Mouse mAB 2E4 immunoreactivity on an EML4-ALK expressing non-small-cell lung cancer patient sample, 100X magnification.

Table 4.4. Summary of results from GP293 cells expressing oncogenic tyrosine kinase constructs.

Tyrosine Kinase	p-MSH2^{Y238} (1)	Inhibition of MutSα (2)	Cytoplasmic retention (3)	Deregulation of MMR (4)
NPM-ALK	Y	Y	Y	Y
EML4-ALK	N/A	N/A	Y*	Y
BCR-ABL	Y	Y	N/A	Y
SRC	Y	Y	N/A	N
HER2	Y	N	N/A	Y
KIT	N	Y	N/A	N
PDGFRα	Y	Y	N/A	Y
PDGFRβ	Y	Y	N/A	Y

Y – yes

* – IHC data only

N – no

N/A – data not available or unknown

cytoplasmic retention of MSH2, I can hypothesize that step 3 is also true for these cells. However, this proposed model does not *necessarily* apply to cells expressing SRC, HER2 and c-KIT. In the case of c-KIT expressing cells, I saw disruption of MutSα formation, but I did not detect MSH2 tyrosine phosphorylation, or MMR dysfunction. In these cells, other unknown post-translational modifications of MSH2 (i.e. acetylation or serine/threonine phosphorylation) induced by c-KIT or its downstream signaling network could underlie the disruption of MSH2:MSH6 binding. Further, although the β-galactosidase reporter plasmid has been used to report MMR dysfunction in the Lai laboratory and by others to great success[7,8], it is not the only method used experimentally to measure MMR deregulation; PCR-based MSI testing[21], IHC for MMR protein expression and/or localization[21], sensitivity to mismatch-inducing drugs[58,59] (i.e. 6-thioguanine, or N-methyl-N-nitrosourea) and a mismatch-based EGFP-reporter plasmid[38] are other methods to measure cellular MMR function. Negative data from one functional assay is not definitive proof that cells retain MMR function, and data from other assays could be used to complement the data already shown. In the case of HER2 expressing cells, although HER2 expression induced MSH2 tyrosine phosphorylation and MMR dysfunction, MSH2:MSH6 binding was not disrupted. In these cells, I hypothesize that other unknown post-translational modifications may promote MutSα formation despite phosphorylation of $MSH2^{Y238}$, but that MutSα may still be unable to translocate to the nucleus to facilitate MMR, or that nuclear translocation occurs, but functional MMR is lacking. Finally, in SRC expressing cells, I found phosphorylation of $MSH2^{Y238}$, and a disruption in MSH2:MSH6 binding, but no MMR dysfunction. Similarly to c-KIT expressing cells, it is possible that SRC expressing cells carry deregulated MMR, but the assay I chose to measure this was not definitive. Thus, although phosphorylation of $MSH2^{Y238}$ is highly suggestive of loss of MMR function, the specific oncogenic tyrosine kinase expressed may induce downstream cellular signaling that overrides this proposed

signaling cascade. Further study is needed in this context.

As I have shown that phosphorylation of MSH2 at tyrosine 238 is likely linked to MMR function, screening of cancer for mAB 2E4 staining has significant implications for cancer treatment. Cells carrying MMR dysfunction have a reported high mutation rate, and an associated chemotherapeutic resistance, especially to DNA adduct-inducing alkylating agents[60], methylating[61], and platinum containing chemotherapeutic agents[62]; thus, positive staining for mAB 2E4 may help direct clinical decisions in regards to patient treatment protocol. In a broader sense, I have shown that mAB 2E4 may screen for the presence of oncogenic tyrosine kinases, and therapeutic targeting using specific tyrosine kinase inhibitors is possible in cancers dependent on the growth-promoting function of the oncogenic tyrosine kinase.

In conclusion, I report on the development and characterization of a novel mouse monoclonal antibody 2E4, which was designed to be specifically reactive to MSH2 phosphorylation at tyrosine 238. This antibody recognizes an epitope of the MSH2 protein with accentuated cytoplasmic staining in ALK-expressing cell lines. I also show for the first time that other clinically relevant tyrosine kinases, including BCR-ABL, PDGFRα and PDGFRβ phosphorylate MSH2 at tyrosine 238, and inhibit MMR. I suggest that phosphorylation of MSH2 at tyrosine 238 is a more global tyrosine kinase phenomenon, leading to a shared mechanism of MMR deregulation. Given these observations, the novel phospho-MSH2^{Y238} antibody, mAB 2E4, may allow for the screening of multiple cancer types for tyrosine kinase expression, with implications for chemotherapeutic targeting and prognosis.

4.6 Acknowledgments

This work was supported by an operating research grant from the Canadian Institute of Health Research (R.L. and S.E.A.). K.M.B. is a graduate student supported by doctoral studentships from the Canadian Institute of Health Research (CIHR Canadian Graduate Scholarship), Alberta Innovates Health Solutions, and the University of Alberta (President's Doctoral Award of Distinction), and is a Killam Scholar (Izaak Walton Killam Memorial Scholarship). The authors would like to thank Dr. T. McMullen (University of Alberta) for the gift of the PDGFRα and PDGFRβ plasmids, Dr. D. Fujita (University of Calgary) for the SRC plasmid, Dr. L. Rönnstrand (Lund University and Malmö University Hospital, Sweden) for the c-KIT plasmid and Dr. J. Dalton (Cambridge Research Laboratory, San Diego) for the EML4-ALK plasmid.

4.7 References

1. Blume-Jensen P, Hunter T. Oncogenic kinase signalling. *Nature* 2001;**411**(6835):355-365.
2. Schlessinger J. Cell signaling by receptor tyrosine kinases. *Cell* 2000;**103**(2):211-225.
3. Lemmon MA, Schlessinger J. Cell signaling by receptor tyrosine kinases. *Cell* 2010;**141**(7):1117-1134.
4. Skorski T. Oncogenic tyrosine kinases and the DNA-damage response. *Nat Rev Cancer* 2002;**2**(5):351-360.
5. Scheijen B, Griffin JD. Tyrosine kinase oncogenes in normal hematopoiesis and hematological disease. *Oncogene* 2002;**21**(21):3314-3333.
6. Wu F, Wang P, Young LC, Lai R, Li L. Proteome-wide identification of novel binding partners to the oncogenic fusion gene protein, NPM-ALK,

using tandem affinity purification and mass spectrometry. *Am J Pathol* 2009;**174**(2):361-370.

7. Young LC, Bone KM, Wang P, et al. Fusion tyrosine kinase NPM-ALK deregulates MSH2 and suppresses DNA mismatch repair function: novel insights into a potent oncoprotein. *Am J Pathol* 2011;**179**(1):411-421.

8. Bone KM, Wang P, Wu F, et al. NPM-ALK mediates phosphorylation of MSH2 at tyrosine 238, creating a functional deficiency in MSH2 and the loss of mismatch repair. *Manuscript submitted for publication* 2014.

9. Swerdlow A, Campo E, Harris NL, et al. WHO Classification of Tumours of Haematopoietic and Lymphoid Tissue. Vol. 2nd (ed 4th). Lyon: World Health Organization; 2008.

10. Campo E, Swerdlow SH, Harris NL, Pileri S, Stein H, Jaffe ES. The 2008 WHO classification of lymphoid neoplasms and beyond: evolving concepts and practical applications. *Blood* 2011;**117**(19):5019-5032.

11. Morris SW, Kirstein MN, Valentine MB, et al. Fusion of a kinase gene, ALK, to a nucleolar protein gene, NPM, in non-Hodgkin's lymphoma. *Science* 1994;**263**(5151):1281-1284.

12. Shiota M, Fujimoto J, Semba T, Satoh H, Yamamoto T, Mori S. Hyperphosphorylation of a novel 80 kDa protein-tyrosine kinase similar to Ltk in a human Ki-1 lymphoma cell line, AMS3. *Oncogene* 1994;**9**(6):1567-1574.

13. Amin HM, Lai R. Pathobiology of ALK+ anaplastic large-cell lymphoma. *Blood* 2007;**110**(7):2259-2267.

14. Lai R, Ingham RJ. The pathobiology of the oncogenic tyrosine kinase NPM-ALK: a brief update. *Ther Adv Hematol* 2013;**4**(2):119-131.

15. Pearson JD, Lee JK, Bacani JT, Lai R, Ingham RJ. NPM-ALK: the prototypic member of a family of oncogenic fusion tyrosine kinases. *J Signal Transduct* 2012;**2012**:123253.

16. Li GM. Mechanisms and functions of DNA mismatch repair. *Cell Res* 2008;**18**(1):85-98.

17. Jascur T, Boland CR. Structure and function of the components of the human DNA mismatch repair system. *Int J Cancer* 2006;**119**(9):2030-2035.

18. Jiricny J. The multifaceted mismatch-repair system. *Nat Rev Mol Cell Biol* 2006;**7**(5):335-346.

19. Jiricny J. Replication errors: cha(lle)nging the genome. *EMBO J* 1998;**17**(22):6427-6436.

20. Peltomaki P. Role of DNA mismatch repair defects in the pathogenesis of human cancer. *J Clin Oncol* 2003;**21**(6):1174-1179.

21. Hegde M, Ferber M, Mao R, et al. ACMG technical standards and guidelines for genetic testing for inherited colorectal cancer (Lynch syndrome, familial adenomatous polyposis, and MYH-associated polyposis). *Genetics in Medicine* 2014;**16**(1):101-116.

22. Wada C, Shionoya S, Fujino Y, et al. Genomic instability of microsatellite repeats and its association with the evolution of chronic myelogenous leukemia. *Blood* 1994;**83**(12):3449-3456.

23. Krskova-Honzatkova L, Cermak J, Sajdova J, Stary J, Sedlacek P, Sieglova Z. Microsatellite instability in hematological malignancies. *Leuk Lymphoma* 2002;**43**(10):1979-1986.

24. Nomdedeu JF, Perea G, Estivill C, et al. Microsatellite instability is not an uncommon finding in adult de novo acute myeloid leukemia. *Annals of Hematology* 2005;**84**(6):368-375.

25. Miyashita K, Fujii K, Yamada Y, et al. Frequent microsatellite instability in non-Hodgkin lymphomas irresponsive to chemotherapy. *Leuk Res* 2008;**32**(8):1183-1195.

26. Karran P. Mechanisms of tolerance to DNA damaging therapeutic drugs. *Carcinogenesis* 2001;**22**(12):1931-1937.

27. Wang P, Wu F, Ma Y, Li L, Lai R, Young LC. Functional characterization of the kinase activation loop in nucleophosmin (NPM)-

anaplastic lymphoma kinase (ALK) using tandem affinity purification and liquid chromatography-mass spectrometry. *J Biol Chem* 2010;**285**(1):95-103.

28. Zhang H, Richards B, Wilson T, et al. Apoptosis induced by overexpression of hMSH2 or hMLH1. *Cancer Res* 1999;**59**(13):3021-3027.

29. He Y, Wertheim JA, Xu L, et al. The coiled-coil domain and Tyr177 of bcr are required to induce a murine chronic myelogenous leukemia-like disease by bcr/abl. *Blood* 2002;**99**(8):2957-2968.

30. Li YM, Pan Y, Wei Y, et al. Upregulation of CXCR4 is essential for HER2-mediated tumor metastasis. *Cancer Cell* 2004;**6**(5):459-469.

31. Bjorge JD, Bellagamba C, Cheng HC, Tanaka A, Wang JH, Fujita DJ. Characterization of two activated mutants of human pp60c-src that escape c-Src kinase regulation by distinct mechanisms. *J Biol Chem* 1995;**270**(41):24222-24228.

32. Sun J, Pedersen M, Ronnstrand L. The D816V mutation of c-Kit circumvents a requirement for Src family kinases in c-Kit signal transduction. *J Biol Chem* 2009;**284**(17):11039-11047.

33. Narayanan R, Yepuru M, Coss CC, et al. Discovery and preclinical characterization of novel small molecule TRK and ROS1 tyrosine kinase inhibitors for the treatment of cancer and inflammation. *PLoS One* 2013;**8**(12):e83380.

34. Anand M, Lai R, Gelebart P. beta-catenin is constitutively active and increases STAT3 expression/activation in anaplastic lymphoma kinase-positive anaplastic large cell lymphoma. *Haematologica* 2011;**96**(2):253-261.

35. Christmann M, Kaina B. Nuclear translocation of mismatch repair proteins MSH2 and MSH6 as a response of cells to alkylating agents. *J Biol Chem* 2000;**275**(46):36256-36262.

36. Christmann M, Tomicic MT, Kaina B. Phosphorylation of mismatch repair proteins MSH2 and MSH6 affecting MutSalpha mismatch-binding activity. *Nucleic Acids Res* 2002;**30**(9):1959-1966.

37. Nicolaides NC, Littman SJ, Modrich P, Kinzler KW, Vogelstein B. A naturally occurring hPMS2 mutation can confer a dominant negative mutator phenotype. *Mol Cell Biol* 1998;**18**(3):1635-1641.

38. Stoklosa T, Poplawski T, Koptyra M, et al. BCR/ABL inhibits mismatch repair to protect from apoptosis and induce point mutations. *Cancer Res* 2008;**68**(8):2576-2580.

39. Slupianek A, Nowicki MO, Koptyra M, Skorski T. BCR/ABL modifies the kinetics and fidelity of DNA double-strand breaks repair in hematopoietic cells. *DNA Repair (Amst)* 2006;**5**(2):243-250.

40. Hoser G, Majsterek I, Romana DL, Slupianek A, Blasiak J, Skorski T. Fusion oncogenic tyrosine kinases alter DNA damage and repair after genotoxic treatment: role in drug resistance? *Leuk Res* 2003;**27**(3):267-273.

41. Slupianek A, Hoser G, Majsterek I, et al. Fusion tyrosine kinases induce drug resistance by stimulation of homology-dependent recombination repair, prolongation of G(2)/M phase, and protection from apoptosis. *Mol Cell Biol* 2002;**22**(12):4189-4201.

42. Fernandes MS, Reddy MM, Gonneville JR, et al. BCR-ABL promotes the frequency of mutagenic single-strand annealing DNA repair. *Blood* 2009;**114**(9):1813-1819.

43. Salles D, Mencalha AL, Ireno IC, Wiesmuller L, Abdelhay E. BCR-ABL stimulates mutagenic homologous DNA double-strand break repair via the DNA-end-processing factor CtIP. *Carcinogenesis* 2011;**32**(1):27-34.

44. Slupianek A, Poplawski T, Jozwiakowski SK, et al. BCR/ABL stimulates WRN to promote survival and genomic instability. *Cancer Res* 2011;**71**(3):842-851.

45. Zhao R, Yang FT, Alexander DR. An oncogenic tyrosine kinase inhibits DNA repair and DNA-damage-induced Bcl-xL deamidation in T cell transformation. *Cancer Cell* 2004;**5**(1):37-49.

46. Genschel J, Littman SJ, Drummond JT, Modrich P. Isolation of MutSbeta from human cells and comparison of the mismatch repair specificities of MutSbeta and MutSalpha. *J Biol Chem* 1998;**273**(31):19895-19901.

47. Claij N, Te Riele H. Methylation tolerance in mismatch repair proficient cells with low MSH2 protein level. *Oncogene* 2002;**21**(18):2873-2879.

48. Ollila S, Sarantaus L, Kariola R, et al. Pathogenicity of MSH2 missense mutations is typically associated with impaired repair capability of the mutated protein. *Gastroenterology* 2006;**131**(5):1408-1417.

49. de Silva CM, Reid R. Gastrointestinal stromal tumors (GIST): C-kit mutations, CD117 expression, differential diagnosis and targeted cancer therapy with Imatinib. *Pathol Oncol Res* 2003;**9**(1):13-19.

50. Kristensen T, Vestergaard H, Moller MB. Improved detection of the KIT D816V mutation in patients with systemic mastocytosis using a quantitative and highly sensitive real-time qPCR assay. *J Mol Diagn* 2011;**13**(2):180-188.

51. Horn L, Pao W. EML4-ALK: honing in on a new target in non-small-cell lung cancer. *J Clin Oncol* 2009;**27**(26):4232-4235.

52. Soda M, Choi YL, Enomoto M, et al. Identification of the transforming EML4-ALK fusion gene in non-small-cell lung cancer. *Nature* 2007;**448**(7153):561-566.

53. Hallberg B, Palmer RH. Mechanistic insight into ALK receptor tyrosine kinase in human cancer biology. *Nat Rev Cancer* 2013;**13**(10):685-700.

54. Janoueix-Lerosey I, Lequin D, Brugieres L, et al. Somatic and germline activating mutations of the ALK kinase receptor in neuroblastoma. *Nature* 2008;**455**(7215):967-970.

55. George RE, Sanda T, Hanna M, et al. Activating mutations in ALK provide a therapeutic target in neuroblastoma. *Nature* 2008;**455**(7215):975-978.

56. Futami H, Sakai R. All-trans retinoic acid downregulates ALK in neuroblastoma cell lines and induces apoptosis in neuroblastoma cell lines with activated ALK. *Cancer Lett* 2010;**297**(2):220-225.

57. Del Grosso F, De Mariano M, Passoni L, Luksch R, Tonini GP, Longo L. Inhibition of N-linked glycosylation impairs ALK phosphorylation and disrupts pro-survival signaling in neuroblastoma cell lines. *BMC Cancer* 2011;**11**:525.

58. Yan T, Berry SE, Desai AB, Kinsella TJ. DNA mismatch repair (MMR) mediates 6-thioguanine genotoxicity by introducing single-strand breaks to signal a G2-M arrest in MMR-proficient RKO cells. *Clin Cancer Res* 2003;**9**(6):2327-2334.

59. Aquilina G, Crescenzi M, Bignami M. Mismatch repair, G(2)/M cell cycle arrest and lethality after DNA damage. *Carcinogenesis* 1999;**20**(12):2317-2326.

60. Fu D, Calvo JA, Samson LD. Balancing repair and tolerance of DNA damage caused by alkylating agents. *Nat Rev Cancer* 2012;**12**(2):104-120.

61. Mojas N, Lopes M, Jiricny J. Mismatch repair-dependent processing of methylation damage gives rise to persistent single-stranded gaps in newly replicated DNA. *Genes Dev* 2007;**21**(24):3342-3355.

62. Martin LP, Hamilton TC, Schilder RJ. Platinum resistance: the role of DNA repair pathways. *Clin Cancer Res* 2008;**14**(5):1291-1295.

CHAPTER 5

General Discussion

5.1 Oncogenic pressure induced by NPM-ALK expression

There are several unanswered questions regarding the regulation of DNA repair pathways, specifically MMR, in the context of NPM-ALK expression that have been addressed in these studies. NPM-ALK, the gene fusion tyrosine kinase central to the pathogenesis of ALK+ALCL[1-4], carries potent transformative potential[5-9], mediating its tumorigenesis through functional and physical interactions with various downstream proteins. Specifically, through its constitutive activation, NPM-ALK initiates the deregulation of a number of downstream signaling pathways, many carrying oncogenic potential on their own, such as the JAK/STAT[10-12], P13K/AKT[13,14], and MEK/ERK pathways[15,16], promoting cellular survival, cell cycle progression, and enhanced cellular proliferation. In an effort to fully understand NPM-ALK-mediated tumorigenesis, in 2009, the Lai Laboratory performed tandem affinity purification followed by mass spectrometry in NPM-ALK-expressing cells to generate a catalog of NPM-ALK-interacting partners. A number of novel interactors were discovered, including the never reported interaction of NPM-ALK with several DNA repair proteins, including the NHEJ/double stranded DNA break repair proteins Ku70/Ku80[17], the DNA polymerase progressivity factor PCNA[18], poly (ADP ribose) polymerase 1 (PARP1)[19], which participates in diverse DNA repair functions, the replication factor minichromosome maintenance complex component 6 (MCM6)[20], and the MMR protein MSH2[21].

5.1.1 Oncogenic tyrosine kinases and DNA repair

Interestingly, although a formal interaction between oncogenic tyrosine kinases and DNA repair factors had never been described, the regulation of DNA repair pathways by gene fusion tyrosine kinases, like NPM-ALK, has been previously reported.[22] Specifically, oncogenic tyrosine kinase have been shown to suppress the normal cellular response to DNA

damage, upregulate the expression of proteins involved in error-prone DNA repair processes, facilitate increased double-strand DNA break repair to induce drug resistance, and protect cells with heavily damaged genomes from apoptosis.[23-29] In regards to DNA MMR, the specific gene fusion tyrosine kinase BCR-ABL expressed by CML cancer cells, was reported to inhibit the MMR process, promoting a cellular "mutator phenotype" and apoptotic protection.[22] Further, the progression of CML from chronic phase to blast phase is associated with the induction of MSI, indicative of MMR dysfunction.[30] The exact mechanisms leading to functional inhibition of MMR has not been reported. The main findings of the three studies presented in this thesis are summarized below.

5.1.2 NPM-ALK suppresses MMR through functional deregulation of MSH2

Using cell lines with enforced NPM-ALK expression, it was found that through binding and phosphorylating MSH2 at undefined tyrosine residue(s), NPM-ALK interferes with the interaction of MSH2 with its main binding partner MSH6, and thus the formation of the integral MMR heterodimer MutSα.[31] The expression of NPM-ALK led to cytoplasmic retention of MSH2, such that it was unable to translocate to the nucleus in the presence of DNA damage in the form of mismatches. Further, NPM-ALK expressing cell lines displayed MMR deregulation, specifically resistance to a mismatch-inducing drug, and measurable β-galactosidase production using an MMR reporter plasmid. ALK+ALCL patient samples showed evidence of MMR dysfunction, including abnormal MSH2 cytoplasmic staining and MSI at defined microsatellite loci. Taken together, these results suggest a novel mechanism by which gene fusion tyrosine kinases, like NPM-ALK, inhibit MMR, through a functional interaction with MSH2. This study represents the first reported post-

translational modification of MSH2 by tyrosine phosphorylation with a direct impact on MMR functionality.

5.1.3 NPM-ALK specifically phosphorylates MSH2 at tyrosine 238

In a follow-up study, mass spectrometry to determine the specific tyrosine residue(s) of MSH2 phosphorylated in the presence of NPM-ALK was performed.[32] Using this information as well as immunoprecipitation studies, I defined the NPM-ALK-induced tyrosine phosphorylation site of MSH2, tyrosine 238. Using an MSH2 mutant that is unable to be phosphorylated, specifically $MSH2^{Y238F}$, I was able to show that tyrosine 238 is an important residue in the context of NPM-ALK-induced regulation, as its enforced expression inhibited the tyrosine phosphorylation of endogenous MSH2, allowing for the restoration of MutSα formation and MMR function. Finally, enforced expression of $MSH2^{Y238F}$ induced spontaneous apoptosis in ALK+ALCL cells. Taken together with the results from the previous study, the data suggest that NPM-ALK phosphorylates MSH2 specifically at tyrosine 238, leading to inhibition of MMR.

5.1.4 Characterization of an anti-phospho-$MSH2^{Y238}$ antibody reveals deregulation of MMR as a shared function of oncogenic tyrosine kinases

In the final study, using the results from the previous studies, and the understanding of the importance of MSH2 phosphorylation in the context of MMR deregulation, with the help of an external biotechnology company, I developed and characterized an anti-phospho-$MSH2^{Y238}$ antibody. In keeping with the previous findings, this mouse monoclonal antibody, mAB 2E4, was preferentially reactive to phospho-$MSH2^{Y238}$ in the presence of NPM-ALK in cells with enforced NPM-ALK expression, and ALK+ALCL

cell lines. Further, this antibody defined an epitope of the MSH2 protein with atypical cytoplasmic localization, and weak MSH6 interaction. Finally, I demonstrated novel interactions between MSH2 and other known clinically relevant oncogenic tyrosine kinases, and phosphorylation of MSH2 specifically at tyrosine 238. These results suggest that MSH2 tyrosine phosphorylation and the subsequent MMR dysfunction may represent a broad oncogenic tyrosine kinase phenomenon.

5.2 Post-translational modification of MSH2

Although functional regulation of the MMR proteins MSH2 and MSH6 (MutSα) through serine phosphorylation has been demonstrated[33-35], little is known regarding the downstream biological significance and the exact circumstances under which phosphorylation occurs, including what specific phosphorylation residue(s) are involved. Interestingly, treatment of cells with alkylating agents[36,37], as well as kinase activators[33], has been reported to positively influence MMR function, inducing both nuclear translocation and chromosomal binding. Further, exposure to various kinase inhibitors caused decreased expression of MMR proteins, as well as a reduction in endogenous MSH6 serine phosphorylation.[33,37] These studies suggest that serine phosphorylation of MutSα, specifically at MSH6, can significantly alter cellular MMR capacity.

Most studies focusing on the phosphorylation-induced regulation of MMR have focused on serine phosphorylation in the N-terminal region of MSH6. MSH6 carries more potential phosphorylation sites than the MSH2 protein[33], and tumor-associated mutations have been identified in N-terminal MSH6 phosphorylation sites.[38] This is especially important as nuclear localization of MutSα is likely mediated through MSH6; in humans, classical NLS sequences have only been identified in MSH6, and it is postulated that MSH2 must first bind MSH6 before nuclear localization

occurs.[39] MSH2 nuclear localization rapidly decreases in cells lacking MSH6 expression[40], despite the fact that independent nuclear and cytoplasmic expression of MSH2 has been noted in the absence of MSH6; this nuclear translocation is thought to occur through importinα and its exact significance is unclear in normal cells.[41-43]

These studies have provided a novel mechanism for MMR regulation via tyrosine phosphorylation of MSH2.[31,32] In keeping with the notion that MSH2 nuclear localization is dependent on MSH6, it was demonstrated that tyrosine phosphorylation of MSH2 has no impact on the movement of MSH6 into the nucleus in the presence of DNA damage.[31] Further, MSH2:MSH6 binding was disrupted upon MSH2 tyrosine phosphorylation, which suggests that the formation of MutSα is needed for MSH2 nuclear translocation. As mentioned, MSH6 was capable of nuclear localization independent of MSH2; the functional significance of this is unknown. Importantly, I was able to show that phosphorylation of MSH2 *does* carry great functional significance and should not be discounted when considering the potential impact of phosphorylation events on MMR function.

5.2.1 Biological significance of MSH2 phosphorylation

5.2.1.1 Naturally occurring disease-relevant mutations surrounding tyrosine phosphorylation site 238

I detected NPM-ALK-induced MSH2 phosphorylation in the MSH2 protein connector domain, located from amino acids 125-299. The connector domain mediates the formation of the MutS ternary complex, connecting the DNA binding subunit to the rest of the heterodimer, allowing for the intramolecular interactions with downstream proteins.[44] A number of the clinically relevant MSH2 missense mutations in Lynch Syndrome patients

have been reported in this domain. In a survey of MSH2 mutants, looking specifically for protein stability, MSH6 interacting ability, and mismatch binding capacity of known MSH2 connector domain missense mutants by Ollila et al., 2008, mutations in the connector domain led to significantly decreased stability over the wildtype MSH2 protein.[45] Connector domain mutants of MSH2 were typically MMR deficient, and exhibited associated loss of MSH2 expression by IHC. Thus, phosphorylation of the connector domain of MSH2 could significantly affect its ability to bind downstream proteins and initiate the MMR signaling cascade.

I performed a search of MSH2 mutations at or near Y238 reported in cancer using the public database COSMIC (The Catalogue of Somatic Mutations in Cancer)[46-48] as well as the online database UNIPROT.[49] I found no reported mutations specifically at the Y238 codon; however, I did find a report of an I->V mutation at amino acid 237.[50] This mutation was detected in a single patient with sporadic colorectal cancer. This patient exhibited MMR deficiency, correlating with MSI at 3/5 loci measured. Since this is the only reported mutation in the literature, it is difficult to determine if the specified mutation was causative in the observed MMR dysfunction phenotype; however, this report, as well as previously mentioned manuscript assessing the function of the connector domain mutants, suggest that mutations affecting the MSH2 protein both at or around Y238 could significantly alter its function.

5.2.1.2 MSH2 and other cellular pathways

On top of the obvious effect that MSH2 tyrosine phosphorylation has on MMR function, MutSα and other MMR proteins participate in non-canonical cellular signaling pathways, including other DNA repair pathways, such as DNA adduct repair, base-excision repair, transcription-coupled repair, double-stranded DNA break repair, and the repair of

intrastrand crosslinks, cell cycle checkpoint activation, apoptotic regulation and trinucleotide repeat (TNR) expansion.[21,39] Interactions of MSH2 and other important cellular proteins from a variety pathways have been extensively documented *in vitro* and *in vivo*: some specific examples include the genome stability promoting protein breast cancer 1, early onset (BRCA1)[51], the oncoprotein c-MYC (V-myc avian myelocytomatosis viral oncogene homolog) and its associated factor MAX (Myc-associated factor X)[52], estrogen-receptor alpha and beta (ERα and ERβ)[53], and the embryonic stem cell factor Sox2 (SRY (sex determining region Y)-box 2).[54] The fact that MSH2 in particular participates in such a diversity of cellular pathways suggests that the MSH2 tyrosine phosphorylation I have described will have numerous implications regarding downstream signaling.

5.2.1.3 Difficulties associated with MSH2 null cell lines

One of the difficulties in studying specific DNA repair proteins comes from the fact that their stability and expression is highly dependent on one another. In my studies, the ideal cell model would be a cell line that is MSH2 null that would allow me to evaluate the downstream MMR signaling effects after re-expression of the MSH2 protein using the MSH2 and MSH2^{Y238F} constructs. There are difficulties with known MMR null cell lines: cells carrying homozygous deletions in the *MSH2* gene will over time lose MSH3 and MSH6 protein expression, and in some cases, their genetic expression as well.[55]

In the T-acute lymphoblastic leukemia (T-ALL) cell line, Jurkat, MSH2 is absent because of homozygous base substitution in exon 13.[56,57] As a result of the genetic loss of *MSH2*, MSH6, which carries a microsatellite in its coding region, is produced as a truncated, non-functional protein due to MSI associated with the loss of MSH2 protein.[58] Genome wide instability

at microsatellite sequences is commonly associated with loss of MSH2.[59] Similarly, the MSH2-/- Lovo cell line, established from human colon adenocarcinoma, carries a homozygous deletion of exons 4-8 in the *MSH2* gene[60], and do not express MSH3 and MSH6 due to protein degradation in the absence of MSH2.[61-63] Finally, the MSH2 null uterine cancer cell line SK-UT-1 carries a homozygous 2bp deletion in exon 14 of the *MSH2* gene that introduces a premature stop codon.[64,65] Upon MSH2 re-expression, MSH3 and MSH6 proteins are undetectable (unpublished observation). The only successful report of re-establishment of MMR in MSH2 null cell lines involved the transfer of mouse chromosome 2 into cancerous cells with homozygous or heterozygous mutations in the *MSH2* gene.[66] Chromosome 2 carries both the *MSH2* and *MSH6* genes, located at 2p21 and 2p16, respectively, and the cells carrying mouse chromosome 2 displayed a restoration of MMR, including a reduction in both MSI and overall mutation rate, and restored sensitivity to the alkylating agent MNNG. Since the experimental approach of introducing a full chromosome with multiple genes is not feasible due to the fact that the other gene products could potentially have significant effects on cellular signaling, using MSH2 null cell lines to study the functional significance of the $MSH2^{Y238F}$ protein was not possible.

5.2.1.4 Experimental issues associated with MSH2 overexpression

The aforementioned issues with MSH2 null cell lines drove us to use over/enforced expression studies to determine the functional significance of $MSH2^{Y238F}$ in the regulation of MMR. These types of experiments carry with them their own set of issues, especially considering that the exogenous protein expression is competing with the expression of the endogenous protein. Further, overexpression of MSH2 and other MMR proteins can actually potentiate MMR dysfunction in a similar manner to cells lacking the expression of the same proteins[67-71]; since MMR proteins

such as MSH2 rely heavily on heterodimerization followed by nuclear translocation for their proper function, too much protein can cause imbalances in protein expression, and in the case of MSH2, change the intracellular ratio of MutSα and MutSβ, leading to decreased cellular MMR function. In keeping with these observations, I have shown that overexpression of HB-MSH2 in GP293 cells increased the β-galactosidase enzymatic activity using the pCAR-OF plasmid, indicative of an increase in MMR dysfunction. Further, immunoprecipitation of MSH2 from GP293 cells expressing NPM-ALK and overexpressing MSH2 led to a 2-fold increase in the observed amount of MSH6 bound to MSH2 (data not shown), suggesting that the increase in MMR dysfunction in these cells was related to improper ratios of MSH2:MSH6. I concluded that cells overexpressing HB-MSH2 were not a good control for my study, and chose to compare enforced expression of HB-MSH2^{Y238F} to HB-EV instead. Luckily for my studies, HB-MSH2^{Y238F} functioned as a dominant negative, preferentially binding to NPM-ALK, not endogenous MSH6, circumventing the issues associated with improper intracellular concentrations of MutSα versus MutSβ.

Overexpression of MSH2 is also associated with the induction of apoptosis[64]; since MSH2 regulates checkpoint activation and the initiation of apoptosis in both MSH2 deficient and proficient cells[72], this observation is not unexpected. It does, however, introduce some issues associated with overexpression studies. In my experiments, I showed that enforced expression of MSH2^{Y238F} in the Tet-on ALK+ALCL MSH2^{Y238F} cell lines induced spontaneous apoptosis. Interestingly, the basal level of apoptosis in these cells was significantly higher than non Tet-on ALK+ALCL cell lines, suggesting that MSH2^{Y238F} expression may be present at a basal level in the absence of doxycycline treatment. Although the pRetro-X Tet-on Advanced System I used to generate the cell lines is said to carry low, or undetectable basal, un-induced expression of the target gene/protein,

tetracycline/doxycycline inducible systems are associated with a variable "leakiness" of expression in the absence of doxycycline.[73] In keeping with these observations, I was never able to generate Tet-on ALK+ALCL cell lines expressing MSH2; after retroviral infection and subsequent selection for antibiotic resistant cells, doxycycline treatment in both Tet-on Karpas 299 and SUP-M2 MSH2 cells resulted in no detectable difference in total MSH2 protein expression (data not shown). These observations underlie the inherent difficulties in overexpression studies. Although I was able to determine that MSH2^{Y238F} and phosphorylation of MSH2 at tyrosine 238 is important in the context of MMR signaling, the imperfect experimental system left a number of questions unanswered.

5.3 Development of the anti-phopsho-MSH2^{Y238} antibody

One of the most important findings of my study is related to the functional significance of tyrosine phosphorylation of MSH2^{Y238} in regards to MMR function. To this end, I characterized a specific anti-phospho MSH2^{Y238} mouse monoclonal antibody, 2E4, which has implications for treatment and prognosis, as well as cancer diagnosis and screening.

5.3.1 Phospho-MSH2^{Y238} antibody: implications for treatment

As I have shown that the presence of phopsho-MSH2^{Y238} correlates with MMR dysfunction, the 2E4 antibody has great potential utility for informing treatment options. MMR dysfunction is associated with varying resistance to common chemotherapeutic agents used in front-line treatment for a variety of cancer types.

5.3.1.1 Chemotherapeutic resistance

Resistance to the platinum-containing chemotherapies cisplatin and carboplatin is multi-factorial[74-76], but MMR has been recognized as one of the key pathways regulating this resistance.[77] These chemotherapies are used to treat cancers such as ovarian cancer, endometrial cancer, NSCLC, colon cancer, and breast cancer, many of which carry MMR deficiency. Both of these agents work by forming DNA adducts, leading to intra- and interstrand crosslinks, which alters the DNA helix causing DNA damage.[78] Functional MMR is required for detection of carboplatin and cisplatin-induced DNA damage by cells; this type of damage interferes with normal MMR activity, which triggers apoptosis. MMR deficient cells are unable to recognize the damage induced by platinating agents, and are thus resistant.[79-81] MMR deficient cells exhibit similar resistance to alkylating agents, topoisomerase inhibitors, and antimetabolites.[21,82,83] Interestingly, cells with loss of MSH2, MSH6, and MLH1 that are resistant to cisplatin are susceptible to treatment with the platinum derivative oxaliplatin, which forms DNA damage derivatives that are poorly recognized by MMR proteins.[84]

5.3.1.1 Synthetic lethality

The knowledge of whether a cancer carries MMR deficiency can be exploited for treatment using synthetic lethality, which is based on the concept that two genes or pathways are synthetically lethal when loss of one is associated with viability, but loss of both induces cell death.[85,86] In the context of MMR deficiency, synthetic lethality has been demonstrated with the inhibition of DNA polymerase γ and the base excision repair (BER) pathway, leading to the lethal accumulation of oxidative damage.[87] Inhibition of PTEN (phosphatase and tensin homolog) -induced putative kinase 1 (PINK1) in MMR deficient cells has also been shown to induce

synthetic lethality through an oxidative stress induction of apoptosis.[88] Treatment strategies based on synthetic lethality have been shown in other MMR deficient cells as well; the ATP depletion associated with gemcitabine treatment increased the sensitivity of MMR null cells to ionizing radiation[89], and methotrexate treatment induced accumulation of 8-oxo-guanidine and apoptosis in cells lacking functional MSH2.[90] The screening of cancer cells with the anti-phospho-MSH2^{Y238} antibody 2E4 could allow for the development of working treatment strategies, including those inducing synthetic lethality associated with MMR loss, in cells that are 2E4 positive.

5.3.2 Screening for oncogenic tyrosine kinase expression

One of the unexpected results from my study was that phosphorylation of MSH2 at tyrosine 238 and the subsequent MMR dysfunction, is a shared tyrosine kinase phenomenon. This is especially exciting considering that a number of cancers carry oncogenic tyrosine kinase drivers, so the mechanism of MMR dysfunction identified in this thesis may be more widespread than ALK+ALCL.

5.3.2.1 Tyrosine kinase inhibitors

Conventional chemotherapeutic strategies don't necessarily differentiate between rapidly dividing normal cells, such as the bone marrow and GI tract, and tumor cells, meaning that there are a number of unintentional toxic side effects.[91,92] Targeted chemotherapies are generally directed towards proteins that are specific to tumor cells with roles in tumor growth and progression. Tyrosine kinase expressing cancers, like ALK+ALCL, and BCR-ABL positive CML, are said to be addicted to the oncogenic tyrosine kinase, such that its inhibition effectively induces cell death and tumor regression.[93-95] Although resistance is an issue when it comes to

targeted therapies with tyrosine kinase inhibitors (as discussed in Chapter 1), targeted therapy has been especially effective for a number of cancers that had poor prognosis prior to its development. For example, the majority of CML patients express BCR-ABL, and before the development of the BCR-ABL inhibitor imatinib, only 30% of patients survived after 5 years[96]; today, the 5-year survival is close to 90%.

The number of cancers found to express oncogenic tyrosine kinases is growing daily, and since the antibody 2E4 may help effectively screen for their expression, therapeutic strategies can be modified to include specific tyrosine kinase inhibitors, if available, on top of first-line chemotherapy.

5.3.2.2 ALK-expressing NSCLC

As I have shown that the 2E4 antibody may effectively discriminate ALK-expressing NSCLC and ALCL from their negative counterparts, the antibody may help in the diagnosis of ALK-expressing cancers. The detection of ALK in NSCLC can be achieved through a variety of experimental techniques with varying success, including: IHC, which is highly dependent on the chosen antibody, and how the tissue is handled and processed[97]; fluorescent *in-situ* hybridization (FISH), which is sometimes difficult to interpret as the results aren't always in concordance with IHC data[97,98]; and RT-PCR, which requires good quality RNA that is not always available.[99] For RT-PCR studies, only known *ALK* alterations are used, and, although there are currently at least 10 different *ALK* rearrangements in NSCLC, there may be more that have not yet been identified.[100] Screening NSCLC tumors for positive 2E4 staining may help in the diagnosis of ALK+NSCLC, especially when IHC and FISH results are not in agreement.

Approximately 5% of NSCLC patients carry *ALK* rearrangements, and treatment with the ALK, MET (HGFR, hepatocyte growth factor receptor), and Ros1 inhibitor crizotinib[101-103] was significantly more effective versus conventional chemotherapy. Crizotinib treatment results in response rates of 60% and a median progressive-free-survival of 8-9 months[104,105], versus response rates of 10% and progression-free-survival of 2-3 months with conventional chemotherapy (the antimitotic agent docetaxel).[106-108] As ALK expression carries better prognosis in NSCLC over patients without ALK expression, better diagnostic strategies would be valuable for improved patient care. With the emergence of ALK as a potential molecular driver in a number of diverse cancers (review by Hallberg and Palmer[109]), screening of cancers for 2E4 expression carries many implications for cancer diagnosis and treatment.

5.4 Future directions

There remain many unanswered questions in regards to the importance of phosphorylation of MSH2 in the context of MMR biology. For example, the importance of restoration of MMR by the expression of $MSH2^{Y238F}$ needs to be elucidated. Although I know that $MSH2^{Y238F}$ expression reestablishes MMR function, presumably through the restoration of endogenous MSH2 and MSH6 formation and inhibition of endogenous MSH2 phosphorylation, the exact mechanisms remain unclear.

Further, the role of phosphorylating $MSH2^{Y238}$ in the progression of cancer induced by oncogenic tyrosine kinase expression needs further study, especially in the context of ALK expression. Although the preliminary data suggest that antibody 2E4 carries great diagnostic utility in regards to ALK+ and ALK− NSCLC and ALK+ALCL, its importance in other ALK-expressing cell lines and patient samples, including neuroblastoma, is currently under investigation. I have yet to show whether oncogenic

tyrosine kinase inhibition affects phosphorylation of MSH2 at tyrosine 238. This would provide us with definitive proof that the expression of the different oncogenic tyrosine kinases underlies the phosphorylation of $MSH2^{Y238}$.

To further the understanding of the importance of $MSH2^{Y238}$ phosphorylation in cancer, the Lai laboratory can consider increasing the effectiveness of the monoclonal antibody; although the current protein G purified antibody 2E4 differentiates between unphosphorylated MSH2 and $MSH2^{Y238}$ by immunoprecipitation of MSH2 and IHC, it is currently not suitable for western blot studies, which would provide a more rapid screening of MSH2 in oncogenic tyrosine kinase expressing cancers. To circumvent this issue, I have recently requested ascites production of the antibody, protein G purification, and a second purification step including the phospho-specific immunizing peptide in hopes to increase the specificity of the antibody, and to decrease the associated background staining. The current antibody is only about 90% pure, and cross-reactivity with other proteins is evident as western blot analysis results in a very dirty film that doesn't differentiate between proteins at the size of MSH2, around 100 kDa. Immunoprecipitation and IHC allow for the differentiation of MSH2 proteins, presumably due to better antigen retrieval and epitope recognition by the 2E4 antibody.

5.5 Conclusions

Determination of the mechanisms underlying NPM-ALK-mediated disruption of MMR signaling may ultimately provide greater understanding of the broader role of oncogenic tyrosine kinases in the deregulation of DNA repair and genomic stability. Through this study, I have shown that tyrosine phosphorylation of MSH2 at tyrosine 238 leads to MMR dysfunction in NPM-ALK-expressing cells. Further, my results suggest that

tyrosine phosphorylation of MSH2 may underlie the deregulated MMR detected in oncogenic tyrosine kinase expressing cancers. I have demonstrated that MSH2 phosphorylation carries functional significance and may be a global tyrosine kinase phenomenon carried by known clinically relevant oncogenic tyrosine kinases

5.6 References

1. Amin HM, Lai R. Pathobiology of ALK+ anaplastic large-cell lymphoma. *Blood* 2007;**110**(7):2259-2267.
2. Lai R, Ingham RJ. The pathobiology of the oncogenic tyrosine kinase NPM-ALK: a brief update. *Ther Adv Hematol* 2013;**4**(2):119-131.
3. Pearson JD, Lee JK, Bacani JT, Lai R, Ingham RJ. NPM-ALK: the prototypic member of a family of oncogenic fusion tyrosine kinases. *J Signal Transduct* 2012;**2012**:123253.
4. Ferreri AJ, Govi S, Pileri SA, Savage KJ. Anaplastic large cell lymphoma, ALK-positive. *Crit Rev Oncol Hematol* 2012;**83**(2):293-302.
5. Zhang Q, Wei F, Wang HY, et al. The potent oncogene NPM-ALK mediates malignant transformation of normal human CD4(+) T lymphocytes. *Am J Pathol* 2013;**183**(6):1971-1980.
6. Chiarle R, Gong JZ, Guasparri I, et al. NPM-ALK transgenic mice spontaneously develop T-cell lymphomas and plasma cell tumors. *Blood* 2003;**101**(5):1919-1927.
7. Giuriato S, Foisseau M, Dejean E, et al. Conditional TPM3-ALK and NPM-ALK transgenic mice develop reversible ALK-positive early B-cell lymphoma/leukemia. *Blood* 2010;**115**(20):4061-4070.
8. Lange K, Uckert W, Blankenstein T, et al. Overexpression of NPM-ALK induces different types of malignant lymphomas in IL-9 transgenic mice. *Oncogene* 2003;**22**(4):517-527.
9. Jager R, Hahne J, Jacob A, et al. Mice transgenic for NPM-ALK develop non-Hodgkin lymphomas. *Anticancer Res* 2005;**25**(5):3191-3196.

10. Chiarle R, Simmons WJ, Cai H, et al. Stat3 is required for ALK-mediated lymphomagenesis and provides a possible therapeutic target. *Nat Med* 2005;**11**(6):623-629.

11. Zamo A, Chiarle R, Piva R, et al. Anaplastic lymphoma kinase (ALK) activates Stat3 and protects hematopoietic cells from cell death. *Oncogene* 2002;**21**(7):1038-1047.

12. Zhang Q, Raghunath PN, Xue L, et al. Multilevel dysregulation of STAT3 activation in anaplastic lymphoma kinase-positive T/null-cell lymphoma. *J Immunol* 2002;**168**(1):466-474.

13. Bai RY, Ouyang T, Miething C, Morris SW, Peschel C, Duyster J. Nucleophosmin-anaplastic lymphoma kinase associated with anaplastic large-cell lymphoma activates the phosphatidylinositol 3-kinase/Akt antiapoptotic signaling pathway. *Blood* 2000;**96**(13):4319-4327.

14. Slupianek A, Nieborowska-Skorska M, Hoser G, et al. Role of phosphatidylinositol 3-kinase-Akt pathway in nucleophosmin/anaplastic lymphoma kinase-mediated lymphomagenesis. *Cancer Res* 2001;**61**(5):2194-2199.

15. Watanabe M, Sasaki M, Itoh K, et al. JunB induced by constitutive CD30-extracellular signal-regulated kinase 1/2 mitogen-activated protein kinase signaling activates the CD30 promoter in anaplastic large cell lymphoma and reed-sternberg cells of Hodgkin lymphoma. *Cancer Res* 2005;**65**(17):7628-7634.

16. Staber PB, Vesely P, Haq N, et al. The oncoprotein NPM-ALK of anaplastic large-cell lymphoma induces JUNB transcription via ERK1/2 and JunB translation via mTOR signaling. *Blood* 2007;**110**(9):3374-3383.

17. Lieber MR, Lu H, Gu J, Schwarz K. Flexibility in the order of action and in the enzymology of the nuclease, polymerases, and ligase of vertebrate non-homologous DNA end joining: relevance to cancer, aging, and the immune system. *Cell Res* 2008;**18**(1):125-133.

18. Moldovan GL, Pfander B, Jentsch S. PCNA, the maestro of the replication fork. *Cell* 2007;**129**(4):665-679.

19. Kim MY, Zhang T, Kraus WL. Poly(ADP-ribosyl)ation by PARP-1: 'PAR-laying' NAD+ into a nuclear signal. *Genes Dev* 2005;**19**(17):1951-1967.

20. Sakwe AM, Nguyen T, Athanasopoulos V, Shire K, Frappier L. Identification and characterization of a novel component of the human minichromosome maintenance complex. *Mol Cell Biol* 2007;**27**(8):3044-3055.

21. Li GM. Mechanisms and functions of DNA mismatch repair. *Cell Res* 2008;**18**(1):85-98.

22. Skorski T. Oncogenic tyrosine kinases and the DNA-damage response. *Nat Rev Cancer* 2002;**2**(5):351-360.

23. Slupianek A, Hoser G, Majsterek I, et al. Fusion tyrosine kinases induce drug resistance by stimulation of homology-dependent recombination repair, prolongation of G(2)/M phase, and protection from apoptosis. *Mol Cell Biol* 2002;**22**(12):4189-4201.

24. Zhao R, Yang FT, Alexander DR. An oncogenic tyrosine kinase inhibits DNA repair and DNA-damage-induced Bcl-xL deamidation in T cell transformation. *Cancer Cell* 2004;**5**(1):37-49.

25. Hoser G, Majsterek I, Romana DL, Slupianek A, Blasiak J, Skorski T. Fusion oncogenic tyrosine kinases alter DNA damage and repair after genotoxic treatment: role in drug resistance? *Leuk Res* 2003;**27**(3):267-273.

26. Skorski T. BCR/ABL regulates response to DNA damage: the role in resistance to genotoxic treatment and in genomic instability. *Oncogene* 2002;**21**(56):8591-8604.

27. Dierov J, Sanchez PV, Burke BA, et al. BCR/ABL induces chromosomal instability after genotoxic stress and alters the cell death threshold. *Leukemia* 2009;**23**(2):279-286.

28. Fernandes MS, Reddy MM, Gonneville JR, et al. BCR-ABL promotes the frequency of mutagenic single-strand annealing DNA repair. *Blood* 2009;**114**(9):1813-1819.

29. Penserga ET, Skorski T. Fusion tyrosine kinases: a result and cause of genomic instability. *Oncogene* 2007;**26**(1):11-20.

30. Wada C, Shionoya S, Fujino Y, et al. Genomic instability of microsatellite repeats and its association with the evolution of chronic myelogenous leukemia. *Blood* 1994;**83**(12):3449-3456.

31. Young LC, Bone KM, Wang P, et al. Fusion tyrosine kinase NPM-ALK deregulates MSH2 and suppresses DNA mismatch repair function: novel insights into a potent oncoprotein. *Am J Pathol* 2011;**179**(1):411-421.

32. Bone KM, Wang P, Wu F, et al. NPM-ALK mediates phosphorylation of MSH2 at tyrosine 238, creating a functional deficiency in MSH2 and the loss of mismatch repair. *Manuscript submitted for publication* 2014.

33. Christmann M, Tomicic MT, Kaina B. Phosphorylation of mismatch repair proteins MSH2 and MSH6 affecting MutSalpha mismatch-binding activity. *Nucleic Acids Res* 2002;**30**(9):1959-1966.

34. Hernandez-Pigeon H, Quillet-Mary A, Louat T, et al. hMutS alpha is protected from ubiquitin-proteasome-dependent degradation by atypical protein kinase C zeta phosphorylation. *J Mol Biol* 2005;**348**(1):63-74.

35. Kaliyaperumal S, Patrick SM, Williams KJ. Phosphorylated hMSH6: DNA mismatch versus DNA damage recognition. *Mutat Res* 2011;**706**(1-2):36-45.

36. Schroering AG, Williams KJ. Rapid induction of chromatin-associated DNA mismatch repair proteins after MNNG treatment. *DNA Repair (Amst)* 2008;**7**(6):951-969.

37. Schroering AG, Kothandapani A, Patrick SM, Kaliyaperumal S, Sharma VP, Williams KJ. Prolonged cell cycle response of HeLa cells to low-level alkylation exposure. *Cancer Res* 2009;**69**(15):6307-6314.

38. Dovrat S, Figer A, Fidder HH, et al. Mutational analysis of hMsh6 in Israeli HNPCC and HNPCC-like families. *Fam Cancer* 2005;**4**(4):291-294.

39. Edelbrock MA, Kaliyaperumal S, Williams KJ. Structural, molecular and cellular functions of MSH2 and MSH6 during DNA mismatch repair, damage signaling and other noncanonical activities. *Mutat Res* 2013;**743-744**:53-66.

40. Christmann M, Kaina B. Nuclear translocation of mismatch repair proteins MSH2 and MSH6 as a response of cells to alkylating agents. *J Biol Chem* 2000;**275**(46):36256-36262.

41. Schroering AG, Edelbrock MA, Richards TJ, Williams KJ. The cell cycle and DNA mismatch repair. *Exp Cell Res* 2007;**313**(2):292-304.

42. Knudsen NO, Andersen SD, Lutzen A, Nielsen FC, Rasmussen LJ. Nuclear translocation contributes to regulation of DNA excision repair activities. *DNA Repair (Amst)* 2009;**8**(6):682-689.

43. Gassman NR, Clodfelter JE, McCauley AK, Bonin K, Salsbury FR, Jr., Scarpinato KD. Cooperative nuclear localization sequences lend a novel role to the N-terminal region of MSH6. *PLoS One* 2011;**6**(3):e17907.

44. Warren JJ, Pohlhaus TJ, Changela A, Iyer RR, Modrich PL, Beese LS. Structure of the human MutSalpha DNA lesion recognition complex. *Mol Cell* 2007;**26**(4):579-592.

45. Ollila S, Dermadi Bebek D, Jiricny J, Nystrom M. Mechanisms of pathogenicity in human MSH2 missense mutants. *Hum Mutat* 2008;**29**(11):1355-1363.

46. Forbes SA, Bhamra G, Bamford S, et al. The Catalogue of Somatic Mutations in Cancer (COSMIC). *Curr Protoc Hum Genet* 2008;**Chapter 10**:Unit 10 11.

47. Forbes SA, Bindal N, Bamford S, et al. COSMIC: mining complete cancer genomes in the Catalogue of Somatic Mutations in Cancer. *Nucleic Acids Res* 2011;**39**(Database issue):D945-950.

48. Forbes SA, Tang G, Bindal N, et al. COSMIC (the Catalogue of Somatic Mutations in Cancer): a resource to investigate acquired mutations in human cancer. *Nucleic Acids Res* 2010;**38**(Database issue):D652-657.

49. UniProt C. Activities at the Universal Protein Resource (UniProt). *Nucleic Acids Res* 2014;**42**(Database issue):D191-198.

50. Chaksangchaichot P, Punyarit P, Petmitr S. Novel hMSH2, hMSH6 and hMLH1 gene mutations and microsatellite instability in sporadic colorectal cancer. *J Cancer Res Clin Oncol* 2007;**133**(1):65-70.

51. Wang Q, Zhang H, Guerrette S, et al. Adenosine nucleotide modulates the physical interaction between hMSH2 and BRCA1. *Oncogene* 2001;**20**(34):4640-4649.

52. Mac Partlin M, Homer E, Robinson H, et al. Interactions of the DNA mismatch repair proteins MLH1 and MSH2 with c-MYC and MAX. *Oncogene* 2003;**22**(6):819-825.

53. Wada-Hiraike O, Yano T, Nei T, et al. The DNA mismatch repair gene hMSH2 is a potent coactivator of oestrogen receptor alpha. *Br J Cancer* 2005;**92**(12):2286-2291.

54. Mallanna SK, Ormsbee BD, Iacovino M, et al. Proteomic analysis of Sox2-associated proteins during early stages of mouse embryonic stem cell differentiation identifies Sox21 as a novel regulator of stem cell fate. *Stem Cells* 2010;**28**(10):1715-1727.

55. Ollila S, Sarantaus L, Kariola R, et al. Pathogenicity of MSH2 missense mutations is typically associated with impaired repair capability of the mutated protein. *Gastroenterology* 2006;**131**(5):1408-1417.

56. Levati L, Marra G, Lettieri T, et al. Mutation of the mismatch repair gene hMSH2 and hMSH6 in a human T-cell leukemia line tolerant to methylating agents. *Genes Chromosomes Cancer* 1998;**23**(2):159-166.

57. Maeck L, Kohaus P, Haase D, Hiddemann W, Alves F. Differential cellular expression of the human MSH2 protein in normal and myelodysplastic haematopoiesis. *Br J Haematol* 2000;**111**(2):650-655.

58. Hosoya N, Hangaishi A, Ogawa S, et al. Frameshift mutations of the hMSH6 gene in human leukemia cell lines. *Jpn J Cancer Res* 1998;**89**(1):33-39.

59. Kinzler KW, Vogelstein B. Cancer-susceptibility genes. Gatekeepers and caretakers. *Nature* 1997;**386**(6627):761, 763.

60. Liu B, Nicolaides NC, Markowitz S, et al. Mismatch repair gene defects in sporadic colorectal cancers with microsatellite instability. *Nat Genet* 1995;**9**(1):48-55.

61. Laghi L, Bianchi P, Delconte G, et al. MSH3 Protein Expression and Nodal Status in MLH1-Deficient Colorectal Cancers. *Clin Cancer Res* 2012;**18**(11):3142-3153.

62. Klingler H, Hemmerle C, Bannwart F, Haider R, Cattaruzza MS, Marra G. Expression of the hMSH6 mismatch-repair protein in colon cancer and HeLa cells. *Swiss Med Wkly* 2002;**132**(5-6):57-63.

63. Oki E, Oda S, Maehara Y, Sugimachi K. Mutated gene-specific phenotypes of dinucleotide repeat instability in human colorectal carcinoma cell lines deficient in DNA mismatch repair. *Oncogene* 1999;**18**(12):2143-2147.

64. Zhang H, Richards B, Wilson T, et al. Apoptosis induced by overexpression of hMSH2 or hMLH1. *Cancer Res* 1999;**59**(13):3021-3027.

65. Risinger JI, Umar A, Boyer JC, et al. Microsatellite instability in gynecological sarcomas and in hMSH2 mutant uterine sarcoma cell lines defective in mismatch repair activity. *Cancer Res* 1995;**55**(23):5664-5669.

66. Umar A, Koi M, Risinger JI, et al. Correction of hypermutability, N-methyl-N'-nitro-N-nitrosoguanidine resistance, and defective DNA mismatch repair by introducing chromosome 2 into human tumor cells with mutations in MSH2 and MSH6. *Cancer Res* 1997;**57**(18):3949-3955.

67. Gibson SL, Narayanan L, Hegan DC, Buermeyer AB, Liskay RM, Glazer PM. Overexpression of the DNA mismatch repair factor, PMS2, confers hypermutability and DNA damage tolerance. *Cancer Lett* 2006;**244**(2):195-202.

68. Drummond JT, Genschel J, Wolf E, Modrich P. DHFR/MSH3 amplification in methotrexate-resistant cells alters the

hMutSalpha/hMutSbeta ratio and reduces the efficiency of base-base mismatch repair. *Proc Natl Acad Sci U S A* 1997;**94**(19):10144-10149.

69. Nicolaides NC, Littman SJ, Modrich P, Kinzler KW, Vogelstein B. A naturally occurring hPMS2 mutation can confer a dominant negative mutator phenotype. *Mol Cell Biol* 1998;**18**(3):1635-1641.

70. Marra G, Iaccarino I, Lettieri T, Roscilli G, Delmastro P, Jiricny J. Mismatch repair deficiency associated with overexpression of the MSH3 gene. *Proc Natl Acad Sci U S A* 1998;**95**(15):8568-8573.

71. Shcherbakova PV, Kunkel TA. Mutator phenotypes conferred by MLH1 overexpression and by heterozygosity for mlh1 mutations. *Mol Cell Biol* 1999;**19**(4):3177-3183.

72. Seifert M, Reichrath J. The role of the human DNA mismatch repair gene hMSH2 in DNA repair, cell cycle control and apoptosis: implications for pathogenesis, progression and therapy of cancer. *J Mol Histol* 2006;**37**(5-7):301-307.

73. Benabdellah K, Cobo M, Munoz P, Toscano MG, Martin F. Development of an all-in-one lentiviral vector system based on the original TetR for the easy generation of Tet-ON cell lines. *PLoS One* 2011;**6**(8):e23734.

74. Perez RP. Cellular and molecular determinants of cisplatin resistance. *Eur J Cancer* 1998;**34**(10):1535-1542.

75. Stewart DJ. Mechanisms of resistance to cisplatin and carboplatin. *Crit Rev Oncol Hematol* 2007;**63**(1):12-31.

76. Vasey PA. Resistance to chemotherapy in advanced ovarian cancer: mechanisms and current strategies. *Br J Cancer* 2003;**89 Suppl 3**:S23-28.

77. Martin LP, Hamilton TC, Schilder RJ. Platinum resistance: the role of DNA repair pathways. *Clin Cancer Res* 2008;**14**(5):1291-1295.

78. Rabik CA, Dolan ME. Molecular mechanisms of resistance and toxicity associated with platinating agents. *Cancer Treat Rev* 2007;**33**(1):9-23.

79. Aebi S, Kurdi-Haidar B, Gordon R, et al. Loss of DNA mismatch repair in acquired resistance to cisplatin. *Cancer Res* 1996;**56**(13):3087-3090.

80. Fink D, Nebel S, Aebi S, et al. The role of DNA mismatch repair in platinum drug resistance. *Cancer Res* 1996;**56**(21):4881-4886.

81. Brown R, Hirst GL, Gallagher WM, et al. hMLH1 expression and cellular responses of ovarian tumour cells to treatment with cytotoxic anticancer agents. *Oncogene* 1997;**15**(1):45-52.

82. Peltomaki P. Role of DNA mismatch repair defects in the pathogenesis of human cancer. *J Clin Oncol* 2003;**21**(6):1174-1179.

83. Aebi S, Fink D, Gordon R, et al. Resistance to cytotoxic drugs in DNA mismatch repair-deficient cells. *Clinical Cancer Research* 1997;**3**(10):1763-1767.

84. Raymond E, Faivre S, Chaney S, Woynarowski J, Cvitkovic E. Cellular and molecular pharmacology of oxaliplatin. *Mol Cancer Ther* 2002;**1**(3):227-235.

85. Kaelin WG, Jr. The concept of synthetic lethality in the context of anticancer therapy. *Nat Rev Cancer* 2005;**5**(9):689-698.

86. Guillotin D, Martin SA. Exploiting DNA mismatch repair deficiency as a therapeutic strategy. *Exp Cell Res* 2014.

87. Martin SA, McCabe N, Mullarkey M, et al. DNA polymerases as potential therapeutic targets for cancers deficient in the DNA mismatch repair proteins MSH2 or MLH1. *Cancer Cell* 2010;**17**(3):235-248.

88. Martin SA, Hewish M, Sims D, Lord CJ, Ashworth A. Parallel high-throughput RNA interference screens identify PINK1 as a potential therapeutic target for the treatment of DNA mismatch repair-deficient cancers. *Cancer Res* 2011;**71**(5):1836-1848.

89. Robinson BW, Im MM, Ljungman M, Praz F, Shewach DS. Enhanced radiosensitization with gemcitabine in mismatch repair-deficient HCT116 cells. *Cancer Res* 2003;**63**(20):6935-6941.

90. Martin SA, McCarthy A, Barber LJ, et al. Methotrexate induces oxidative DNA damage and is selectively lethal to tumour cells with defects in the DNA mismatch repair gene MSH2. *EMBO Mol Med* 2009;**1**(6-7):323-337.

91. Arora A, Scholar EM. Role of tyrosine kinase inhibitors in cancer therapy. *J Pharmacol Exp Ther* 2005;**315**(3):971-979.

92. Chabner BA, Roberts TG, Jr. Timeline: Chemotherapy and the war on cancer. *Nat Rev Cancer* 2005;**5**(1):65-72.

93. Tabbo F, Barreca A, Piva R, Inghirami G, European TCLSG. ALK signaling and target therapy in anaplastic large cell lymphoma. *Front Oncol* 2012;**2**:41.

94. Sharma SV, Gajowniczek P, Way IP, et al. A common signaling cascade may underlie "addiction" to the Src, BCR-ABL, and EGF receptor oncogenes. *Cancer Cell* 2006;**10**(5):425-435.

95. Donato NJ. Bcr-Abl adds another twist to cell fate. *Blood* 2011;**118**(10):2646-2647.

96. Druker BJ, Guilhot F, O'Brien SG, et al. Five-year follow-up of patients receiving imatinib for chronic myeloid leukemia. *N Engl J Med* 2006;**355**(23):2408-2417.

97. Thunnissen E, Bubendorf L, Dietel M, et al. EML4-ALK testing in non-small cell carcinomas of the lung: a review with recommendations. *Virchows Arch* 2012;**461**(3):245-257.

98. Yoshida A, Tsuta K, Nakamura H, et al. Comprehensive histologic analysis of ALK-rearranged lung carcinomas. *Am J Surg Pathol* 2011;**35**(8):1226-1234.

99. Just PA, Cazes A, Audebourg A, et al. Histologic subtypes, immunohistochemistry, FISH or molecular screening for the accurate diagnosis of ALK-rearrangement in lung cancer: a comprehensive study of Caucasian non-smokers. *Lung Cancer* 2012;**76**(3):309-315.

100. Sasaki T, Rodig SJ, Chirieac LR, Janne PA. The biology and treatment of EML4-ALK non-small cell lung cancer. *Eur J Cancer* 2010;**46**(10):1773-1780.

101. Kwak EL, Bang YJ, Camidge DR, et al. Anaplastic lymphoma kinase inhibition in non-small-cell lung cancer. *N Engl J Med* 2010;**363**(18):1693-1703.

102. Ou SH, Kwak EL, Siwak-Tapp C, et al. Activity of crizotinib (PF02341066), a dual mesenchymal-epithelial transition (MET) and anaplastic lymphoma kinase (ALK) inhibitor, in a non-small cell lung cancer patient with de novo MET amplification. *J Thorac Oncol* 2011;**6**(5):942-946.

103. Bergethon K, Shaw AT, Ou SH, et al. ROS1 rearrangements define a unique molecular class of lung cancers. *J Clin Oncol* 2012;**30**(8):863-870.

104. Camidge DR, Bang YJ, Kwak EL, et al. Activity and safety of crizotinib in patients with ALK-positive non-small-cell lung cancer: updated results from a phase 1 study. *Lancet Oncol* 2012;**13**(10):1011-1019.

105. Gambacorti Passerini C, Farina F, Stasia A, et al. Crizotinib in advanced, chemoresistant anaplastic lymphoma kinase-positive lymphoma patients. *J Natl Cancer Inst* 2014;**106**(2):djt378.

106. Hanna N, Shepherd FA, Fossella FV, et al. Randomized phase III trial of pemetrexed versus docetaxel in patients with non-small-cell lung cancer previously treated with chemotherapy. *J Clin Oncol* 2004;**22**(9):1589-1597.

107. Shepherd FA, Rodrigues Pereira J, Ciuleanu T, et al. Erlotinib in previously treated non-small-cell lung cancer. *N Engl J Med* 2005;**353**(2):123-132.

108. Shepherd FA, Dancey J, Ramlau R, et al. Prospective randomized trial of docetaxel versus best supportive care in patients with non-small-cell lung cancer previously treated with platinum-based chemotherapy. *J Clin Oncol* 2000;**18**(10):2095-2103.

109. Hallberg B, Palmer RH. Mechanistic insight into ALK receptor tyrosine kinase in human cancer biology. *Nat Rev Cancer* 2013;**13**(10):685-700.